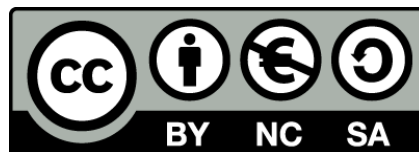UNIVERSITAT DE
BARCELONA

Targeting tumor microenvironment crosstalk through GPCR receptors and PI3K pathway

Martina Guerrero Hernández

PhD in Biomedicine

Targeting tumor microenvironment crosstalk through GPCR receptors and PI3K pathway

Martina Guerrero Hernández
Barcelona 2019

DOCTORAL PROGRAMME IN BIOMEDICINE

Research line- Molecular and cellular biology of cancer

2015-2019

University of Barcelona- Faculty of Medicine

Targeting tumor microenvironment crosstalk through GPCR receptors and PI3K pathway

Doctoral thesis presented by:

Martina Guerrero Hernández

Institut d'Investigacions Biomèdiques August Pi i Sunyer (IDIBAPS)

Hematology-Oncology department

Martina Guerrero Hernández	**Patricia Pérez Galán**	**Jordi Camps Polo**	**Elías Campo Güerri**
Doctorand	Thesis director	Thesis director	Thesis tutor

Barcelona, February 2019

INDEX

Table of contents

Cancer begins and ends with people. In the midst of scientific abstraction,

it is sometimes possible to forget this one basic fact.

—June Goodfield

INTRODUCTION

1.Cancer history and evolution

Cancer. What does cancer mean? It is a term for disease in which abnormal cells divide without control and can invade nearby tissues or can also spread to other parts of the body through the blood and the lymph systems (definition from National Cancer Institute). Cancer is not one disease but many diseases. We call all of them "cancer" because they share a fundamental feature: the abnormal growth of cells. But what else?

Cancer is one of the most relevant problems that has been affecting the human race since the beginning of time, going through 4000-years of history, with its importance increasing in the last 300 years.

The first medical description of cancer was in an original Egyptian text written in 2500 BC, where it is described as "a building tumor in breast … like touching a ball of wrapping". Then, the Greek Hippocrates was the first to use the term 'karkínos' (καρκίνος), which means crab, to refer to the cancer, due to its similarity in hardness to a crab shell, according to some historians. Later, during medieval times, Andreas Vesalius (1514-1564) launched a new search for the real cause and cure of cancer. There is a lot of evidence demonstrating the attempts to fight against cancer throughout this period. Johannes Scultetus (1595-1645) described a mastectomy, the surgical removal of breast cancer, using fire, acid and leather bindings. A few years later, Giovanni Battista Morgagni (1682-1771) was the first to establish the scientific basis for the surgical removal of complicated tumors. Between 1800 and 1900, surgeons devised increasingly aggressive operations to attack the roots of cancer in the body. In the 1890's, William Stewart Halsted at Johns Hopkins University devised the radical mastectomy (an operation to extirpate the breast, the muscle beneath the breast and the associated LNs). Until the XIX century, medicine focused on the study of where the tumor mass appeared and how to remove it from the organism. In 1838 a botanist named Matthias Schleiden and Theodor Schwann, a physiologist, proposed that all living things were composed of fundamental units called cells. Shortly after the introduction of this idea, in 1858, Rudolf Virchow wrote the Diecellulare Pathologie book, where he described the main actor in all diseases as our cells, including cancer. Virchow was the first to understand that our cells are the promoters of cancer and proposed that cells only arose from other cells and that growth could only occur as a result of hyperplasia. Virchow studied cancers under a microscope and recognized that they represented hyperplasia in an extreme form that he called "neoplasia".

In the development of new strategies to fight against cancer, in 1898 radium was discovered by Marie and Pierre Curie, and oncologists and surgeons began to deliver high doses of radiation to tumors, without knowing that radiation itself was carcinogenic. Later, during World War I, mustard gas was indiscriminately used with horrible consequences. This led to the study by Louis S. Goodman and Alfred Gilman, two pharmacologists from Yale University, to use a mustard gas derivate (clormetina, Mustargen) in the treatment of neoplasic diseases in 1942. But it was not until the Bari incident in Italy during World War II in 1943, when the gas decimated normal white blood cells in the victim's bodies reinforcing the hypothesis made by the pharmacologist from Yale that the use of these derivatives became important in killing cancers of white blood cells, such as Hodgkin's lymphomas and leukemia. The results were published in 1946. It was the beginning of **Chemotherapy**. In 1947, Sidney Farber discovered that a folic acid analog called aminopterin, was able to kill dividing cells in the bone marrow. Using aminopterin, Farber obtained good results in the remission of lymphoblastic leukemia. In 1955, **radiotherapy** was born at the hands of Henry Kaplan, a physician-scientist. It was initially used for the treatment of retinoblastoma in a baby, and then used to cure Hodgkin's lymphoma. In the 1960's physicians Emil Frei and Emil Freireich at the National Cancer Institute (NCI) began to use highly toxic drugs to cure acute lymphoblastic leukemia. In the 1990's, Barbara Bradfield was among the first women to be treated with the drug, Herceptin, that specifically attacks breast cancer cells with good results[1]. Continuing on, in 1997, rituximab (anti CD20) was one of the first monoclonal antibody used in cancer treatment in NHL[2].

1.1 Cancer biology

Rolling underneath these medical, cultural, and metaphorical interceptions of cancer over the centuries was the biological understanding of the illness, an understanding that had evolved from decade to decade. Cancer is a disease caused by the uncontrolled growth of a cell. This growth is unleashed by dynamic changes in the genome, specifically mutations that produce oncogenes with dominant gain of function and tumor suppressor genes with recessive loss of function[3]. In a normal cell, powerful circuits regulate cell division and cell death. In a cancer cell, these circuits have been broken, unleashing a cell that cannot stop growing and in some cases have acquired the ability to migrate and invade other tissues and organs of the organism.

That this seemingly simple mechanism, cell growth without barriers, can lie at the heart of this grotesque and multifaceted illness demonstrates the power of cell growth. Cell division allows us as organisms to grow, to adapt, to recover, to repair, and to live. In cancer cells, this skill is distorted

and intensifies all of those abilities, thus creating perfect versions of themselves within our cells. Cancer cells can grow faster and adapt better.

Tumors, unlike what was previously believed, are more than insular masses of proliferating cancer cells; they are complex tissues composed of multiple distinct cell types, which interact with each other. In the biology of tumors it is necessary to understand the role of **tumor microenvironment** in tumorigenesis. This tumor microenvironment is made up of stromal cells, which contribute to certain hallmarks and cancer capabilities[4].

The hallmarks of cancer were described for the first time by Hanahan and Weinberg in 2000[5], where they enumerated six different essential alterations in cell physiology that collectively dictate malignant cell growth, a common set of rules that govern the development of all types of human tumor cells. A few years later, in 2011, the same authors revised the original hallmarks including four more and expanded the functional roles and contributions made by recruited stromal cells to tumor biology. The hallmarks of cancer represent acquired functional capabilities by different tumor types through distinct mechanisms during the course of multistep tumorigenesis, that allow cancer cells to survive, proliferate and disseminate (described below)[4].

-Genome Instability and Mutation

Multistep tumor progression is the succession of clonal expansions, where some of them may be triggered by non-mutational changes affecting the regulation of gene expression[6,7]. The role of p53 is crucial in the maintenance of genome integrity[8]

-Tumor-Promoting Inflammation

Already in the 1980´s, several pathologists recognized that some tumors are infiltrated by cells of innate and adaptive immune system[9]. In the ensuing decade, the important effect of immune cells (from innate immune system) in neoplastic progression[10], where inflammation can participate in hallmark capabilities by supplying bioactive molecules to the tumor microenvironment[11] was demonstrated.

-**Sustaining Proliferative Signaling**

This represents the most essential feature in cancer cells, which involves the ability to maintain chronic proliferation. Cancer cells are able to sustain proliferative signaling by different mechanisms that include: the autocrine production of growth factor ligands themselves [12], the production of

stimulus to the supportive tumor-associated stroma [13], and the deregulated expression of protein receptor levels on the cancer cell surface[14]. Moreover, somatic mutations in certain tumors are associated with constitutive activation of signaling pathways usually triggered by activated growth factor receptors, such as mutations in the catalytic subunit of phosphoinositide 3-kinase (PI3K) isoforms, and another example such as EGFR which triggers the hyperactivation of the signaling pathway[15,16].

-Evading Growth Suppressors

Cancer cells must escape the control of powerful programs that negatively regulate cell proliferation, which mostly depend on tumor suppressor genes. The two principal tumor suppressors are the retinoblastoma-associated protein (RB), which transduce growth-inhibitory signals from outside of the cell[17], and the p53 transcription factor, which receives inputs from stress and abnormal intracellular functions[18]. They are the central control nodes that regulate cell proliferation, or alternatively, activate senescence or apoptotic programs. Another mechanism that inhibits cell proliferation is cell contact, such as Merlin (the cytoplasmic NF2 gene product) which scores contact inhibition via coupling cell-surface adhesion molecules (E-cadherin) to trans-membrane receptor tyrosine kinases (EGFR)[19]. In many late-stage tumors, TGF-β signaling is able to activate the epithelial-to-mesenchymal transition (EMT)[20,21].

-Resisting/Withstanding Cell Death

Apoptosis (programmed cell death) has been established as a natural control in cancer development[22-24]. The apoptosis induced stress signaling is imbalanced due the elevated levels of oncogene signaling and DNA damage, however some tumors are able to attenuate apoptosis in high-grade malignancy state and in resistance to therapy. The apoptotic program is divided into the extrinsic and intrinsic programs, the latter is more implicated as a barrier to cancer pathogenesis[24]. The apoptotic machinery and programs will be described in detail in later sections. The most common strategy for avoiding apoptosis in cancer cells is the loss of p53 function[25,26]. Alternatively, tumors cells are able to increase the expression of antiapoptotic regulators (Bcl-2, Bcl-x, Bfl-1, Mcl-1), or they can downregulate proapototic factors (Bax, Bim, Puma)[26]. Autophagy and necrosis are alternative cell death mechanisms that tumor cells are able to overcome (autophagy)[27] or to take advantage of (necrosis)[10].

-Enabling Replicative Immortality-

Cancers cells require unlimited replicative potential to maintain cell proliferation. One of the mechanisms that tumor cells use to acquire this feature is to increase the levels and activity of telomerase, a specialized DNA polymerase that add telomere repeat segments to the end of telomeric DNA to protect the end of chromosomes[28]. Senescence is another natural barrier to proliferation, that is induced by various proliferation-associated abnormalities, including high levels of oncogenic signaling[29].

-Inducing Angiogenesis

The tumor-associated neo-vasculature, generated by the angiogenesis process, is required for the maintenance and expansion of the tumor[30]. This process is controlled by angiogenic regulators, which are signaling proteins that bind cell-surface receptors displayed by vascular endothelial cells, such as vascular endothelial growth factor-A (VEGF-A), which can be upregulated by hypoxia and by oncogene signaling[31,32]. The upregulation of these angiogenic factors is triggered by the expression of oncogenes such as *Ras* and *Myc*, or by inductive signals produced by immune inflammatory cells[33,34]. It is also known that cells of the innate immune system (macrophages, neutrophils, mast cells and myeloid progenitors) are capable of infiltrating tumor masses and assembling at the margins of lesions, helping to sustain ongoing angiogenesis and conferring a protection against therapy [35-37].

-Activating Invasion and Metastasis

During the development of some tumors, the cells from the primary tumor acquire the ability to move out and invade adjacent tissues, and ultimately they are able to travel to distant sites and colonize themselves. This processed denominated metastasis is responsible for 90% of human cancer deaths[38]. The detailed outline of the invasion-metastasis process will be described in a later section (3.3). One of the main proteins involved in preventing tumor invasion and metastasis is E-cadherin, and it is frequently downregulated as an occasional mutated in human carcinomas[39,40]. Another well-described process implicated in metastasis, dissemination an apoptosis resistance , is the regulatory process "epithelial-mesenchymal transition" (EMT)[41,42]. Moreover, the crosstalk between cancer cells and the tumor microenvironment cells through the secretion of several stimuli[36,43,44], also contributes to this acquired capability of invasion and metastasis of tumor cells.

-Reprogramming Energy Metabolism

In uncontrolled proliferation state of cancer cells, adjustments of energy metabolism are necessary to sustain cell growth. This phenomenon was observed for the first time in 1930 by Otto Warburg[45] and then termed "aerobic glycolysis". Under hypoxic conditions, this dependence on glycolysis increases[46].

-Evading Immune System

The immune system (innate and adaptive) has a crucial role as a barrier for tumor development and progression in both animal models[47] and clinical epidemiology[48]. But in the cancer context, tumors cells are able to impede the infiltration of immune cells such as NK cells and CTLs[49] and inactivate their cytotoxic activity by secreting immunosuppressive factors.

1.2 The tumor microenvironment

The biology of a tumor is the result of the genetic alterations in the tumor cell together with an active interaction among tumor cells and the microenvironment cells. Tumor cells are a heterogeneous group of distinct clonal subpopulations which reflect clonal heterogeneity[50,51]. And a tumor microenvironment is integrated by different types of cells that contribute to the progression of the tumor and to the acquisition of new features and new resistances.

There are substantial differences in the composition of the tumor microenvironment between hematologic malignancies and solid tumors. A noticeable immune B-cell non-Hodgkin's lymphoma (NHL) is characterized by immune infiltrate in secondary lymphoid organs (Lymph nodes (LN) and the spleen),while the infiltration of immune cells in solid tumors is more limited[52].

In many lymphomas, such as follicular lymphoma (FL), mucosa-associated lymphoid tissue lymphomas and classical Hodgkin's lymphoma, the tumor microenvironment plays a crucial role in the proliferation of the lymphoma cells, as well as in the activation of the B-cell receptor an antigen presentation [53]. (An expanded description of tumor microenvironment in FL in the section 2.4).

 In solid tumors, different types of normal cells constitute the tumor stroma, including fibroblast, immune cells, vascular cells, and pericytes. These groups of cells secrete a variety of growth factors and other molecules, such as cytokines and chemokines, which promote cell growth, tumor

progression, and the recruitment of other cells into the tumor[54]. (An expanded description of tumor

microenvironment in CRC in the section 3.3).

2. Follicular Lymphoma

Follicular lymphoma (FL) is the most common indolent non-Hodgkin lymphoma, and the second most frequent subtype of nodal lymphoid malignancies in Western Europe. The annual incidence of this disease has rapidly increased during recent decades, from 2-3/100.000 during the 1950s to 5/100.000 recently[55] , with a median age of presentation of 60 years[56]. FL is slightly more frequent in females[57].

FL is a biologically heterogeneous disease, and the prognosis varies widely among individuals [58]. The disease is characterized by the clonal proliferation of neoplastic lymphoid cells that share morphological, immunophenotypic and molecular attributes of germinal center B cells[59]. These tumors contain a mixture of neoplastic centrocytes and centroblasts along with various non-neoplastic cells including T-cells, follicular dendritic cells, and macrophages[60].

Although FL is generally characterized by slow progression and high response rates to therapy, it is still considered incurable, because virtually almost all the patients relapse [61,62]. Currently, the median survival for newly diagnosed patients has significantly increased and is now approaching 20 years [63]. Moreover, it has been recently reported that the life expectancy of patients in complete response at 30 months is similar to that of the Spanish general population[64]. However, response duration and survival shorten after each relapse[65]. Additionally, there is a risk of transformation to an aggressive lymphoma of approximately 20% at 5 years and 30% at 10 years[66].

2.1 FL Pathogenesis

The genetic hallmark of FL is the reciprocal translocation t(14;18)(q32;q21), which is present in 85-90% of cases[67] [68,69]. The small series of FL cases that lack a t(14;18) were divided in two subgroups: one with BCL2 protein overexpression not related to an IGH/BCL2 rearrangement and a second without BCL2 overexpression (characterized prominently by the presence of t(3;14)(q27;q32), implying a role for BCL6)[70]. Moreover, these cases shown an increased Ki67 proliferation rate, MUM1 higher expression, and CD10 reduced expression. Although overall survival and patient characteristics did not differ between FL with and without t(14;18) supporting the notion that both belong to the same lymphoma entity[71,72].

The somatic rearrangement, which is thought to constitute the first step of lymphomagenesis, is initiated within the bone marrow during B-cell lymphopoiesis as a result of erroneous immunoglobulin heavy chain gene (IGH) rearrangement[73,74]. The t(14;18) translocation leads to placement of the B cell Lymphoma 2 (BCL2) gene under the inductive influence of transcriptional enhancers associated with IGH, resulting in overexpression of anti-apoptotic BCL2 (the hallmark of the disease) leading to increased cell survival in germinal centers [75-77]. BCL2, along with other anti-apoptotic proteins, inhibits apoptosis by binding and neutralizing activated pro-apoptotic proteins including the mitochondrial outer membrane permeabilizers BAX and BAK, as well as the intracellular stress sensors BIM and PUMA that activate BAX and BAK [78-80]. This prolonged survival favors the acquisition of further genetic lesions and ultimately may lead to the development of FL in some such cells[81].

The t(14;18) translocation is also present at low frequency (0.1-10 cells/million) in peripheral blood of 50-70% of healthy individuals, suggesting that the rearrangement itself is insufficient for malignant transformation and therefore secondary genetic alterations are required for cellular transformation to FL [67,82-84]. That circulating t(14;18) positive cells have been named FL-like B cells (FLLCs) and their abundance has been linked to the development of FL[85].

Recently, the notion that the t(14;18) is the first, or the only genetic event initiating FL has been challenged by the identification as early genetic events [86,87] the presence of mutation in 1 or more chromatin-modifying genes; the most frequent being those in the histone-lysine N-methyltransferase 2D (KMT2D; previously known MLL2), the histone acetyltransferases CREB-binding protein (CREBBP), and the Polycomb-group catalytic protein histone-lysine N-methyltransferase (EZH2). In addition, recent results have revealed the importance of the glycan modification (mannosylation) of surface immunoglobulin evident in 74% to 90% of cases. (Table 1). The amino acid sequence motifs are cues for addition in the endoplasmatic reticulum (ER) of a dolichol-linked oligosaccharide chain to the Asn residue, a process known as N-glycosylation. Although germ line-encoded motifs are present in the constant regions of normal immunoglobulin and in a few immunoglobulin variable (IGV) sequences, motifs introduced into the IGV regions during somatic hypermutation are rare in normal memory B cells. However, they are present in almost all cases of FL where they accumulate in the antigen-binding sites. They are found in most soluble IgM+ cases (90%) but there are slightly fewer (73.5%) in IgG+ cases [81,88]. Almost all cases of FL express unusual mannosylated glycan in the antigen-binding site, and these mannosylated

surface immunoglobulins present on the surface of the FL cells, bind with DC-SIGN present in tumor-associated macrophages (TAM) and promote a persistent signaling mechanism for tumor survival/proliferation[89,90]. In addition the mannosylation of the surface immunoglobulin-binding sites could be used to assist diagnosis and, because they are clonal markers, could also be used for monitoring[81].

Table1. Genetic changes found in earliest inferable progenitor of FL

Genetic change	Approximate frequency in FL, %
Translocation of BCL2	80-90
Mutations in 1 or more chromatin-modifier genes	95
Acquisition of N-glycosylation sites in IGV region of BCR	74-90

2.2 Landscape of genomic alterations across the FL genome

The development of next-generation sequencing technologies has led to the discovery of additional recurrent somatic mutations that have provided new insights into the molecular pathogenesis of FL, that include epigenetic deregulation, increased stimulation of survival pathways and immune evasion (Table 2).

2.2.1 Epigenetic deregulation

Alteration of chromatin-modifying genes

Disruption of histone-modifying enzymes by genetic lesions is recognized as a central hallmark of FL, arising in nearly every patient. These mutations principally target the gene encoding **KMT2D KMT2C**, **EZH2**, **CREBBP** and **EP300**[87,91-95]. Chromatin conformation is determined by a dynamic equilibrium between active and repressive histone marks placed at gene promoters and enhancers to control their transcription. The active regulation of these marks, due to both internal and environmental signals, allows B cells to undergo rapid transcriptional and phenotypic changes during the differentiation process. Inactivating mutations in *KMT2D*, *CREBBP* and *EP300* lead to a loss of active marks of transcription (mainly histone H3 lysine 4 methylation (H3K4me) and histone H3 lysine 27 acetylation (H3K27ac))[96,97], whereas hotspot gain-of-function mutations in EZH2 increase the repressive mark H3K37 trimethylation (H3K27me3)[98]. Together, these mutations lead to the aberrant repression of gene transcription in networks with central roles in GC and post-GC

cell fate decision. This phenomenon may maintain the GC phenotype by suppressing programs required for exiting the GC reaction and promoting terminal differentiation, while enhancing survival pathways such as CD40, nuclear factor-κB (NF-κB), Janus kinase (JAK)-signal transducer and activator of transcription (STAT), Toll-like receptor (TLR) and B cell receptor (BCR) signaling[96-102].

Others participants in epigenetic remodeling are the transcription factors **BCL-6**, myocyte-specific enhancer factor 2B (**MEF2B**), and **FOXO1.** While not considered histone-modifying by themselves, they are able to recruit demethylases and deacetylases to promoters and enhancers. BCL-6 can selectively recruit histone deacetylase 3 (HDAC3) to promote H3K27 deacetylation and consequently inactivate B cell enhancers, contrasting the effects of CREBBP and EP300. Even so, BCL-6 represses expression of genes implicated in cell cycle checkpoints and plasma cell differentiation in collaboration with EZH2[103]. The transcriptional activator MEF2B interacts with both the transcriptional co-repressor calcineurin-binding protein (CABIN1) or class II HDACs, and this interaction modulates the activity of MEF2B. The mutations in MEF2B (15% of FL patients) alter its activity to bind to DNA or to the co-repressor CABIN1, resulting in an increased transcriptional activity of MEF2B, and hence increased expression of *BCL6* and *MYC* oncogene[104,105]. Mutations in FOXO1 (present in 5% to 10% in FL patients) lead to a gain of function and cause its nuclear retention and consequent activity, which consists of maintaining the dark-zone program in GC B cells and cooperating with BCL-6[106,107]. Finally, mutations in genes encoding members of the switch/sucrose non fermentable (SWI/SNF) nucleosome remodeling complex or in the linker and core histone genes such as **ARID1A**, **ARID1B**, **BCL7A** and **SMARCA4** , identified in 5-10% of patients with FL, might modify chromatin structure and DNA accessibility to histone-modifying enzymes [87,94,108,109].

All these alterations induce the arrest of B cells in a GC phenotype, sustaining proliferation programs and genetic instability in cells that overexpress **BCL-2** and therefore are resistant to apoptosis[110].

Aberrant DNA methylation

Another type of epigenetic deregulation in FL is the aberrant DNA methylation. In normal GC B -cells a massive redistribution of cytosine methylation mediated by activation-induced cytidine deaminase (AID)[111] occurs ,which mediates the hypomethylation of heterochromatin, and local hypermethylation of Polycomb-repressed regions[112]. In FL tumors, a hypomethylation of their DNA

but increased DNA methylation at the promoters of tumor suppressor genes such as BCL6 and EZH2 and in their target genes has been demonstrated [113-115].

Moreover, the high levels of intra-tumoral heterogeneity in the DNA methylation pattern are associated with higher FL histological grade, therefore contributing to disease aggressiveness[114].

2.2.2 Survival and proliferation signals

One of the most important signaling pathways in FL is the BCR signaling, responsible for antigen activation and promoting cell survival, [53,116]. Approximately 30% of FL patients show mutations in gene encoding proteins in the BCR-NF-κB signaling pathway, mainly in the genes encoding the Bruton tyrosine kinase (**BTK**), accounting for 5-10% of FL patients, and the caspase recruitment domain-containing protein 11 (**CARD11**), accounting for 10-15% of FL patients[109,117,118]. The functional consequences of these mutations are still unclear. Moreover, antigen-independent BCR activation also exists, due to the mannosylation of the surface immunoglobulins, which binds to dendritic cells and macrophages present in the tumor microenvironment that express the DC-SIGN, leading to activation of downstream BCR signaling pathway[89,90].

Equally important, mutations in gene encoding components of the mTOR complex 1 (mTOR1) pathway have been observed in approximately 25% of FL patients[119] . mTOR1 activation increases protein synthesis in response to growth factors and nutrient signals. The levels of amino acids are tightly regulated by a complex located in the lysosomal surface, which includes the RRAG GTPases, the Regulator complex, the V-ATPase complex and sodium-coupled neutral amino acid transporter 9 (SLC38A9)[120,121]. Almost exclusively, activating mutations in *RRAGC* (which encodes RAS-related GTP-binding protein C (RAGC)) occur in FL, and is able to activate mTORC1 in amino acid deprivation conditions[119]. Mutations in V-ATPase complex components specifically in **ATP6V1B2**, **ATP6AP1** and **VMA21** have been found in 10% of the patients, and lead to defects in signaling or alter the interaction between the complex[109].

Additional signaling pathways that collaborate in maintaining the proliferation and survival of tumors cells are JAK-STAT and NOTCH pathways. Activating mutations in the gene encoding **STAT6** cause the constitutive activation of interleukin-4(IL-4)-JAK-STAT pathway, moreover, mutations in genes encoding **STAT3** or suppressor of cytokine signaling 1 (**SOC1**), sustain cell survival and proliferation[94,122] (20%). Mutations in C-terminal PEST domain of the **NOTCH1**, **NOTCH2** proteins,

and alterations in the **NOTCH3** and **NOTCH4** genes and in **DTX1** and **SPEN**, which encode NOTCH signaling regulators, are present in 18% of patients with FL (one of these mutations in NOTCH pathway components), even so, the contribution of these mutations to FL pathogenesis is still unclear[94,122,123].

Finally, inactivating mutations in **GNA13** gene (present in 10% of FL patients) promote B-cell growth and lymphoma cell dissemination[92]. GNA13 encodes the alpha subunit of a heterotrimeric G-protein coupled receptor responsible for modulating RhoA activity[124].

2.2.3 Immune evasion

As mentioned above, mutations in CREEBP and EP300 are very frequent in FL. Recently, it has been demonstrated that CREBBP participates in the control of major histocompatibility complex (MHC) class II expression. Specifically, the decrease of H3K27ac in the enhancers of genes involved in MHC class II presentation reduces its expression and consequently the capacity to stimulate T cell proliferation (in vitro) and changes the population of T-cells that infiltrate the tumors, with a decrease in the stimulation of anti-tumoral CD4$^+$ helper T cells (in vivo)[87].

On the other hand, the inactivation of the receptor herpes virus entry mediator A (**HVEM**; also called TNFRSF14) by point mutation or 1p36 deletions (in 50% of FL) increases the recruitment and activation of protumoral follicular helper T Lymphocytes (T$_{FH}$) through impaired interaction with B and T lymphocytes attenuator (BTLA) receptor expressed on B and T Lymphocytes. Moreover, BTLA expression is under the control of KTM2, frequently mutated in FL, as described before. Altogether, this defect in HVEM-BTLA axis results in the secretion of different cytokines of tumor necrosis factor (TNF) family that activate the lymphoid stroma, creating a tumor-supportive environment containing a high amount of T$_{FH}$[125-128].

Table 2 Genetic alterations in FL

Pathway	Gene	Approximate frequency of mutated cases, %	Proposed functional consequences
Epigenetic and transcriptional regulation	KMT2D (MLL2)	70-90	Reduced H3K4 methylation, promotion of GC B-cell proliferation
	CREBBP	50-70	Reduced histone acetylation, enhances BCL6 function, impaired TP53 function
	EZH2	10-30	Increased bi- and trimethylation of H3K27, reduced expression of target genes
	EP300	10-20	Reduced histone acetylation
	MEF2B	10-20	Enforces activity of BCL6
	KMT2C	13	Reduced histone methyltransferase
	BCL7A	~10	Alteration of chromatin remodeling, specific consequences unclear
	ARID1A	~10	
	ARID1B	~5	
	SMARCA4	~5	
	BCL6	Mutations ~5; translocations ~10	Increased H3K27 deacetylation, reduced expression of target genes
BCR signaling	IGV regions	~80	Promotes N-glycosylation of the surface immunoglobulins favoring microenvironment crosstalk
	CARD11	10-15	Activation of NF-κB signaling
	BTK	5-10	Function of these mutations are still unclear
	FOXO1	5-10	Mutations cause nuclear retention, maintains dark-zone B-cell program, cooperates with BCL6
mTORC1 signaling	RRAGC	10-15	mTORC1 activation, promotes cellular metabolism and growth
	ATP6V1B2	~10	Defects in mTORC1 signaling or alter the interaction between the complex
	ATP6AP1	~10	
	VMA21	5	
Migration	GNA13	5-10	Inactivating mutations promote B-cell growth and lymphoma cell dissemination
Survival	BCL2	~85	Rescue from apoptosis in the GC
	SOCS1, STAT6 and STAT3	20	Hyperactivation of JAK/STAT signaling
	NOTCH1, NOTCH2, NOTCH3, NOTCH4, DTX1 and SPEN	18	Function of these mutations to lymphomagenesis is still unclear[94,122,123]
Immune evasion	HVEM	~50	Loss-of-function mutations may prevent inhibitory HVEM signaling
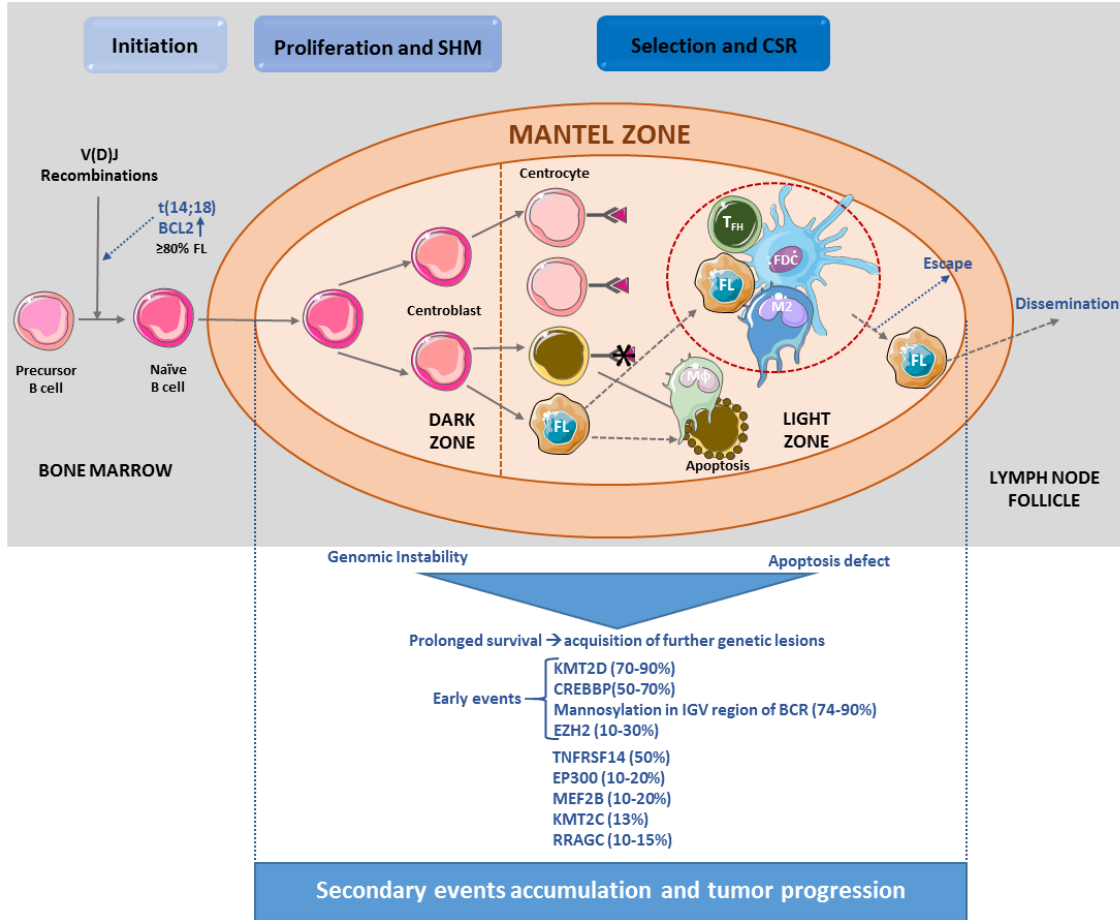
Figure 1. Pathogenesis and genomic alterations. Scheme representing the different steps of FL pathogenesis in bone marrow and then in the lymph node, and the most frequent mutations (including early mutational events).

2.3 FL transformation

FL transformation to an aggressive lymphoma occurs in 2% to 3% of patients per year, and it has been linked to adverse prognosis[129,130]. The most common histology at the time of transformation is diffuse large B-cell lymphoma (DLBCL) (80%), sometimes composite lymphomas (14%) followed by rare instances of lymphomas resembling morphologically high-grade B-cell lymphoma (6%)[131,132].

The factors involved in transformation remain unclear but appear not to be single genetic events but rather multiple hits within a varying molecular landscape[133], summarized in table 3. The tracking of multiple clones in patients shows that transformation to an aggressive B-cell lymphoma occurs either by direct clonal evolution or by divergent evolution from a common progenitor cell[134].

Diagnosis of Follicular (FL)
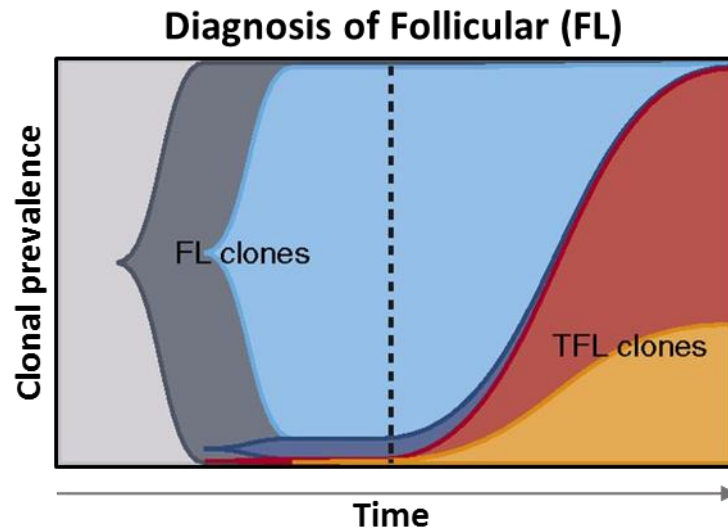
Figure 2. Analysis of FL clonal evolution. Graph represents the origin and evolution of transformed FL.

The common event driving the transformation to aggressive lymphoma is *MYC* translocation. A significant proportion of transformed FLs (TFLs) are double-hit lymphomas and are classified as high-grade B cell lymphoma, with translocations in *MYC* and *BCL2* and/or *BCL6*, according to 2016 WHO classification[135]. Transformation occurs via the activation of known or putative oncogenes (MYC and CCND3) and inactivation of known or putative tumor suppressors genes (TP53, CDKN2A/B, B2M, S1PR2, GNA13)[94,122,136-141]. These changes lead to an increase in proliferation (resulting from cell cycle reregulation), defects in DNA damage response, alterations in B cell migration and escape from immune surveillance[142]. Moreover, mutations in EBF1 and regulators of NF-κB signaling (MYD88 and TNFAIP3) were gained at transformation[94].

The development of a new noninvasive approach for monitoring tumor evolution, the sequence of circulating tumor DNA (ctDNA) by liquid biopsies, is a promising method for early detection of transformation[143].

Table 3. Biological risk factors that increase FL transformation.

Category	Variable with reported risk of transformation
Microanatomical structure	Disrupted CD21^{+} FDC meshwork's[144]
	Intrafollicular localization of CD14^{+} FDCs[145]
Tumor microenvironment	Predominantly intrafollicular localization of CD4^{+} T cells[144]
	Diffuse pattern of PD1^{+} cells[145]
	Higher FOXP3 expression[146]
	Intra- or perifollicular distribution of FOXP3^{+} cells[147]
	Increased vessel density[148]
FL grade	Grade 3A[132]
	IRF4 tumor cell staining by IHC[132]
Germ line polymorphism	Single nucleotide Polymorphism (SNP) rs6457327[149]
Gene expression signatures	Embryonic stem cell-like signature[150]
	NF-κB target signature scores[151]
Large-scale genetic alterations	Deletions of chromosome 1p or 6q; gain of chromosomes 2, 3q or 5[152-155]
	Higher numbers of structural rearrangements[136]
Single gene alterations	*TP53* mutations or deletions[138,156]
	MYC translocations or mutations[139]
	FAS mutation[137]
	BCL6 translocations[132,157]
	BCL2 mutations[158]
Circulating tumor DNA	Proportion of mutations uniquely found in plasma[143]

Adapted from Kridel et al., Blood, 2017[133].

2.4 Role of tumor microenvironment

FL is probably the NHL with the highest dependence on microenvironment, which sustains cell growth and survival creating a specific FL tumor niche[60]. In fact, FL was the first lymphoma where the composition of microenvironment was related to prognosis[159].

Several highly frequent genetic alterations are not oncogenic *per se* but favor the crosstalk of FL cells with their neighboring cells. As mentioned above, the recent demonstration that the inactivation of HVEM contributes to the immune escape of FL, sheds more light on the relation between genetic alterations and development of a permissive microenvironment.

The FL tumor is characterized by the maintenance of the follicular structure indicating that FL B cells remain dependent on cellular and molecular events that contribute to the normal germinal center (GC) reaction. The formation pattern of tumor microenvironment in FL has been defined as a 're-education' process, meaning that tumor cells take advantage of follicle structure and organization

to promote their survival. This organization similar to GC is supported by follicular dendritic cells(FDCs) and T follicular helper (T$_{FH}$) cells[160]. Beyond T lymphocytes, FL tumor cells also indirectly influence the polarization of monocytes towards an immunosuppressive phenotype. Lastly, the differentiation of mesenchymal stromal cells to lymphoid-like stromal cells (fibroblastic reticular cells) is an important process that accounts for the production of chemotactic cytokines that attract FL cells and may modulate the composition of FL microenvironment [161,162].

In summary, it is now accepted that FL microenvironment, including stromal cells, T$_{FH}$ or tumor associated macrophages (TAM), supports malignant B-cell survival, proliferation and drug resistance. Thus, the FL cell niche should be envisioned as a dynamic network of cell interactions where factors secreted by a certain cellular type may impact the activation, expansion, polarization and migration of a different one [163].

2.4.1 Stromal cells

The stromal cell subset is the non-hematopoietic cell type present in LNs and is responsible for making up the parenchyma. These cells are fibroblastic reticular cells (FRCs), follicular dendritic cells(FDCs), marginal reticular cells (MRCs) and bona fide mesenchymal stromal cells (MSC) that can differentiate to FRC. The main common feature of lymphoid stromal cells is to derive from resident local precursors and need both tumor necrosis factor (TNF)-α and lymphotoxin (LT)-α1β2 (produced by B and T cells) for their maturation and maintenance as immunologically competent cells. Furthermore, they play a central role in FL pathogenesis through both a direct tumor B-cell supportive activity and an indirect effect on the orchestration of FL cell niche[164].

FRCs: they form the mesenchymal stromal network on the T-cell zone. These cells provide a purchase for antigen delivery, immune cell recruitment, motility, interaction, and homeostasis within the release of extracellular matrix components (ECM) (such as the collagen-rich reticular fibres, ER-TR7 antigen, fibrillin, laminin and fibronectin), IL-7, VEGF, nitric oxide, and homeostatic chemokines CCL19, CCL21 and CXCL12. This latter cytokine induces FL tumor cell migration and adhesion, and also dendritic cell migration to T cell zone. FRCs also express integrin subunits, the adhesion ligand intercellular adhesion molecule 1 (ICAM1), and vascular cell adhesion molecule 1 (VCAM1)[165].

FDCs: they represent the cluster of the germinal center (GC) of B follicles promoting the recruitment of B cells and T$_{FH}$ through CXCL13-dependent attraction into the light zone of GC. These cells present

antigens as immune complex to B-cells, thereby contributing to affinity maturation and BCR survival. FDCs express Fc receptors (such as CD16, CD23 and CD32), complement receptors (such as CD21 and CD35) and complement components (such as C4). They also express high levels of VCAM1, desmin, laminin and B cell-activating factor of the TNF family (BAFF)[165]. Equally important is the production of Hedgehog (Hh) ligands, IL-15, hepatocyte growth factor (HGF), and the adhesion molecule VCAM1 that has been proposed to contribute to their anti-apoptotic effect on malignant GC B cells[166-169].

MRCs: they have different phenotype than FRCs and FDCs but also share markers in common with them, such as ER-TR7 antigen, demin, laminin, VCAM1 and MADCAM1, and secrete the chemokine CXCL13[165].However, MRCs seem to uniquely express the tumor necrosis factor family member RANKL (receptor activator of NF-κB ligand).

MSC: these cells present in the LN can be triggered to FRC differentiation in response to TNF-α and LT-α1β2[170]. They also overexpress CCL2 chemokine that causes the recruitment of monocytes promoting their differentiation into proangiogenic and anti-inflammatory macrophages phenotype (TAMs)[161].

2.4.2 T cells

T cells are one of the major immune cell types found within TME and coordinate the specific immune response to cancers cells, due the differentiation of naïve T cells to distinct specialized T cell subpopulations. These specialized subsets produce specific cytokines and exhibit different effector functions. Two different classes of T cells are of interest, CD4+ T lymphocytes and CD8+ cytotoxic T cells (CTLs)[171].

2.4.2.1 CD8+ T cells

The presence of CD8+ **CTLs** in the tumor, is associated to anti-tumoral immunity by the host, therefore inhibiting FL cell growth. They are activated by the engagement of their T-cell receptor (TCR) with complexes formed between antigenic peptides and MHC class I molecules displayed on the surface of target cells. TCR signaling leads to the rapid secretion of the pore-forming protein perforin, granzyme B, and other proteases stocked in CTL cytoplasmic granules (named lytic granules) at the CTL/ target cell contact site. Penetration of granzyme B in target cells triggers an

apoptotic cascade ultimately leading to target cell annihilation, in fact granzyme B expression is associated with prolonged PFS [172].

2.4.2.2 CD4^{+} T cells

CD4^{+} T cells have pivotal role in tumor cell growth. In the area around the tumor, five different types of CD4+T cells have been described:

Th1 cells: they perform an essential role protecting the body against intra-cellular pathogens through macrophage activation. Also, they promote and regulate the CD8+ CTLs activity[173]. Th1 cells by producing some cytokines such as IFN-γ, IL-2 and TNF-β can mediate inflammation and delayed hypersensitivity. High numbers of Th1 cells in the TME have been associated to a good prognosis in many cancers[174].

Th2 cells: they are not directly cytotoxic immune cell types, so they mediate their effector functions by the release of cytokines that activate other immune cell types[175]. The IL-10 secretion by Th2 cells mediate the inhibition of DC antigen processing, presentation, and/or the activation of the immune suppressive regulatory T cells[176]. However, the secretion of IL-4 was linked to tumor clearance through recruitment of infiltrating eosinophils and macrophages[177].

Th17 cells: they are part of TIL sub-sets within the TME, and are more abundant near the tumor mass. The rich environment of pro-inflammatory cytokines secreted by fibroblast and other cells types in TME, favor the recruitment of Th17 cells[178]. These cells are able to generate pro- or antitumor growth effects depending on the cancer type[179]. Th17 cell, with a specific phenotype (CD45RA-, CD45RO+), express CD49, CCR2, CCR5 and CCR7 receptors, allowing their trafficking to peripheral tissues and limit their retention in lymph nodes[180].

T regulatory cells (Treg): they are able to suppress effector T-cells mediated antitumor functions within the TME, supporting disease progression, and would result in poor outcome in lymphoma. Treg express CD25 and secrete IL-10, IL-35 and TGF-β.[181]. However, in FL the presence of these FOXP3 [+] cells have been described as a good prognostic marker and associated with improved overall survival[182,183]. The role of regulatory T cells in the context of this lymphoma has been controversial and some authors failed to found a positive correlation[144], or even associated the follicular location of Treg with poor outcome[147].

In the germinal center, two different types of T cells have been characterized:

T follicular helper (T$_{FH}$): they were initially identified as CD4$^+$ T cells expressing CXCR5 and PD-1 and they are located in follicular areas of secondary lymphoid organs, but recent studies defined them as a distinct helper T-cell lineage, under the control of BCL6, the master regulator of T$_{FH}$ differentiation pathway, playing a central role in GC B-cell localization, selection and differentiation in normal follicles[184]. FL-T$_{FH}$ display a specific gene expression profile compared to tonsil-T$_{FH}$, with an overexpression of *IL4, IL2, IFNG* and *TNF*. T$_{FH}$ produces high levels of IL-4, and it has been associated with a STAT6 and Erk-dependent FL activation in a paracrine mode. Moreover, the interaction T$_{FH}$ CD40 ligand (CD40L) with CD40-FL cells promotes FL cell survival. FL-T$_{FH}$ could also modulate the FL supportive niche through their expression of *TNF* and *LTA* that activate differentiation and maintenance of B-cell supportive lymphoid stroma network. In addition, the overexpression of IL-4 may contribute to the polarization of TAM within the malignant cell niche.

T follicular regulatory (T$_{FR}$): these cells are Foxop3^{pos}CXCR5^{hi}, sharing some phenotypic characteristics with T$_{FH}$, such as a high levels of BCL6 compared to classical Treg[185]. T$_{FR}$ have opposite functions in follicular lymphoma, they are able to suppress CD4+T cells (including T$_{FH}$) and follicular lymphoma cells[186], and conversely, they could inhibit CD8$^+$ CTLs from the GC border[172]. They also strongly express the co-stimulatory molecule ICOS, with strong immunesuppressive functions[185].

2.4.3 Myeloid cells

These types of cells are recruited into tumor as monocytes from the bloodstream by the release from tumor of chemokines such as CCL2[60].

TAMs are highly plastic cells involved in tumor survival, growth and immunity. It is well accepted that the presence of macrophages in tumor microenvironment has a bad prognosis, but on the other hand, it has been reported that a high content of them predicts favorable outcome in FL patients treated with Rituximab-chemotherapy[187]. A later study, demonstrated that CD163-positive macrophages predict outcome in follicular lymphoma, but their prognostic impact is highly dependent on treatment received. Increased staining for CD163 was associated with poor PFS and OS in the patients treated with R-CVP, and favorable PFS in the patients treated with R-CHOP. On the other hand, CD68 staining cells did not predict outcome in these patients[188].

Once they reach the tumor, the secretion of IL-4 by Th2 leads to M2 polarization of monocytes (via STAT6), a phenotype that is associated with tumor dissemination, immunosuppression and

angiogenesis[189,190]. M2 classical phenotype is characterized by the co-expression CD68 and CD163, and the low expression of IL-12 and high expression of IL-10[190]. TAMs also secrete suppressive cytokines such as TGF-β that inhibit antitumor immunity[191]. On the other hand, the secretion of IFN-ɣ by Th1 in tumor microenvironment[185], promotes and increases the migration of macrophages in response to CCL2 through an upregulation of STAT1 expression[192]. Macrophages interplay with FL cells also occurs through the cytokine B cell activating factor (BAFF) secreted by TAMs, which is a survival factor for FL patients. Moreover, it has been reported a germline mutation in TNFRSF13 C/BAFF-R in 10% of FL patients, which induces a strong activation of BAFF-signaling[193]. Another important pathway activation by TAM interaction with FL is the BCR signaling. M2 macrophages overexpress C-type lectins DC-SIGN (CD209) and Mannose Receptor (CD206), which bind mannosylated BCR in FL cells and might help tumor progression by contributing to the proliferation and survival[194]. Moreover, the overexpression of CD40L and IL-4 secretion by T_{FH} in FL tumor, increase the secretion of IL-15 by myeloid cells promoting B cells proliferation[195]. Finally TAMs in FL release immunosuppressive molecules such as IL4I1, which contribute to local immune escape[196].

Figure 3. Tumor microenvironment in FL. FL B-cells are supported by a variety of cell such as TAMs, FDCs and T-cells, which support tumor growth and survival through a complex set of cytokines, chemokines, adhesion molecules, angiogenic factors and stimulating molecules.

2.5 Diagnosis and prognosis

For FL diagnosis purposes a specimen/excisional LN biopsy is necessary. Due to the heterogeneity of the tumor sample, core biopsies and fine needle aspirations are not recommended because the FL grading is difficult. The histological report should give the diagnosis according to the World Health Organization (WHO) classification. Grading of FL based on lymph node biopsies is carried out according to the number of blast/high-power field (table 1 summarize the different grade classifications)[197], and the staging is carried out according to the Ann Arbor classification system[198] (table 2), with mention of bulky disease (>7cm) when appropriate[197].

Table 4. Grading of follicular lymphoma

Grade	Description
1	≤5 blasts/high-power field
2	6-5 blasts/high-power field
3A	>15 blasts/high-power field/ centroblasts with intermingled centrocytes
3B	>15 blasts/high-power field/ pure sheet of blasts

Grade 1,2 and 3A should be treated as indolent disease[199], whereas grade 3B is considered an aggressive lymphoma[200].

Table 5. Staging of follicular lymphoma according to the Ann Arbor classification system.

Stage	Area of involvement
I (I$_E$)	One lymph node region or extralymphatic site (I$_E$)
II (II$_E$)	Two or more lymph node regions or at least one lymph node region plus a localized extralymphatic site (II$_E$) on the same side of the diaphragm
III (III$_E$, III$_S$)	Lymph node regions or lymphoid structures (e.g. thymus) on both sides of the diaphragm with optional localized extranodal site (III$_E$) or spleen (III$_S$)
IV	Diffuse or disseminated extralymphatic organ involvement

The diagnostic work-up consists of[197]:

1. Physical examination of peripheral LNs , liver and spleen.

2. Computed tomography (CT) scan of the neck, thorax, abdomen and pelvis.

3. Bone marrow aspirate and biopsy to carry out histology and cytology. Carrying out an immunophenotype by flow cytometry and PCR for BCL2 rearrangement is also recommended.

4. Positron emission tomography (PET)-CT (improves the accuracy of staining for nodal and extranodal sites)

5. Complete blood count, routine blood chemistry which includes lactate dehydrogenase (LDH), β2 microglobulin and uric acid. Likewise, carrying out flow cytometry on peripheral blood and PCR for BCL2 rearrangement is also recommended.

6. Screening test for human immunodeficiency virus (HIV), hepatitis B virus (HBV) and hepatitis C.

For prognosis purposes, due to the heterogeneity in both disease presentation and response to treatment among patients with FL, different models have been developed to assist in the pretreatment assessment of prognosis. The first established Follicular Lymphoma International Prognostic Index (FLIPI)[201], was derived from a database of over 4000 FL patients treated largely in the pre-rituximab era, and the five strongest prognostic factors in multivariate analysis were: number of nodal sites of disease (>4), elevated LDH, age >60, stage III or IV disease, and hemoglobin >12g/dl. Later on, in the rituximab-chemotherapy (R-chemo) era, FLIPI2 was developed incorporating β2 microglobulin, diameter of largest LN, bone marrow involvement and hemoglobin levels[202]. Both indexes are prognostic tools that classified patients into low-, intermediate-, and high-risk groups that correlate with overall survival (OS) or progression-free survival (PFS), respectively[203]. These models have several limitations though, as they are not useful in treatment decisions, response to treatment and they do not incorporate molecular data into the assessment[58,204-207].

Gene-expression profiling of 191 biopsy specimens obtained from patients with untreated FL suggested a more favorable clinical course in cases with infiltrating T cells, in comparison with cases with non-specific macrophages bystander cells, therefore the length of survival among patients correlates with the molecular features of nonmalignant immune cells present in the tumor at diagnosis[159]. But subsequent studies on the clinical significance of non-malignant cell populations have generated conflicting results, which may partly be influenced by poor reproducibility in immunohistochemical marker quantification[208].

For all these problems, recently a new model has been developed, m7-FLIPI score, which incorporates the Easter Cooperative Oncology Group (ECOG) performance status, FLIPI, and the mutational status of seven candidate genes (*EZH2, ARID1A, MEF2B, EP300, FOXO1, CREBBP* and *CARD11*), which are commonly affected in FL, to improve the prognosis in patients with high tumor burden receiving first-line chemoimmunotherapy[58,204-206]. In spite of this, the m7-FLIPI remains primarily a research tool and it has not been established in the clinical routine practice[58,204]. Biological parameters are still being researched for prognostic assessment, for example gene

expression profiling techniques are currently being explored to develop more clinically relevant models. A recent reported 23-gene expression panel is able to predict the risk of progression in FL patients at diagnosis, independently of the FLIPI score and use of anti -CD20 maintenance therapy.[209].

2.6 Current treatments

Despite the fact that FL remains largely an incurable disease with the current available treatment options, it is a treatable disease mostly responsive to several regimens of chemotherapy, immunotherapy, radiation and targeted therapies. Initial treatment decision must be individualized according to the patient characteristics such as age and performance status, disease factors such as stage of the tumor, and goals of care. The varied presentation at diagnosis and frequent lack of significant symptoms result in differences in initial management strategies, from observation to chemoimmunotherapy[210].

2.6.1 First-line treatment

Low tumor burden

Stage I-II. For those patients who present localized disease, radiotherapy (24 Gy) is the preferred treatment with a good curative potential, 10-year OS rates in up to 80% of the cases and with a median OS of nearly 20 years[211,212]. In selected patients, elderly patients or patients with other problems, to avoid the side-effects of radiation, "watch and wait" or rituximab (anti-CD20 monoclonal antibody) therapy is the recommended treatment[58,213,214].

Stage III-IV. In patients with low-risk profile, the current therapeutic approach is based on clinical risk factors, symptoms and patient perspective. Thus "watch and wait" is recommended, and when symptoms appear, antibody monotherapy (rituximab) is recommended [215].

High tumor burden

Stage I-II. In patients with adverse clinical or biological prognosis features, or when radiotherapy is not applicable (lung and liver), systemic therapy (the same that is indicated for advances stages) is recommended[214].

Stage III-IV. For those patients, no curative therapy is yet established. The disease is characterized by spontaneous regression in 10-20% of cases and varies from case to case, therapy should be initiated upon the symptoms appearance[197]. The recommended treatment is the addition of chemotherapy to rituximab, however, there is no consensus among experts in the field regarding the selection of chemotherapy. The most commonly regimens are **R-CHOP** (rituximab, cyclophosphamide, doxorubicin, vincristine and prednisone), **R-CVP** (rituximab, cyclophosphamide, vincristine and prednisone) and **BR** (bendamustine and rituximab). In the past, R-CHOP regimen was the most commonly selected by clinicians, but it has changed in recent years due to the favorable reports from BR treatment, improving PFS and reducing the toxicity compared to R-CHOP treatment[216-219]. Even so, in patients with more aggressive histology it is reasonable to choose first-line R-CHOP treatment[220]. In elderly patients, a brief course of chemoimmunotherapy with a full rituximab course is an alternative with good efficacy and low toxicity[221,222].In patients when conventional chemotherapy is contraindicated, antibody monotherapy (rituximab) or chlorambucil plus rituximab as an alternative[223,224] is recommended. Recently, the development of a type II monoclonal antibody to CD20 (**obinutuzumab**), provides a novel antibody approach in combination with chemotherapy for untreated high tumor burden FL patients. The GALLIUM trial demonstrated that the treatment obinutuzumab plus chemotherapy (**G-chemo**) improves the PFS significantly , although with increased serious adverse effects compared to R-chemo[225].
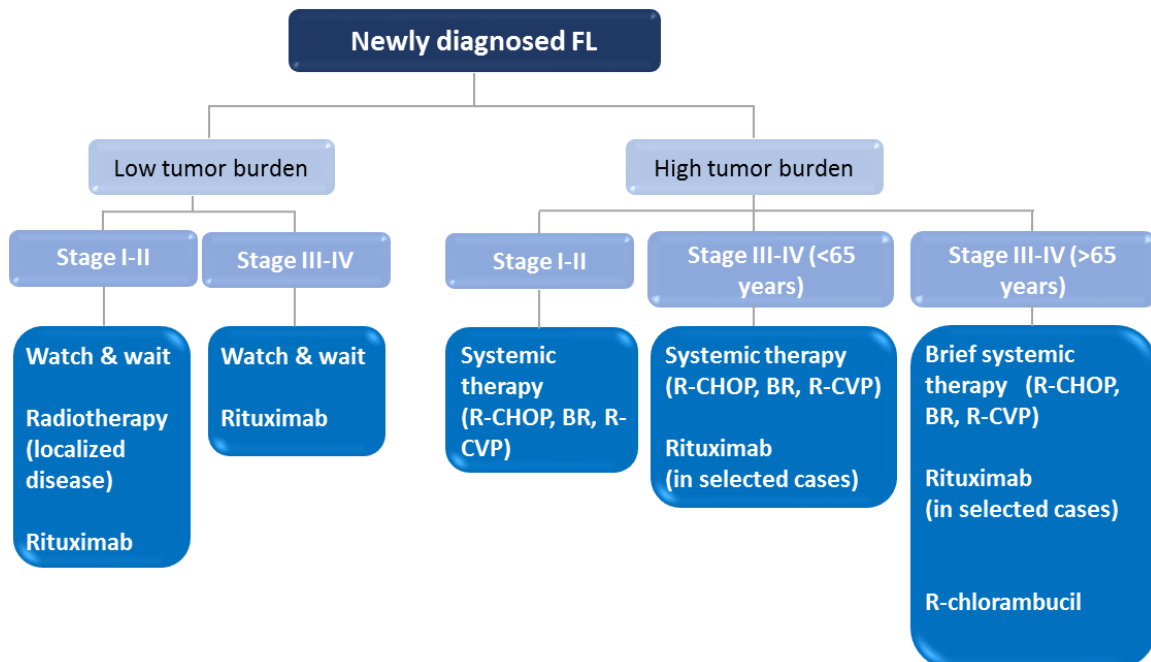
Figure 4. Representative scheme of treatment decision in newly diagnosed FL.

2.6.2 Consolidation/maintenance

The PRIMA trial revealed that rituximab maintenance for 2 years improves PFS (51% versus 35% after 10 years)[226]. In addition, the use of rituximab maintenance in patients treated with frontline BR, improves the PFS with an acceptable safety profile[227]. Radioimmunotherapy consolidation after chemotherapy (this combines rituximab with the radioactive isotype Ytrium90, **Zevalin®**, that is delivered to tumor site) also improves PFS, but effects are inferior in comparison with rituximab maintenance[228].

2.6.3 Second-line treatment

Even though the improved effectiveness of chemoimmunotherapy regimens, approximately 20% of patients with FL relapse within 2 years of first-line therapy[221,226]. This remains the case despite the benefit of additional rituximab in the form of maintenance as previously mentioned. The remarkably consistent frequency of early relapse across studies is suggestive of a group of patients with different disease biology who are uniquely at risk and who may benefit from alternate therapies, at frontline or at the time of relapse. Nowadays, the clinical significance of early relapse in FL is unknown[229].

At relapse obtaining a new biopsy to exclude transformation into an aggressive lymphoma is recommended. In asymptomatic patients with low tumor burden, observation is indicated. In early relapses (<12-24 months), a non-cross-resistant scheme should be preferred (for example bendamustine after CHOP or vice versa). In symptomatic cases with low tumor burden, rituximab monotherapy is suggested. In later relapses, R monotherapy is the recommendation with palliative intent in low tumour burden patient[197]. In younger patients with high tumour burden, early relapse and refractory disease an allogenic stem cell transplantation[230] is indicated. In double (rituximab and alkylating agents)-refractory FL, PI3k inhibitor **idelalisib** is suggested[231], although the use of appropriate prophylaxis to avoid the mortality risks as a consequence of opportunistic infections[197] is needed. Recently, the GADOLIN study suggests the use of obinutuzumab in combination with bendamustine in relapsed rituximab treated cases[232]. More details in figure 5.

Relapsed FL

Biopsy

FL

Transformed

R-chemo ± high dose therapy and AutoSCT

Low tumor burden

High tumor burden

Stage I-II

Stage III-IV

Stage III-IV (<65 years)

Stage III-IV (>65 years)

Relapse/progression

Watch & wait

R-monotherapy

Palliative radiation (in selected cases)

Watch & wait

Chemoimmunotherapy

R-monotherapy (in selected cases)

Dependent on first-line regimen and remission duration:

Chemoimmunotherapy +R maintenance

Radioimmunotherapy (alternatively)

High-dose consolidation with ASCT (in early relapses)

Dependent on first-line regimen and remission duration:

Chemoimmunotherapy (BR, R-CHOP, R-CVP) + R maintenance

Radioimmunotherapy (alternatively)

Later relapse/progression

Watch & wait

R-monotherapy

Palliative radiation (in selected cases)

Watch & wait

R-monotherapy

Chemoimmunotherapy (long prior remission)

Idelalisib (double refractory cases)

Dependent on prior regimens and remission duration:

Chemoimmunotherapy (long prior remission) +R maintenance (if not previously applied)

High-dose consolidation with ASCT (in early relapsed)

Radioimmunotherapy or R monotherapy

Idelalisib (double refractory cases)

Allogenic transplantation (in selected casese)

Dependent on prior regimens and remission duration:

Chemoimmunotherapy (long prior remission) + R maintenance (if not previously applied)

Radioimmunotherapy or R monotherapy

Idelalisib (double refractory cases)

Figure 5. Representative scheme of treatment decision in relapsed FL.

2.7 New treatments for relapsed/refractory Follicular Lymphoma

FL is characterized by successive lines of therapy resulting in progressively shorter periods of disease-free survival followed eventually by the development of either chemo-refractoriness, large cell transformation, or death from treatment related toxicities[233]. For this reason, it is necessary to develop new treatments with new mechanisms of action to offer therapeutic options for patients with relapse and R-chemo refractory FL to improve disease control and to maintain high quality of life with minimal therapy related toxicity.

One of the most important pathways in FL is the B cell receptor (BCR) signaling pathway that represents a crucial component in the survival of normal B cells throughout their development. And in many non-Hodgkin lymphomas (NHLs) such as FL, deregulated BCR signaling has been identified as a potent contributor to lymphomagenesis and tumor survival. PI3K is a common denominator transducing the signaling from FL crosstalk with the tumor microenvironment making it an attractive target.

Equally important, considering the genetic FL hallmark t(14;18), the Bcl-2 family proteins play a crucial role in the regulation of apoptosis in cancer cells.

2.7.1 PI3K Pathway

The phosphatidylinositol-3-kinase (PI3K) pathway plays an important role in multiple cellular functions, including proliferation, differentiation, and trafficking[234], and also contributes to cancer-promoting aspects of the tumor environment, such as angiogenesis and inflammatory cell recruitment[235,236].

PI3K class I are heterodimeric enzymes that have both regulatory (p85) and catalytic (p110) subunits. The p110 subunit exists in four different isoforms: α, β, γ and δ, with different functions and sites of expression. The isoforms α and β are ubiquitous, while the isoforms γ and δ are restricted mainly to lymphocytes[237].

The activation of PI3K pathway is mediated by the activation of the Receptor Tyrosine Kinase (RTK) or the BCR, among others, such as the stimulation of CD40L, which recruit PI3K to the cell membrane. PI3K mediates the conversion of PIP_2 to **PIP_3**., while, the dephosphorylation of PIP3 to generate PIP2 is accomplished by the 3-phosphatase **PTEN** (which has tumor-suppressor function).

PIP3 recruits AKT through its PH domain to the inner surface of cell membrane. AKT is activated by a dual regulatory mechanism: translocation to the plasma membrane and phosphorylation at Thr308 (by PDK1) and Ser473 (by PDK2). The main biological consequences of AKT activation in cancer cell growth are survival, proliferation (increased cell number) and growth (increased cell sizes). In the matter of survival, cancers cells have several mechanisms to inhibit apoptosis and prolong their survival, and AKT is able to block the apoptosis blocking **IGF1**, phosphorylating **BAD** (preventing its interaction with BCL-X$_L$), **caspase-9** and **FKHR** (a member of Forkhead family of transcription factors). Also it is able to influence positively in **NF-κB** (promoting its nuclear translocation and activation of targets genes) and negatively in **p53** (pro-apoptotic tumor suppressor) via the phosphorylation of **MDM2**, which is a negative regulator of p53, that is translocated efficiently to the nucleus and it can bind p53. Regarding cell proliferation, AKT has an important role in preventing cyclin D1 degradation by the phosphorylation of **GSK3β**. Once phosphorylated, GSK3β is not able to phosphorylate cyclin D1 therefore avoiding its degradation. Moreover, AKT can regulate indirectly in a negative manner **p27** and **p21**. In cell growth, AKT target directly **mTOR**, which is important regulator of cell growth[238].
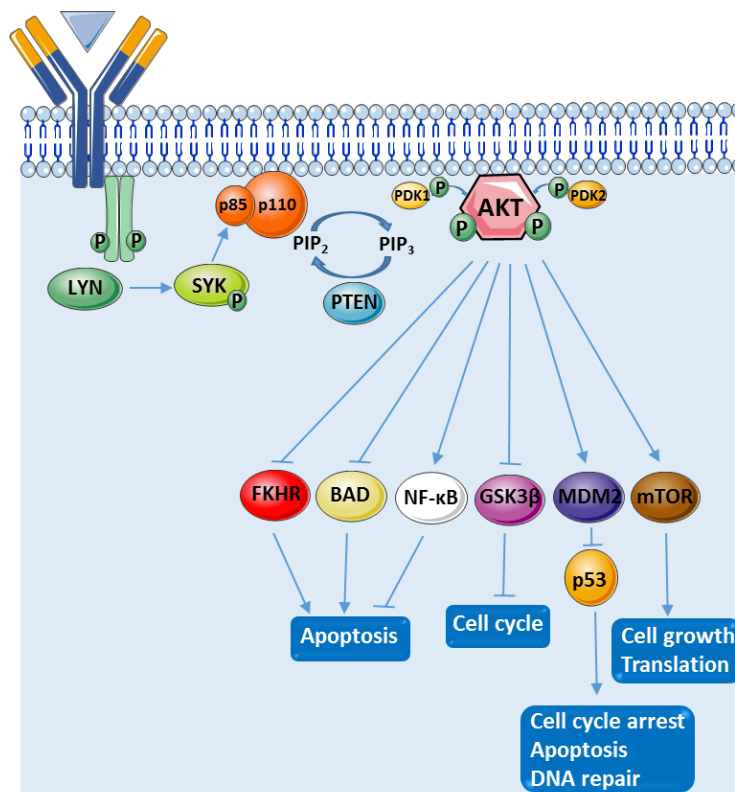
Figure 6. PI3K pathway. Representative sheme of PI3K patwhay activation downstream of BCR receptor.

Currently there are two Food and Drug Administration (FDA)-approved PI3K inhibitors for R/R FL patients with two or more prior therapies: idelalisib and copanlisib.

2.7.1.1 Idelalisib

Idelalisib (GS-1101; Zydelig; Gilead Sciences) is δ isoform specific inhibitor, orally available, which was the first in class isoform-specific inhibitors to receive regulatory approval for relapsed CLL, SLL and FL in 2014. Idelalisib blocks PI3K δ I(C_{50}=2.5nM) while the IC50s for other PI3K isoforms are 40 to 300-fold higher. On a screening assay at 10nM for 401 kinases, idelalisib did not present significant off-target activity[239]. In addition to its recommended use to R/R FL, other indications for Idelalisib include relapsed chronic lymphocytic leukemia (CLL) in combination with rituximab in comorbid patients, and small lymphocytic lymphoma (SLL)[240].

PI3Kδ plays an essential, non-redundant role in B-cell receptor signaling critical to the pathogenesis of indolent NHL. Selective inhibition of PI3Kδ on lymphoma cells, reduces AKT phosphorylation. This leads to induce caspase-dependent death at high doses (10uM) in malignant cells, suppresses protumoral cytokines production by NK and T cells (such as IL10 and CD40L), and revokes microenvironmental signals that promote tumor cell survival such as B-cell activating factor (BAFF), tumor necrosis factor (TNF), and fibronectin, blocking the adhesion of tumor cells to supporting stromal cells[241]. It also blocked survival signals derived from BCR and nurse-like cells, and it reduced the secretion of CXCL13, CCL3 and CCL4 chemokines[242]. On the other hand, to a lesser extent than ibrutinib, idelalisib, it has been shown to partially abrogate antibody-mediated cytotoxicity induced by anti-CD20 monoclonal antibodies (Rituximab). It is important to note that FL patients that present severe immune toxicity have decreased number and function Treg cells in peripheral blood. This lead to a deregulation in T-effectors cells activity, therefore it increases antitumoral immunity and loss of self-tolerance with autoimmune toxicity[243].

In the phase II trial (DELTA trial,NCT01282424) 125 patients were treated with 150 mg of idelalisib twice daily until disease progression or unacceptable toxicity . A total of 72 patients (58%) had FL, 28 (22%) had SLL, 15 (12%) had Marginal Zone Lymphoma (MZL), and 10 (8%) had Lymphoplasmacytic Lymphoma (LPL). The median age was 64 years. And the median of prior treatments in these patients was 4. After a median of 6.6 months of Idelalisib as a single-agent treatment, 90% of the patients showed tumor reduction, and they presented an ORR of 54% with a

median PFS of 11 months[244]. In a subset of 37 patients with FL and early disease progression (defined as EFS >= 24 months after frontline chemotherapy), idelalisib retained significant activity with an ORR of 57% and an PFS of 11.1 months[245].

A post hoc analysis by Gopal et al. idelalisib showed antitumor activity in high-risk FL patients who relapsed within 24 months following initial chemoimmunotherapy[246].

Due the importance of the PI3K pathway in the pathogenesis of Mantle cell lymphoma (MCL)[247], it was logical to explore the activity of Idelalisib in MCL. On a phase Ib study (NCT00710528), with 40 patients with relapsed/refractory MCL which included many heavily pre-treated (with a median of 4 prior therapies), but excluded patients treated previously with ibrutinib. The dose range was the same used in indolent NHL. The ORR was 40% and the PFS was 3.7 months, with a trend toward longer PFS among less heavily pre-treated patients. 22% of the patients experienced clinical benefit exceeding 12 months. The limited duration of response in patients with MCL suggest the rapid development of resistance to p110δ inhibition[248].

The most common adverse events (AEs) reported in these studies were fatigue, diarrhea, nausea, rash chills, pyrexia and pneumonitis, reversible in most of the cases. Monitoring liver function during the treatment[244,248] is also recommended. Moreover, Idelalisib decrease the function of neutrophils and adaptive immune cells, as well as the function of Tregs[249]. In addition, toxicities seem to be more severe in non-previous treated patients, in first-line treatment, causing immune-mediated hepatotoxicity in CLL patients, leading to the closure of clinical trial[250].

In a phase III trial of idelalisib (NCT01539512) in combination with rituximab in 220 relapsed CLL patients an ORR of 81% was reported and PFS was not reached, but 40% of the patients presented serious adverse events[251]. The triplet of lenalidomide, idelalisib and rituximab treatment in relapsed/refractory indolent lymphoma studies (A051201 and A051202) caused serious toxicity (unacceptable rates of hepatotoxicity), including two deaths, resulting in the closure of these studies[252].

2.7.1.2 Copanlisib

Copanlisib (BAY 80-6946; Bayer AG) is an intravenous pan-class I PI3K inhibitor, which shows potent activity against the isoforms α and δ. The PI3Kα isoform is expressed to a lesser extent than PI3Kδ

in various forms of lymphoma. Moreover, PI3Kα is fundamental for processes such as angiogenesis[253].

In September 2017, the FDA granted copanlisib accelerated approval for its use in relapsed FL after two previous lines of therapy[240] Approval was based on a phase II study (NCT01660451) of 104 heavily pretreated patients (median of 3 prior treatments) with FL and with a median age of 63 years, in which the ORR was 58.7%, with a 14.4% complete response (CR) rate, and with a median duration of response 22.6 months[254].

The most common toxicities were transient hyperglycemia, transient hypertension, diarrhea, neutropenia, fatigue and fever, and the less frequent adverse events were pneumonitis, elevation of liver enzymes, opportunistic infections and colitis[254].

Although copanlisib is currently approved in third-line treatment and as monotherapy, new clinical trials are in progress to examine its use at earlier stages and in combination with other agents, such as rituximab (phase III NCT02367040 study in 450 iNHL patients), and R-CHOP or RB (phase III NCT02626455 study in 546 iNHL patients).

Phase III testing is currently ongoing for several experimental PI3K inhibitors, including **duvelisib**, wich in September 2018 has granted FDA approval for R/R CLL and SLL after at least two prior therapies, –(NCT02049515 and NCT02004522). In addition, it received accelerated approval for R/R FL after two prior systemic therapies (NCT02204982). **Umbralisib** (TGR-1202; NCT02612311, NCT02793583). RP6530, **buparlisib** (BKM120)[255], and INCB050465 are undergoing earlier-phase testing[256].
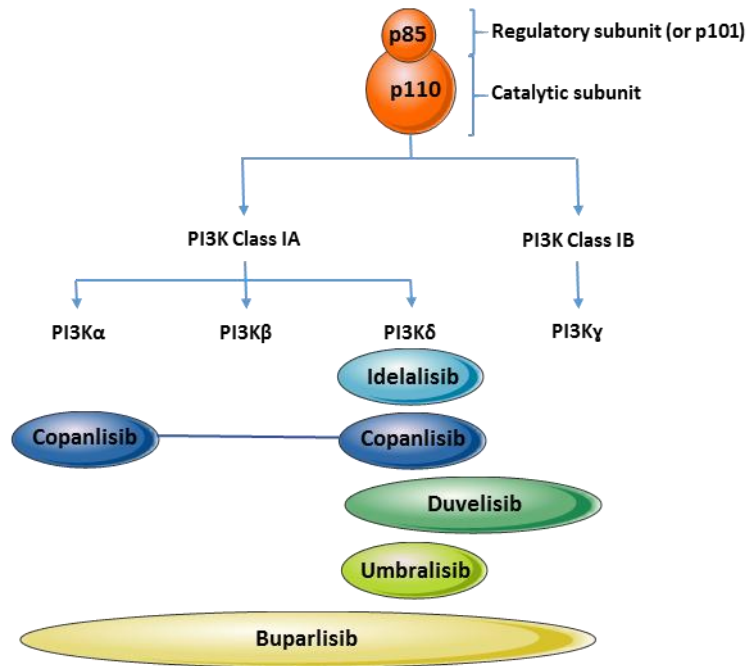
Figure 7. Different PI3K inhibitors. Representative scheme of the different PI3K subunits and classes, and the specificity of the different types of PI3K inhibitors to these classes.

2.7.2 BCL2 family proteins

BCL-2 deregulation is paramount in the pathogenesis of FL and it is therefore an attractive target for novel therapeutic approaches. Indeed, the BCL-2 protein, encoded on chromosome 18, was the first anti-apoptotic protein described and was discovered to be a chromosomal fusion product with the immunoglobulin heavy chain machinery, t(14;18) in FL in 1985[69]. Since then, more than 20 proteins belonging to BCL-2 family have been described. The relevance of BCL-2 proteins in cell death and survival includes externally (extrinsic pathway) and internally (intrinsic pathway) initiated pathways of cell death. The extrinsic pathway of apoptosis is the result of binding ligands to the cell-surface death receptors (Fas, TNF or TRAIL receptors); these death ligands are predominantly produced by cells of the immune system such as T cells, NK cells, macrophages and dendritic cells[257]. The intrinsic pathway is initiated by different stimuli, such as DNA damage, growth-factor or cytokine deprivation, viruses and oxidative stress. Both pathways conclude in the activation of caspase-mediated cell death, where the cell is progressively disassembled and then consumed by phagocytic cells, but in intrinsic pathway BCL-2 family proteins are the main mediators of this

process. This family of proteins is divided into 2 groups, depending on their structure and function (all of them containing at least one BH domain):

- **Anti-apoptotic**: These proteins contain four conserved BCL-2 homology (BH) domains, BH1-BH4 and include BCL-2, BCL-X$_L$, BCL-W, BFL-1 (A1), myeloid cell leukemia 1 (MCL-1) and BCL-B proteins, and are antagonistic to pro-apoptotic BCl-2 family proteins.
- **Pro-apoptotic:**
    - BH3-only members: BID, BIM, BIK, BAD, BMF, HRK, NOXA, and PUMA, proteins are in this category. They just have the BH3 domain, thus they are denominated BH3-only proteins. In response to an apoptotic signal, multidomain proteins are released from the anti-apoptotic proteins by being displaced by sensitizer BH3-only proteins that bind to anti-apoptotic proteins with higher affinity, thus promoting the activation of Bax and Bak, and finally the apoptosis[258].
    - Multidomain members: BCL-2 associated X protein (BAX), it is located in cell cytoplasm, BCL-2 related ovarian killer (BOK), it is located in Golgi apparatus and in endoplasmatic reticulum[259], and BCL-2 antagonist killer (BAK), which is embedded in the mitochondrial outer membrane. They contain the BH1-BH3 domains. Based on the sequence similarity of BOK with BAX and BAK, it has been assumed that they might function similarly[259]. BAX and BAK activated are cell death mediators, as they disrupt the integrity of the outer mitochondrial membrane (MOMP) causing the release of apoptogenic factors such as cytochrome c, second mitochondrial activator of caspases/direct IAP-binding protein with low pI (Smac/DIABLO), Omi/HtrA2[260], apoptosis-inducing factor (AIF) and endonuclease G[261] from the mitochondria into the cytoplasm[262]. BAX/BAK activity is inhibited by its binding to anti-apoptotic BCL-2 family proteins, and they may be directly activated or sensitized by their interaction with other family members.
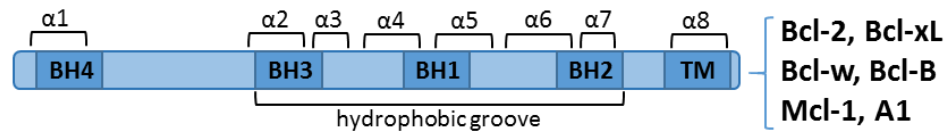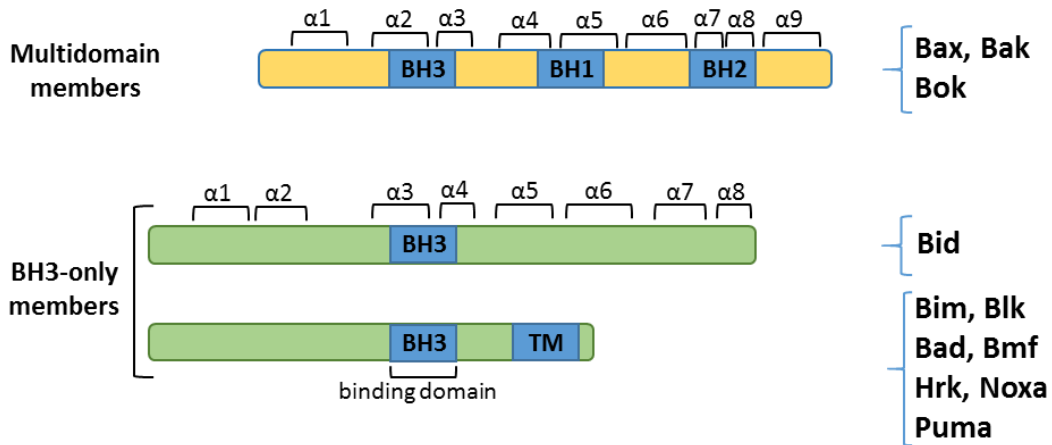
Figure 8. BCl2 family protein. Classification according them functions.

Intrinsic pathway
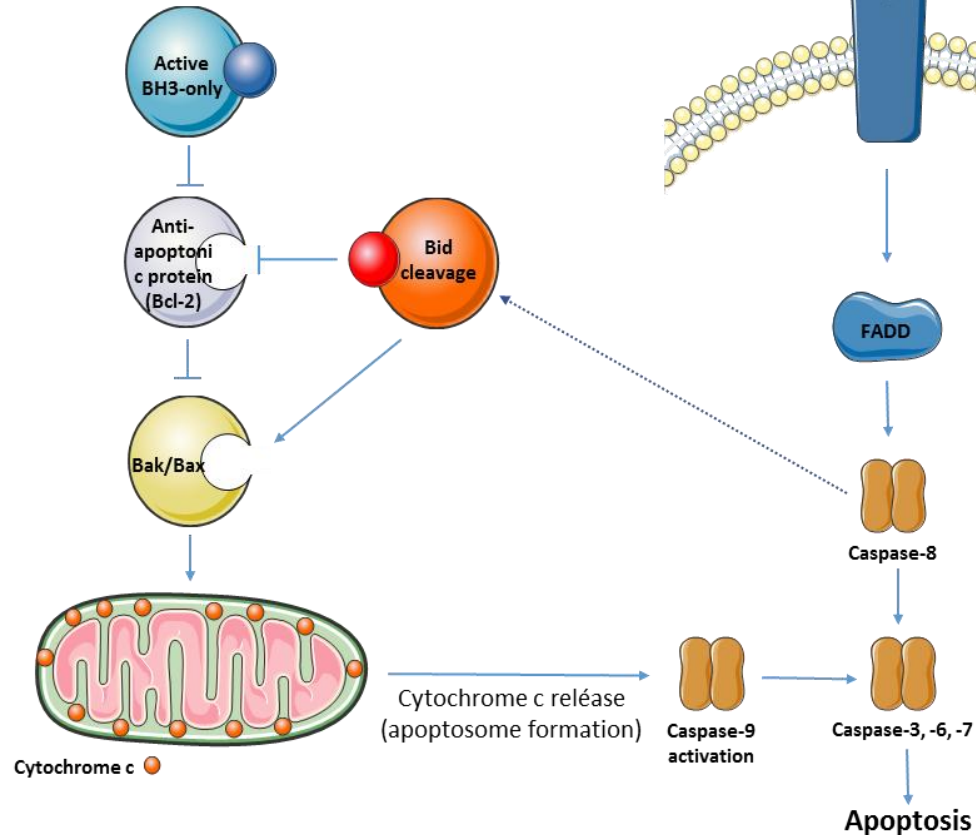
Extrinsic pathway

Figure 9. Intrinsic and extrinsic pathways of apoptosis.

Altering the balance among these opposing fractions, mainly by anti-apoptotic protein increase, and rarely by mutations in BAX and BAK genes[263], provides one means by which cancer cells undermine normal apoptosis and gain a survival advantage[24,264,265].

The role of BCL-2-related chemotherapy resistance has been described in MM, myelodysplastic syndrome (MDS), acute myeloid leukemia (AML), acute lymphoid leukemia (ALL), DLBCL, MCL, FL and in CLL, this latter showing high sensitivity to BCL-2 antagonists[266].

The development of BH3-mimetics, which binds anti-apoptotic proteins and promote apoptosis, has been explored as an anti-cancer therapy. Two different strategies were explored. In an initial attempt to inhibit the expression of BCL-2 such as Oblimersen (an anti-sense RNA) were developed

to target the start codon of BCL-2 mRNA, thus reducing the expression of BCL-2[267]. More recently, small molecules compounds that inhibit the function of BCL-2 were developed. ABT-737 was the first anti-BCL-2 agent developed by Abbot, and it was found to inhibit BCL-2, BCL-X$_L$ and BCL-W[268]. ABT-737 is not an orally bioavailable compound, and also presented unfavorable pharmacologic properties, Consequently, Abbot developed ABT-263 (navitoclax), an oral bioavailable compound, which demonstrated significant activity in early phase clinical trials, but also presented a significant dose-limiting toxicity (specifically it caused thrombocytopenia in patients), due to the off-target binding to BCL-X$_L$, highly expressed in platelet precursors[269,270].

2.7.2.1 Venetoclax

Venetoclax (ABT-199, AbbVie) is a small molecule, orally administrated, and the third compound in Abbott's series of BCL-2 inhibitors. It presents more than 100-fold higher affinity to BCL-2 compared to other BCL-2 family members, such as BCL-X$_L$, thus reducing thrombocytopenia, in addition to other side effects[271]. Furthermore, Venetoclax is the first BCL-2 inhibitor approved by the FDA for the treatment of CLL[266].

Two clinical trials in R/R patients with CLL in monotherapy with venetoclax (NCT01328626[272] and NCT01889186[273]) were evaluated with similar results. In the first study, after the dose escalation phase, an expansion cohort of 60 CLL patients were evaluated showing an ORR of 79% and PFS of 15 months. In the second study in phase II, 107 patients with RR disease and del(17p) were evaluated showing a result similar to the previous study, an ORR 85% and the median PFS was not reached at the 12-month median follow-up time. Additional studies of venetoclax in combination with other agents in CLL are in progress[266]. Phase Ib venetoclax + rituximab in 49 R/R CLL (NCT01682616[274]) study, showed an ORR of 86% and 51% of complete response. The efficacy and the durability of responses observed with the combination offers an attractive potential treatment option.

In FL, even though 85% of patients harbor the t(14;18), which accounts for the overexpression of BLC2, the results of the first clinical trial with venetoclax were not satisfactory. This reduced activity of Venetoclax in FL may be the result of a complex interplay among other anti-apoptotic proteins regulated by microenvironment, such as and BLF-1 and MCL-1, and BH3-family members[266]. In a phase I trial (NCT01328626) of Venetoclax in R/R B-NHL (M12-175[275]), which included a total of 106

patients, 28 with MCL, 29 with FL, and 34 DLBCL, ORR was 44% and the estimated median PFS was 6 months. However in FL patients ORR was 38%, and, PFS 11 months. The recommended single-agent dose for FL and DLBCL was 1200 mg.

In order to increase response rates and durability, additional investigations using venetoclax in combination with chemo-immunotherapy in indolent lymphomas, including FL, are in progress. A completed phase II study (NCT02187861[276]), combining venetoclax (VEN)+ rituximab(R) + bendamustine(B) in 164 R/R FL patients, showed an ORR of 33% in VEN+R group, ORR of 64% BR group, and ORR of 68% in VEN+BR group. Currently, there are several studies in progress, a phase Ib of venetoclax+ bendamustine+ rituximab in 60 R/R NHL (NCT01594229[277]), phase I/II Ibrutinib + Venetoclax in 41 R/R FL patients (NCT02956382), phase I Obinutuzumab+ Venetoclax in 25 previously untreated FL Patients (NCT02877550), phase II Venetoclax +Obinutuzumab +Bendamustine in 56 patients with high tumor burden FL as front line therapy (NCT03113422), among others (information from ClinicalTrials.gov).

Table 6. Summary of Venetoclax Clinical trials.

Drugs combinations	Name of study	Patients
Venetoclax + Bendamustine + Rituximab[277]	Phase Ib (NCT01594229)	R/R NHL
Ibrutinib + Venetoclax	Phase I/II (NCT02956382)	R/R FL
Obinutuzumab+ Venetoclax	Phase I (NCT02877550)	Untreated FL
Venetoclax +Obinutuzumab +Bendamustine	Phase II (NCT03113422)	High tumor burden FL

2.7.3 Other Novel agents

As we mentioned above, it is known that the pathogenesis of FL, as in others NHLs, is dependent on the crosstalk with the tumor microenvironment, the activation of B-cell receptor (BCR) and the interaction with the immune system[278]. For this reason, the development of new therapeutic agents that target these pathways such as immune modulators, immune checkpoint inhibitors, and BCR signaling pathways inhibitors, with favorable toxicity profiles[220] is being worked on. Table 7 summarizes the current trials in R/R FL with these novel agents.

Table 7. Summary of the current clinical trials in R/R FL with novel agents.

	Name of study	Activity	ORR/PFS
Lenalidomide[279]	Phase II (NCT00179673)	Immune modulator (interact with the E3 ubiquitin ligase cereblon (CRBN))	23% 4.4 months
Ibrutinib[280]	Phase II (NCT01849263)	Immune modulator (Bruton tyrosine kinase (BTK) inhibitor)	37% 14 months
Vorinostat[281,282]	Phase II (NCT00253630; NCT00875056)	Histone deacetylase (HDAC)	47-49% 15-20 months
Abexinostat[283,284]	Phase II (NCT00724984)	Pan-HDAC	56-64% 10-20.5 months
Tazemetostat[285,286]	Phase II (NCT01897571)	Enhancer of zeste homolog 2 (EZH2) inhibitor	EZH2 mutants: 63-92% EZH2 wt: 26-28%
Nivolumab[287]	Phase Ib (NCT01592370)	Programmed cell death (PD-1) mAb	40% not reached
CAR-T therapy (CTL019) [288-290]	Phase IIa (NCT02030834)	Anti CD19 chimeric antigen receptor	CR 70%, not reached
CC-122 + Obinutuzumab [291,292]	Phase Ib (NCT02417285)	Cereblon-modulating agent+ anti-CD20 mAb	75% 11 months

CR: complete response.

Other clinical trials combining some of these new agents with the current treatments are being carried out with promising results. One good example is the Rituximab and Lenalidomide combination in untreated FL patients (RELEVANCE study)[293], where the efficacy results were similar with rituximab plus lenalinomide and rituximab plus chemotherapy (with both regimens followed by rituximab maintenance therapy), showing a 3 years PFS of 77% in the first group and 78% in the second, and a 3 years OS of 94% in both groups. But rituximab plus lenalinomide showed a safer profile[294].

3. Colorectal cancer

Colorectal cancer (CRC) is the third most common cancer in males (10%) and the second in females (9.2%), with between one and two million new cases being diagnosed every year, and the fourth most common cause of cancer-related death worldwide, with 700.000 deaths per year[56,295]. The incidence of CRC has risen by more than 200.000 new cases per year from 1990 to 2012 due to diets and lifestyles in western countries, among others factors. However, the mortality has been progressively declining since 1990[296]. In contrast to these declines, the incidence of CRC in people under the age of 50 has been increasing at a rate of 1.7% per year from 2000 thought 2013[56].

Most CRCs are sporadic and are diagnosed at a median age of 65-75 years; nevertheless some 20-30% of the cases might have a familiar predisposition despite the absence of known germ-line defect[297]. Well-established hereditary syndromes that have a Mendelian pattern are familial adenomatous polyposis (FAP) (<1%)[298], Lynch syndrome (2-3%)[299], and CRC associated to *MUTYH* (<1%)[300]. On the other hand, serrated polyposis syndrome (SPS), a syndrome characterized by multiple serrated polyps (SPs) throughout the colon and accompanied by an increased risk of developing CRC (1.9% in 5 years)[301], represents a rate ranged from 0% to 0.5%, which increased to 0.4% to 0.8% after follow-up colonoscopy[302].

Currently, about 60-70% symptomatic patients are diagnosed with advanced stage of disease. Fortunately, the screening for the disease has become more available, using colonoscopy as a routine method, and less invasive technologies are being development to replace colonoscopy. As a result, earlier stage detection would allow for better outcomes in term of reducing the disease burden[303].

Although in patients with non-advanced CRC (stage I and III) 5- year survival rate is above 63%, patients with advanced and distant metastatic disease (stage IV), this survival rate drops to 10%, which accounts for approximately 18% of cases. Approximately, 20 % of patients in the United States have distant metastatic disease at the time of presentation[56]. CRC can spread by lymphatic and hematogenous dissemination, as well as by contiguous and transperitoneal routes. The most common metastatic sites are the regional lymph nodes, liver, lungs, and peritoneum. Albeit, the main organ that harbors 60% of the metastasis is the liver[304].

3.1 CRC Pathogenesis

CRC is a heterogeneous disease according to clinical manifestations, molecular characteristics, response to treatments and prognosis.

The main feature of CRC formation is the accumulation of acquired genetic and epigenetic changes that transform normal glandular epithelial cells into invasive adenocarcinoma. In 1988, Volgestin and Fearon proposed the adenoma-carcinoma sequence model to explain the pathogenesis of CRC, as a normal epithelial cell that undergoes a series of changes until it becomes a carcinoma[305]. The process begins with a first step that initiates the formation of benign neoplasm (adenomas or serrated polyps), followed by a step that promotes the progression to more histologically advanced neoplasm, and the final step that transforms the tumor to invasive carcinoma. Since this model was proposed, the knowledge about molecular pathogenesis of CRC has increased, and led to numerous revisions of the original Volgestin and Fearon model[306]. The alteration of different molecular pathways leads to the progression and transformation of adenoma to carcinoma.

Aberrant crypt foci

The search for the earliest morphological precursors to CRC led to the description of **aberrant crypt foci (ACF)**[307]. They were observed for the first time in carcinogen-treated rodents by Bird and colleagues, resulting in the identification of lesions in the colons of animals treated with carcinogens suggestive of preneoplastic lesions[308]. Subsequently, these lesions were also observed in human patients, showing that an increased frequency of these very early lesions predisposes the patient to colon cancer[309,310]. Aberrant crypts foci are characterized macroscopically by enlarged diameter, thickened hypercellular epithelium, altered mucin pattern, and typically occur in clusters. Their luminal openings can have a round, slit like, or serrated appearance. The role for ACF in colorectal carcinogenesis is supported by the presence of histopathological intraepithelial neoplasia (dysplasia) in some ACF, and is further corroborated by the presence in some ACF of genetic alterations that are present in colorectal carcinomas, such as mutations in the adenomatous polyposis coli (*APC*) tumor suppressor gene and *KRAS* proto-oncogene, microsatellite instability (MSI)[307,311,312], and cytosine-guanine base pair (CpG island) hypermethylation[313,314]. Despite this, some reports don't identify ACF as a CRC precursor[315-317].

3.1.1 Adenomatous polyposis coli (APC)-type Tubular Adenomas (Conventional)

Approximately 70% of CRC arise via APC-type tubular adenomas[318]. The biallelic APC mutation is the genetic event that produces the distinctive nuclear and cytoplasmatic alteration termed *adenomatous*. A truncated APC protein results in altered apoptosis and cell-cycle control through dysfunction of the Wnt/β-catenin/Axin pathway, which drives the neoplastic cell proliferation[319,320]. The APC protein also controls microtubule function in the nucleus and the cytoplasm. In the nucleus, microtubules attach to the kinetochore during mitosis. Truncated APC protein produces abnormal microtubule attachment, resulting in a defective spindle checkpoint system that allows the cell to prematurely exit out of mitosis into anaphase[321-323]. This premature exit, before each chromosome pair can segregate to their daughter cells, produces dicentric chromosomes that are potent initiators of chromosome instability (CIN)[323] . In the cytoplasm, truncated APC alters microtubule formation, bundling and transport.

3.1.2 Serrated Neoplasia Pathway Polyps

Serrated polyps are an alternative pathway to malignancy (which represents 30% of CRC cases), where a subset of hyperplastic polyps, most likely microvesicular hyperplastic polyps, progress to serrated neoplasms, and a fraction of them progress to CRC[324]. In this type of neoplasia there is no direct association between specific genetic mutations and unique cytogenetic feature. Several key genetic mutations seem to initiate, facilitate, and/or actively enhance progressive changes in cell-signaling pathways, causing a spectrum of specific cytologic features in the cells that form serrated neoplasia pathways polyps[325]. The early genetic changes found in right colon serrated neoplasia pathway polyps are the *BRAF* (or *KRAS* in some cases) activating mutation and CpG island hypermethylation[326-329]. CpG island hypermethylation is also an early event in a subset of aberrant crypt foci lesions[313,314], as we mentioned above, and in a spectrum of serrated polyps, including hyperplastic polyps (HP), sessile serrated adenomas/polyps (SSA/Ps), and traditional serrated adenomas (TSA). The gene *SLC5A8,* which is especially sensitive to hypermethylation, has been characterized as potential early genetic alteration, along with *BRAF*, necessary for the development of right colon serrated neoplasia pathway polyps[314].

3.2 Genomic pathogenesis in CRC.

The hallmark features of colorectal carcinogenesis are the presence of genomic instability and epigenetic changes, which result in the main difference between normal colon epithelium and neoplasia[4]. According to the genetic model for colorectal tumorigenesis proposed by Fearon and Volgestin in 1990[330], three different molecular carcinogenesis pathways with distinct clinic-pathologic features, and with important implications for prevention, screening, and therapy have been described:

-**Chromosomal Instability (CIN).** The most common form of genomic instability, which is found in 70% of colorectal tumors, is the so called sporadic tumor[331,332]. Aneuploidy, defined as the presence of numerical chromosomes changes or multiple structural aberrations of the chromosomes, is the result of an abnormally high rate of CIN that persists throughout the progression of the tumor[333]. Moreover, there is some evidence that CIN promotes cancer progression by increasing clonal diversity[334,335]. The deregulation of mitotic spindle checkpoint regulators, such as BUB1, entails gains and losses of whole arms or whole chromosomes, while the deregulation of the double strand DNA break repair mechanism, results in smaller gains and losses through structural chromosome aberrations[336,337]. It is also known that oncogene-driven stress, telomere erosion and DNA hypomethylation play a role in CIN in CRC[338,339].

-**Microsatellite Instability (MSI).** This accounts for approximately 15% of colorectal tumors[340]. MSI in CRC has been defined as the presence of at least 30% unstable microsatellite loci in a panel of 5-10 loci selected at a National Cancer Institute consensus conference [341]. Tumors with 10-29% unstable loci have been classified as MSI-low, and tumors with <10% unstable loci have been classified as microsatellite stable (MSS). The presence of MSI in conventional polys is unfrequent; however, it is almost always present in serrated polyps, and in tubular adenomas from Lynch syndrome patients [342,343]. The mechanism leading to MSI involves inactivation of genes in the DNA Mismatch Repair (MMR) family, which include *MLH1, MSH2, MSH6* and *PMS2*, aberrant DNA methylation, or by somatic mutations[335]. Mutations in *POLE* and *POLD1* are associated with hypermutated CRCs as well[344].

-**CpG Island Methylator Phenotype (CIMP).** The hypermethylation of loci that contain CpG islands and the global DNA hypomethylation are the result of epigenetic changes in CRC. DNA methylation is a post-replicative DNA modification that consists of the covalent attachment of a methyl-group to the 5' position of cytosine residues in cytosine and guanosine (CG) dinucleotides, called CpG

islands, regions of the genome[345]. The addition of methyl groups in these regions can inhibit binding of transcription factors, and permits recruitment of methyl-CpG-binding domain proteins to promote regions, which can repress transcription initiation[346]. Hypermethylation is present in essentially all CRCs; however, there is a subset of 10-20% CRCs that have a higher proportion of aberrantly methylated CpG loci, which includes the majority of sporadic CRC with MSI associated with hMLH1 methylation[347]. CIMP is defined as increased methylation of at least three loci from a selected panel of five CpG islands-associated genes[348] .The mechanism responsible for aberrant DNA methylation in colon tumor is still unclear. Recently, some suggestions have indicated that overexpression of the DNA methyltransferases *DNMT3B* or *DNMT1*[332], mutations in genes involved in chromatin remodeling, such as *CHD7* and *CHD8*[349], and changes in the chromatin structure and histone modification state of histone H3[350,351], correlate with CIMP. Consequently, CIMP induces the expression of oncogenes, impedes the expression of tumor suppressor genes, and thus collaborate in the tumorigenesis process.

3.2.1 Key genes mutated in CRC

Adenomatous Polyposis Coli (*APC*). *APC* inactivation is one of the first event in adenoma development. The gene is located at the chromosome band 5q22.2 [352] and encodes APC protein, which is a negative regulator of the β-catenin, the effector of the Wnt signaling pathway[353]. The Wnt signaling pathway controls the colon epithelial homeostasis[354], and increases the levels of intracellular β-catenin levels which stimulates cell proliferation by transcriptional activation of *C-MYC, CCND1*, growth factors, among others[355]. *APC* mutations occur in the mutational cluster region in codons 1286-1513 (most common point mutations or small Indels leading to stop codons and therefore a truncated protein), and arises early in colon cancer tumorigenesis[355].

Kirsten Rat Sarcoma virus mammalian homolog (*KRAS*). The mutations in *KRAS* are early events in the adenoma-carcinoma sequence, though they are only approximately in one-third of CRCs[356]. *KRAS* is an oncogene from the *RAS* gene family and is located on chromosome 12q12.1. *RAS* proto-oncogenes regulate key cellular signaling pathways including phosphoinositide-3 kinase (PI3K) and mitogen-activated protein kinases (MAPK) pathways[357]. *KRAS* mutations are found in exon 2 from codons 12 and 13, and in exon 3 from codon 61. These mutations compromise the ability of GTPase activing proteins[358]. *KRAS* is a good biomarker and also good negative predictor to EGFR inhibition response, 99% of patients that show *KRAS* mutation do not respond to EGFR inhibition[359,360].

V-Raf murine sarcoma viral oncogene homolog B (*BRAF*). A single, activating, point mutation in *BRAF* (V600E) results in constitutive signaling of the mitogen-activated protein kinase (MAPK) pathway through KRAS signaling, resulting in cell proliferation, survival, and inhibition of apoptosis. Mutations in *BRAF* correlates with CIMP, establishing CIMP as a biologically relevant phenotype with a key role in the serrated pathway[326]. Additionally, *BRAF* is mutated very early in the serrated pathway, in 70-76% of cases[342,361], and it has even been observed in aberrant crypt foci (in serrated hyperplastic aberrant crypt foci), which, as described above, are probably the earliest histologically evident lesions in the serrated pathway[313,362]. In CRC 10%-17% of patients show activating *BRAF* mutations[363].

Tumor protein p53 (*TP53*). *TP53* is the gene that encodes for p53 transcription factor, which is a central coordinator of cellular response to stress[364]. P53 controls the transcription of several genes involved in, cell cycle regulation, DNA metabolism, apoptosis, senescence, cell differentiation, angiogenesis, immune response, motility and migration[357,365]. *TP53* gene is located on chromosome 17p13.1. Missense mutations represent about the 80% of *TP53* mutations in codons 175, 245, 248, 273, and 282[366]. The loss of function of p53 due the mutations in *TP53* is present in 4-26% of adenomas, 50% of adenomas with invasive foci within adenomatous polyps, and 50-75% of sporadic CRCs[367].

Phosphatidylinositol-4,5-bisphosphate 3-kinase catalytic subunit alpha (*PIK3CA*). The phosphatidylinositol-3-kinase (PI3K) signaling pathway plays and important role in CRC tumorigenesis[368]. *PIK3CA* gene is located at chromosome 3q26.32. Amplifications of this gene have been observed in adenomas, and are frequent events in the carcinogenesis of CRC. The amplifications in *PIK3CA* have been proposed as an independent prognostic factor for longer survival[369]. Mutations in the gene were observed in 10-30% of CRC cases[370] and have been associated with CIMP, KRAS mutation and fatty acid synthase (FASN) expression in colorectal cancer[371]. The most frequent mutations are E542k, E545K, and H1047R, which result in dominantly active form of PI3K protein, that stimulates cancer cell growth and survival[372].

Mothers against decapentaplegic homolog 4 (*SMAD4*). *SMAD4* is a tumor suppressor gene located in chromosome 18q21.2, and is associated with juvenile polyposis syndrome (JPS)[373,374]. SMAD4 protein is an intracellular mediator that responds to transforming growth factor-β (TGF-β). When TGF-β binds to its receptor it activates the internalization of SMAD4 into the nucleus to promote apoptosis and cell cycle regulation[374]. *SMAD4* mutations lead the progression of adenoma to

carcinoma, and approximately 30% of CRC patients carry that mutation[375]. In addition, the loss of chromosome 18q is the most common cytogenetic abnormality in CRC (up to 70%) called "deleted in colorectal carcinoma" gene (*DCC*)[330], therefore, SMAD4 alteration is also due to aneuploidy[376].
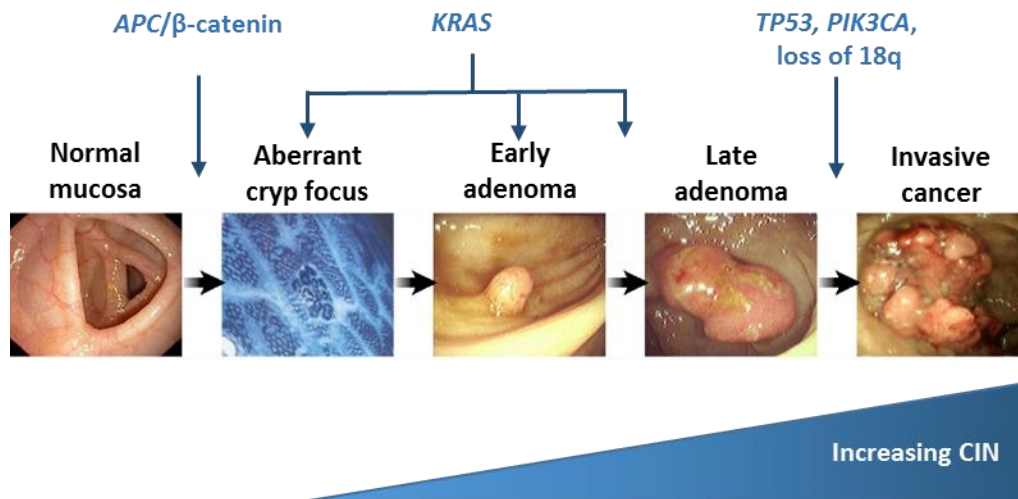
Figure 10. Stepwise progression from normal epithelium to invasive colorectal carcinoma. Adapted from [377]

3.3 Role of the tumor microenvironment (TME)

As explained in the epidemiology of CRC, the survival of patients has been significantly increased in the recent years, but some patients undergo tumor relapse and resistance to the initially effective drugs. It is for that reason that the importance of tumor microenvironment in the development, expansion and maintenance of tumor cells is gaining value. In addition, it has been shown that the dependence of tumor cells on external signals from their microenvironment is determining carcinogenesis[378,379].

TME in solid tumors, including CRC, represents a complex network composed of different type of cells, such as different population of T cells, macrophages, fibroblasts, or endothelial cells, which are interacting among themselves.

3.3.1 Immune Inflammatory cells

The incidence of developing CRC increases in conditions of chronic inflammation[380]. In sporadic CRC, an extensive inflammatory infiltrates with high levels of cytokine expression in tumor microenvironment, such as interferon ɣ[381,382] or interleukin-17A and interleukin-22[383-385] are

present. However, the role of adaptive immune response in human cancer progression is still controversial[10]. For many solid tumors, the presence of natural killer cells (NK) and natural killer T cells in the TME predicts good prognosis[386]. Due to its importance, a specific cancer classification (Immunoscore) was developed using the immune infiltration on CRC cancer[387,388].

Tumor-infiltrating lymphocytes (TILs)

TILs are the host immune response to cancer cells and predict clinical outcome in CRC patients[389]. The two principal types of T cells present in CRC are CD8$^+$ cytotoxic T cells (CTL), which are able to attack and kill the tumor cell directly (through the release of granzyme B, perforin, such others), and the heterogeneous group of CD4$^+$ helper cells (Th), which secrete different types of cytokines[390]. T-helper type 1 lymphocytes (Th1s) are able to activate CTL, and T-helper type 2 lymphocytes (Th2s) stimulate humoral immunity[391]. In contrast, other types of CD4$^+$ T cells, such as regulatory T cells (Tregs), are able to suppress the activity of CTL by cell to cell contact or by the releasing different cytokines, such as transforming growth factor-β (TGF-β) or forkhead box P3 (FoxP3)[392]. On the other hand, the mechanism of interaction between programmed death-1 (PD-1)$^+$ T-cells and PD-Ligand 1/2$^+$ tumor cells, is a new approach for treatment of CRC patients (following the successful development of anti-PD-1 for melanoma, renal cell carcinoma, and non-small cell lung cancer). Several clinical trials provide some evidence indicating that PD-L1 expressing CRC tumors and MSI tumors may show signals of anti-tumor activity during PD-1 targeting therapy, due to high infiltration of immune cells[393] .

Tumor-Associated Macrophages (TAMs)

TAMs are the major population of inflammatory cells in tumor stroma, and they come from circulating monocytes or from tissue-resident macrophages[36]. TAMs are abundant in most human and experimental murine cancers, and their activities are usually pro-tumorigenic[394]. They are essential components of the immune inflammatory response, and are very important players in tumor progression[395]. Also, it has been demonstrated that TAMs facilitate tumor invasion and metastasis in CRC patients through the secretion of different growth factors, proteolytic enzymes and inflammatory mediators[396-398]. M2 macrophages subtype are those commonly known as TAMs, as described previously in FL, and they produce anti-inflammatory cytokines, and TGF-β[399]. The main functions associated with TAMs are immune suppression and angiogenesis stimulation[400], participating in remodeling the extracellular matrix (ECM)[401]. In addition, the production of ROS and nitrogen intermediates by TAMs contributes to genetic instability in cancer cells[402].

Others

Other type of tumor-promoting inflammatory cells are mast cells and neutrophils[43,403]. NKs are other type of immune inflammatory cells but they act as tumor-antagonizing cells[4].

3.3.2 Cancer-Associated Fibroblast (CAFs)

CAFs are mesenchymal-like cells and are part of the diverse connective tissue components[404]. A fibroblast is a resting mesenchymal cell with potential to proliferate when stimulated by a growth factor, such as TGF-β or IL-6, among others[405,406]. Once activated, they are able to secrete chemokines and cytokines, and synthesize extracellular matrix[407]. CAFs are the dominant cellular population in the stroma of CRC[408]. The interaction of CAFs and cancer cells is mediated through oxygen and extracellular metabolite availability, and cytokine and chemokine signaling[409]. Chemokine secretion by CAFs (such as CXCL12) and other cytokines leads to infiltration of immune cells[410], which further contributes to angiogenesis[411] and metastasis[412]. Another key molecule secreted by CAFs is TGF-β. On the other hand, CRC cells also secrete TGF-β, which stimulates the secretion of IL-10 by CAFs cells that increase the efficiency of organ colonization by CRC cells, and confers a survival advantage to metastatic cells[413]. Moreover, TGF-β secretion by CAFs in tumor microenvironment elicits epithelial CXCR4 expression in prostate cancer cells, which triggers tumor cell growth when stimulated by CXCL12[414].

3.3.3 Endothelial cells

The vascular cells are a very important component in the tumor microenvironment due to their function of providing nutrients and oxygen to the growing tumor cells[415]. Quiescent endothelial cells are activated through different signals present in the tumor compartment, described as a "angiogenic switch"[416], which activates molecular pathways in endothelial cells that promote the formation of tumor-associated vasculature. These biological programs include the activation of VEGF, FGF, and Notch pathways, among others[417,418].

Other important types of vessels developed in tumor microenvironment are lymphatic vessels, which are located at the peripheries of tumors, and are closely related to the endothelial cells of the general circulation[419].

3.3.4 The extracellular matrix (ECM)

The ECM is another very important component of the TME[420]. ECM is mainly composed of fibronectin, laminin, collagens type I and IV (30%), proteoglycans, and hyaluronic acid[421], and it forms a physical and biochemical framework. Some of the cells that form TME are responsible for suppling distinct ECM proteins. As mentioned above, different TME cells are able to remodel the ECM, and facilitate angiogenesis and inflammation. This structure plays a critical role in tumor development, which is commonly deregulated and becomes disorganized in later stage of tumor progression[422]. Interestingly, the composition of ECM differs in primary tumors of diverse metastatic potential. In fact, the composition of the extracellular TME has been used as a predictor of clinical prognosis[423].

3.3.5 Pericytes

Pericytes are contractile mesenchymal cells similar to smooth muscle cells, which are located around the endothelial tubing of blood vessels[4]. These types of cells are implicated in the synthesis of the vascular basement membrane in collaboration with endothelial cells[424]. Some signaling pathways are implicated in the recruitment, differentiation and function of pericytes, such as transforming growth factor (TGF)-β[425].
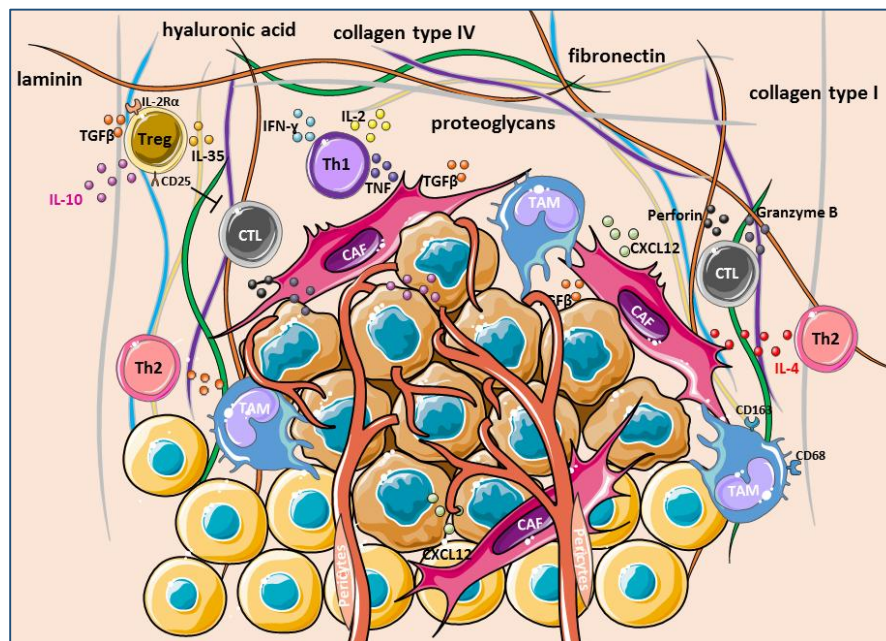
Figure 11 Tumor microenvironment in CRC. TME in CRC represents a complex network composed by different type of cells, such as different population of T cells, macrophages, fibroblasts, or endothelial cells, which are interacting among themselves and support tumor growth and survival through a complex set of factors and stimulating molecules.

3.4 CRC progression and metastatic disease

Tumor development is based on the crosstalk between tumor cells and their surrounding TME, and is mediated by the receptors and their ligand expression levels in both cellular components[426]. Specifically, carcinogenesis is the process that leads the epithelial tissue progression to higher pathological grades of malignancy, reflected in local invasion and distant metastasis[4]. Distant metastasis is preceded by previous invasion of tumor cells to their most adjacent tissue layers. This multistep process, also known as the invasion-metastasis cascade, starts with local invasion, intravasation into nearby blood and lymphatic vessels, transits through the hematogenous and lymphatic systems (lymph nodes), followed by escape into the parenchyma of distant tissues (extravasation), and finally the growth of metastatic lesions (colonization)[427]. However, metastasis is not the last step in tumor progression; some evidences indicates that cancer cells (from CRC, breast cancer and prostate cancer, among others) can disseminate early from the noninvasive lesion[428-430].

The metastatic cells have specific features, the most important ones are: deregulation in cell fate determinants, losing differentiation-inducing factors[431]; and activation of stem cell signaling, such as WNT-β-catenin signaling[432] or Notch[433], among others. The epigenomic reprogramming in cancer cells is a key regulator in cell fate determination[434]. The epithelial-mesenchymal transition (EMT) program, conditioned by hypoxia and inflammation in a reactive stroma, is another important fact to promote invasion and metastasis[435]. The EMT is a critical mechanism where epithelial tumor cells lose their intracellular junctions, cell-to-cell contact capacities, and cellular polarity acquiring a more motile and mesenchymal phenotype[436,437].

Different cancers have preferential sites of metastasis (known as seed and soil hypothesis)[427]. In CRC, metastatic dissemination seems to follow a stepwise manner[438], the first place of hematogenous distant dissemination is usually the liver, as mentioned before, due to the venous drainage of the intestinal tract through the portal venous system, followed by the lungs, bone, and other sites, including the brain. In tumors originating in distal rectum, the inferior rectal veins drain into the inferior vena cava, and this might be the reason to explain as to why the initial site to metastasize in these patients are the lungs[439]. However, the mechanisms by which metastatic cells seem to choose their organ of preference to invade remains unresolved.

As mentioned in the previous section, stromal cells are crucial for promoting tumor cell dissemination in primary sites, and for contributing to the tumor cell proliferation in the metastatic

sites[379,440]. Different cell populations of the tumor stroma can participate in the orchestration of tumor dissemination. For example, TAMs induce the intrinsic mobility of tumor cells through the stimulation with CSF1 in breast cancer[441]. In CRC, CAFs secrete IL-11 in response to TGF-β, as mentioned above, which activates STAT3 signaling, conferring survival advantages to metastatic tumor cells in lung and liver[413].

Nevertheless, not all cells that are able to arrive to the blood vessels can survive in the circulation and form metastasis[442]. The activation of survival signals, such as AKT signaling pathway in response to CXCL12, is necessary for the survival of cancer cells in the circulation[443]. Another system that supports cancer cell dissemination is the lymphatic system. The lymphangiogenesis (regulated by VEGF-C) in tumor mass is not only used by cancer cells to disseminate to lymph nodes[444], but also to the liver in CRC[445].

Once tumor cells are in blood, or in lymphatic vessels, a substantial amount of evidence indicates that chemokines play an important role in the organ-selective metastasis process[446,447]. For example, cancers cells that express CXCR4 receptor disseminate and form metastasis in organs that express its specific ligand CXCL12, such as the lungs, liver, lymph nodes, bone marrow[446,448-450].
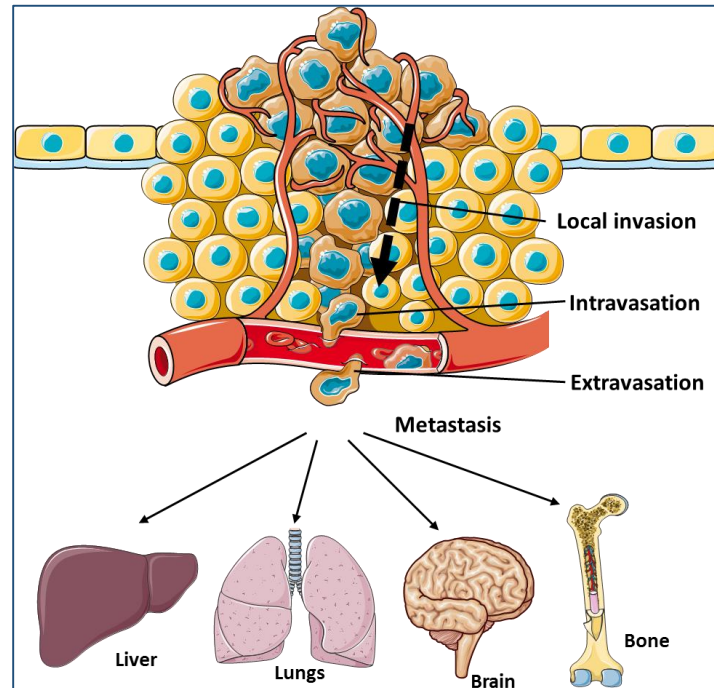
Figure 12. Schematic representation of multistep process known as the invasion-metastasis cascade, which begins with local invasion, intravasation into nearby blood and lymphatic vessels, transit through the hematogenous and lymphatic systems (lymph nodes), follow by escape into the parenchyma of distant tissues (extravasation), and finally growth of metastatic lesions (colonization).

3.5 GPCRs in Cancer

G protein-coupled receptors (GPCRs) are an important family of membrane signaling receptors with seven α-helical transmembrane (7TM) structural motif, which have an important role in cancer growth and development through the regulation of cell proliferation, immune cell-mediated functions, angiogenesis, invasion, migration and survival in metastatic sites[451,452]. There are approximately 1000 GPCRs encoded by the human genome and are divided in five families based on sequence homology: rhodopsin, secretin, glutamate, adhesion and frizzled[453]. The most relevant and largest group are the rhodopsin family GPCRs[454]. Different types of cancers exhibit unusual overexpression of GPCRs and G proteins[451].

Upon the interaction of an extracellular ligand to its receptor, GPCRs undergo a conformational change that activates a signaling cascade by coupling to intracellular heterotrimeric G-proteins (α, β, and ɣ subunits) associated with the inner surface of the plasma membrane [455], which binds the guanine nucleotide GDP in its basal state. When the receptor is activated by its ligand, GDP is released and replaced by GTP, triggering the subunit dissociation (into βɣ dimer and α monomer). This dissociation leads to the activation of multiple downstream effectors, including ERK1/2, mitogen-activated protein kinase (MAPK), JNK, and AKT. The α monomer binds to GTP, and this is rapidly hydrolyzed to GDP in re-association with the receptor and the trimeric G-protein complex. Other pathways are activated by different subunits of Gα, such as adenyl cyclase; PLCβ (via PLC) to activate phosphatidylinositol-specific phospholipases, which hydrolyze PIP2 to generate IP3 and DAG (which increase intracellular concentrations of free Ca^{2+} and activate some proteins kinases such as PKC); and the transcription factor NFκB via PYK2. Besides, a specific Gα12 is associated with Rho and Ras[456].
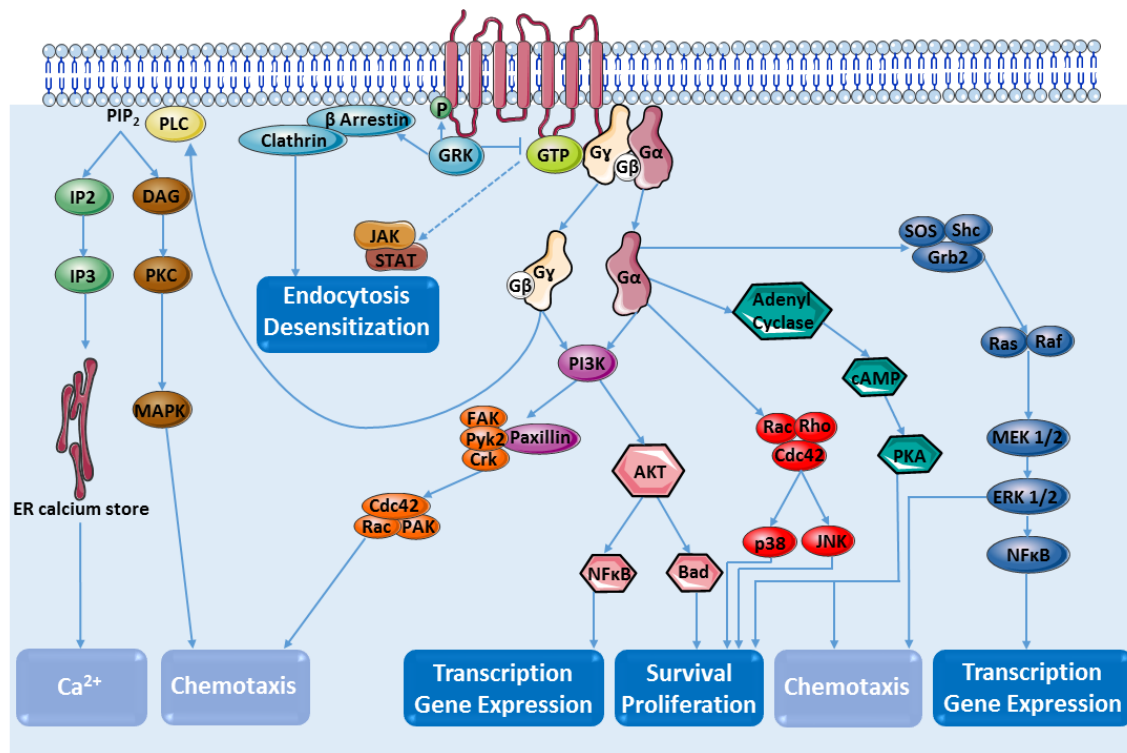
Figure 13. GPCR activation pathway

GPCR dimers formation

Classically, GPCRs were considered as monomeric functional entities, which activate a single signaling cascade. Nevertheless, in recent years it has become evident that GPCRs are able to form dimers with other GPCRs in the cell membrane[457], and this dimer formation may modify the cellular response[458-461]. There are different mechanisms involved in receptor coupling to regulate the activation of downstream pathways. Three different mechanisms are proposed to understand the biological function of dimer formation:

- GPCR dimerization plays a role in trafficking, thus both receptors are co-internalized after their activation. This is the example for D1 and D2 dopamine receptors[461].
- Transantagonism, which implies that the activation of one receptor induces the inhibition of the signaling activity of the other receptor[462].
- Transactivation, the ability to initiate the signaling cascade of one receptor upon the agonist binding to the other receptor[463].

Such heterodimerization increases the range of intracellular responses[464] and it is proved to alter the pharmacodynamics of certain drugs[465].

GPCRs show differential expression in cancer cells compared to normal tissues, and they are highly druggable targets. In fact, 35% of drugs approved by FDA are GPCR-targeted drugs[466,467]. However, a more accurate evaluation of interactions and off-target effects is needed[468,469], which is the main reason as to why most of these drugs are currently in clinical trials for cancer treatment.[467].

3.5.1 Chemokines receptors

Chemokines are chemotactic cytokines (approximately 8-17kDa), which bind a chemokine receptor rhodopsin family GPCRs[470], and are produced by tumor cells and tumor microenvironment. While there are approximately 50 chemokines, only 20 chemokine receptors have been identified so far, thus some receptors interact with more than one chemokine, and some chemokines share the same receptor[471]. In addition, some receptors bind specifically to only one cytokine molecule. This is the example of CXCR4, CXCR5, CXCR6, CCR6, CCR9 and CX3CR1[472]. Besides, depending on the cellular type and context, chemokine receptor activation generates a variety of cellular responses[473].

In normal tissue, chemokines cause leucocytes migration, and their secretion is induced by growth factors, inflammatory cytokines and pathogenic stimuli[474]. Within the GPCR family, chemokine receptors are associated with tumor metastasis[472]. In addition, these chemokine receptors have been involved in chronic inflammation, which is a very important feature to induce tumor initiation and progression of different cancer types, such as colon, liver, breast and lung[475,476]. In addition, chemokines are able to recruit different cell types to form the tumor microenvironment, which in turn, represents a secondary source of chemokines, thus further promoting tumor growth, cell survival, angiogenesis and metastasis[470]. Cancer cells from different types of solid tumors express high levels of CXCR4, CCR7, CCR9 and CCR10 chemokine receptors[477]. Specifically, in CRC the expression of CCR7 predicts lymph node metastasis[478]. Furthermore, the overexpression of CXCR4 by CRC cells is significantly associated with lymphatic and distant dissemination[447], and with an increased risk of recurrence and poor survival in patients with colorectal cancer [479].

3.5.1.1 CXCR4 receptor

Among the well-known chemokine receptors, CXCR4 and its ligand, the stromal cell derived factor-1 (SDF-1) or CXCL12, have been studied extensively. CXCR4 is a rhodopsin-like GPCR[480] and is

functionally present in different cell types in adult tissues, such as peripheral blood lymphocytes, monocytes, dendritic cells, intestinal and alveolar epithelial cells, and neurons, among others[481]. The stimulation of CXCR4 by CXCL12 binding activates the prolonged ERK-2 and PI3K response[482], enhances tyrosine phosphorylation, association with components of focal adhesion, and the NF-κB activity[483].

The physiological role of the CXCR4/CXCL12 axis in normal cells is to modulate developmental processes, such as hematopoiesis, organogenesis, immune response, and vascularization. Likewise, this axis participates in other important processes such as tissue renewal, lymphocytes maturation and stem cell homing[484,485]. During development, the CXCL12-CXCR4 axis has an important role in the spatial organization of stem cells and progenitor cells during the formation of specific organs, such as in cardiac septum formation (defects in the axis cause vascular defects)[486]. In kidney development, CXCL12 drives vascular and epithelial progenitor cells to form anatomical interactions between glomerular and tubular epithelium with their vascular networks[487]. Finally, it has been also described that CXCL12 gradients support stem cell migration in embryonic development[488]. In contrast, the role of chemokine signaling in stem cell homing in the bone marrow is in the opposite direction compared to the organ development. In fact, CXCL12 signaling maintains CXCR4+ hematopoietic stem cells (HSCs) within the bone marrow[489]. CXCL12 also regulates the number of mature granulocytes and monocytes in the blood through the regulation of HSCs mobilization inside the bone marrow[490]. During the leukocyte maturation, immature T and B cells travel to the thymus and secondary lymphoid organs, where they are selected. CXCL12 in collaboration with other chemokines such as CCL17, CCL21 and CCL22, are responsible for regulating migration to different compartments of these secondary lymphoid organs in order to complete the maturation process[491,492]. During the tissue renewal process, CXCL12-CXCR4 axis plays an important role in neurogenesis of the hippocampus in adults, as well as in neural stem cells and neural progenitor cells, aiding the maintenance of their stemness or regulating the migration of their neural progeny[493]. This axis also participates in the homing of stem cells in mammalian testes[494]. In summary, the CXCL12–CXCR4 axis is responsible for maintaining peripheral stem cell pools that have important functions in homeostatic tissue renewal and regeneration .

In cancer cells, CXCR4 plays an important role at different stages of cancer development[495], and is involved in the metastasis of tumor cells in colorectal, breast, prostate, ovary, and lung

cancers[446,447,477]. Furthermore, the upregulation of CXCR4 has been found in many tumor types[481,496], including CRC, where the overexpression of CXCR4 correlates with a poor prognosis[497].

At the transcriptional level, expression of CXCR4 is induced by several processes. Activation of the hypoxia-inducible factor-1 (HIF-1α), which occurs under hypoxia conditions, increases CXCR4 expression[498,499]. Moreover, vascular endothelial growth factor (VEGF), as part of its autocrine action induces the expression of CXCR4 in breast cancer[500]. Furthermore, in breast cancer too, the transcription factor NF-κB, which controls cell motility, upregulates CXCR4[501]. Recently, gene-fusion events, such as *PAX3-FKHR* in embryonal rhabdomyosarcoma cells, have been also associated with CXCR4 transcriptional activity[502]. In addition, apart from the functions described above, it has been demonstrated that CXCR4 regulates other important processes in cancer progression. This receptor establishes a permissive tumor microenvironment and immune evasion in cancer[450]. Also, it has been reported that CXCR4 expression is responsible for the outgrowth of micrometastasis in animal models of CRC[503].

As far as CXCL12 is concerned, it is well known that its production is high in lung, liver, bone marrow, and lymph nodes[446], which usually are the main sites for CRC metastasis. Moreover, CXCL12 through the upregulation of Akt/PKB pathway, is capable to increase survival upon specific death signals, such as TRAIL signals[504].

The CXCR4-CXCL12 axis is likely to be a rather dynamic process. Whereas in some areas of the tumor protease production or other events could degrade or reduce CXCL12, in some tumor regions CXCR4 expression might be increased. Consequently, gradients of CXCL12 released in other body locations may trigger sub-populations of tumor cells to leave the primary site[472].

Finally, the fact that CXCR4 plays a crucial role in cell stemness, its expression by sub-population of cells in a primary tumor might indicate that these cells could have cancer stem cell properties[505].

3.5.1.1.1 Current treatments targeting CXCR4/CXCL12 axis

It is well established that the central role of CXCR4-CXCL12 axis in regulating HSC homing has been used for clinical purposes. A single injection of a CXCR4 antagonist is sufficient to mobilize HSCs and other progenitor cells from the bone marrow into the blood[506], used for therapeutic stem cell

transplantation. Plerixafor (AMD3100) is the unique CXCR4 antagonist approved by the FDA and the EMA for clinical use.

CXCR4 antagonist was developed in 1994 as anti-HIV drug. Results from several clinical trials showed that the main side effect of the drug was HSC mobilization into the blood[506]. This fact leads to its use in stem cells transplantation in hematologic neoplasm, and therefore numerous studies were developed to test the efficacy and safety of AMD3100 for this purpose. These clinical trials in Phase I-II are a clear example of the high interest in improving the use of this compound to mobilize stem cells: NCT00075335, NCT00082329, NCT00241358, NCT00291811, NCT00914849 and NCT00322127 (from ClinicalTrials.gov).

Moreover, AMD3100 is under the focus of attention to assess its efficacy in cancer treatment, but only in combination with regular chemotherapeutics or other current treatments, in resistant or recurrent patients. (Summary in table 8). In patients with relapsed/refractory acute myeloid leukemia (AML), a study in phase I/II was carried out to determine the safety and efficacy of CXCR4 inhibitor in combination with mitoxantrone, etoposide, and cytarabine (NCT00512252). In pediatric patients with relapsed or refractory acute lymphoblastic leukemia (ALL), AML and myelodysplastic syndromes (MDS), the effect and safety of combining plerixafor and standard anti-cancer drugs (i.e. cytarabine and etoposide) was tested to enhance the cytotoxic effect of chemotherapy (phase I, NCT01319864). With the same objective, the effect of AMD3100 to sensitize chronic lymphocytic leukemia/small lymphocytic lymphoma (CLL/SLL) patients to rituximab was also prescribed (phase I, NCT00694590). Finally, another study in phase I in recruitment status, is preparing to evaluate how plerixafor may help the body to overcome resistance to immune therapy in patients with advanced pancreatic, ovarian and CRC (NCT02179970).

Table 8. Summary of plerixafor (CXCR4 inhibitor) clinical trials.

Clinical trial number	Drug	Combination	Disease	Study phase
NCT00512252	plerixafor	mitoxantrone, etoposide, and cytarabine	AML	phase I/II
NCT01319864	plerixafor	cytarabine and etoposide	Pediatric ALL, AML and MDS	phase I
NCT00694590	plerixafor	rituximab	CLL and SLL	phase I
NCT02179970	plerixafor	immune therapy	advanced pancreatic, ovarian and colorectal cancer	phase I (recruitment)

Other CXCR4 inhibitors, some improved versions of AMD3100 and others antibodies against CXCR4, are under evaluation in clinical trials for cancer treatment.

Table 9. Summary of CXCR4 inhibitors and antibodies in clinical trials.

Clinical trial number	Drug	Combination	Disease	Study phase
NCT01010880	BKT140		Multiple Myeloma	Phase I-II
NCT01359657	Anti-CXCR4 (BMS-936564)	Lenalidomide/Dexamethasone or Bortezomib/Dexamethasone	Multiple Myeloma	Phase I
NCT01120457	Anti-CXCR4 (BMS-936564)		Acute Myelogenous Leukemia, Diffuse Large B-Cell Leukemia, Chronic Lymphocytic Leukemia, Follicular Lymphoma	Phase I
NCT02737072	CXCR4 peptide antagonist (LY2510924)	Durvalumab (anti PD-1)	Advanced Refractory Solid Tumors	Phase I

3.5.2 Endocannabinoids receptors

The endocannabinoid system is composed of endogenous cannabinoids (endocannabinoids), the enzymes that regulate the amount of endocannabinoids, and the cannabinoid receptors (mainly CB_1[507] and CB_2[508], which are GPCR receptors). Recently, it has described the function of the endocannabinoids as lipid mediator synthesized from common precursors, which acts in other receptors besides cannabinoids receptors[509]. Historically, in Western medicine in the XIX century, *Cannabis* (derived from marijuana plant *Cannabis* sp.), has been used to treat a variety of gastrointestinal disorders[509-511]. The most important compound of Cannabis is Δ^9-tetrahydrocannabinol (THC), which produces a variety of biological effects by mimicking endocannabinoid ligands[512].

The two better described endocannabinoid ligands are: 2-arachidonylglycerol (2-AG)[513,514], expressed in the ilium and colon, and generated via phospholipase C or by turnover of diacylglycerol (DAG) via DAG lipase (DAGL)[515], and anandamide (AEA)[516], which is expressed in the mucosa, submucosa and muscular layers of colon and ilium, and is endogenously synthesized from membrane phospholipids by the enzyme N-acylphosphatidylethanolamine-phospholipase D (NAPE-PLD) and through alternative biosynthetic pathways[515]. Both ligands are increased in CRC patients[517].

The typical endocannabinoid enzymes expressed in the gastrointestinal tract are: fatty acid amide hydrolase (FAAH)[518,519], which degrades AEA and is placed in stomach and intestine in cells of myenteric plexus, and monoacylglycerol lipase (MALG)[520,521], which hydrolases 2-AG and is expressed in fibers and in the nerve cells through mucosal layers and muscle of the duodenum, ileum, and colon. It has been shown that MALG is downregulated in CRC[522].

The CB_1 receptor is mainly expressed in the central nervous system, in colonic epithelial, vascular smooth muscle cells of the colon, and plasma cells in normal tissues[509,523,524]. The CB_2 receptor is mainly expressed in peripheral and inflammatory tissues, in macrophages, and lightly in plasma cells[508,523]. Both CB_1 and CB_2 receptors are important in modulating inflammatory processes *in vitro*. CB_1 promotes epithelial wound healing in human normal colon[525], and CB_2 activation inhibits the effect of IL-8 release in human colonic epithelial normal cells[526]. The expression of both receptors is found in B cells, natural killer cells and mast cell[527-529]. The stimulation of other cells, such as macrophages, mononuclear cells and dendritic cells lead to an increase in the production of endocannabinoids[529]. In addition, cannabinoids are able to inhibit activated macrophages and mast cells, as well as the secretion of some cytokines[530-532].

The first study testing cannabinoids (specifically phytocannabinoids THC and cannabinol) in cancer regression was in 1975 by Munson et al., showing suppression of tumor growth in Lewis lung adenocarcinoma in animal models[533]. In recent decades, different studies demonstrated that the use of cannabinoids (endocannabinoids, phytocannabinoids and synthetic cannabinoids) or blocking endocannabinoid enzymes confer a cancer growth inhibition by blocking cell proliferation and inducing apoptosis in breast cancer[534] and in glioma[535]. In addition, several reports showed anti-invasive and anti-metastatic characteristics in prostate cancer[536], in CRC[537] and in lung cancer[538], and anti-angiogenic properties in microenvironmental sites of malignant tissues such as breast[539] and lung cancer[540].

Furthermore, it has been demonstrated that cannabinoids are able to modulate cell cycle checkpoints in melanoma [541] and in breast cancer[542].

In CRC a down-regulation of CB_1 has been described[543]. Otherwise, an up-regulation of CB_2 receptor expression was reported in a series of 175 colorectal patients, where high CB2 expression was detected in lymph nodes positive patients, and it was expressed with great intensity in tumor epithelial cells. In addition, it correlates to tumor growth and predicts disease free survival and overall survival in colon cancer[544].

3.5.2.1 CB_2 receptor

CB_2 receptors are rhodopsin family serpentine receptors that bind primary to $G_{i/o}$ proteins to modulate the downstream signaling. They are able to activate a wide range of signaling pathways, but recent investigations are focused on modulation of adenylyl cyclase[545,546] and extracellular signal-regulated kinases 1/2 (ERK1/2)[547], this latter indicating potential control of gene transcription by MAP kinase network with varied responses and outcomes[548]. As other GPCRs, CB_2 exhibit variable internalization following agonist binding, some agonist promoting internalization and others being inactive[549,550]. In healthy organisms, it is known that CB_2 receptor is expressed by cells of macrophage lineage, and to a lesser extent by other immune cells[551]. CB_2 receptor, unlike CB_1, does not produce psychotropic effects[552], which makes it a good therapeutic target[553,554].

Recent reports have described the capacity of CB_2 receptors to form heterodimers with other receptors, and this phenomenon contributes to the heterogeneity of receptor signaling, and thus cellular consequences[458,555,556]. A recent investigation demonstrates that the heterodimer formation

of CB_2 with GPR55 (another GPCR receptor) exhibited a negative crosstalk and cross-antagonism between both receptors in breast cancer and glioblastoma[557]. In addition, another recent study suggested that the heterodimerization of CXCR4 and CB_2 has an impact on cancer cell invasion[556].

Finally, specifically targeting CB_2 with a selective CB_2 receptor agonist (JWH133), it has been reported to show tumor regressive action on glioma cells[558].

3.5.2.1.1 Current treatments

Nabilone (analogue of THC) and Epidiolex (cannabidiol analogue) are the only synthetic cannabinoid drugs approved by the FDA for clinical use, unfortunatly these are not used for cancer treatment.

The anticarcinogenic effects of cannabinoids have been demonstrated in *in vitro* studies and *in vivo* models, however, cannabinoids have not been used as anticancer therapy in clinical trials until recently. Several studies are testing the effects of cannabinoids as palliative treatment in combination with current chemotherapeutics, reducing their cytotoxic effects such as nausea, loss of appetite, etc (for example NCT00380965).

The first study that demonstrated similar effects in animal models and patients was a clinical pilot study in glioblastoma patients, which proved THC to be safe when administrated intracranially[559].

Recently, a few clinical trials have started to test the efficacy of cannabinoids as anticancer treatment. In recurrent glioblastoma patients, the combination of THC and cannabidiol (CBD, other cannabis component) with temozolomide (chemotherapy) (NCT01812616 and NCT01812603) have shown improvement in patient's viability. In advanced solid tumors, synthetic cannabinoid (a mixed of CB1/CB2 receptors agonist) was used to evaluate the efficacy to destroy cancer cells (NCT01489826).

On the other hand, as mentioned above, CB_2 receptor is a very interesting druggable target due to non-psychoactive effect and also reducing pathogenic effects on liver health[560].

Table 10. Summary of cannabinoids clinical trials in cancer.

Clinical trial number	Drug	Disease	Study phase
NCT01812616, NCT01812603	Sativex (THC+CBD) + Temozolomide	Recurrent Glioblastoma	Phase I-II
NCT01489826	Dexanabinol (mixed CB1/CB2 receptor agonist)	Solid tumor	Phase I

3.6 Diagnosis and prognosis of CRC

CRC is diagnosed after the onset of symptoms[561], or through screening colonoscopy or fecal occult blood testing in the majority of patients. Routine screening of asymptomatic with high risk individuals for CRC (according to the edge) is supported by major societies and preventive care organizations. Also, this method has been shown to detect asymptomatic early-stage malignancy, thus improve mortality.

Patients with colorectal cancer (CRC) may present in three ways[562]:

●Symptoms and/or signs (abdominal pain, otherwise anemia, and/or a change in bowel habits, or rectal bleeding)[563]

●Asymptomatic individuals discovered by routine screening

●Emergency cases that show intestinal obstruction, peritonitis, or rarely, an acute gastrointestinal bleed

In the last type of patients, or in patients with intolerance to colonoscopy, colonography (CT) can provide a radiographic diagnosis.

The tumor-node-metastasis (TNM) classification of the American Joint Committee on Cancer (AJCC) at diagnosis is used for initial patient management, as the TNM provides prognosis information and aids in treatment decision[564].

The T, N, and M categories for colon cancer are assigned based upon:

●Whether there are signs of cancer spread on physical examination or radiographic imaging tests

●Findings from surgical resection and histologic examination of the resected tissues

Table 11. TNM classification.

Primary tumor (T)	
T category	**T criteria**
TX	Primary tumor cannot be assessed
T0	No evidence of primary tumor
Tis	Carcinoma in situ (intramucosocal carcinoma)
T1	Tumor invades the submucosa (muscularis mucosa9
T2	Tumor invades the muscularis propria
T3	Tumor invades through the muscularis propria into pericolorectal tissues
T4	Tumor invades the visceral peritoneum, or invades or adheres to adjacent organs or structures
Regional lymph nodes (N)	
N category	**N criteria**
NX	Regional lymph nodes cannot be assessed
N0	No regional lymph node metastases
N1	One to three regional lymph nodes are positive
N2	Four or more regional nodes are positive
Distant metastasis (M)	
M category	**M criteria**
M0	No distant metastasis
M1	Metastasis to one or more distant sites or organs, or peritoneal

Table 12. Stage according to the TNM classification

Stage	TNM
0	Tis; N0;M0
I	T1,T2; N0; M0
II	T3, T4; N0; M0
III	Any T; N1, N2; M0
IV	Any T; Any N; M1

Table adapted from the AJCC Cancer Staging Manual, Eighth Edition (2017) published by Springer International Publishing.

Albeit, in patients with stage II and III colon cancer, TNM staging is less useful for distinguishing patients with different prognosis (https://seer.cancer.gov/). Also in stage II patients, new biomarkers are needed to select high-risk patients for adjuvant therapies after surgery[565]. For this reason, recently biomarkers studies and other histologic features have been under evaluation to incorporate them in current routine diagnosis[566]. The most important aspects to consider when making decisions about treatment but which are not yet incorporated into the formal staging criteria are:

- Clinicopathological features (primary site localization, among others)[567].

- Microsatellite instability, which reflects deficiency of mismatch repair enzymes and is both a prognostic factor and predictive of a lack of response to fluoropyrimidine therapy[568].

- Mutation status of KRAS and BRAF, because mutations in these genes are associated with lack of response to agents targeting the epidermal growth factor receptor (EGFR)[569].

- Immunoscore has been defined to quantify the in situ immune infiltrate in tumor[570].

- The tumor-stroma ratio (TSR), which estimates the proportion of malignant epithelial cells and stroma, besides its prognostic value, might be used as an additional high-risk factor to select patients for adjuvant therapy[571,572].

- Tumor budding (TB), which reflects the EMT at invasive tumor front, and thus represents the cell-biological correlate of the tumor-stroma interphase. Moreover, it has prognostic value[573].

Currently, the biomarkers routinely tested are:

Table 13. Currently tested biomarkers.

Mutation	Incidence (%)	Method of testing	Prognostic or predictive	Clinical utility
KRAS	35-45%	Whole genome sequencing	Predictive	Predicts resistance to EGFR inhibitors
BRAF	8-10%	Whole genome sequencing	Prognostic	Indicative of aggressive disease
MSI-H (high)	15%	Polymerase chain reaction, immunohistochemistry	Predictive	Predictive response to immunotherapy

Adapted from [574]

Finally, a new model was developed and has been proposed in order to improve the progression and thus prognosis of CRC. The consensus molecular subtypes (CMS) was described to classify

patients by integrating gene expression, mutations, copy number alterations (CNAs), methylations, microRNA expression, as well as patient's outcome, to perform an accurate classification of CRC[575].

Table 14. CMS classification (molecular features).

CMS1 MSI immune	CMS2 Canonical	CMS3 Metabolic	CMS4 Mesenchymal
14%	37%	13%	23%
MSI, CIMP high, hypermutation	SCNA high	Mixed MSI status, SCNA low, CIMP low	SCNA high
BRAF mutation		KRAS mutations	
Immune infiltration	Wnt and MYC activation	Metabolic deregulation	Stromal infiltration, TGF-β activation, angiogenesis
Worse survival			Worse relapsed-free and overall survival

CIMP, CpG island methylator phenotype; MSI, microsatellite instability; SCNA, somatic copy number alterations

3.7 Current treatments in CRC

Adenocarcinomas in the colon are the principal lesions in primary cancers. Therefore, the only curative treatment for localized colon cancer is **surgical resection**, where the tumor is removed completely, also the major vascular pedicles and the lymphatic drainage basin of the affected colonic segment are resected. This is only indicated in an attached or infiltrated tumor into resectable organ or structure. In addition, surgical resection may be indicated in selected patients with limited resectable metastatic disease (liver o lung)[576].

Neoadjuvant chemoradiotherapy

In locally **advanced rectal cancer**, neoadjuvant chemoradiotherapy (RT + fluorouracil) or chemotherapy (fluorouracil), rather than initial surgery, is a common approach supported by randomized trials[577].

On the other hand, in locally **advanced colon cancer** invading adjacent organs, neoadjuvant chemoradiotherapy might be considered, whereas, in patients with early **colon cancer**, benefits are limited to isolated case reports. There is no consensus agreement as to which patients, if any, are suitable for this approach [578,579]. Besides, the utility of neoadjuvant chemotherapy alone for patients

with primary colon cancers is unclear; this approach will be directly studied in the phase III FOxTROT trial, which completed accrual in 2016[580].

Adjuvant chemotherapy

The postoperative chemotherapy (adjuvant) is indicated for patients who present occult micrometastasis that are present at the time of surgery (stage III-IV). The aim of this therapy is to eradicate these micrometastasis, thereby increasing the cure rate and reducing the likelihood of disease recurrence.

Early studies of 5-fluorouracil (5-FU) monotherapy failed to show a survival benefit relative to resection alone[581]. Interest in adjuvant chemotherapy was revived in the late 1980s with reports that suggested a survival benefit from FU-based combination regimens[582], and by the discovery of modulators of FU activity, such as leucovorin (LV)[583] and oxaliplatin[584].

A combination of several chemotherapy drugs are given intravenously, incorporating irinotecan (semisynthetic inhibitor of topoisomerase), oxaliplatin (third-generation platinum compound that causes mitotic arrest via the formation of DNA adducts), and capecitabine (5-FU prodrug). These are now all established options for use as first-line, second-line and sequential treatment of CRC[585].

In stage II patients (lymph node-negative), the benefits of chemotherapy (5-FU and oxaliplatin-based or non-oxiloplatin-based regimens) are controversial. Treatment decision must be individualized depending on the presence of high-risk clinicopathologic features (fewer than 12 nodes in the surgical specimen, T4 stage, perforated/obstructed tumor, poorly differentiated histology, lymphovascular or perineural invasion, and tumor budding), mismatch repair protein status, assessment of comorbidities and anticipated life expectancy, and given the relatively good prognosis of stage II disease, the potential risks associated with treatment[586]. If adjuvant chemotherapy is chosen, most patients receive a fluoropyrimidine alone, unless they have a tumor with deficient mismatch repair status, in which case adjuvant fluoropyrimidines alone are ineffective. For patients receiving a non-oxaliplatin-based adjuvant therapy regimen (i.e., a fluoropyrimidine alone), six months of adjuvant therapy remains the standard approach[587].

In stage III patients (with node-positive), oxaliplatin-containing chemotherapy for six months is recommended as a standard approach for most patients, although oxaliplatin's benefits are controversial in older adults[588].

In general, **older adult** patients gain as much benefit from adjuvant fluorouracil (FU)-based chemotherapy as younger individuals do, although it is used less often in older adults, and rates of treatment-related toxicity may be higher. The role of oxaliplatin as a component of adjuvant therapy in older adult patients is controversial[589,590].

The most commonly used oxaliplatin-based regimens are FOLFOX[591] (folinic acid (Leucovorin) + 5-fluorouracil (5-FU) + oxaliplatin (Elotaxin) and CAPOX[592] (capecitabine (Xeloda) + oxaliplatin (Elotaxin); also called XELOX).

Patients with stage II disease are more often offered a regimen that does not include oxaliplatin, typically LV-modulated FU or single-agent oral capecitabine.

In stage IV patients (with metastasis), treatment has been considered palliative for many years. Chemotherapy has expanded the therapeutic options for these patients and improved median survival from less than one year in the single-agent fluoropyrimidine era to more than 30 months, fewer than 20 percent of those treated with chemotherapy alone are still alive at five years, and only a few are free of disease, unless resection or ablation of metastases has been performed[593] . For this reason, it is important to evaluate KRAS and BRAF mutations (as it has been demonstrated that they have an impact in the efficacy of specific anti-cancer agents) to decide the best adjuvant treatment combination[585]. FOLFOX, FOLFIRI (folinic acid (Leucovorin) + 5-FU + irinotecan (CPT-11)) or FOLFOXIRI (folinic acid (Leucovorin) + 5-FU + oxaliplatin (Elotaxin) + irinotecan (CPT-11)) are the current chemotherapeutic treatments. Three different types of targeted therapies have been developed and approved for metastatic CRC to use in combination with the previous mentioned chemotherapeutics[594]:

- Monoclonal antibodies against VEGF (Bevacizumab[595]) and EGFR (Cetuximab[596] and Panitumumab[597].
- Recombinant fusion proteins against angiogenic factors (Aflibercept[598]).
- Molecules that inhibit tyrosine kinase receptors (Regorafenib[599]).
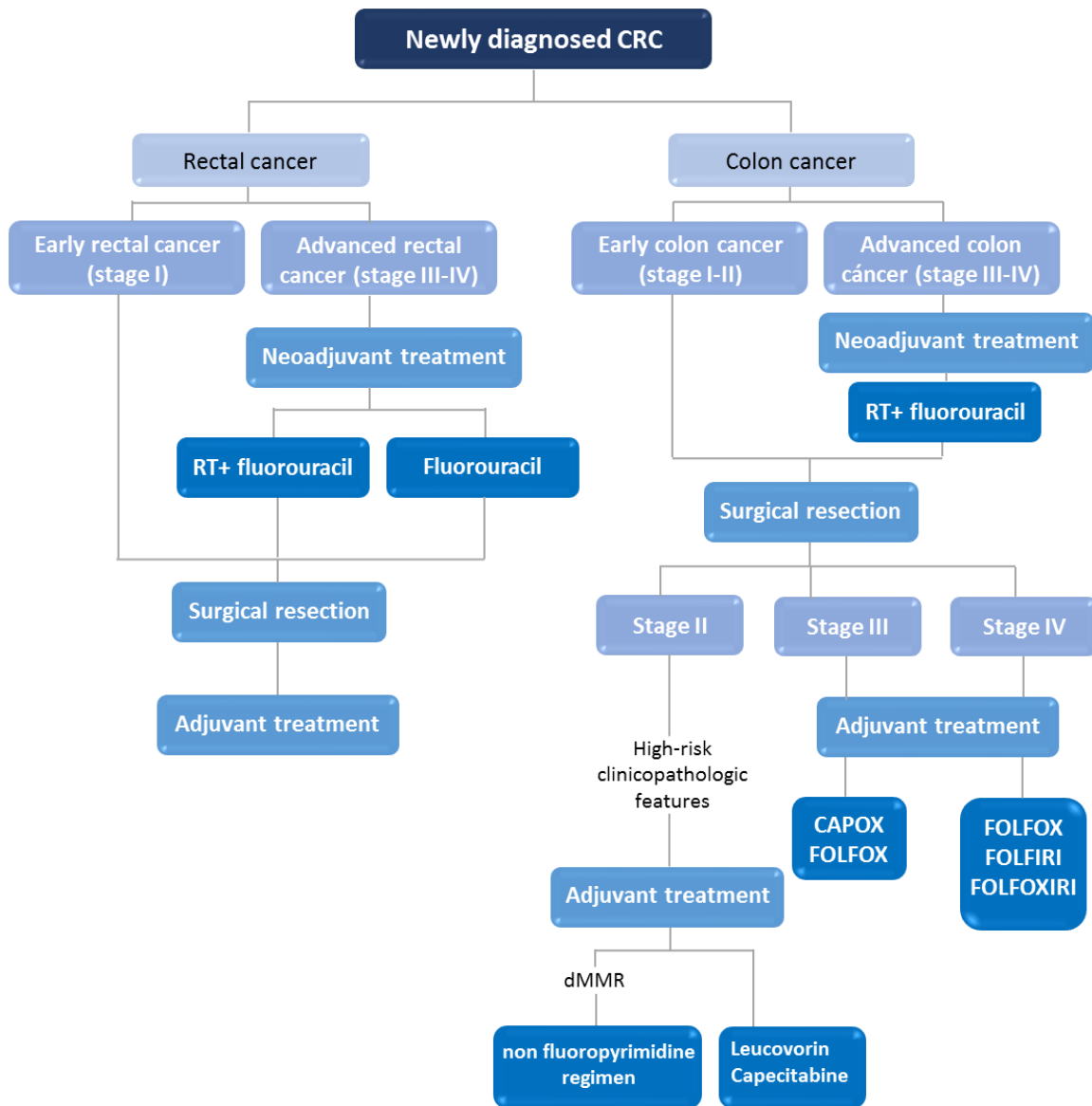
Figure 14. **Representative scheme of treatment decision in newly diagnosed CRC.** High-risk clinicopathologic features: fewer than 12 nodes in the surgical specimen, T4 stage, perforated/obstructed tumor, poorly differentiated histology, lymphovascular or perineural invasion, and tumor budding. dMMR, deficient mismatch repair; FOLFOX, folinic acid (Leucovorin) + 5-fluorouracil (5-FU) + oxaliplatin (Elotaxin); CAPOX capecitabine (Xeloda) + oxaliplatin (Elotaxin); FOLFIRI folinic acid (Leucovorin) + 5-FU + irinotecan (CPT-11)); FOLFOXIRI folinic acid (Leucovorin) + 5-FU + oxaliplatin (Elotaxin) + irinotecan (CPT-11).

HYPOTHESIS AND AIMS

The tumor microenvironment is gaining momentum due to its contribution to cancer progression and therapy resistance. This tumor microenvironment has a direct crosstalk with tumor cells that involves the activation of different pathways that promote cell survival, invasion and migration, among others benefits.

Study 1. Idelalisib Interferes with the Crosstalk of Follicular Lymphoma and its Immune Microenvironment and Potentiates the Activity of Venetoclax

In FL, PI3K is a common denominator transducing the signaling from tumor-microenvironment crosstalk. Likewise, the Bcl-2 family proteins play a crucial role in the regulation of apoptosis in cancer cells.

Our hypothesis: PI3Kdelta targeting may interfere with tumor-microenvironment crosstalk while Venetoclax may target the tumor cells, thus representing a promising combination therapy that may improve FL outcome.

Aims:

-To characterize by gene expression profiling (GEP) the molecular effects of idelalisib in this primary FL co-culture system with follicular dendritic cells (FDC), and identify the potential mechanism of resistance

- To delineate the effects of PI3K in FL immune microenvironment

-To analyze the combinatorial effect of idelalisib with the BCL-2 inhibitor ABT-199 in the presence of FDC and M2 macrophages

Study 2. GPCRs heterodimers as a new therapeutic target in colorectal cancer

In CRC, GPCRs have an important role in cancer growth and in the regulation of the angiogenesis, invasion, migration and survival in metastatic sites. In addition, tumor or stromal cells from the microenvironment may secrete GPCR ligands.

Our hypothesis: targeting the heterodimerization of GPCRs (CXCR4 and CB_2) that are biologically relevant in cancer can be an effective way to reduce proliferation and dissemination.

Aims:

-To characterize CXCR4 and CB_2 receptor expression and heterodimer formation in CRC

-To decipher the functional role of CXCR4- CB_2 heterodimers

-To analyze the potential as cancer therapeutic agent in vitro and in vivo models of single compounds (CXCR4 and CB_2 inhibitors).

METHODS

Study 1: Idelalisib and Venetoclai in FL

1. Patient samples

Primary FL cells isolated from lymph nodes or peripheral blood of 34 patients (see clinical characteristics in Table 15), diagnosed according to the World Health Organization (WHO) classification criteria were used. Written informed consent was obtained in accordance with the Ethics Committee of the Hospital Clínic, University of Barcelona and the Declaration of Helsinki. Mononuclear cells were isolated by gradient centrifugation on Ficoll (GE healthcare) and used fresh or cryopreserved in liquid nitrogen in RPMI 1640 containing 10% DMSO (Sigma-Aldrich) and 60% heat-inactivated fetal bovine serum (FBS; Life Technologies) and conserved within the Hematopathology collection of our institution (IDIBAPS-Hospital Clínic Biobank). The percentage of tumor cells was evaluated by flow cytometry as $CD20^+$ $CD10^+$ showing light chain restriction lymphocytes. FL primary samples were cultured in RPMI 1640 (Life Technologies) supplemented with 10% FBS, 2 mM L-glutamine, 50 μg/mL penicillin/streptomycin and were maintained in a humidified atmosphere at 37ºC containing 5% CO_2.

2. FL microenvironment models

For the co-cultures with follicular dendritic cell line (FDC), the HK non-immortalized cell line generated from normal tonsils was kindly provided by Dr. Yong Sung Choi[600] was cultured in IMDM medium supplemented with 20% FBS, 2 mM L-glutamine, and 50 μg/mL penicillin/streptomycin (all from Life Technologies).

M2-macrophages were generated from monocytes isolated from buffy coats of healthy donors (Banc de Sang i Teixits (BST Barcelona)) previously enriched by Rosette Sep (Human monocyte enrichment cocktail, from Stem Cell) and followed by differentiation with 20ng/ml M-CSF for 7 days. FDC or macrophages cells were seeded on day 0, and FL cells (1-2 x10^6cells/mL) were added the following day onto confluent stroma layers at 1:20 ratio (FDC:FL) and 1:4 (M2:FL) and cultured for the times indicated in the presence or absence of Idelalisib (Gilead Sciences).

Table 15. FL patient characterictics.

Study label	Sex/ Age	Histol. Grade	Ann Arbor stage	FLIPI	Disease status	Genomic alterations	Initial Therapy	DFS (years)	Num. of Relapsed	Progression
FL1	M/71	2	IV	I	D	na	R	6	0	no
FL2	M/77	na	na	na	na	1,2,3	na	na	na	na
FL3	F/83	2	III	I	D	1,2,3	R	5	0	no
FL4	M/65	2	I	L	D	1,2,3,5	R	5	0	2th neo
FL5	F/73	2	IV	H	D	na	R-Lena	1	1	no
FL6	M/80	2	IV	I	D	1	R-Benda	2	0	no
FL7	M/73	2	IV	H	D	1,3	R-Benda	mon	2	yes
FL8	M/75	2	I	L	D	1,2,3,6	CFM-PDN	2	0	no
FL9	M/69	2	IV	H	D	1,2,3,9	R-CHOP	2	0	no
FL10	F/55	3a	IV	H	D	1,3,4,7,8	R-CHOP	mon	2	yes/death
FL11	M/50	2	II	L	D	1,3,5,8	R-CHOP	5	1	1st rescue
FL12	F/73	3a	III	I	D	2	R-CHOP	3	1	yes/death
FL13	F/60	2	IV	I	D	3,6	R-FCM	14	0	no
FL14	F/70	2	I	L	R	1,3	RX	3	1	yes
FL15	F/54	2	IV	L	D	1,4	R-CHOP	1	0	no
FL16	M/54	2	IV	H	D	1,3,7,9	FCM	5	1	no
FL17	F/69	2	IV	I	D	3,5	R-CHOP	5	0	no
FL18	M/58	3a	IV	L	R	1	CHLORAM	10	1	no
FL19	M760	2	IV	L	D	2,3,7	R	1	1	no
FL20	F/66	1	IV	I	R	1,3	CHOP	mon	1	yes
FL21	F/50	2	IV	L	D	3	FCM	17	0	no
FL22	M/70	2/3	IV	I	R	1,2,3	RX	3	1	2th neo
FL23	M/50	1	I	L	R	3	CHOP	6	1	no
FL24	F/80	2	III	H	D	1,2,3,4,6	R-CHOP	13	0	no
FL25	F/32	2	IV	I	D	1,2,3	R-CHOP	1	0	no
FL26	M/53	3a	IV	I	R	2,3,4	R-CHOP	4	2	2th rescue
FL27	F/59	2	IV	I	R	1,2,3	R-CHOP	5	2	2th rescue
FL28	F/59	2/3	IV	H	D	no data	R-CHOP	14	0	no
FL29	M/56	2	IV	I	R	1,2,3,6	R-CHOP	1	2	2th rescue
FL30	F/66	1	IV	H	D	no data	R-CHOP	1	0	no
FL31	M/60	1/2	III	I	D	1,3,5,6,7	R-CHOP	1	0	no
FL32	F/77	3	IV	H	D	7	R-CHOP	2	0	no
FL33	M/57	1	IV	I	R	no data	R-CHOP	2	1	no
FL34	F/	2	na	na	na	1,2,3,6	na	na	na	na

Grade was evaluated by two different pathologists; FLIPI: Follicular Lymphoma International Prognostic Index: >3 high-risk (H), 2 intermediate risk (I), and 0-1 low-risk (L); Samples are obtained at D: diagnosis, or R: relapse; Somatic mutations identified by NGS: (1) CREBBP, (2) TNFRSF14, (3) KMT2D, (4) EP300, (5) MEF2B, (6) EZH2, (7) TNFAIP3, (8) TP53, and (9) RRAGC. Initial therapy consisted of R: Rituximab; Lena: Lenalidomide; Benda: Bendamustine; CFM: Cyclophosphamide; PDN: Prednisone; CHOP: Chemotherapy combination of Cyclophosphamide, Hydroxydaunorubicin, Oncovin and Prednisone; FCM: Chemotherapy regimen composed of Fludarabine, Cyclophosphamide and Mitoxantrone; RX: Radiotherapy; or Chlorambucil. DFS (Disease free survival) is referred to time passed from initial therapy to first relapse.

3. Gene expression profiling (GEP) and data meta analysis

Total RNA was isolated from FL cells, previously purified using CD20 magnetic beads (Miltenyi), using the TRIzol reagent (Life Technologies) followed by a cleaning step using the RNAeasy kit (Invitrogen). RNA integrity was examined with the Agilent 2100 Bioanalyzer (Agilent Technologies). Only high quality RNA was then retrotranscribed to cDNA and hybridized on HGU219 microarray. All samples were simultaneously run in a GeneTITAN platform (Affymetrix). For the identification of differentially expressed genes, MEV platform (v4.9) and Rank Products test were used, applying a paired analysis with False Discovery Rate (FDR)≤0.05. Multiplot Studio Tool v.1.1 was used to plot differences between FL patients in Idelalisib response.

Gene Set enrichment Analysis (GSEA) v2.0 (Broad Institute) interrogating C2, C3, GO and Hallmark 0.5 gene sets from the Molecular Signature Database v2.5, and experimentally derived custom gene sets[601]. A two classes analysis with 1000 permutations of gene sets and a weighted metric was used. Bonferroni correction for multiple testing was applied and only gene sets with FDR ≤0.05 and a normalized enrichment score (NES) of ≥1.5 were considered significant. The leading edge genes were displayed using Morpheus (https://software.broadinstitute.org/morpheus).

4. Targeted Next Gene Sequencing (NGS)

We performed NGS of 10 genes (TNFRSF14, CREBBP, TP53, MEF2B, RRAGC, EP300, KMT2D, EPHA7, TNFAIP3 and EZH2), targeting all exons and their flanking regions. Libraries were generated using HaloPlex HS target enrichment system (Agilent technologies, Santa Clara, CA; following the manufacturer's protocol) with an input of 60 ng of genomic DNA. Libraries were sequenced in a MiSeq instrument (Illumina, San Diego, CA) in a paired-end run of 150 bp.

<u>Bioinformatics analysis</u>

The variant calling was performed using an updated version of our in-house pipeline[602]. Briefly, quality control and trimming of the raw sequencing reads was done using the FastQC (v0.11.5) and Surecall Trimmer (v4.0.1) algorithms, respectively. Trimmed reads were aligned to the GRCh37/hg19 human reference genome using the Burrows-Wheeler Aligner-MEM algorithm (v0.7.17)[603]. Base quality score recalibration and indel realignment steps were subsequently performed according to the GATK Best Practices (GATK, v3.8)[604,605]. The mean coverage obtained was 2585x, with 96% of the

target region covered at >100x (Samtools (v1.6)[606], custom scripts). The variant calling was done in parallel using VarScan2 (v2.4.3)[607], Mutect2 (GATK, v4), VarDict (v1.4)[608], and deep SNV-shearwater (v1.24.0)[609]. The post processing fpfilter was used to filter the mutations detected by VarScan2. All variants detected by any of the variant callers were combined and annotated using SnpEff and SnpSift (v4.3)[610,611]. Finally, a custom script was applied to filter out recurrent artifacts, low quality, low variant allele frequency (VAF <2%), intronic and synonymous variants. Polymorphisms described in the Single Nucleotide Polymorphism Database (dbSNP149) with a European population frequency higher than 1% (1000 Genomes Project database) were also excluded. All programs were executed following the authors' recommendations.

5. ELISA cytokine quantification

CCL22, IL-10, VEGF-C were determined using specific Raybiotech ELISA Kits, and VEGF-A was evaluated by Mini TMB ELISA Development from Peprotech. Cytokines levels were assessed in duplicates in supernatants harvested from FL primary cells ($2x10^6$ cells/mL) from monocultures or co-cultures. A standard curve was generated for each cytokine, and mean absorbance for each set duplicate were interpolated and transformed into concentrations. The optical density at 450nM was analyzed in a spectrophotometer (Synergy Bio-tek Instrument).

6. HUVEC tube formation assay

Human umbilical vein endothelial cells (HUVEC) were kindly provided by Dr Maria C. Cid and were cultured as previously described[612]. Supernatants from FL primary cells ($2x10^6$ cells/mL) were harvested after 48 hours of incubation with/without (w/wo) Idelalisib in co-culture with FDC or monoculture. 24-well plates were coated with Matrigel (Becton Dickinson) and allowed to polymerize for 45 minutes at 37ºC. Afterwards, the supernatants of interest were mixed (1:1) with HUVEC cells ($4x10^4$ cells) in HUVEC medium (RPMI 1640 medium that contains 25% of Bovine Calf Serum(HyClone), 150 µg/ml medium endothelial cell growth supplement (ECGS) (BD Bioscience), and 4U/ml medium of sodium heparin salt(AppliChem)) and incubated for 24 hours. Photos were taken at x40 magnification in a DMIL LED Leica microscope coupled to a DFC295 camera and analyzed with Suite v 3.7 software (Leica). Then, the number of nodes and junctions was quantified in 5 randomly chosen fields using the Image J software (angiogenesis analyzer plugin).

7. Adhesion assay to HUVEC cells

HUVEC cells were plated in 96 wells plate at final concentration of $1x10^5$cells/well. in HUVEC medium and incubated overnight (ON) with TNF-α (10ng/ml) (R&D System). Otherwise, FL co-cultured with FDC w/wo idelalisib were recovered after 48 hours of incubation and were counted and labeled with 1 μM Calcein, AM (Invitrogen) for 30 minutes at 37ºC. After washing twice the cells with PBS, $1x10^5$ cells/well were seeded in a plate containing activated HUVEC cells for 3hours with RPMI 1640 medium at 37ºC. Then, the plate was washed extensively with RPMI 1640 to remove non-adhered cells. Adhered cells were lysed with 1% Triton X-100, supernatant was transferred into black plates (Thermo Scientific, Nunc) and fluorescence was measured in a spectrophotometer (Synergy Bio-Tek Instrument) (excitation filter: 485 ± 20 nm; band-pass filter: 530 ± 20 nm). Data were expressed as relative fluorescent units (RFU) after subtraction of non-specific adhesion (empty well).

8. Transendothelial migration

HUVEC cells ($0.2x10^6$ cells/well) were seeded on gelatin 0.1% coated transwells (Costar) and incubated ON with TNF-α (10ng/ml). The next day, $0.5x10^6$ FL cells coming from 48 hours of FDC co-culture w/wo idelalisib were seeded into transwells with the endothelial monolayer in RPMI 1640 medium with 10% FBS, and were allow to migrate for 6 hours in a gradient of FBS. (RPMI medium + 20% FBS) $CD20^+$ cells crossing HUVEC barrier were counted by flow cytometer (Attune Classic Acoustic Focusing Cytometer (Life technologies)).

9. T cell migration assays

Freshly tonsils were minced and mechanically disaggregated in RPMI 1640 medium with piston syringe and 70um Nylon Cell strainer (Falcon), then samples were purified using Ficoll gradient to obtain PBMCs. PBMCs from freshly tonsils and healthy donors were enriched in T cells (depletion of B cells and monocytes). Migration of T cell subpopulation ($0.2x10^6$ cells/well) was evaluated in 24-well chemotaxis chambers containing 5 μM pore size inserts (Corning, Life Science) to supernatants of 48h HK (FDC) co-cultures w/wo idelalisib. Cells migrated for 3h, and then Attune flow cytometer was used to count the cells. Treg cells ($CD4^+$, $CB25^+$ and $FOXP3^+$) from blood were selected; T_{FH} cells ($CD4^+$, $CXCR5^+$, $CD25^-$) and T_{FR} cells ($CD4^+$, $CXCR5^+$, $FOXP3^+$) from tonsil were selected too. Cell viability from these selected cells were assed using Live/Dead Fixable Aqua Dead Cell Stain kit (Invitrogen). Net migration was used to evaluate the migration.

$$\text{Net migration} = \frac{\text{num of migrate cells (subpopulation)} - \text{num of cells of the same subpopulation from Neg Ctrl}}{\text{num of cells of the same subpopulation from the input}}$$

Neg Ctrl = Negative controls. Migration vs medium+ 0.5% BSA

10. iBH3 profiling

BH3 profiling assesses the dependence of a certain cell on a specific anti-apoptotic BCL-2 protein. As we explained previously, the intrinsic pathway of apoptosis is regulated at the level of the mitochondria where different members of the BCL-2 family of proteins interact to make this life or death decision. The apoptosis induced by therapeutic agents often involves changes in the levels and interactions of BCL-2 family members. BH3 profiling relies on our understanding of how several broad groups of BCL2 family members interact with each other. The iBH3, or intracellular BH3, method relies on the quantification of retained cytochrome c as measure of how close is a cell to death, the so-called priming. A thorough method explanation and complete protocols, as buffers preparations could be find in https://letailab.dana-farber.org/bh3-profiling.html).,

FL cells were co-cultured with FDC or M2 w/wo idelalisib for 24h in a cell density of 2x10^6 cells/ ml. First, isolated FL cells were stained using Live/Dead Fixable Aqua Dead Cell Stain kit for 30min. Cells were washed with PBS +2% of FBS. Then cells were labeled with CD19-PE (BD Bioscience) for 30 min. Again, cells were washed with PBS +2% of FBS. At this point, cells were placed in 96 wells plate, resuspendend in MEB Buffer (1x10^5 cells/well), permeabilized with 0.002% digitonin, and exposed to peptides for 1 hours at room temperature (RT). At this time, 4% of Formaldehyde were added and incubated for 10 min at RT. Then N2 buffer is added to neutralize the formaldehyde and terminate fixation at least for 5 minutes. Next, cells were incubated with anti-cytochrome c antibody (Biolegend) in 1:40 dilution (in 10X CytoC Stain Buffer) ON at 4ºC. Finally, cytochrome c release was analyzed by flow cytometer in viable and CD19$^+$ cells, and then calculated using the next formula:

$$\% \, Cytochrome \, c \, loss = 1 - \frac{MFISample - MFIPos \, Ctrl}{MFINeg \, Ctrl - MFIPos \, Ctrl}$$

Pos Ctrl = Positive release controls. Alamethicin
Neg Ctrl = Negative release controls. DMSO

Peptides and/or small molecules are the heart of the assay. Because of their unique interaction patterns (a summary of these interactions can be found in table 16), the BH3 peptides make it possible to determine priming class and subclass. The relative response of mitochondria to a fixed dose or a series of doses allows priming to be ranked across cell types or primary samples.

Table 16. EC50 of BH3-only peptides to N-terminal GST

	BIM	BAD	NOXA	HRK	FS-2[613]
Bcl-2	<10	11 (3)	-	-	-
BcL-xL	<10	<10	-	92 (11)	-
Bcl-w	38 (7)	60 (19)	-	-	-
Mcl-1	<10	-	19 (2)	-	-
Bfl-1	73 (3)	-	-	-	<10

C-terminal truncated anti-apoptotic proteins Values listed are in nM. Grayed values are greater than 1 µM.

11. Flow cytometry

Cells were seeded in co-culture or monoculture w/wo idelalisib and Venetoclax (Selleck Chemicals) as single agents or in combination for 72 h. Drugs cytotoxicity was evaluated by staining FL cells with CD19-PE (BD Bioscience), including Annexin V-FITC (eBioscience) and 7-Aminoactinomycin D (7AAD) (Sigma). Finally, cells were acquired and analyzed by flow cytometry. FL viable cells were identified as $CD19^+$, Annexin V-FITC$^-$ and 7AAD$^-$.

12. Western blot

FL pellets were lysated and proteins were extracted with RIPA buffer (Sigma-Aldrich) completed with protease and phosphatases inhibitors to perform Western blot analysis. Proteins extracts were quantified using the Lowry reagent (DC Protein Assay, BioRad). Next, protein samples were resolved by 12% SDS-PAGE gels, and electroblotted onto a PVDF membranes (Immobilon-P, Millipore). Membranes were blocked in Tris-buffered saline and 0.1% Tween 20 (TBST) with 5% powdered milk for 1h. Then, membranes were incubated with primary antibodies diluted in TBST with 5% BSA overnight at 4ºC. Finally, membranes were visualized on a mini-LAS4000 device (Fujifilm) by enhanced chemiluminescence (ECL, Amersham Life Science). Densitometry analysis of bands was performed with Multi Gauge V3.0 software (Fujifilm, Tokio). Data was represented using the control conditions as a reference.

Table 17. Antibody used for Western Blot analysis.

Primary Antibody	Species	Reference	Dilution	Source
Bcl-xL (54H6)	Rabbit	2764	1/1000	Cell signalling
Mcl-1(s-19)	Rabbit	sc-819	1/500	Santa Cruz
Bfl-1	Rabbit	ABC498	1/1000	Millipore
α-tubulin	Mouse	T5168	1/5000	Sigma Aldrich

13. Simple Western Methods (Peggy Sue)

FL cells were harvested in lysis buffer (Cell Signaling Technology) containing: Protease Inhibitor Cocktail (Roche Diagnostics Corp), and phosphatase inhibitor sets 1 and 2 (EMD Millipore). Following 30 minutes on ice, cell lysates were cleared by centrifugation at 12,500 RPM for 10 minutes at 4°C. Lysates were analyzed by Simple Western using Peggy Sue™ or Sally Sue™ (ProteinSimple, San Jose, CA) according to manufacturer's standard protocol. Data was processed using Compass software (ProteinSimple). The following antibodies were purchased from Cell Signaling Technology (Danvers, MA): p-AKT (S473) (#4058), pBAD (S112) (#9291), pBAD (S136) (#4366) and actin (#4968).

14. Statistical analysis

Unpaired and paired *T-tests* were used to assess differences between two groups using GraphPad Prism software 7.0.

Study 2: GPCRs heterodimers in CRC

1. Cell lines and patient samples

1.1. CRC cell lines and cell cultures

SW480, SW620, Colo320, HT29, DLD1 and HCT116 were obtained from American Type Culture Collection (Manassas, VA, USA), and were cultured in RPMI 1640, DMEM-F-12 or McCoy 5A medium supplemented with antibiotics 1% pencillicin/streptomycin (10.000 Units/ml Pencillicin, 10.000 µg/ml streptomycin) and 10% fetal bovine serum (FBS) (all from Life Technologies). The cells were maintained at 37ºC in a humidified atmosphere with 5% carbon dioxide. Mycoplasma infection was routinely tested by PCR.

1.2. Generation of SW620-GFP+/Luc+ (Cell transduction)

SW620 cells were transduced by retrovirus infection of LPNIG plasmid to generate a stable green fluorescence protein (GFP) and luciferase (Luc) expressing cells. Phoenix cells were used to generate the retrovirus supernatants. These cells were transfected with X-tremeGENE HP DNA transfection reagent (Roche) in 3:1 (reagent, DNA). Supernatant containing the virus was collected after 3 days, filtrated (0.4 µm) and then concentrated (ultracentrifugation in Sorval during 2h at 12ºC). After the centrifugation, the viral pellets were concentrated 100 times with PBS and added to the SW620 cells. Then cells were treated with 1 mg/ml of Neomycin (G 418 (sigma)) antibiotic for 1 week for a first selection, and then were flow-sorted by fluorescence-activated cell sorting using FACS Aria cell sorter (BD Bioscience) recovering 5% of GFP^{+++} cells. Luciferase expression was assayed *in vitro* using the luciferase assay system (Promega).

1.3. Patient samples: Tissue MicroArray (TMA)

Colorectal primary tumors, metastasis and normal mucosa that form TMA samples were cases operated on the Hospital Clínic de Barcelona between 2005 and 2012. This resulted in 10 series of 99 different patients. A tissue microarray (TMA) was constructed using multiple normal mucosa and tumor punches taken from formalin-fixed paraffin-embedded blocks (FFPE) using a tissue cylinder with a diameter of 1 mm. Those punches were transferred into one recipient paraffin block (20 x 15 mm) using a semi-automated tissue arrayer. Four cores were obtained from the tumor center, four cores from the invasive tumor front and one from the normal adjacent mucosa. All patients signed

the corresponding informed consent form, and the Hospital Clinic Ethic Committee (IRB).approved the sample collection. Complete histopahological and clinical information were available.

2. Immunohistochemistry

2.1. TMA samples

Tissue sections from TMA were subjected to citrate buffer (pH6) antigen retrieval for 20 minutes before to exposure to immunohistochemical staining using primary antibody against CXCR4 receptor (1/600) or primary antibody against CB_2 receptor (1/500) for 1h at room temperature. Immunodetection was performed using automated immunostainer system (Bond maX Processing Modul, Vision Biosystems, Leica) with DAB for 8 minutes at room temperature as the chromogen. Preparations were scanned on VENTANA iScan HT slide scanner (Roche Diagnostics), and then images were processed using Virtuoso v.5.6.2 Software. For the evaluation of the expression of both antibodies, cases were scored as 0 (no staining, only at CXCR4 staining samples), 1 (weak staining), 2 (moderate staining), or 3 (high staining). CXCR4 and CB_2 staining was scored by two independent pathologists from Hospital Clínic de Barcelona on U-DO3 microscope (Olympus, Tokyo, Japan). In order to evaluate all samples together, scores were divided into low expression (scores 0 and 1), or high expression (scores 2 and 3).

2.2. In vivo samples

Xenograft tumor samples from liver, lung and cecum, were subjected to fixation in 4% paraformaldehyde for at least 8h, and then incubated with 30% ethanol solution until paraffin-embedded blocks performance. Paraffin-sections on silane-coated slides were exposed to immunohistochemical staining using anti-Ki-67 (clone 30-9, ready to use Roche), or subjected to hematoxylin and eosin staining in Tissue-Tek® Prisma™ automated slide stainer (Sakura) and were evaluated on BX41 microscope (Olympus, Tokyo, Japan).

3. In situ Proximity Ligation Assay (PLA)

Cells were grown on Poly-L-Lysine Cellware glass coverslips (Corning) and fixed in 4% paraformaldehyde, and then permeabilized with 0.1 % Saponin buffer (PBS +10% FBS). CXCR4-CB_2 heteromers were identified using the Duolink In Situ PLA detection kit (Olink, Bioscience). The cells

were incubated at 37ºC for 1h with the blocking solution of the kit in a preheated humidity chamber, after that, cells were incubated overnight in the antibody dilution medium containing the mouse anti-CXCR4 antibody (1:200, BD) and rabbit anti-CB$_2$ antibody (1:100, Cayman chemical). Then, cells were incubated with a mixture of equal amounts of secondary antibody anti-mouse coupled directly to a DNA minus chain and anti-rabbit coupled directly to a DNA plus chain. Next, cells were incubated in a preheated humidity chamber for 30 min at 37ºC with the ligation solution from the kit to induce anneling and ligation of the two DNA probes. Amplification was done with the Duolink Detection Reagents Red kit, which contains Texas Red fluorescence nucleotides. Finally, the cells were mounted using mounting medium with DAPI from the kit. This technique requires both receptors to be close enough (<17 nm) to allow the two DNA probes from the secondary antibodies to be able to ligate[614].

1. Proximity probe binding   2. Circularization and ligation of connector oligonucleotides   3. Rolling circle amplification   4. Detection of rolling circle product
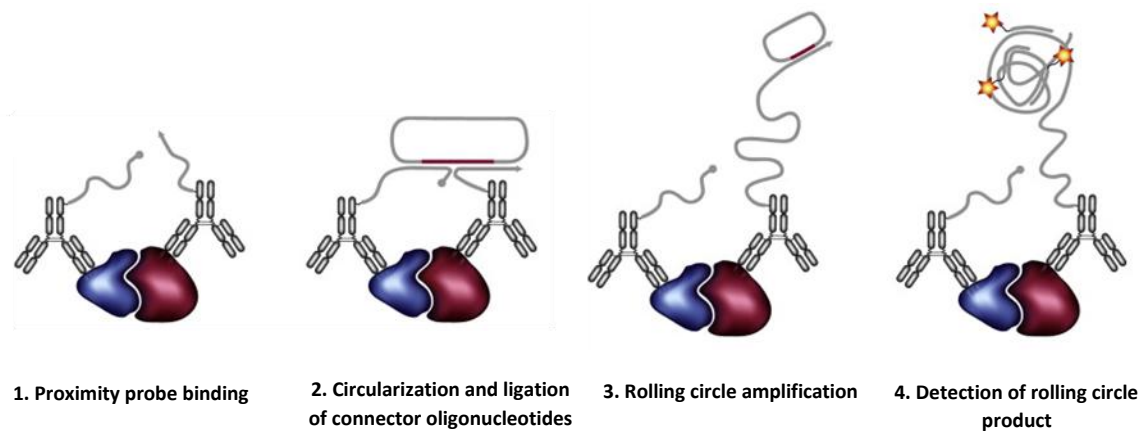
Figure 15. PLA functional scheme.

If both receptors are enough closer, a punctate red fluorescent signal can be detected by confocal microscopy.

4. Confocal microscopy

The samples were observed under a Leica TCS SP5 laser scanning confocal microscope (Leica Microsystems Heidelberg GmbH, Manheim, Germany) equipped with a DMI6000 inverted microscope, blue diode (405nm), Argon (458/476/488/496/514), diode pumped solid state (561nm) and HeNe (594/ 633nm) lasers, and APO 63x oil (NA 1.4) immersion objective lenses was used at the Unitat de Microscòpia Òptica Avançada (Centres Científics i Tecnològics , Universitat de Barcelona).DAPI and Alexa Fluor 633 images were acquired sequentially using 405, and 633 laser

lines, AOBS (Acoustic Optical Beam Splitter) as beam splitter and emission detection ranges 415-480 and 643-680nm respectively and the confocal pinhole set at 1 Airy units. Simultaneously, bright field transmitted light images were acquired. Sections were acquired at a 1µm step size. Images were acquired at 600 Hz in a 1024 x 1024 pixels format, zoom at 3 and pixel size of 60 x 60 nm. Finally, acquired images were processed counting red fluorescence dots signals with ImageJ software.

5.Image Analysis

5.1 Cell lines PLA

In order to analyze PLA signals on cells automatically, a macro of instructions was written to be executed in the open source software ImageJ (Wayne Rasband, NIH, USA) [615]. First, in order to determine PLA particles, PLA stack images (red channel) were projected along z axis with maximum intensity method, Gaussian Blur filtered (sigma 0.5). Local background was subtracted from PLA labelling regions and labelled particles were segmented by intensity thresholding (Li AutoThreshold)[616]. Salt and pepper noise was removed by median filtering (radius 1). Second in order to separate close PLA structures, Find Maxima command was used to determine local maxima were (noise tolerance 10) and creates a watershed segmented particles binary image Minimum operation between intensity thresholded PLA image and segmented particles image allows to encode a new image with the limits between PLA structures. Finally, cells were drawn manually by the user from Bright Field Image and Area and number of PLA structures were measured from each cell.

5.2 TMA samples PLA

In order to analyze PLA signals on tissue automatically, a macro of instructions was written to be executed in the open source software ImageJ. First, in order to determine cellular regions, DAPI image was mean filtered (radius 2), intensity thresolded (Li autoThreshold method), and converted to a binary image. Small regions, not considered as cells, were size filtered with the Analyze Particles and excluded from the final quantification. A selection of the cells from the mask image was created and added to the ROI Manager. Next, in order to segment PLA structures, PLA image was Gaussian Blur filtered (sigma 0.5) and particles were determined as local intensity maxima that stand out from

neighbor pixels by more than a noise tolerance (4). Finally, PLA local maxima were counted on the cells selection.

6. Flow cytometry

Cells were detached using Cell stripper, a non-enzymatic cell dissociation solution (Corning). Immediately, 2×10^5 cells were used for each condition. For surface detections, fresh cells were stained with anti-CXCR4-PE, anti-CB$_2$-FITC label antibody, and Aqua Dead Cell stain in a buffer containing 10% of mouse serum and 10% of rabbit serum for 20 minutes. Moreover, for intracellular detection, cells were fixed in 4% paraformaldehyde, next permeabilized with 0.1 % Saponin buffer (PBS +10% FBS), and then stained with the same antibodies and buffer for 20 minutes also. Finally, cells were washed and resuspended in Attune 1x Focusing Fluid (Life Technologies), and a total of individualized 10.000 cells were acquired and analyzed on Attune Classic Acoustic Focusing Cytometer (Life technologies). Only life cells were evaluated, and Mean fluorescence ratio (MFIR) was calculated as the ratio between mean fluorescence intensity (MFI) of each sample and the MFI of fluorescence minus one (FMO) sample. FMO sample contained all the antibodies except the antibody that you are evaluating.

7. Determination of ERK1/2 phosphorylation levels

ERK1/2 (Thr202/Tyr204) phosphorylation levels were measured by Western Blot Cells were deprived ON in culture medium without FBS. Then were incubated for 3h with the drugs (100µM AMD3100 (Sigma) or 50µM JTE907 (Tocris)). After this 3 h, cells were stimulated with 200ng/ml of Human SDF-1α (CXCL12, Peprotech) or 50nM of JWH133 (Tocris) for 20 minutes. Finally, cells were washed with cold PBS and detached from the plate with a scraper.

8. Western blot

Cells pellets were lysated and proteins were extracted with Triton buffer (20nM Tris-Hcl pH7.6, 0.15 M NaCl, 1M EDTA, 1% TritonX-100 (Sigma-Aldrich)) completed with protease and phosphatases inhibitors to perform Western blot analysis. Proteins extracts were quantified using the Lowry reagent (DC Protein Assay, BioRad). Next, protein samples were resolved by 4% to 12% precast SDS-

PAGE gels (NuPAGE gels, Life Technologies) and electroblotted onto a PVDF membranes (Immobilon-P, Millipore). Membranes were blocked in Tris-buffered saline and 0.1% Tween 20 (TBST) with 5% powdered milk for 1h. Then, membranes were incubated with primary antibodies diluted in TBST with 5% BSA overnight at 4ºC, anti-phospo-ERK1/2 antibody (Cell Signaling Technology), 2h at RT for anti-ERK1/2 (Santa Cruz) and 1h at RT for anti-α-tubulin (Sigma Aldrich) antibodies. Finally, membranes were visualized on a mini-LAS4000 device (Fujifilm) by enhanced chemiluminescence (ECL, Amersham Life Science). Densitometry analysis of bands was performed with Multi Gauge V3.0 software (Fujifilm, Tokio). Data was represented using the control conditions as a reference.

Table 18. Summary of antibodies used in the different technics.

Primary Antibody	Species	Reference	Dilution	Source	Use
CXCR4 PE Anti-Human (CD184)	Mouse	555974	1/20	BD Biosciences	Flow
CXCR4 clon 12GS Anti-Human	Mouse	555972	1/200	BD Biosciences	PLA
CXCR4 [UMB2] monoclonal	Rabbit	ab124824	1/600	Abcam	IHQ
CB2-FITC polyclonal	Rabbit	10010712	1/20	Cayman Chemical	Flow
CB2 receptor polyclonal	Rabbit	101550	1/100	Cayman Chemical	PLA
CNR2 polyclonal Anti-Human	Rabbit	PA1-744	1/500	Thermo Fisher (Pierce)	IHQ
phospo-ERK1/2 antibody	Rabbit	9101	1/1000	Cell Signaling Technology	WB
ERK 1 (K-23)	Rabbit	sc-94	1/500	Santa Cruz	WB
α-tubulin	Mouse	T5168	1/5000	Sigma Aldrich	WB

9. KRH -3955 synthesis

All air sensitive manipulations were carried out under a dry argon or nitrogen atmosphere. THF and CH2Cl2 were dried using a column solvent purification system. Analytical thin-layer chromatography was performed on SiO2 (Merck silica gel 60 F254), and the spots were located with 1% aqueous KMnO4 or hexachloroplatinate. Chromatography refers to flash chromatography and was carried out on SiO2 (SDS silica gel 60 ACC, 35-75 mm, 230-240 mesh ASTM). NMR spectra were recorded at 300 or 400 MHz (1H) and 100.6 MHz (13C), and chemical shifts are reported in δ values downfield from TMS or relative to residual chloroform (7.26 ppm, 77.0 ppm) as an internal standard. Data are reported in the following manner: chemical shift, multiplicity, coupling constant (J) in hertz (Hz),

integrated intensity, and assignment (when possible). Assignments are given only when they are derived from definitive two-dimensional NMR experiments (HSQC-COSY). IR spectra were performed in a spectrophotometer Nicolet Avantar 320 FT-IR and only noteworthy IR absorptions (cm-1) are listed. High resolution mass spectra (HMRS; LC/MSD TOF Agilent Technologies) were performed by Centres Científics i Tecnològics de la Universitat de Barcelona.

(Dipropylamino)butanenitrile (1)

Potassium iodide (1.55 g, 93.0 mmol) and potassium carbonate (12.2 g, 88.0 mmol) were added under an argon atmosphere at RT to a solution of dipropylamine (5.48 mL, 40.0 mmol) in dry acetonitrile (74 mL). The resulting mixture was heated to reflux and then a solution of bromobutyronitrile (10.0 g, 6.7 mL, 67.5 mmol) in dry acetonitrile (20 mL) was added dropwise. After 20 h at reflux, the reaction was cooled to RT, filtered, and evaporated under vacuum. The residue was diluted in an 1N aqueous hydrochloride acid solution (200 mL) and washed with diethyl ether (3 x 100 mL). The water layer was basified to pH 9 with an 1N aqueous sodium hydroxide solution and extracted with diethyl ether (3 x 100 mL). The combined organic extracts were dried over sodium sulfate, filtered, and concentrated under reduced pressure to give nitrile 1 as a yellow oil (8.85 g, 78%), which was used in the next reaction without further purification.

N,N-Dipropylbutane-1,4-diamine (2)

A solution of nitrile 1 (2.89 g, 17.20 mmol) in anhydrous THF (50 mL) was added dropwise at −78 °C and under an argon atmosphere to a solution of lithium aluminium hydride (636 mg, 16.7 mmol) in anhydrous THF (20 mL). The mixture was allowed to reach to RT and then stirred overnight. The excess of lithium aluminium hydride was hydrolyzed by the successively addition of distilled water (0.6 mL), a 10% NaOH solution (0.6 mL), and distilled water (1.8 mL). Sodium sulfate was added to the resulting mixture, and filtered through a Celite® pad. The resulting solution was concentrated under reduced pressure to give compound 2 as a yellow oil (2.93 g, 99%) which was used in the next reaction without further purification.

[4-(aminomethyl)phenyl]methanol (3)

Methyl 4-(aminomethyl)benzoate (2.0 g, 9.94 mmol) in anhydrous THF (30 mL) was added at 0°C dropwise under an argon atmosphere to a solution of LiAlH4 (756 mg, 19.4 mmol) in anhydrous THF (40mL). The reaction mixture was heated up to reflux for 4 h. The reaction was cooled to 0°C, and distilled water (756 uL), 15% NaOH solution (756 uL) and water (2.2 mL) were successively added.

Sodium sulfate was the added, the precipitate was filtered off using a Celite® pad, and the filtrate was concentrated under reduced pressure. Flash chromatography of the residue (from CH2Cl2 to 9:1 CH2Cl2/MeOH) afforded amino-alcohol 3 (1.07 g, 82%).

[4-(Phthalimidemethyl)phenyl]methanol (4)

N-Carbethoxyphthalimide (1.71 g, 7.8 mmol) and amine 3 (1.07 g, 7.8 mmol) were added at RT under an inert atmosphere into two neck flask containing MeOH (48 mL), and the mixture was stirred and degassed with argon for 30 min. Triethylamine (4.3 mL, 31.2 mmol) was added and, the resulting mixture was stirred at RT overnight. The solvent was removed by rotary evaporation and then the residue was treated with a 1 M solution of HCl (20 mL), and the mixture was extracted with ethyl acetate. The combined organic extracts were washed with 1 M HCl and distilled water, dried over NaSO4, filtered, and concentrated under reduced pressure. Flash chromatography (hexane to 1:2 hexane/EtOAc) afforded phthalimide 4 (1.68 g, 81%).

4-(Phthalimidemethyl)benzaldehyde (5)

MnO2 (1.09 g, 12. 6 mmol) was added at RT to a solution of alcohol 4 (334 mg, 1.26 mmol) in CH2Cl2 (20.0 mL). After being stirred at RT for 20 h, the reaction mixture was diluted with Et2O (20 mL) and filtered through a pad of Celite®. The filtrate was concentrated under reduced pressure. Flash chromatography of the residue (hexane to 1:1 hexame/EtOAc) afforded aldehyde 5 (310 mg, 93%).

Phthalimide derivativa (6)

Aldehyde 5 (4.83 g, 18.2 mmol) was added under an argon atmosphere at 0 ºC to a suspension of primary amine 2 (4.07 g, 23.6 mmol) and anhydrous sodium sulfate (5.1 g, 36.4 mmol) in MeOH (100 mL), and the resulting mixture was stirred for 24 h at RT. The reaction was filtrated through a Celite® pad, and the filtrated was concentrated under reduced pressure to give an imine derivative, which was used in the subsequent step without further purification. A solution of di-tert-butyl dicarbonate (8.8 g, 40 mol) in anhydrous MeOH (20 mL) and Pd/C (850 mg) were added to a solution of the above imine in anhydrous MeOH (40 mL), and the resulting mixture was stirred under a hydrogen atmosphere at RT overnight. After this time the suspension was filtered over Celite® and the solvent was evaporated under reduced pressure. Flash chromatography of the residue (from 2:1 hexame/EtOAc to EtOAc) afforded N-Boc derivative 6 (5.5 g, 58%).

Tert-Butyl (4-(aminomethyl)benzyl)(4-(dipropylamino)butyl)carbamate (7)

A solution of methylamine (40 wt % in water, 26 mL) were added at RT to a solution of N-Boc derivative 6 (2.6 g, 4.98 mmol) in MeOH (26 mL), and the mixture was stirred overnight at 50 ºC. The resulting mixture was concentrated under reduced pressure, and the excess of MeNH2 and water was removed under high vacuum rotavapor. CH2Cl2 and sodium sulfate were added to the residue, and the mixture was filtered and concentrated under reduced pressure affording deprotected amino derivative 7 (quantitative), which was used directly in next step without further purification.

Tert-Butyl carbamate derivative (8)

1H-Imidazole-2-carbaldehyde (413 mg, 4.3 mmol) was added at 0 ºC under an argon atmosphere to a suspension of primary amine 7 (4.98 mmol) and anhydrous sodium sulfate (1.4 g, 10.12 mmol) in MeOH (50 mL). The reaction was allowed to stir overnight at RT after which it was filtered through a Celite® pad, and the filtrated it was concentrated under reduced pressure. The residue was solved in anhydrous MeOH (50 mL) and a solution of sodium cyanoborohydride (405 mg, 6.4 mmol) in methanol (3 mL) was added at 0 ºC under an argon atmosphere to the reaction. The resulting mixture was then allowed to stir for 20 h. The reaction was concentrated under reduced pressure, and the resulting yellow oil was dissolved in water and extracted three times with CH2Cl2 (50 mL). The combined organic extracts were washed with brine, dried over anhydrous sodium sulfate, filtered and concentrated. Flash column chromatography (Biotage® SNAP KP-NH, from 1:9 hexane/EtOAc to EtOAc) afforded imidazole derivative 8 (890 mg, 38%).

Tert-Butyl carbamate derivative (9)

1-methyl-1H-imidazole-2-carbaldehyde (45 mg, 0.418 mmol) was added at 0 ºC under an argon atmosphere to a suspension of secondary amine 8 (160 mg, 0.31 mmol) and anhydrous sodium sulfate (142 mg, 1.0 mmol) in anhydrous MeOH (5 mL). The reaction was stirred at RT for 8 h. A solution of sodium cyanoborohydride (36 mg, 0.57 mmol) in MeOH (1 mL) was added at 0 ºC under argon atmosphere to the reaction, and the resulting mixture was stirred at room temperature for 20 h. The mixture was filtered through a Celite® pad, and the filtrated it was concentrated under reduced pressure. The resulting yellow oil was dissolved in water and extracted three times with CH2Cl2 (5 mL). The combined organic extracts were washed with brine, dried over anhydrous

sodium sulfate, filtered and concentrated. Flash column chromatography (Biotage® SNAP KP-NH, 1:9 hexane/EtOAc to EtOAc) afforded imidazole derivative 9 (104 mg, 60%).

KRH-3955 derivative (10)

TFA (1.0 mL) was added at RT under an argon atmosphere to a stirring solution of N-Boc derivative 9 (110 mg, 0.19 mmol) in anhydrous CH_2Cl_2 (1.0 mL), and the solution was stirred at this temperature for 4 h. Saturated solution of $NaHCO_3$ was then added and the resulting mixture was extracted with CH_2Cl_2. The combined organic extracts were dried over sodium sulfate, filtered and concentrated under reduced pressure to afford deprotected amine (86 mg, 95%).

In summary, the synthesis of the monomer **KRH-3955**-linker starts with the preparation of diamine **2** (two steps, 77% overall yield) and aldehyde **5** (three steps, 62% overall yield).
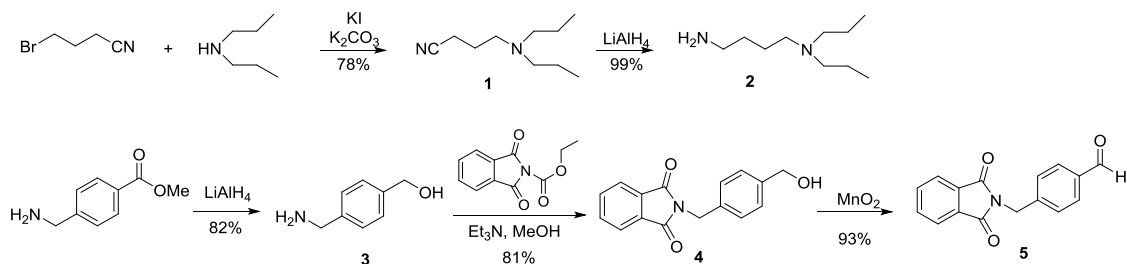
Next, the reductive amination between **A** and **B** was satisfactorily accomplished in presence of Boc_2O using H_2 as the reductive reagent, directly affording compound **C** in 58% yield.
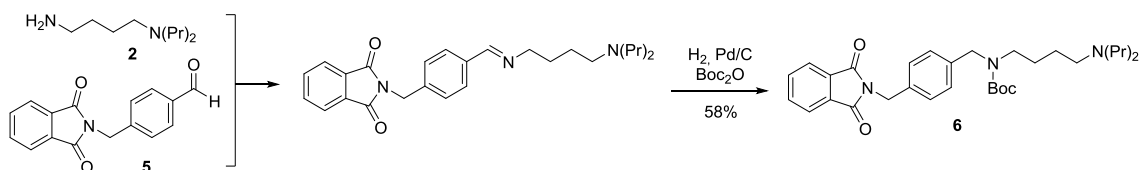
Finally, the phathalimide deprotection was accomplished with aqueous methylamine and the resulting primary amine was submitted to two consecutive reduction aminations under usual conditions ($NaCNBH_3$ as a reductive agent) for the incorporation of the imidazole rings.
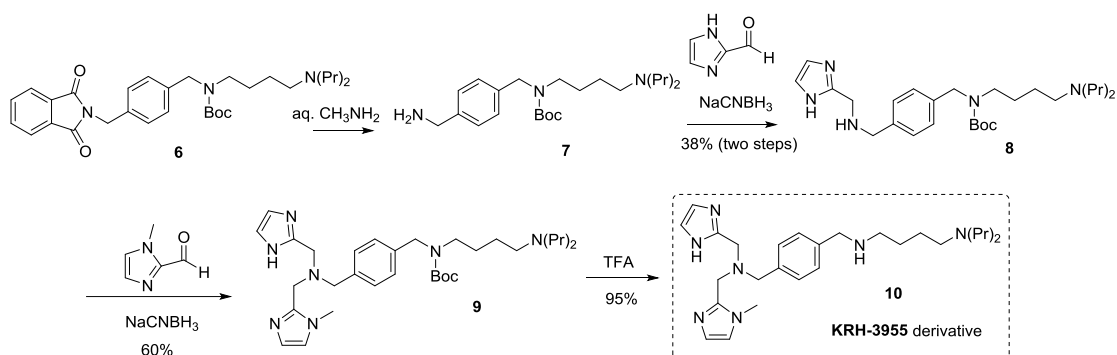
10 Wound-healing assays

The wound-healing (scratch) assay was performed using IncuCyte®S3 Live-Cell Analysis System. A total number of $6x10^4$ cells per well were seeded in a 96-well plate and allowed to adhere overnight. When cells were confluent, they were treated with mitomycin (Sigma-Aldrich) for 1 h at 37°C. Next cells were washed with saline solution to remove completely mytomycin. Mytomicin inhibit cell proliferation for 48 hours. Wound Maker tool from IncuCyte® was used to create straight-line wound area. Wells were washed twice with saline solution again to remove detached cells to avoid reattach of these cells into the wound area. Finally, 100µl of complete medium containing treatments and stimulators were added in each well. Wells containing only complete medium were used to normalized all the other conditions. Cells seeded in wells containing CXCL12 stimuli (200ng/ml of Human SDF-1α (Peprotech)) were used as a positive migration control. In the rest wells, drugs were added to prove its modulator power in cell migration induced by CXCL12 100µM AMD3100 (Sigma), or 10µM KRH-3955 (synthesized), or 50µM JTE907 (Tocris), or both 10µM KRH3955 and 50µM JTE907. Migration was monitored by acquiring images every 2 hours using IncuCyte® system for 42 hours. Images were analyzing by IncuCyte® Scratch Wound Cell Migration Software Module to determine the wound closure area.

1. SEED CELLS **2. CREATE WOUND AREA** **3. ADD TREATMENT**

Plate cells (100µl/well, 60.000 cells/well) and allow to adhere overnight

Wound confluent cell monolayer using a 96-well Wound Maker.

Add treatments and stimulis (100µl/well) and image in the IncuCyte® system.
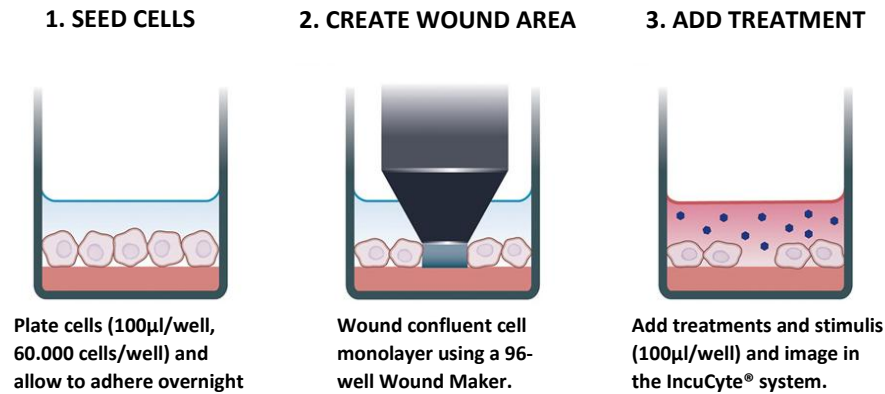
Figure 16 Scratch assay scheme.

11 *In vivo* experiments

The Animal Ethics Committee of the University of Barcelona approved all the protocols used in animal work. Mice were housed and bread in the specific pathogen free (SPF) animal facility of the Faculty of Medicine of the University of Barcelona. NOD scid gamma (NSG®) (NOD.Cg-PrkdcscidIl2rgtm1Wjl/SzJ (005557)) female mice (Charles River) of 6-8 weeks of age were used for orthotopic studies, and CB17-Scid (CB-17/Icr-Prkdcscid/scid/Rj) female mice (Janvier Labs) of 6-8 weeks of age were used for intrasplenic injections studies.

For both studies, animals were anaesthetized with a mixture of ketamine (Imalgene® 100mg/ml (100 mg/kg) and xilacine (Rompun®2% (10 mg/kg).

For intrasplenic injections, $3x10^6$ cells resuspended in 100 µl of RPMI 1640 serum free medium were injected under the spleen capsule via a 27-gauge needle. Previously, the spleen was carefully exposed after small cutaneous incision in the left flank (carried down through the peritoneal wall). A visible "paling" and slight swelling of the spleen were the parameters to establish a successful inoculation (as previously reported [617]). After 2 min, splenectomy was performed (necessary time to allow injected cells pass from the spleen to portal circulation and then enter the liver) as previously reported[618]. Finally, the abdominal wall and the skin were closed with sutures. Liver tumor formation was followed by luminescence imaging for 3-4 weeks. Mice's livers were evaluated *ex vivo* by bioluminescence imaging, and then metastatic lesions were isolated under sterile conditions. Lesions were minced and mechanically disaggregated in RPMI 1640 medium with piston syringe and

70um Nylon Cell strainer (Falcon) to isolate SW620 GFP$^+$/Luc+. Then cells were centrifuged and seeding with RPMI medium and 1 mg/ml of Neomycin (G 418 (sigma)) antibiotic for 1 week.
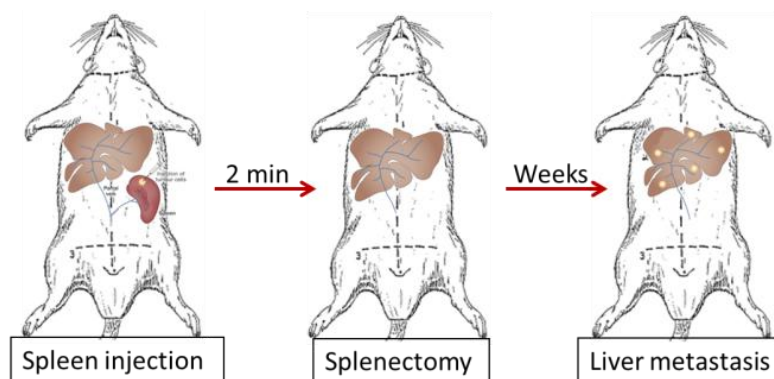
Figure 17 Intrasplenic injection scheme.

Orthotopic injections were done as previously described[619]. The mice cecums were exteriorizing by laparotomy, then 2x10^6 SW620-L cells suspended in 50µl of RPMI 1640 medium and placed into a sterile micropipette were slowly injected with an approximate 30º angle. Micropipette tip were introduced 5mm into the cecal wall. Subsequently, a slight pressure with a cotton stick was applied at 2 mm from the injection point in the pipette axis direction. After pulled the pipette out, the area around the injection was cleaned with saline solution to avoid growing of undesired refluxed tumor cells into the abdominal cavity. The small diameter, and flexible tip of the pipette, and the angular and slow rate of administration diminish resistance to the injection, limiting tissue damage and bleeding and ensuring the absence of cell reflux. Finally, the gut was returned to the abdominal cavity, and the abdominal wall and the skin were closed with metal wound clips. Animals were treated with buprenorphine (Buprex® 0.3mg/ml (0.1mg/Kg)) by subcutaneous route for pain, and enroploxacino (Enrovet 100mg/ml (1.5 ml/250ml water)) were used by drinking water to avoid infections, both for 3 days. Four days after cecum inoculation of SW620-L cells, mice were daily treated with vehicle (0.5% methylcellulose and % DMSO in PBS), KRH-3599, a CXCR4R antagonist (10mg/kg intraperitoneal injection), JTE907 (Tocris) a CB$_2$R antagonist (10mg/kg oral administration) or both, for five and a half weeks. Animals were monitored until death because of their neoplastic process or until the end of the experiment (40 days).

Tumor development were followed weekly (or once a week) by bioluminescence imaging (BLI) using a Aequoria Luxiflux device equipped with an ORCA-ER camera (Hamamatsu). For tumor and metastasis tracking ventral images were quantified. Color maps generated with Matlab and BLI

signal was quantified using Wasabi software and Image J software. On orthotopic studies, at the experiment end point, on necropsy, ex vivo liver and lung bioluminescence images were done to confirm the development of metastasis.

12 Statistical analysis

The Fisher's exact test was used for statistical analysis of the distribution of CXCR4 and CB_2 expression in the different samples contained in TMAs. The Pearson's chi-squared test was used for correlation analysis between high expression of CXCR4 and CB_2. Kaplan-Meier disease free survival curves were statistically compared by the Gehan-Breslow-Wilcoxon test. Unpaired and paired T-tests were used to assess differences between two groups for the rest of the analyses. All statistical analyses were done using GraphPad Prism software 7.0. Data are expressed as mean ± SD.

RESULTS

STUDY 1: Idelalisib Interferes with the Crosstalk of Follicular Lymphoma and its Immune Microenvironment and Potentiates the Activity of ABT-199

1. Idelalisib modulates key signaling pathways in the germinal center

To examine the molecular effect of idelalisib in a relevant in vitro FL model we established primary FL co-cultures with FDC as previously described[264,620] to mimic the germinal center (GC) microenvironment. GEP was performed in B cells isolated from these co-cultures that were treated in the presence or absence of idelalisib (500nM, 48h). GSEA revealed that gene sets related to the GC program, including CD40L signaling and targets of the transcriptional repressor BLIMP were downregulated by Idelalisib treatment (Table 19, Figure 18A).

Table 19. Common gene sets regulated by idelalisib in monoculture and in FDC-FL co-culture

GSEA analysis	CONTROL vs IDELA		FDC vs FDC IDELA	
Gene sets	NES	FDR, q-value	NES	FDR, q-value
BLIMP1 targets	2.51	<0.0001	2.21	<0.0001
CD40 signaling during GC development	2.37	<0.0001	2.20	<0.0001
GC B CELL	2.24	<0.0001	2.46	<0.0001
mTORC1 pathway	2.26	<0.0001	2.30	<0.0001

Gene sets regulated by IDELA were identified by Gene Set Enrichment Analysis (GSEA) using custom genes set (http://lymphochip.nih.gov/signaturedb/index.html). NES: Normalized Enriched Score; FDR: False Discovery Rate. Threshold FDR<0.05 and NES>1.5

Likewise, the genes pertaining to MTORC1 signature were also diminished by idelalisib. Of note, these gene sets were similarly downmodulated in the presence or absence of FDCs. We then validated this data at protein and functional levels. We first demonstrated the complete blockade of PI3K/AKT pathway by western blot showing a reduction of the activating phosphorylation of Ser473-AKT (Figure 18B). Likewise, idelalisib was able to downregulate the expression of several genes related to CD40L signaling, Blimp targets and GC program in larger patient cohort (n=26). These genes included the anti-apoptotic protein BCL2A1 (A1/BFL-1) (p<0.001) and the chemokine CCL22 (p<0.001) responsible to induce the migration of different immune cell type regulated by BLIMP-1 (Figure 18C). CD40/CD40L interaction between B and T cells is essential for germinal center response to the point that abrogation of CD40L signaling in established GCs causes their fast dissolution. Genes downregulated by Idelalisib included some proteins directly involved in the B-T immunological synapse, such as co-stimulatory protein CD80 (p=0.011), Signaling Lymphocytic

Activation Molecule SLAMF1 (p=0.006) or the intercellular adhesion molecule ICAM1 (p=0.027) (Figure 18D-E)

Taken together these results indicate that idelalisib is interfering with B-T cell interaction in the GC together with a putative arrest release related to the regulation of Blimp genes.

D

E
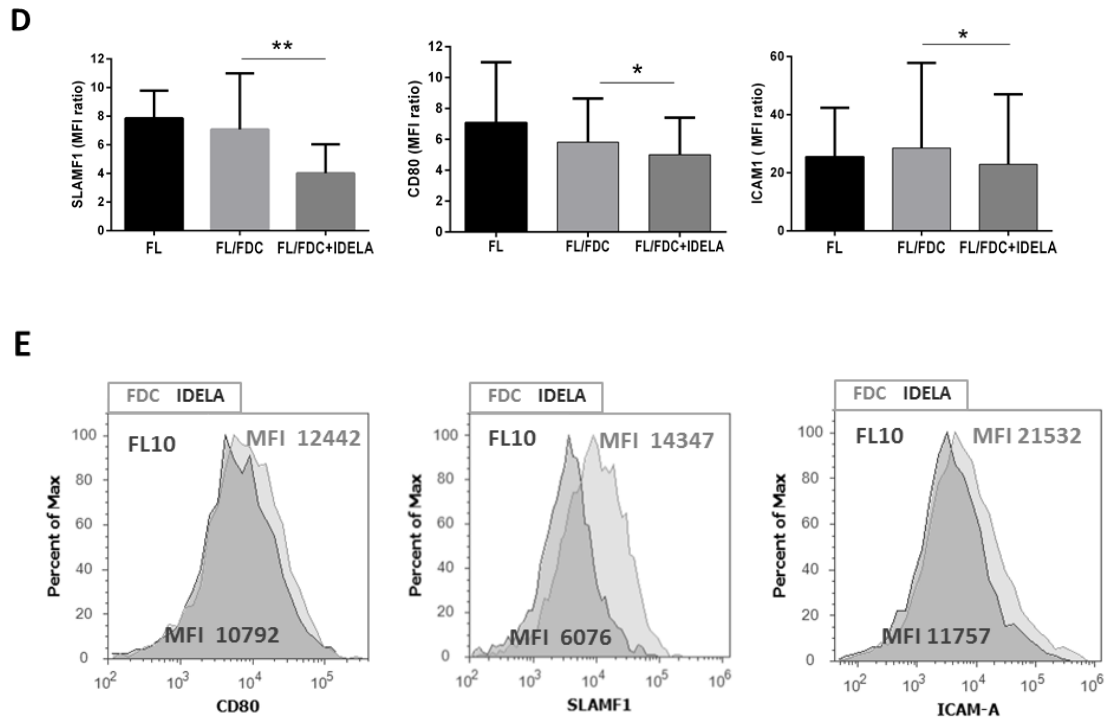
Figure 18. Idelalisib inhibits gene sets elated to GC program and CD40 signaling. (A) FL cells (n=5) were cultured for 48h with idelalisib (500nM), and B cells were purified and subjected to GEP. Gene sets regulated by IDELA in the presence or absence of FDC coculture were identified by Gene Set Enrichment Analysis (GSEA) using custom genes set (http://lymphochip.nih.gov/signaturedb/index.html). Heatmaps of the corresponding leading edge of selected gene sets are shown including the relative gene expression of FL cells cultured w/wo IDELA. **(B)** Primary follicular lymphoma cells were treated for 3 hours with Idelalisib (500nM) and phosphorylation of Akt1, mTOR were assessed by Peggy Sue simple western and quantified by densitometry (n=3). **(C)** BCL2A1 and CCL22, gene expression was measured by real-time PCR in primary samples of FL patients (n=26). **(D)** Primary follicular lymphoma cells in monoculture or FDC co-culture were treated for 48 hours w/wo Idelalisib (500nM) and expression of were measured using flow cytometry (n=8), **(E)** representative histograms of SLAMF1, CD80 and ICAM1 expression.

2. Idelalisib shapes the FL immune microenvironment

Macrophages and many tumor types including FL secrete the immunosuppressive chemokine CCL22[621-623]. CCL22 and CCL17 are the ligands for CCR4 receptor, predominantly expressed by circulating memory lymphocytes, especially T regulatory (Treg) cells and T helper2 (Th2)[624].To gain insights into the effect of CCL22 downregulation by Idelalisib, we first validated the GEP results at protein level. Analysis of CCL22 by ELISA in supernatants from FL-FDC co-cultures treated w/wo idelalisib (500nM, 48h), demonstrated that CCL22 is secreted in the FL-FDC niche and idelalisib induced a significant reduction of this chemokine (Figure 19A, p=0.003). Then we checked if FL co-culture supernatants were effectively able to recruit Treg cells from blood. To this aim PBMC from

healthy donors, enriched in the T cell fraction, were challenged to migrate towards those FL+FDC supernatants (w/wo idelalisib), where CCL22 was determined previously, and counted by flow cytometry (CD4$^+$/CD25$^{+/}$FOXP3$^+$). FL-FDC supernatant favored Treg recruitment and idelalisib reduced this event (Figure 19B, p=0.0094).

Infiltrating macrophages that contribute to CCL22 secretion also composes FL microenvironment, showing in fact higher expression that FL cells (Figure 19C, p=0.022). Thus, we sought to determine the repercussion of idelalisib in FL-M2 crosstalk. As displayed in Figure 19D, FL-M2 co-culture increased the expression of CCL22 in M2 macrophages and idelalisib treatment was able to decrease (Figure 19D, p=0.0364). Moreover, idelalisib reduced the secretion of the immunosuppressive cytokine IL-10 identified in FL-M2 co-cultures (Figure 19E, p=0.0156).

Another T cell subpopulation fundamental for FL survival are T follicular helper cells (T$_{FH}$). Using PBMC from fresh tonsils enriched in the T cell fraction we quantify the effect of idelalisib on T$_{FH}$ cells (CD4$^+$CXCR5$^+$CD25$^-$) migration. As shown in figure 19F, FL-FDC supernatants recruited T$_{FH}$ and idelalisib diminished this migration. However, Idelalisib did not affect the recruitment of T follicular regulatory cells (T$_{FR}$) (CD4$^+$CXCR5$^+$FOXP3$^+$) (Figure 19G).

In summary, idelalisib shapes the immune FL microenvironment by decreasing the levels of the immunosuppressive cytokines CCL22 and IL10, and by hampering the recruitment and function of supportive T$_{FH}$ to the FL niche.
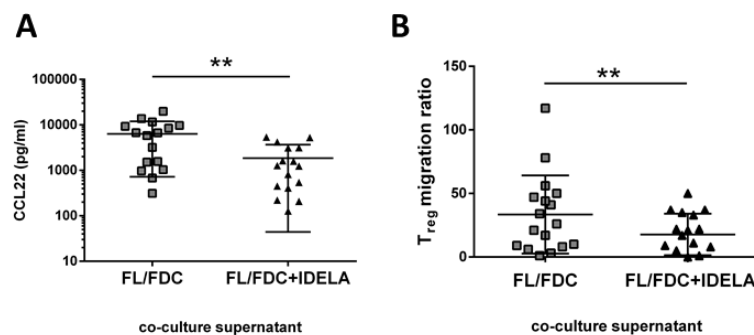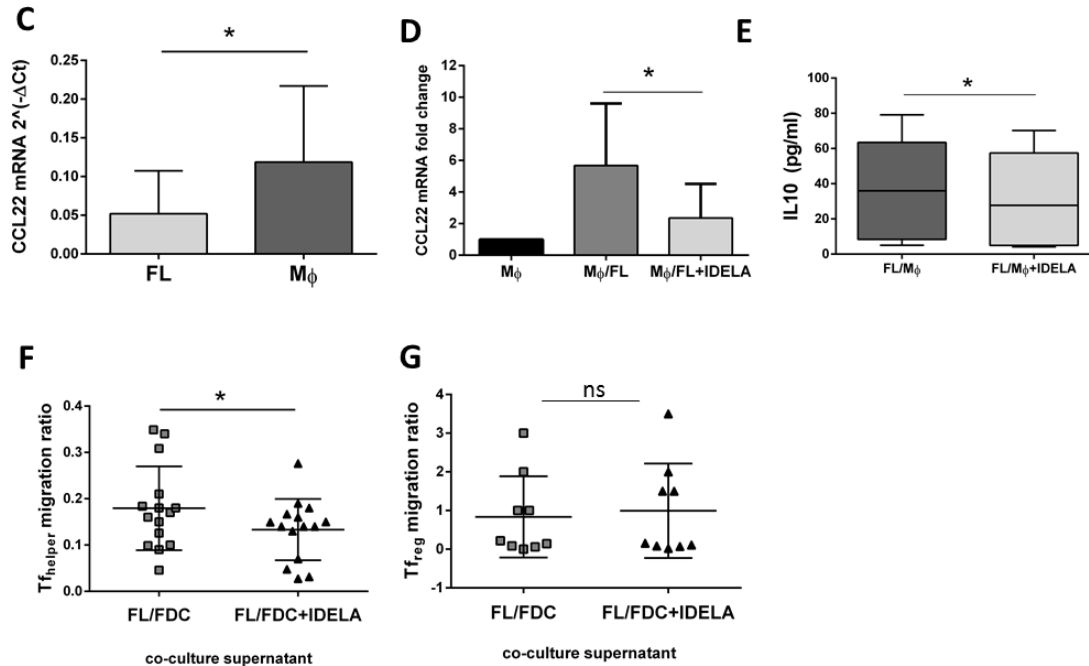
Figure 19. Idelalisib shapes FL immune microenvironment. FL-FDC co-culture supernatants (n=26) w/wo idelalisib were used to determine: **(A)** CCL22 expression assessed by ELISA **(B)** Migration of Treg cells (CD4$^+$ CD25$^+$ FOXP3$^+$) obtained from PBMCs of healthy donors (n=16) versus supernatants obtained from FL-FDC co-cultures w/wo idelalisib. **(C)** Basal expression of CCL22 was assessed using RT-PCR in FL cells (n=27), and peripheral blood derived macrophages (n=7). **(D)** M2-macrophages derived from PBMCs were co-cultured for 24h with FL cells (n=5) w/wo idelalisib (500nM) and CCL22 expression was determined by real-time PCR **(E)** IL-10 expression assessed by ELISA and **(F)** Migration of specific T$_{FH}$ (CD4$^+$ CXCR5$^+$CD25$^-$) (n=15) obtained from tonsils (n=15). **(G)** Migration of specific T$_{FR}$ (CD4$^+$ CXCR5$^+$ FOXP3$^+$) (n=9) obtained from tonsil.

3.   Idelalisib modulates FDC-induced gene sets in selected FL patients

We then sought to determine the impact of idelalisib on the genes specifically induced by FDC co-culture. FDC significantly changed FL transcriptome, a LIMA analysis identified 306 genes significantly upregulated (p<0.05 and fold change >2) in patients FL1-FL4, while FL5 was not responsive to FDC co-culture (Figure 20). GSEA analysis of the whole expression data set uncovered an enrichment of genes related to extracellular matrix formation, cell migration, transendothelial migration and cell-cell/cell-matrix adhesion among others, in accordance with previous results[620] (Table 20, Figure 21A).).

Table 20 Gene sets regulated by IDELA treatment in FL-FDC co-cultures in sensitive patients

Gene sets	# of enriched gene sets	NES	FDR, q-value
Custom gene sets			
Human angiogenesis	1	2.63	<0.0001
IRF4 pathway	1	1.98	0.0045
Cell cycle regulation	2	1.97	0.0039
Integrin pathway	1	1.92	0.0067
Serum response	1	1.84	0.0075
Canonical Pathways (C2CP)			
Focal adhesion-Integrins	12	2.80	<0.0001
Extracellular matrix formation	7	2.76	<0.0001
Angiogenesis (VEGF/PDGF pathways)	6	2.29	<0.0001
Transendothelial cell migration	3	2.30	<0.0001
Cell adherent junctions –ECadherin	5	2.08	0.0009
Cell cycle G1-M	8	2.01	0.0027
Motif gene sets (C3 TFT)			
SRF	6	2.31	<0.0001
IRF	2	1.85	0.0080
NFAT	1	1.73	0.021
NFκB	1	1.64	0.041
Hallmark genesets (H)			
Epithelial mesenchymal transition	1	3.25	<0.0001
Angiogenesis	1	2.26	<0.0001
mTOR	1	1.95	0.0002
Interferon α and γ_responses	2	1.6	0.015
GO genesets (C5)			
Extracellullar matrix organization	8	2.9	<0.0001
Adhesion-intergrins	9	2.56	<0.0001
Vasculature-angiogenesis-EC growth	15	2.49	<0.0001
Cell cycle G1-S and G2-M	5	2.09	0.0007

Gene sets regulated by IDELA were identified by Gene Set Enrichment Analysis (GSEA) using custom genes set experimentally derived (http://lymphochip.nih.gov/signaturedb/index.html) C2 canonical pathways, C3 motif gene sets, Hallmark and C5-GO signatures obtained from the Molecular Signature Database (v2.5). NES: Normalized Enriched Score; FDR: False Discovery Rate. Threshold FDR<0.05 and NES>1.5. The number of enriched gene sets and the best FDR and NES scores are indicated for each biological process
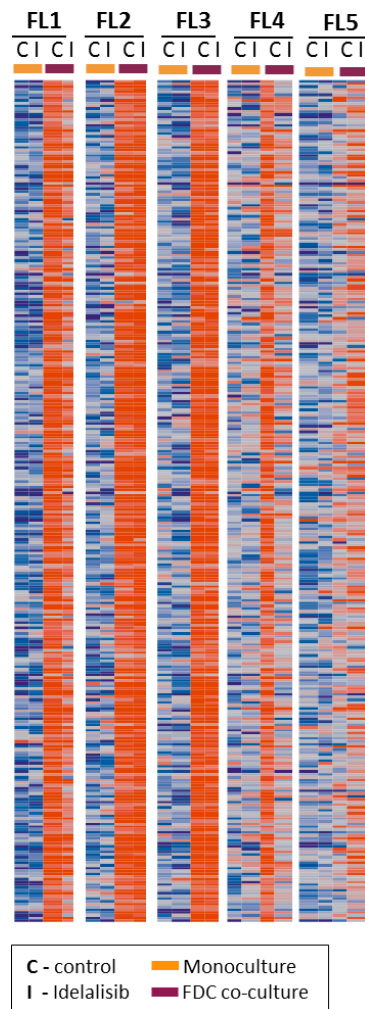
Figure 20. Idelalisib modulates FDC-induced gene sets in selected FL cases. FL primary cells were isolated from monocultures or FL-FDC co-cultures w/wo idelalisib (500nM, 48h) and subjected to GEP. Lima Analysis from GEP results. FL cells (n=5) Heatmaps of the corresponding leading edge of selected gene sets are shown including the relative gene expression of FL cells cultured w/wo Idelalisib.

In vitro treatment with idelalisib uncovered differential gene regulation among patients leading to two different patterns of response (Figure 21B and C), being FL1 and FL4 sensitive to idelalisib while FL2 and FL3 appeared resistant to the inhibitor.

A
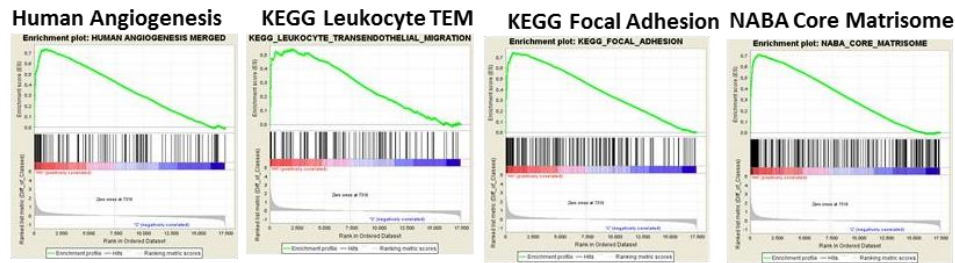
B
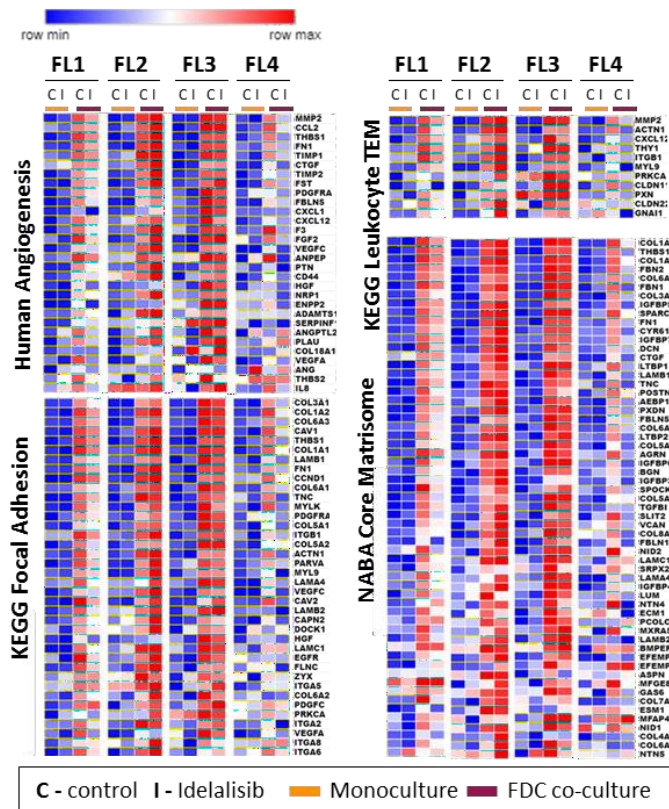
C
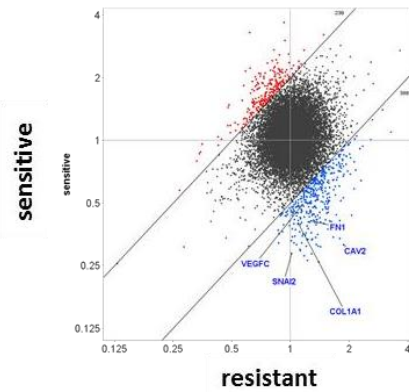
Figure 21. Idelalisib uncovered differential gene regulation among patients leading to two different patterns of response. FL primary cells were isolated from monocultures or FL-FDC co-cultures w/wo idelalisib (500nM, 48h) and subjected to GEP. Gene sets regulated by idelalisib were identified by GSEA using custom genes sets, C2 canonical pathways, C3 motifs, Hallmark and C5-GO signatures. Enrichment plots **(A)** and heatmaps **(B)** of the corresponding leading edges of selected gene sets are shown. **(C)** Scatter plot comparison of gene expression regulation by idela in FL cells from FL-FDC co-cultures of FL1 and FL4 (responsive) vs FL2 and FL3 (unresponsive)

In order to validate these results in a larger patient cohort, 39 genes were selected following the criteria of upregulation by FDC co-culture (fold change >2, p<0.05) and differential regulation by idelalisib (fold change <0.5 in sensitive *vs* no change in resistant patients). The effect of idelalisib in this custom gene signature was analyzed in 26 FL-FDC primary co-cultures. Figure 22A illustrates the power of this gene signature to discriminate between idelalisib sensitive and resistant FL-FDC

primary cultures. We then were able to reduce this signature to 18 genes maintaining the same predictive power (Figure 22B), providing an easy and manageable fingerprint of idelalisib sensitivity.
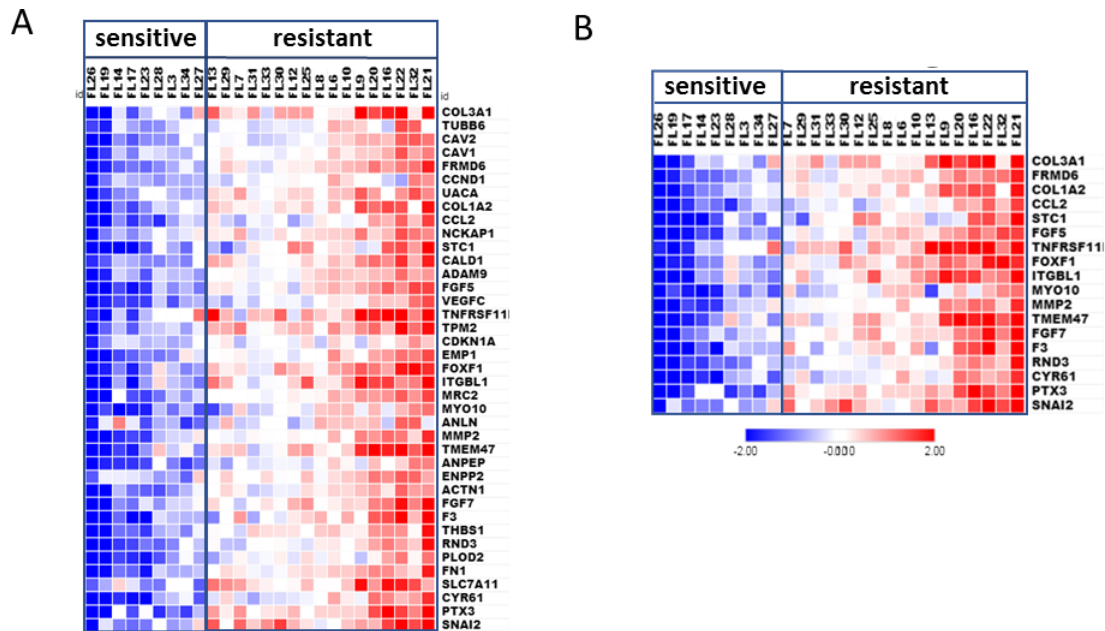
Figure 22. Fluidigm analysis showed a putative gene signature for Idelalisib responsiveness. FL primary cells were isolated from monocultures or FL-FDC co-cultures w/wo idelalisib (500nM, 48h) and subjected to GEP. RNA from 26 different FL samples co-cultured with FDC w/wo idelalisib were used for this analysis. Rows were clustered by Euclidean distance. **(A)**Heatmap displays expression fold change of 39 selected genes, in response to Idelalisib. Genes were chosen according to microarray data from a total of 152 genes, all them upregulated by FDC co-culture (fold change >2) but differently modulated by idelalisib (fold change <0.5 in sensitive patients versus no change in resistant). **(B)** Heatmap displays expression fold change of a 18–genes signature in response to Idelalisib in FL-FDC co-cultures showing differential regulation in sensitive and resistant FL samples.

4. Idelalisib reduces FDC-induced angiogenesis and transendothelial migration in sensitive patients

We then sought to determine the functional consequences of this differential gene regulation of idelalisib between sensitive and resistant patients.

It is well documented that PI3K/AKT plays a key role in angiogenesis, both through regulation of VEGF-A expression, and as a transducer of VEGF-A–VEGFR downstream signaling. Analysis of VEGF-A and VEGF-C secretion by ELISA on supernatants from FL-FDC co-cultures w/wo idelalisib, uncovered a selective and significant (p=0.0062 and p=0.0072, respectively) downregulation of both proangiogenic factors only in idelalisib sensitive patients (Figure 23A) in accordance with GEP results (Figure 21B). We then used these supernatants in a tube formation assay. HUVEC endothelial cells were cultured with supernatants recovered as described above. Supernatants from FL-FDC co-cultures significantly increased the number of nodes and junctions compared to those from FL monocultures (p=0.0056). Importantly, the presence of idelalisib diminished the proangiogenic potential of those supernatants, exclusively in idelalisib sensitive patients (p=0.0138), in accordance with the results obtained for VEGF-A and VEGF-C (Figure 23B).

A
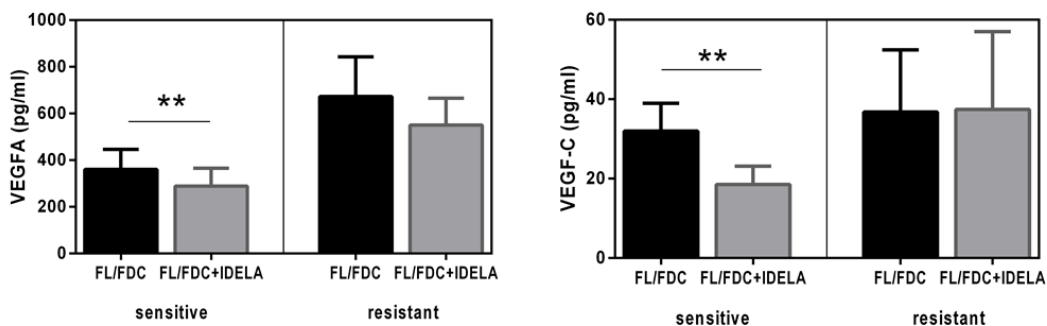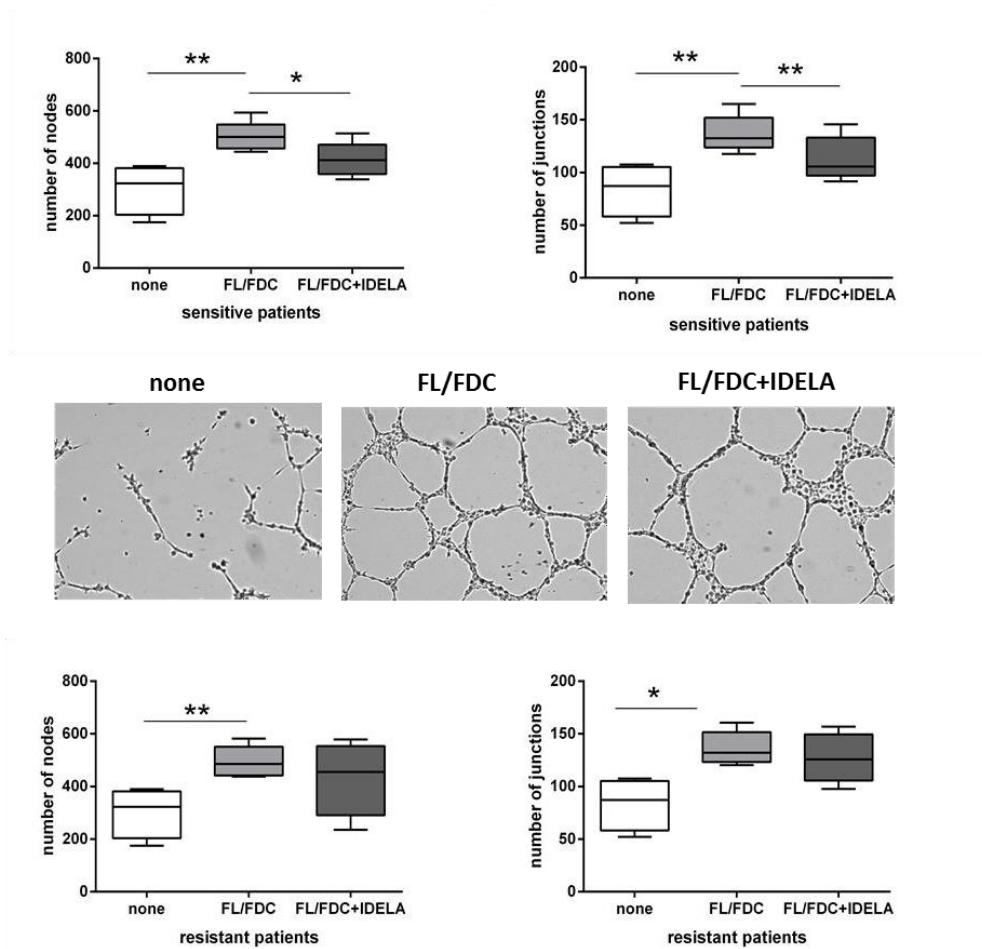
Figure 23. Idelalisib reduces FDC-induced angiogenesis in sensitive patients. FL-FDC co-culture supernatants w/wo idelalisib (500nM, 48h) were used to determine: **(A)** VEGF-A and VEGF-C protein secretion by ELISA in sensitive (n=7) and resistant (n=6) patients and **(B)** Tube formation assay of endothelial HUVEC cells cultured for 24h with their own media plus the corresponding supernatants (ratio1:1). 5 Representative images of each condition were captured using a phase-contrast microscope and analyzed by IMAGE J software (Angiogenesis analyzer plug-in). Node and junction numbers from sensitive (n=5) and resistant (n=5) are shown.

As described in Figure 20 and 21B, FDC co-culture significantly modulated the expression of some adhesion-related molecules with a differential regulation by idelalisib between sensitive and resistant patients as displayed in Figure 24A. The main integrins upregulated by the co-cultured were ITGA2, ITGA6, ITGB1 and ITGBL1, while the main corresponding ligands were the Extracellular Matrix Components (ECM) collagens (COL1A2, COL3A1, COL6A3 and COL1A1), fibronectin (FN1), laminin (LAMB1, LAMA4, LAMB2), tenascin (TNC) and CYR61; and the glycoprotein THBS1, which is involve in angiogenesis, cell-to cell interaction and cell to matrix interaction. We then validated the

functional consequences of this gene regulation. FL cells from FL-FDC co-cultures w/wo idelalisib were challenged to cell adhesion experiments to HUVEC cells and idelalisib reduced this even just in sensitive patients (Figure 24B, p=0.004).

Adhesion represents a precedent step for cell migration onset. The simultaneous reduction observed in both integrins and their ligands in sensitive patients may indicate a decrease in the migratory capacity of these cells inside the lymph node and through the blood vessel wall. To demonstrate that hypothesis, we carried out a trans-endothelial migration (TEM) assay. FL cells were challenged to migrate through trans-wells coated with HUVEC and Matrigel towards supernatants from FL- FDC co-cultures w/wo Idelalisib. In the line with the adhesion assay results, idelalisib reduce TEM in sensitive patients (p=0.043) while did not affect this phenomenon in resistant ones (Figure 24C).
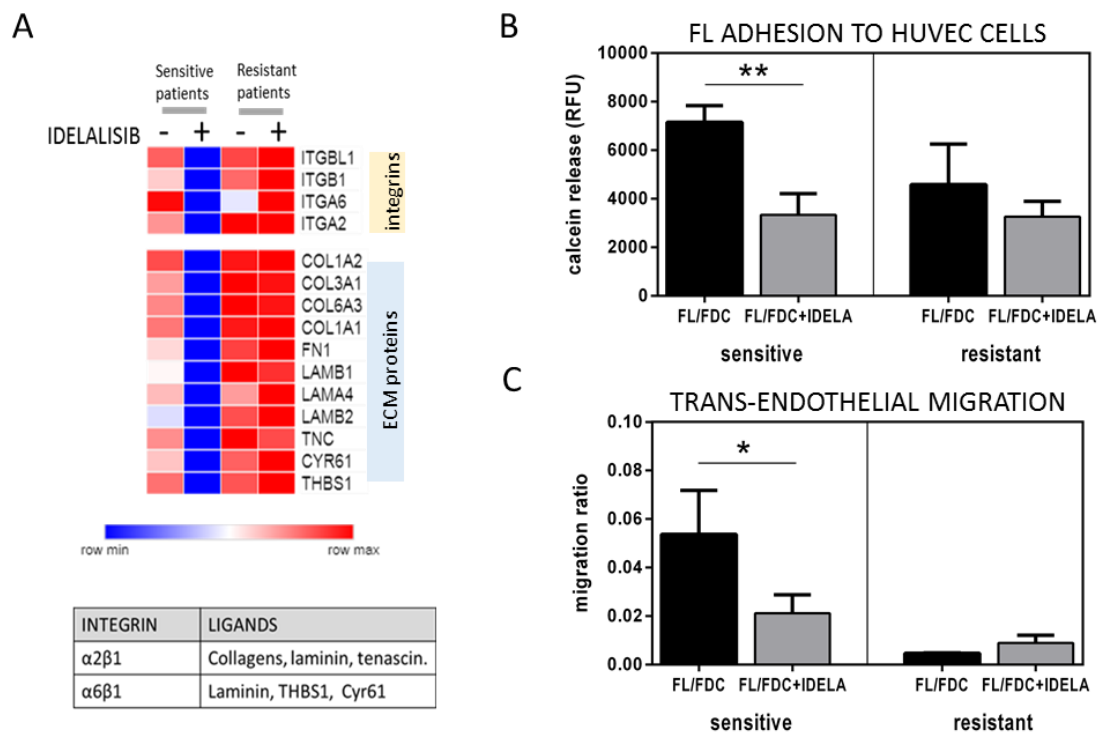
Figure 24. Idelalisib reduces FDC-induced trans endothelial migration in sensitive patients. (A) Heatmap displaying the regulation induced by idelalisib in the expression of integrins and their ligands in FL cells from FL-FDC co-cultures of sensitive (FL1 and FL4) and resistant patient samples (FL2 and FL3) **(B)** FL cells from FL-FDC co-cultures w/wo idelalisib (500nM, 48h) of sensitive (n=3) and resistant (n=5) patients were stained with calcein and allow to adhere for 3h to HUVEC cells. After extensive washing the cells that remain attached were lysed and fluorescence measured in Synergy HT microplate reader. **(C)** FL cells from FL-FDC co-cultures w/wo idelalisib (500nM, 48h) where challenged to migrate for 6 h in a gradient of FBS through trans-wells coated with HUVEC cells seeded on gelatin 0.1% coated + TNF-α (10ng/ml). CD20+ cells crossing HUVEC barrier were counted by flow cytometry. Sensitive patients (n=7) and resistant patients(n=6).

5. **Mutational load does not predict sensitivity to idelalisib and mutated RRAGC correlates with resistance to idelalisib**

In order to further characterize possible patterns of clinical responses to idelalisib we analyzed the mutational load of commonly recurrent mutations in a set of FL patients with characterized molecular responses to idelalisib. These genes included *CREBBP, KTM2D, TNRFS14, EP300, EZH2, MEF2B, EZH2, TNFAIP3, TP53* and *RRAGC.* The frequency of these mutations in our patient series was in accordance with published results in larger patient cohorts (Figure 25 and Supplemental Table 1)).

Although we did not observe any correlation between molecular responses to idelalisib and mutational load, the presence of activating *RRAGC* mutations (FL9 and FL16) did correlate with idelalisib resistance. Mutations of *RRAGC* on the nucleotide binding domain impairs the exchange of nucleotides, causing continuous mTORC1 activation, independently of PI3K/Akt1 pathway[119].
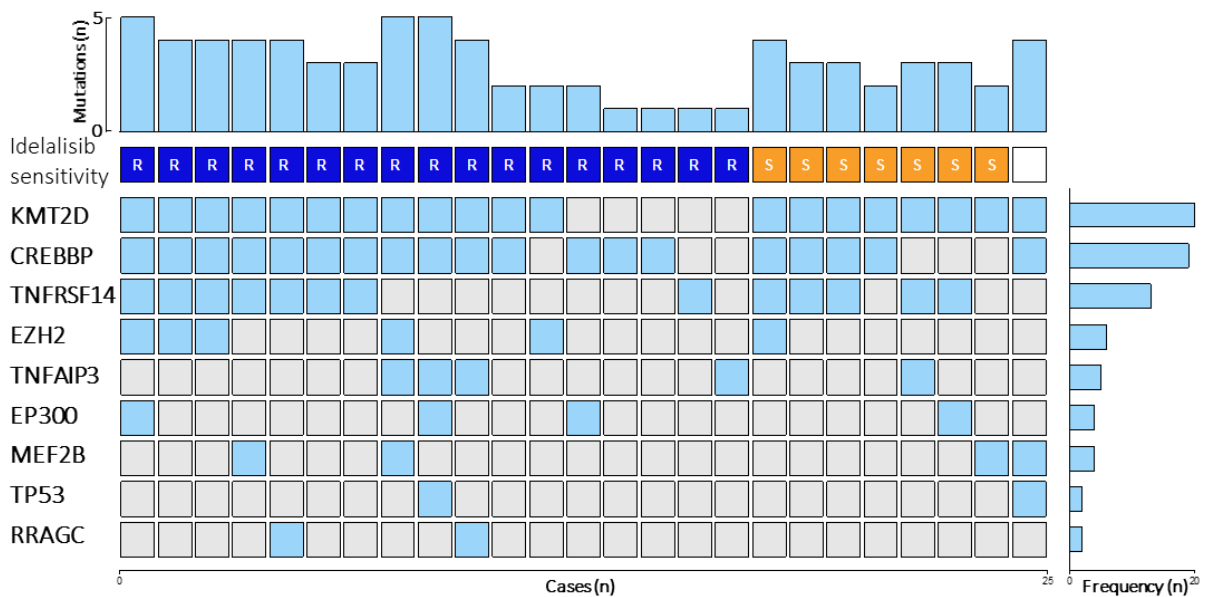
Figure 25. Recurrent somatic mutation present in FL patients. A total number of 25 patients were analyzed by NGS. Found mutations are represented in the figure. Genes mutations rates correlated with the literature. R (resistant to idelalisib); S (sensitive to idelalisib).

6. Idelalisib bypasses microenvironment derived resistance to ABT-199

As we have described, FL microenvironment is a prominent source of pro-survival and cell dissemination signaling. As a result, FDC-FL and M2-FL co-cultures (p=0.0002 and p<0.0001, respectively), significantly increased the viability of FL cells (Figure 26). Idelalisib induced moderate direct cytotoxicity on tumor cells that was maintained in theses co-cultures.
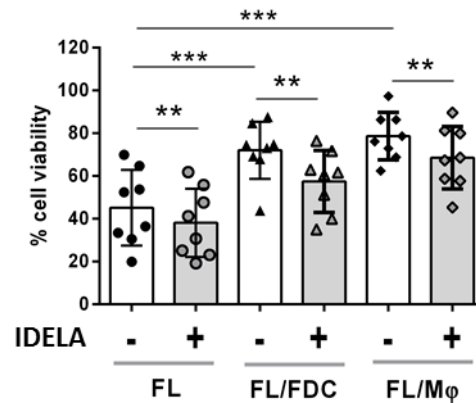
Figure 26. Idelalisib induced moderate direct cytotoxicity on tumor cells. Cell viability (AnnexinV-/7AAD-) was assessed in FL cells from monocultures, FL-FDC and FL-M2 w/wo idelalisib (500nM, 72 h).

Antiapoptotic BCL-2 family of proteins tightly control cell viability and may be well regulated in these co-cultures. We have found that FDC-FL co-cultures augmented the expression of BCL-XL and MCL-1, while M2-FL co-cultures increased BFL-1 on tumor cells (Figure 27A). We then characterize the dependence of FL cell on antiapoptotic BCL2 proteins by BH3 profiling[625]. In the absence of co-culture we found that FL cells showed mainly patterns of either BCL-2 (n=6) or BCL-XL dependence (n=6), while only one FL case manifested dependence on MCL-1 (Figure 27B). Interestingly, we identified that FDC co-cultures increased the sensitivity to HRK (p=0.031) and NOXA (p=0.042) peptides, indicating a higher dependence on BCL-XL and MCL-1 targets respectively, whereas M2 sensitized FL cells to a synthetic peptide specific for BFL-1 (FS2) (p=0.047), indicating a higher dependence on this antiapoptotic protein (Figure 27C). In summary, microenvironment renders FL more dependent on apoptotic proteins different from BCL-2, reducing their priming for apoptosis[626].
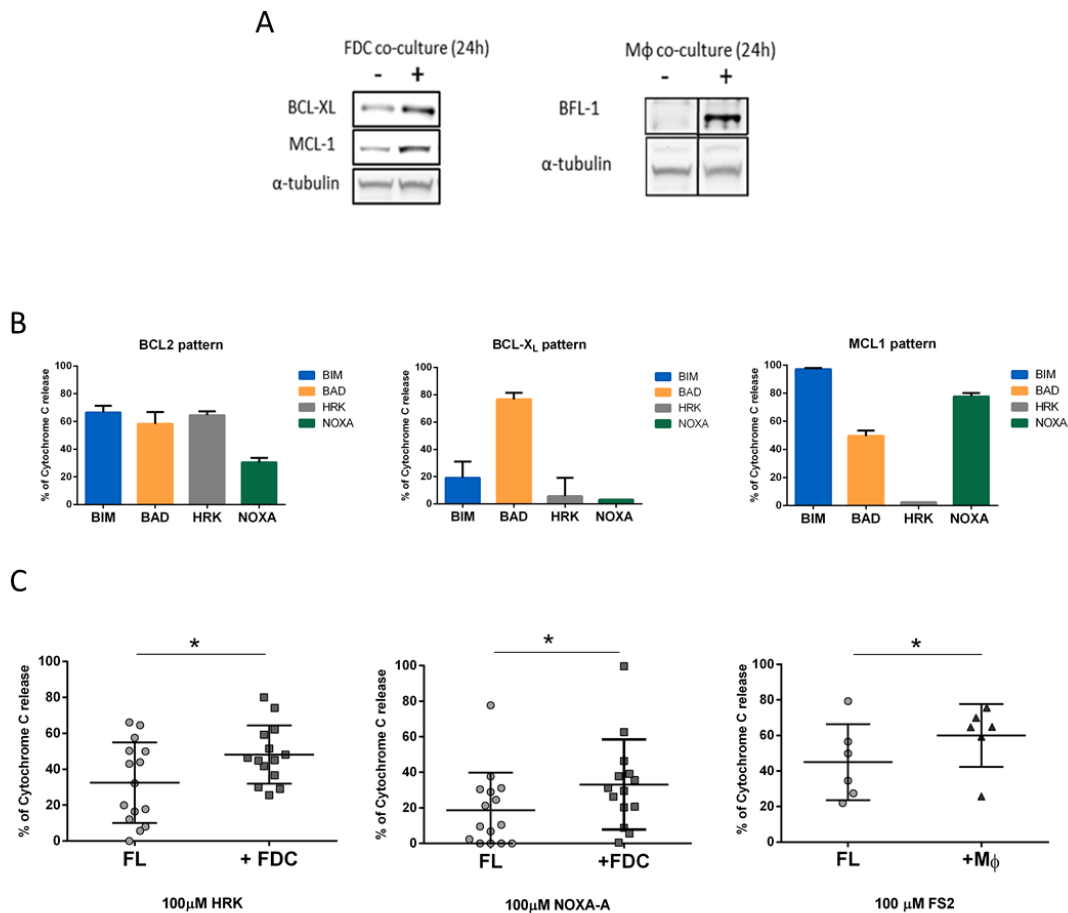
Figure 27. Microenvironment renders FL more dependent on apoptotic proteins different from BCL-2, reducing their priming for apoptosis. **(A)** BCL2 protein expression regulation in FL cells form FL-FDC and FL-M2 co-cultures (24h) **(B)** Examples of BH3 profiles from 3 individual FL patients showing pattern of relative dependence on BCL-2 (n=6), BCL-XL (n=6) and MCL-1 (n=1). **(C)** BCL2 protein family dependence was assessed by BH3 profiling using HRK (BCL-XL dependence), NOXA (MCL-1 dependence) or FS2 (BFL-1 dependence) peptides.

This fact may lay at the basis of the reduced clinical benefit observed with ABT-199 / Venetoclax in FL patients[275]. Likewise, when we evaluated the priming (by Cytocrome C release, as described in material and methods) induced by ABT-199 in FL cells alone or from FDC-FL and M2-FL co-cultures, we observed a marked reduction of this priming in the co-culture set up. Noteworthy, idelalisib counteracted the tumor microenvironment induced resistance to ABT-199 by restoring BCL-2 dependence and increasing apoptosis priming (Figure 28A). Moreover, idelalisib induced the expression of BH3-only protein HRK and reduce BAD phosphorylation, probably facilitating apoptosis induction by ABT-199 (Figure 28B).
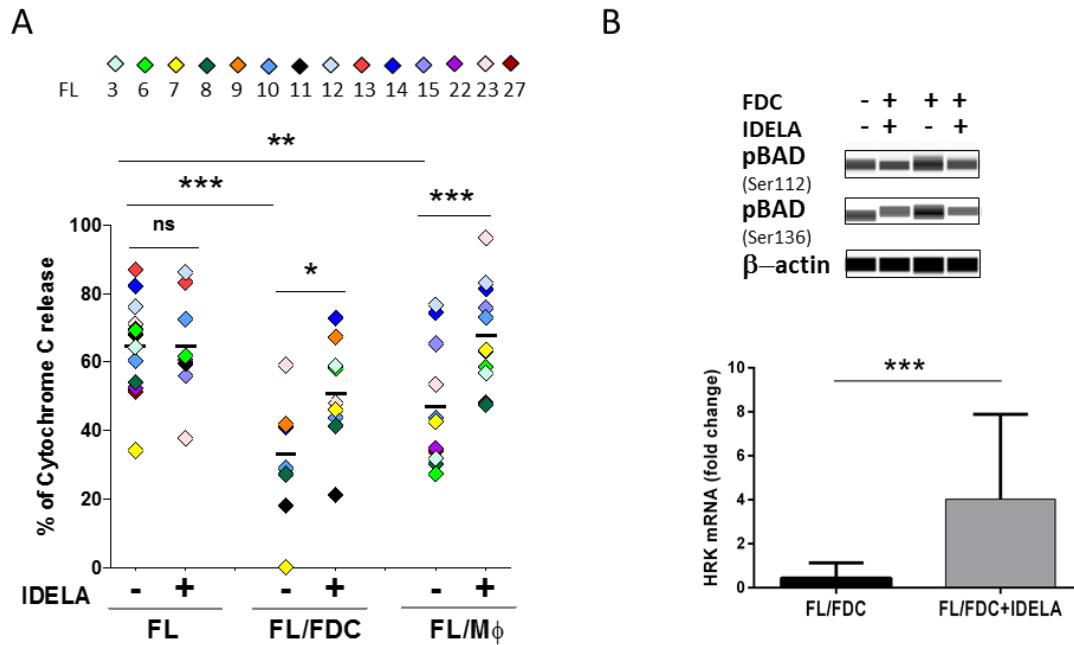
Figure 28. Idelalisib counteracted the tumor microenvironment induced resistance to ABT-199 by restoring BCL-2 dependence and increasing apoptosis priming. (A) FL cells from monocultures, FL-FDC and FL-M2 w/wo idelalisib (500nM, 24h) were permeabilized, incubated for 1 h with ABT 10µM, fixed and stained for intracellular cytochrome C. The percentage of induced apoptosis was evaluated by flow cytometry, measuring the release of cytochrome C. **(B)** .BAD phosphorylation in Ser112 and Ser136; HRK expression, a pro-apoptotic protein that target specifically BCL-XL

The therapeutic cooperation of idelalisib with ABT-199 on apoptosis induction was further assessed by flow cytometry measuring the percentage of viable cells after 3-day co-culture with each agent alone or in combination, using two doses of ABT-199 (10 and 50nM). We concluded that the treatment of FL cells with ABT-199 and idelalisib resulted in a synergistic reduction of cell viability compare to ABT-199 10nM alone in FDC-FL co-cultures(p=0.0135). Besides, the combinatorial treatment of both drugs in M2-FL co-cultures showed also a synergistic reduction of cell viability at both doses of ABT-199 (p=0.0006; 10nM and p=0.016; 50nM) (Figure 29).
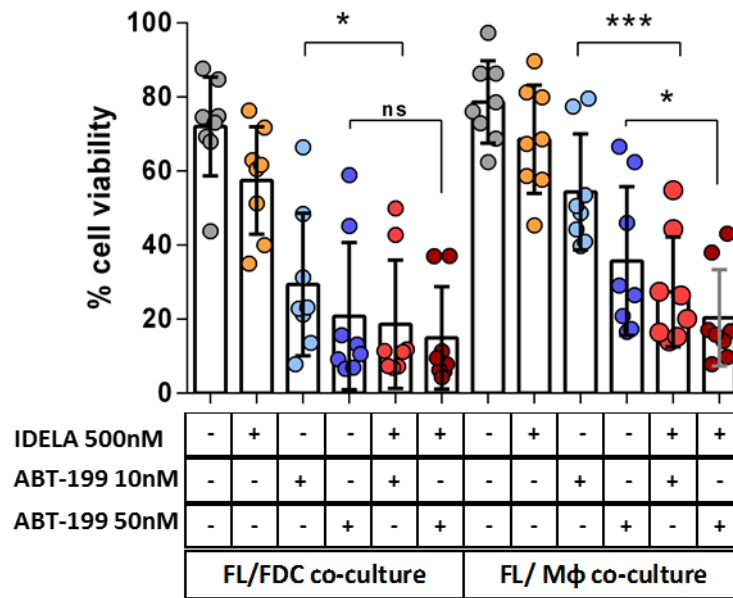
Figure 29. Idelalisib bypasses microenvironment derived resistance to ABT-199. Cell viability (AnnexinV-/7AAD-) was assessed in FL cells from FL-FDC and FL-M2 w/wo idelalisib (500nM) and w/wo ABT-199 (10 or 50nM) after 72h of treatment.

STUDY 2: GPCRs heterodimers as a new therapeutic target in colorectal cancer

1. **CB$_2$ and CXCR4 are simultaneously overexpressed in primary colon tumors.**

Different tissue microarrays were used to characterize the expression of CB$_2$ and CXCR4receptors in a cohort of (n=74 CB$_2$, n=73 CXCR4) prospective primary stage II (pT1-2N0) colon cancers with their associated matched normal mucosa (n=61 CB$_2$, n=48 CXCR4), invasive fronts, and paired metastasis, when available (n=19) (Figure 30A and B).
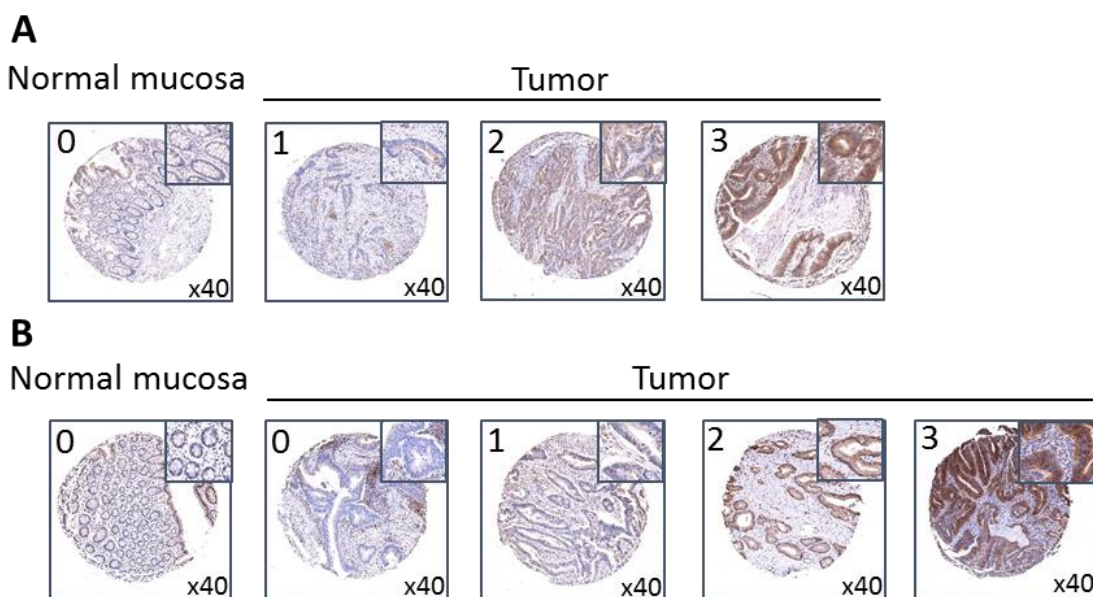
Figure 30. CB$_2$ and CXCR4 expression characterization in primary colon tumor cells and normal mucosa. (A) Representative images of CB$_2$ immunostaining representing the different scores established according to the intensity staining in tumors and normal mucosa in tissue microarrays sample (TMA). **(B)** Representative images of CXCR4 immunostaining of the same TMA samples. Scores: 0 and 1 correspond to low intensity, 2 and 3 correspond to high intensity. Zoom x200.

We observed that the expression levels of both receptors were higher in primary colon tumor samples and their associated metastasis compared to normal mucosa epithelial cells (p<0.0001). However, differences in the expression of CB$_2$ and CXCR4 in primary tumor cells compared to their paired metastatic lesion were not significant (Figure 31A and B). Furthermore, we identified a significant correlation between expression levels of CB$_2$ and CXCR4 (P=0.031) (Figure 31C). When we compared the relapsed -free survival between patients with high levels of both receptors and

patients with low levels of them, we observed a tendency showing that patients with high levels of both receptors showed worse prognosis (Figure 31D). Nevertheless, this trend was absent when either the expression of each receptor was considered individually or their expression values were not in the same directionality (Supplemental Figure 1).
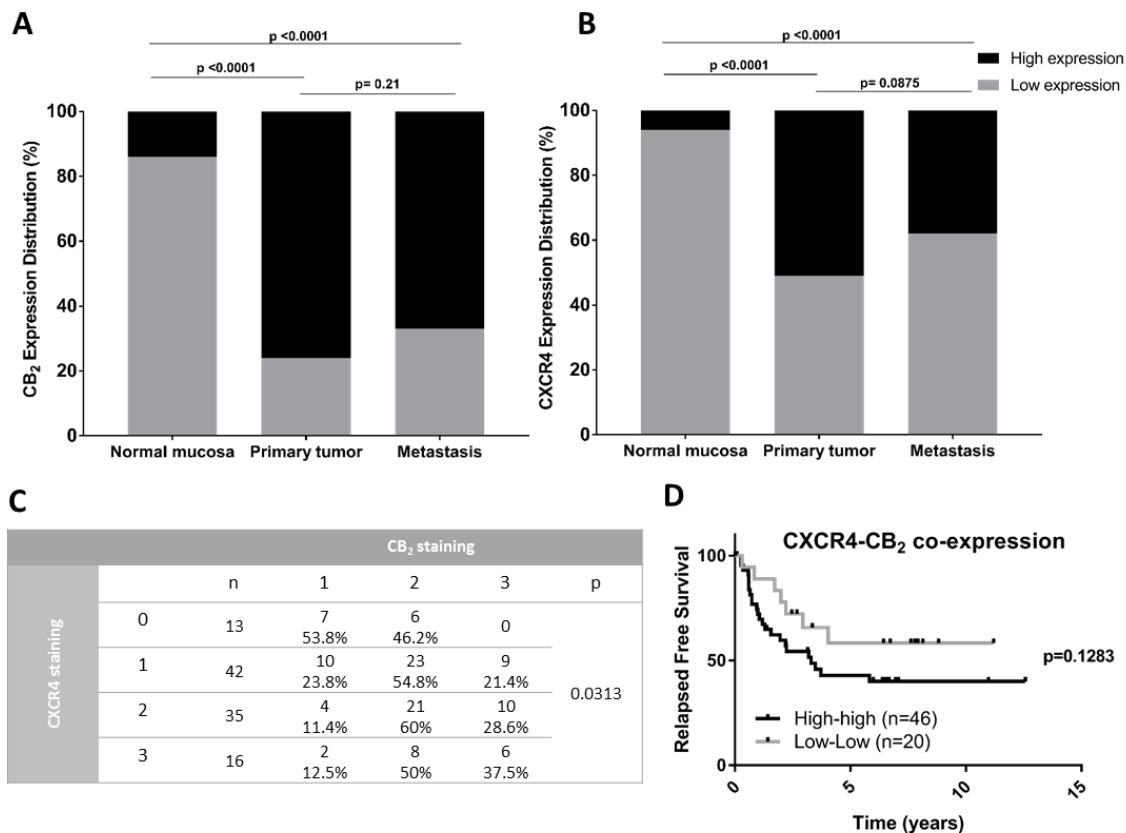
Figure 31. CB$_2$ and CXCR4 were simultaneously overexpressed in primary colon tumors. (A) CB$_2$ expression distribution in the three different types of samples: normal mucosa, primary tumor and metastasis. Black bar represents high expression, and grey bar represent low expression. The results show the percentage of patients of each group (low or high) in total patients. **(B)** CXCR4 expression distribution analyzed in the same way than CB$_2$ expression distribution. **(C)** Representation of percentage of patients in all the possible combination of expression of both receptors, shows the correlation between high expression of CXCR4 and CB$_2$. **(D)** Data plotted in Kaplan-Meier curves for relapsed free survival show differences between patients with high expression levels of both receptors and patients with low expression levels of both, those patients with high expression of CXCR4 and CB$_2$ receptors has worst prognosis

2. Prognostic value of CXCR4 – CB$_2$ heterodimerization.

Next, we sought to identify whether co-expressed CXCR4 and CB$_2$ receptors were physically nearby using the proximity ligation assay, in which two antibody-DNA probes are able to hybridize if the two receptors are close enough, thus considered they are forming heterodimers. By performing this methodology to our cohort of primary stage II colon cancers on TMAs, we detected different amounts of heterodimer formation between CXCR4 and CB$_2$. First, analyzing epithelial cells forming the intestinal glands, we detected a greater presence of CXCR4-CB$_2$ heterodimers in primary tumor samples than matched normal mucosa (p<0.0001) (Figure 32A and D). Second, when we divided the primary tumors according to the presence of disease relapse, our analysis showed that tumors from patients with relapse presented a higher amount of heterodimers compared to those from patients which did not show relapse (p=0.0089) (Figure 32B, C and E), thus suggesting that the formation of CXCR4-CB$_2$ heterodimers might be indicative of worse prognosis. However, differences in the heterodimers formation in primary tumor cells compared to their paired metastatic lesion were not significant.

A

Zoom 4x

x630

Normal mucosa

B

Zoom 4x

x630

Primary tumor (non relapsed)

C

Zoom 4x

x630

Primary tumor (relapsed)
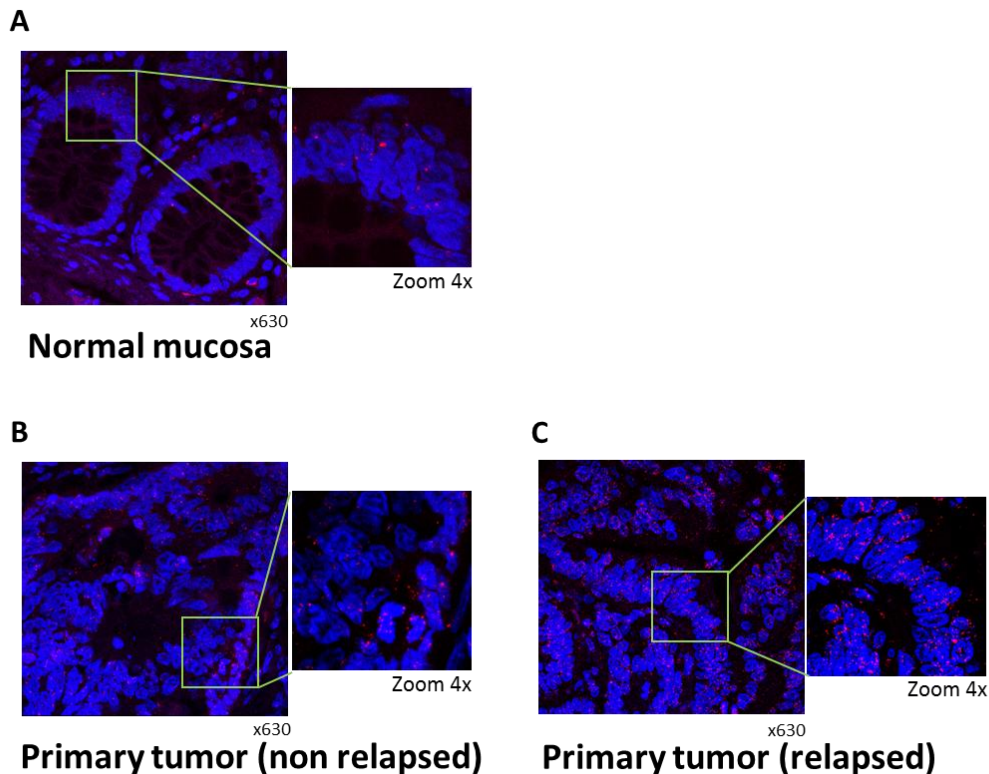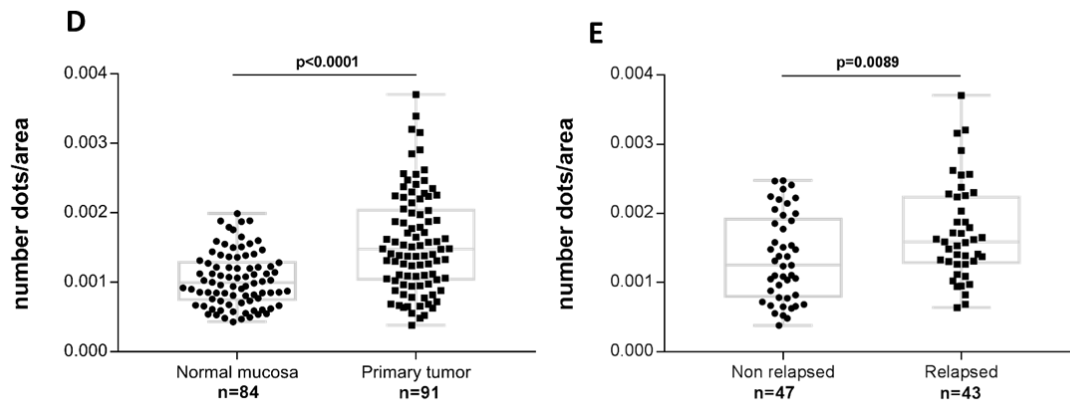
Figure 32. Prognostic value of CXCR4-CB$_2$ heterodimerization. (A-C). Representative images of PLA signal in normal mucosa samples, primary tumor non-relapsed, and primary tumor relapsed, respectively, from TMA. **(D)** Dotted plot represent the number of PLA signals per area of sample for each patient. Significant differences were observed between normal mucosa and primary tumor, tumor samples shown higher number of heterodimers. **(E)** Tumor relapsed samples shown higher number of heterodimers compare to tumor non relapsed.

3.   Heterogeneous formation of CXCR4 and CB$_2$ heterodimers in *in vitro* models.

In order to functionally asses the role of CXCR4-CB$_2$ heterodimers in cancer cells, we then investigated the cell membrane expression levels and the total cellular expression levels of individual CXCR4 and CB$_2$ in a total of six CRC cell lines (SW480, SW620, Colo320, HT-29, DLD-1 and HCT116) by flow cytometry (Figure 33A and B). While SW480 (MFIR= 5.01; p=0.0001 SW480 vs others (excluding Colo320)) and Colo320 (MFIR= 5.36; p<0.0001 vs others (excluding SW480)) showed the highest expression levels of CXCR4 at the cell membrane, only Colo320 showed a significantly greater amount of total CXCR4 expression (MFIR= 13.18; p=0.0095) (Figure 33A). In contrast, only slight difference among cell lines were detected for both cell membrane and total levels of CB$_2$expression (Figure 33B). In addition, our analysis showed that the overall levels of CB$_2$ expression, including cell membrane and total, were significantly lower than CXCR4 (Table 21).
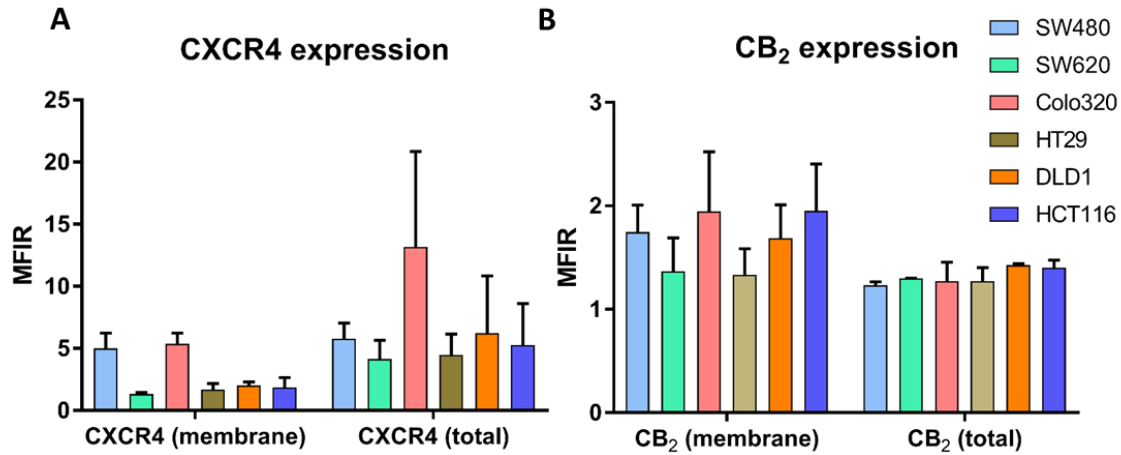
Figure 33. CRC cell lines showed different CXCR4 and CB$_2$ expression levels. (A) CXCR4 MFIR of membrane expression, or total expression of SW480, SW620, Colo320, HT29, DLD1 and HCT116 cells were represented. **(B)** CB$_2$ MFIR of membrane expression, or total expression of SW480, SW620, Colo320, HT29, DLD1 and HCT116 cells were represented.

Table 21 Summary of CXCR4 and CB$_2$ obtained by flow cytometry in six different CRC cell lines

		Membrane expression	Total expression
		MFIR	MFIR
SW480	CXCR4	5.01	5.78
	CB$_2$	1.75	1.23
SW620	CXCR4	1.32	4.16
	CB$_2$	1.37	1.30
Colo320	CXCR4	5.36	13.18
	CB$_2$	1.95	1.27
HT29	CXCR4	1.67	4.47
	CB$_2$	1.33	1.27
DLD1	CXCR4	2.01	6.23
	CB$_2$	1.69	1.43
HCT116	CXCR4	1.88	5.28
	CB$_2$	1.95	1.40

Since heterodimer formation was a distinctive feature in primary colon tumors, we also performed PLA in the panel of six cell lines. Our results indicated that SW480 cell line showed the highest amount of heterodimer formation compared to the others cell lines (p<0.0001). In contrast, HT-29 and HCT116 presented the lowest level of heterodimer formation. Intermediate levels were detected for SW620, Colo320 and DLD-1 cells (Figure 34A and B). Taken together, CRC cell lines

showed different CXCR4 and CB_2 expression levels and distinctive amounts of heterodimers. Subsequent analyses for this study were performed using SW480 and SW620, providing their differences in heterodimer formation and highly invasive capacity
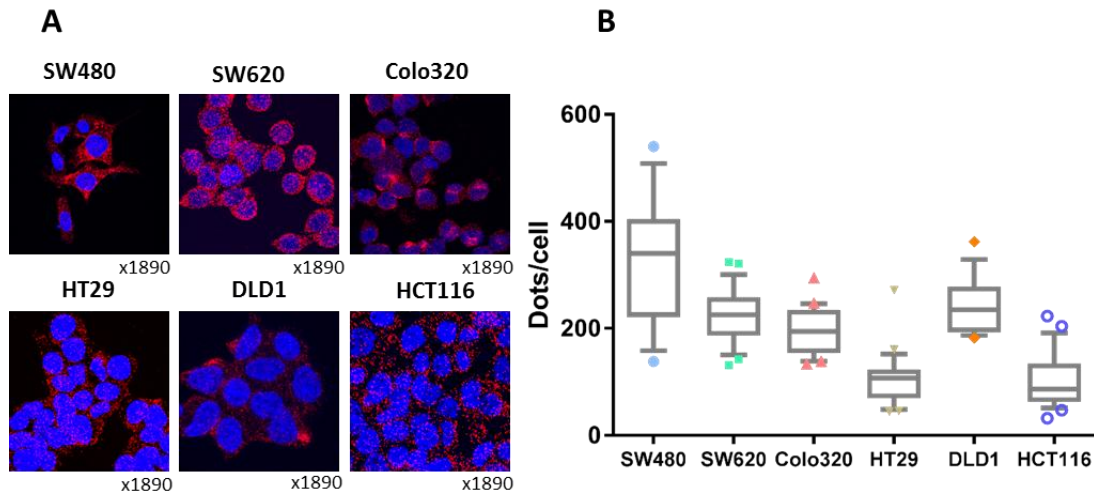
Figure 34. Heterogeneous formation of CXCR4 and CB₂ heterodimers in *in vitro* models. (A) PLA signal images of the different cells lines (SW480, SW620, Colo320, HT29, DLD1 and HCT116 cells). **(D)** PLA signals quantification using Image J software.

4.   CXCR4-CB₂ heterodimers crosstalk.

Next, we sought to determine whether the formation of heterodimers affected the signaling pathway properties of each individual receptor. To test this, we assessed phosphorylation of ERK-1/2 compared to total ERK-1/2 as a surrogate marker of both CXCR4 and CB_2 signaling pathways (Figure 35A). After 20 minutes exposure in SW480 cells, the CXCR4 agonist, CXCL12, produced an increment in the pERK-1/2/ERK-1/2 ratio. Likewise, CB_2-selective inverse agonist, JWH133, produced a robust increment in pERK-1/2 over ERK-1/2 after the same exposure time. Nevertheless, co-activation of both receptors resulted in a slight reduction of ERK-1/2 phosphorylation compared to CXCL12 and JWH133 induction alone. Unsurprisingly, CXCL12 signaling induction was blocked by the CXCR4 antagonist, AMD3100. Intriguingly, AMD3100 was also able to block the signal induced by the CB_2 inverse agonist, JWH133. Similarly, the JWH133 induced signal was blocked by the CB_2 antagonist, JTE907; nevertheless, the signal induced by CXCL12 was also blocked by the CB_2

antagonist JTE907. These results were further confirmed in SW620 (metastatic cells isolated from the liver of intrasplenic mouse model (SW620-L)) (Figure 35B). Thus, our results suggest a bidirectional cross-antagonism through the formation of heterodimers, by which one receptor can be targeted using its partner receptor antagonist, and vice-versa
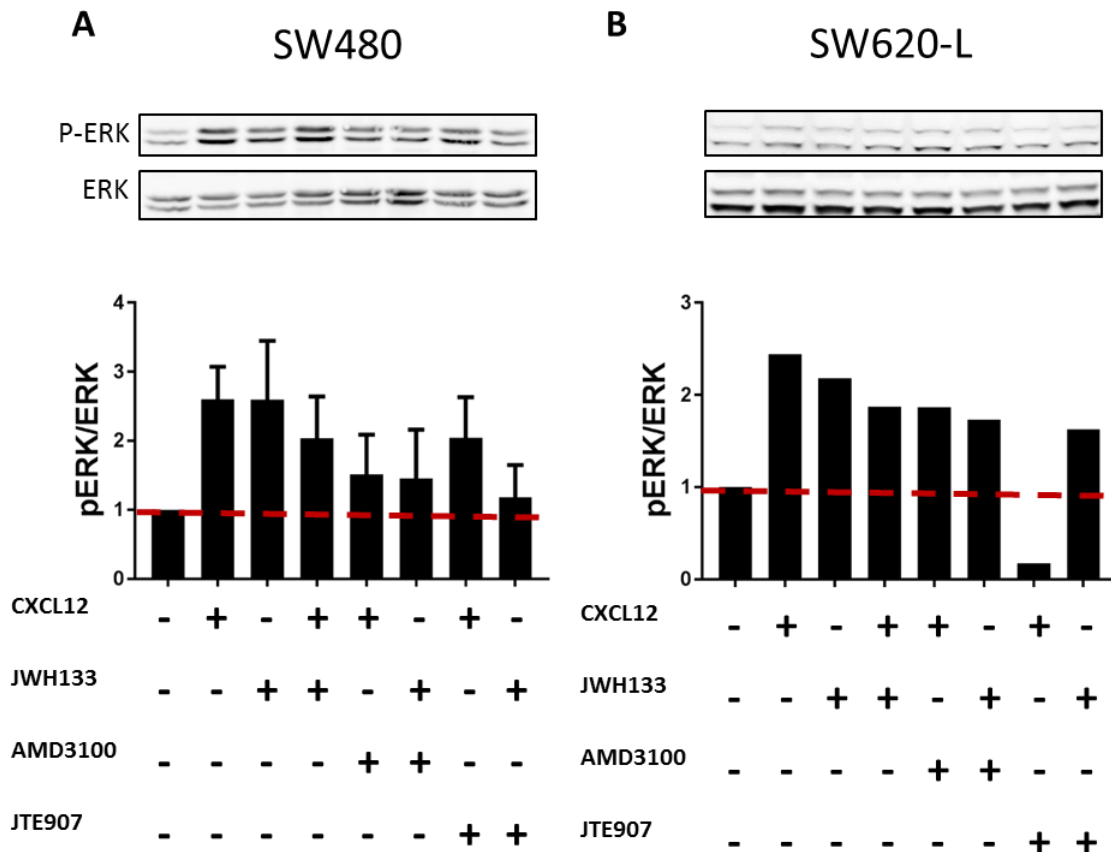
Figure 35. CXCR4-CB$_2$ heterodimers show crosstalk. (A) Confluent SW480 cell lines were stimulated after ON deprivation and 3h of CXCR4 inhibitor or CB$_2$ inhibitor treatment. Cells were stimulated for 20 minutes with CXCR4 or CB$_2$ ligands. Changes in pERK were used as a read-out of pathway inhibition. Bar graph represent the mean of 4 independent assays. **(B)** SW620 derived from mouse liver after intraspleenic injection (SW620-L), were used to confirm the results observed in SW480 assays. The experiment was performed using the same experimental conditions.

5.   Inhibition of CXCR4 and CB$_2$ compromises phospho-ERK mediated cell migration.

The activation of ERK1 and ERK2 signaling pathway by CXCL12 has been shown to be associated with cell migration[456]. Hence, we analyzed whether the bidirectional cross-antagonism between CXCR4 and CB$_2$ affected cell migration induced by the CXCR4 agonist, CXCL12. For these propose, wound healing assays were performed using 200 ng/ml of CXCL12 together with CXCR4 antagonists, (AMD3100 and KRH-3955), CB$_2$ antagonist JTE907, and the combination of the last two to stimulate the wound closure by cell migration. Our results showed that after 42 hours stimulation of SW480 cells with CXCL12, cell migration was significantly induced (p=0.0045) (Figure 36A-B). However, treatment of cells with CXCR4 antagonists significantly reduced the amount of wound closure (p= 0.0958 and p=0.0005, for AMD3100 and KRH-3955 respectively). In fact, CXCR4 antagonist KRH3955 was more effective in reducing the migration capabilities of these cells than AMD3100 (p=0.0004). Interestingly, CB$_2$ receptor antagonist, JTE907, also blocked the migration induced by CXCR4 agonist CXCL12 (P<0.0001), suggesting dysfunctional consequences of CXCR4 and CB$_2$ heterodimer crosstalk (Figure 36B). The combination of CXCR4 and CB$_2$ antagonists, however, did not provide an additional reduction of migratory capability.

B
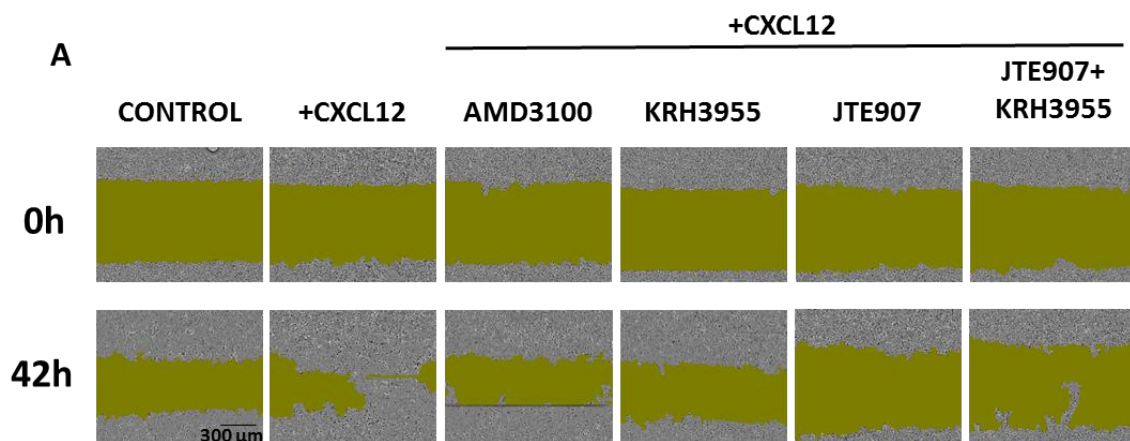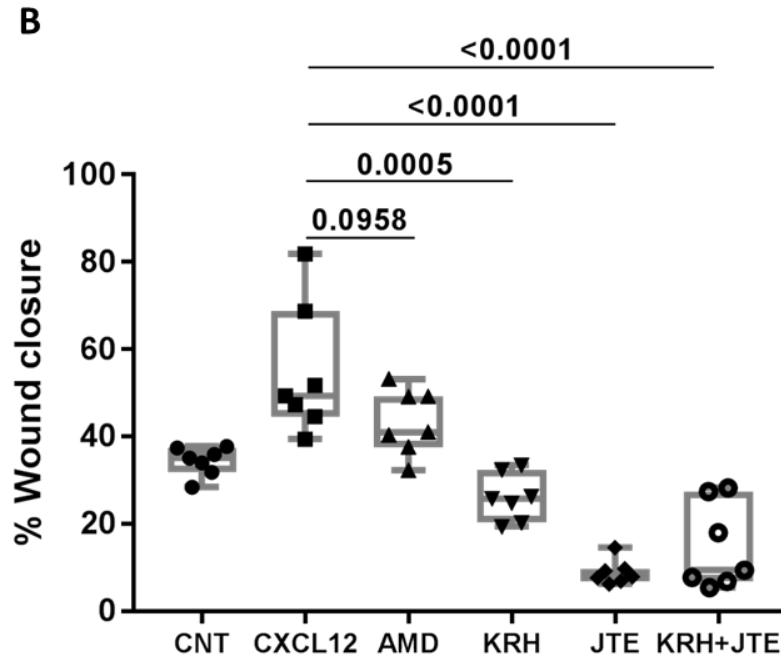
Figure 36. Crosstalk between CXCR4 and CB$_2$R affects cell migration. SW480 confluent cells were seeded in 96 well plates. Before the beginning of wound healing assay, cells were treated with mytomicin for 1h to inhibit the proliferation for 48h. The assay was performed using complete medium complemented with CXCL12 (CXCR4 ligands), which stimulate cell migration, for 42h. Every 2h images were taken. **(A)** Representative images of wound healing assay, comparing the cells at time 0 and after 42h of stimulation. **(B)** Quantification of percentage of wound closure in the different conditions. A total of 7 replicates were assed to each condition.

6. **Targeting the crosstalk between CXCR4 and CB$_2$ showed anti-metastatic and anti-proliferative effects *in vivo*.**

To investigate whether the heterodimer formation was involved in the formation of liver and lung metastasis in CRC, we first infected SW620 cells with an expression vector for GFP and luciferase (SW620-GFP-luc) to monitor the kinetics of growth and colonization ability of these cells by quantitative bioluminescence imaging. Subsequently, SW620-GFP-luc cells were inoculated into the spleen of SCID mice followed by splenectomy, and cells that colonize the liver of the animals and thus showing a more aggressive phenotype were isolated. These isolated metastatic cells from the liver with increased liver metastatic activity, SW620-L-GFP-luc, were expanded in culture and subsequently used in orthotopic injections using NOD-scid gamma (NSG) mice. SW620-L cells

showed more metastatic capacity than SW620 *in vitro*. (Figure 37 A). Moreover, SW620-L cells showed a less local aggressive phenotype in ortothopic mouse model (p=0.0042), which were able to slowly grow in the cecum of the mice to provide sufficient time to allow the cells to migrate to distant organs (Figure 37B).
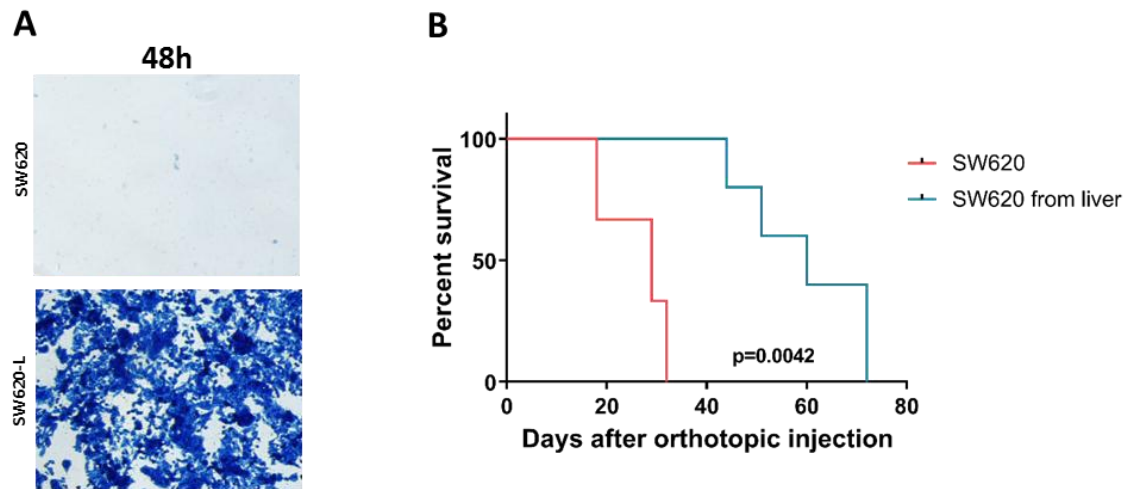
Figure 37. SW620-L cells showed high metastatic capacity. SW620-L isolated from liver after intrasplenic injection was compared to it parental cell line. **(A)** SW620 and SW620-L cell lines *in vitro* migration towards CXCL12 gradient. **(B) M**ice survival after ortothopic injection.

At day 4 after injection of SW620-L-GFP-luc cells in the mouse cecum, mice were intraperitoneal or orally treated in a daily basis with the CXCR4 antagonist, KRH-3955, with the CB_2 antagonist, JTE907, or with both antagonists for 40 days. We used KRH-3955 instead of AMD3100 due to its higher efficiency in reducing cell migration *in vitro*. At the experiment endpoint, we detected a significant decrease in primary tumor size in animals treated with a combination of CXCR4 antagonist, KRH3955 and CB_2 antagonist JTE907 (p=0.027). Animals treated with either only KRH-3955 (p=0.110) or only JTE907 (p=0.291) barely suffered a non-significant decrease in primary tumor size compared with untreated animals, (Figure 38A-C). Despite a reduction in the mitotic index in tumors from mice treated with either KRH-3955 or combination of KRH-3955 and JTE907, differences were not statistically significant when compared to tumors from non-treated mice (Figure 38D). IHC against Caspase 3 did not show differences between samples from different treatment groups. (Figure 38E).
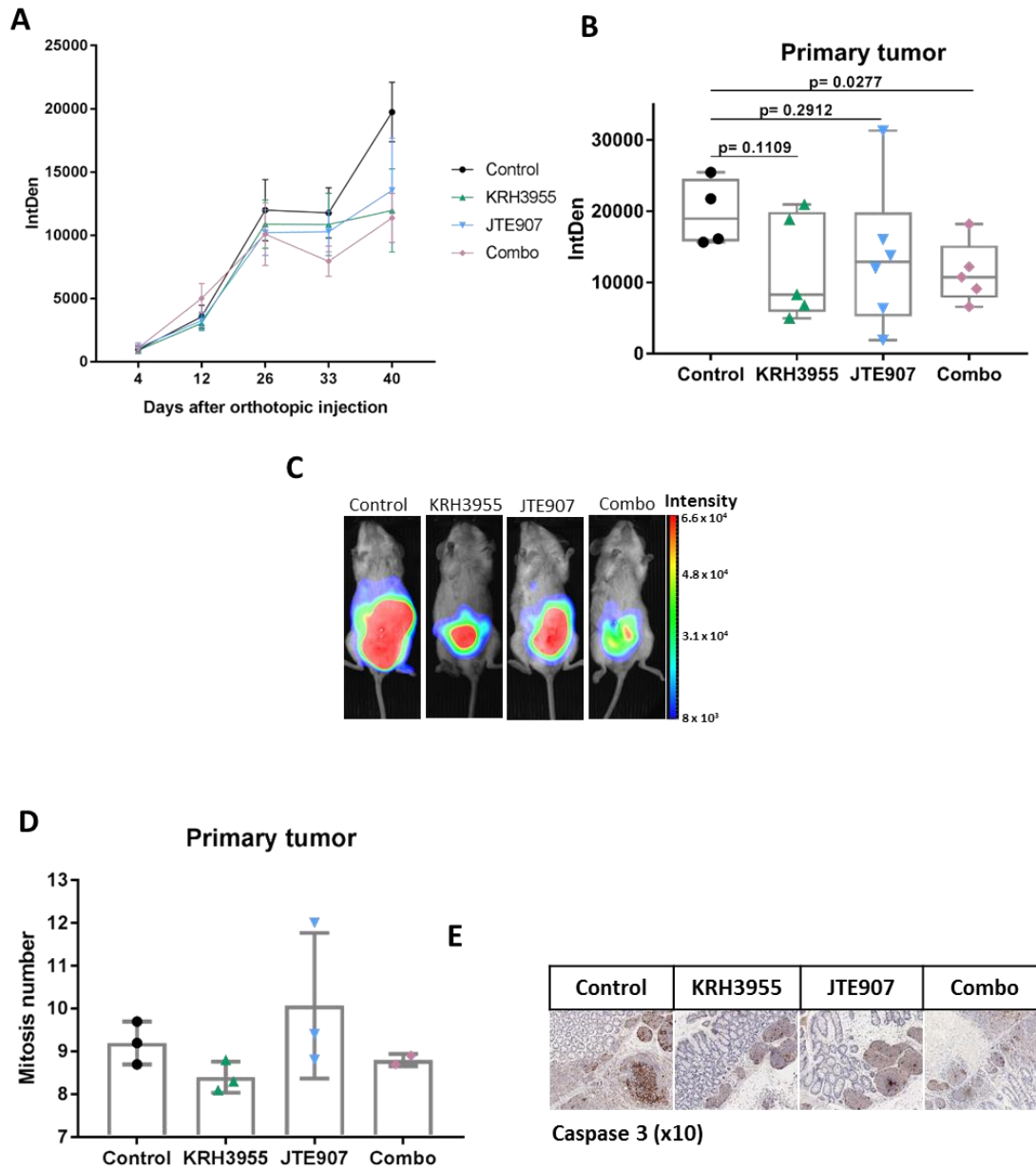
Figure 38. CXCR4 antagonist and CB₂ antagonist show anti-proliferative effect in a orthotopic mouse model of CRC. Four different group of 6 animals each one were used to assay the potential of CXCR4 and CB₂ inhibitors. **(A)** Primary tumor sizes monitoring using Hamamtsu Bioluminiscence device weekly. **(B)** After 40 days of treatment, animals were euthanized, and the sized of cecum tumors were evaluated at the end point. **(C)** Representative bioluminescent images of primary tumors**. (D)** Mitosis number in primary tumors was evaluated counting 10 different fields of 3 samples for each group. **(E)** Caspase 3 representative images.

Finally, we assessed the capacity of orthotopic injected SW620-L-GFP-luc cells to colonize the liver and the lungs (Supplemental Figure 2) upon treatment. Of note, while no differences were observed in regards to the number of metastatic nodes, the size of liver metastases were diminished in mice treated with the combination of KRH-3955 and JTE907 (p=0.0320), but not when mice were treated with either only CXCR4 or only CB_2 antagonists (p=0.2272 and p=0.2049 for KRH-3955 and JTE907 treatment, respectively) (Figure 39A and B). Further histological analysis of Ki67 staining in the metastatic lesions confirmed the results detected by bioluminescence. Smaller liver metastases were detected in animals treated with both antagonists, suggesting the biological orchestrated role of CXCR4 and CB_2 receptors to promote cell migration and metastasis *in vivo* (Figure 39C).
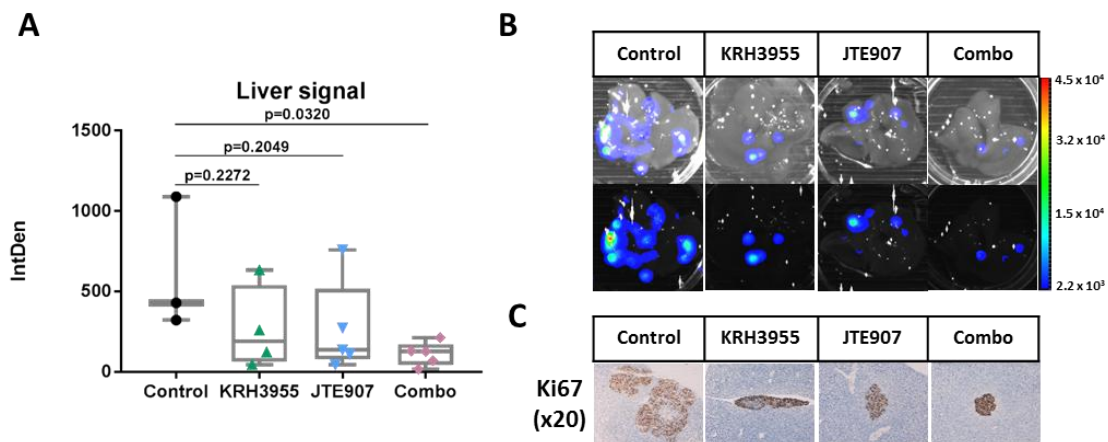
Figure 39. Targeting the crosstalk between CXCR4 and CB_2 showed anti-metastatic effect in a orthotopic mouse model of CRC. Four different group of 6 animals each one were used to assay the anti-metastatic potential of CXCR4 and CB_2 inhibitors. **(A)** *Ex-vivo* evaluation of mice livers was done. The combination of both inhibitors decreased the signal (tumors cells) in livers. **(B)** Representative images of bioluminescence in mouse livers. **(C)** Ki67 immunostaining was performed to confirm the reduction of liver metastasis volume in animals treated compared to control animals

.

DISCUSSION

The tumor microenvironment is a crucial player in tumor development and progression. Targeting specifically tumor crosstalk is a promising approach to overcome drug resistances or cancer relapses in those patients that present unsuccessful response to standard therapies.

In this thesis, we propose two new combinatorial therapies based on the disruption of crosstalk between tumor cells and their tumor microenvironment in two different cancer types. In Follicular lymphoma we explored the use of the well described and clinically used PI3K δ inhibitor (Idelalisib) and the BCL2 inhibitor Venetoclax (ABT-199). On the other hand, in colorectal cancer we examined the innovative combinational therapy of the chemokine receptor (CXCR4) inhibitor and the cannabinoid receptor inhibitor (CB$_2$), both receptors implicated in cancer progression.

Combinatorial therapy of Idelalib and Venetoclax in R/R FL

The microenvironment of human follicular lymphoma (FL), an incurable B cell non-Hodgkin's lymphoma, is thought to play a major role in its pathogenesis and course. Thus, in the recent years therapies targeting FL-microenvironment crosstalk have reached the clinic. Idelalisib has been the first-in-class PI3Kδ inhibitor approved for the treatment of Relapsed/Refractory (R/R) FL[244,627]. Despite its introduction in the clinic, a precise characterization of the interference of Idelalisib with the crosstalk of FL and its microenvironment remains ills defined. Moreover, it is highly possible that the described side effects are consequence of the same immunoregulation responsible for its therapeutic activity[628-630].

In the present study, to determine the molecular effect of idelalisib *in vitro*, we selected GEP to identify/characterize the pathways regulated by idelalisib in B cells isolated from FL samples with or without FDCs co-cultures. We demonstrated that idelalisib may modulate germinal center pathways, including CD40L signaling and targets of transcriptional repressor BLIMP, as well as, the downregulation of genes pertaining to MTORC1 signature, regardless of the presence of FDCs.

Using a meaningful *in vitro* co-culture system of FL primary cells and supportive FDCs, we have uncovered that idelalisib modulates CD40/CD40L interaction between B and T cells, essential for germinal center reaction. Idelalisib also downregulated the expression of several membrane proteins critical for B-T cell synapses such as the costimulatory molecule CD80, the activation receptor SLAMF1, required for IL-4 secretion by T$_{FH}$ [631] and the adhesion molecule ICAM1. From the specific genes regulated by CD40L-CD40 system stood out CCL22, a chemokine fundamental for the

migration of diverse T cell subpopulations[624]. This decrease in CCL22 by idelalisib had consequences in the composition of FL microenvironment. By means of *in vitro* migration assays, we have been able to demonstrate a significant decrease in the recruitment of Treg and T_{FH} when these cells were challenge to migrate towards supernatants from FL-FDC co-cultures treated with idelalisib.

PI3Kδ is fundamental for the generation of T_{FH} [632] and the presence of these supportive T_{FH} has been associated with poor prognosis in a number of hematologic malignancies[633]. Intra-tumoral T_{FH} induce production of CCL22 by FL tumor cells and facilitate active recruitment of Treg and IL-4-producing T cells, which, in turn, may stimulate more chemokine production in a feed-forward cycle. In this regard, based on previous studies[631], the decrease in the activation receptor SLAMF-1 we observed in our system may reduce IL-4 production by T_{FH}.

More importantly, the crosstalk between FL-T_{FH} contributes to FL pathogenesis and promotes immune evasion in FL microenvironment[623]. Thus, the coordinated decrease in T_{FH} and Treg recruitment may allow the host to mount superior immune responses against the tumor, and control the disease. To this end may also contribute the decrease induced by idelalisib in CCL22 and the immune suppressive cytokine IL-10[634] both secreted by pro-tumoral M2-macrophages, contributing to ameliorate the immune suppressive FL microenvironment.

It is important to note that despite Treg have long been associated to immune evasion mechanisms employed by solid tumors, in FL the presence of high numbers of FOXP3+ Treg , mostly located in the intrafollicular areas, has been associated to improved overall survival[182,183]. This apparent contradiction has been clarified by the recent discovery of a new subpopulation of FOXP3+ cells in the germinal center which co-expresses CXCR5, that may be those FOXP3+ T cells referred by Carreras and cols[182]. These cells, known as follicular regulatory T cells (T_{FR}) specifically inhibit B cell responses, controlling both GC cell number and T_{FH} function, thus justifying its correlation with good prognosis[635]. Our results indicate that idelalisib impaired Treg recruitment from peripheral blood although it did not change T_{FR} cells migration, that may be explained by the lack of expression of CCR4, precluding their response to CCL22[636].

Another key observation of our study is that idelalisib interferes with specific genes induced by the supportive FDCs just in a subset of FL primary samples. These genes were implicated in processes related to angiogenesis, extracellular matrix formation, cell migration, trans-endothelial migration, and cell-cell/cell-matrix adhesion, allowing us to define a gene signature to discriminate between

idelalisib sensitive and resistant FL primary cultures in an expanded cohort of patients. Ideally, the predictive value of this signature should be further validated in pre-treatment samples from FL patients enrolled in Idelalisib clinical trials, in order to correlate in vivo responses with this *in vitro* predictor.

Regarding angiogenesis, as we have previously reported FL-FDC interactions promote the generation of an "angiogenic niche"[620] which is of key importance in FL, as vascularization predicts overall survival and risk of transformation[148]. Just in those patients defined as sensitive based on the signature described above, idelalisib reduced the secretion of the pro-angiogenic factors VEGF-A and VEGF-C. In consequence these supernatants were significantly less efficient in the generation of endothelial HUVEC cells microtubules, used a read-out of their pro-angiogenic potential. However, it is important to note that idelalisib anti-angiogenic effect was moderate compared to previous results obtain using the pan-PI3K inhibitor BKM-120[620]. This may be explained by the prominent role of PI3Kα in angiogenesis[253] not targeted by idelalisib.

FL patients usually present with disseminated disease at diagnosis indicating the high mobility properties of these tumor cells. To enter lymphoid organs, B cells must adhere to endothelium and transmigrate across the endothelial barrier. Thus, chemokines and adhesion molecules are important in the homing of normal and malignant B cells and in lymphoma dissemination. Both firm adhesion and transmigration of the tumor cells are mediated through selectin ligands, integrins or CD44[637]. Importantly, in several models of lymphoma, including FL, the expression of several β-integrins has been associated with disease dissemination and patient prognosis[638]. Thus the regulation of this process is of paramount importance to control the disease and idelalisib has shown significant activity in sensitive patients. In this regard, studies of the interference of idelalisib with the process of adhesion have been used as a read-out of antitumor activity[639].

In an attempt to associate a specific mutational profile with idelalisib responses, we characterized the presence of somatic mutations in genes described as recurrently mutated in FL[110] (*CREBBP, KTM2D, TNRFS14, EP300, EZH2, MEF2B, EZH2, TNFAIP3, TP53* and *RRAGC*). We found that mutations in *RRAGC* correlated with idelalisib resistance, as mutations of this adaptor cause continuous mTORC1 activation, independently of PI3K/Akt1 pathway[119]. This mutation is present in 10-15% of FL patients[110], and our results are the first to support this observation that may be considered on treatment decisions.

Otherwise, *BCL-2* overexpression induced by the reciprocal translocation t(14;18)(q32;q21) is the genetic hallmark of FL, which is present in 85-90% of cases[67] [68,69], and is one of the first events in FL pathogenesis. Therefore, this fact would lead to hypothesized that inhibition of BCL-2 could be a really useful approach to treat FL patients, and obtain good responses to the treatment. But the first clinical trial with venetoclax (BCL-2 inhibitor) were not satisfactory, the ORR was 38%, and the PFS 11 months . It was proposed that the reduced activity of venetoclax in FL may be the result of a complex interplay among other anti-apoptotic proteins regulated by microenvironment, such as and BLF-1 and MCL-1, and BH3-family members[266, 640]. In this regard, we have uncovered that FL-FDC co-cultures augmented the levels of BCL-XL and MCL-1 on FL cells, while BFL-1 was increased in FL-M2 co-cultures. These events were validated using BH3 profiling[625], a technique that using peptides specific for certain anti-poptotic proteins, evaluate the degree of dependence on those proteins. BH3 profiling demonstrated that FL cells co-cultured with FDC increased their dependence on MCL-1 and BCL-XL, while FL cells co-cultured with M2 rely on BFL-1. The consequence of these microenvironment-derived changes was a decrease activity of the BCL-2 inhibitor venetoclax in FL-FDC or FL-M2 co-cultures compared to FL mono-cultures. In summary, microenvironment renders FL more dependent on apoptotic proteins different from BCL-2, reducing their priming for apoptosis. These results are in agreement with those reported by several groups in CLL and MCL[641-644] and may well lay at the basis of the reduced clinical benefit observed in FL patients treated with venetoclax[275]. Noteworthy, idelalisib counteracted the tumor microenvironment induced resistance to ABT-199 by restoring BCL-2 dependence and increasing apoptosis priming, and induced the expression of BH3-only protein HRK and reduce BAD phosphorylation, probably helping apoptosis induced by Venetoclax, supporting the use of this combinatorial regimen in FL patients.

Lastly, we concluded that the treatment of FL cells with venetoclax + idelalisib regimen resulted in synergistic reduction of cell viability compare to the treatment of venetoclax alone in FDC co-cultures. Besides, the combinatorial treatment of both drugs in M2 co-cultures showed also a synergistic reduction of cell viability.

In summary, idelalisib constitutes a valuable therapeutic tool in R/R patients, and the introduction of venetoclax in the combined therapy adds more chance of success in resistant patients. Profitably, a phase II trial of this combination will be initiated in the hematology department of Hospital Clinic based on these results.

Combinatorial therapy of KRH-3955 and JTE907 in CRC

The standard clinical procedure in advanced colon cancer treatment is the surgical resection of primary tumors and the subsequent adjuvant treatment with chemotherapy. However, a substantial number of patients show metastasis after the treatment. This highlights the need to find targeted therapies to target those tumor cell populations that acquired a more aggressive phenotype.

A large number of studies demonstrated the importance of the CXCR4/CXCL12 axis in metastatic disease, including CRC cancer. This fact has brought about the increasing number of studies related to gain insights into the biological effects of the overexpression of both CXCR4 and CXCL12 in some cancer types, and the druggable possibilities of CXCR4/CXCL12 axis to prevent the migration of these tumoral cells to secondary distant sites.

The correlation between CXCR4 expression and CRC has been extensively studied in the recent years. It has been shown that its expression might vary by anatomic location and by tumor stage, rectal cancer samples and stage III and IV colon cancer present a strong CXCR4 expression[447]. Different studies have demonstrated a positive correlation between the expression of CXCR4 in tumor cells overall survival[479], liver metastasis[645], and with LN metastasis[646]. In fact, a recent report showed results from 12 studies and performed meta-analysis with 1.913 CRC patients in order to determine the prognosis and pathological value of CXCR4 expression. The authors conclude that high CXCR4 expression was associated with poor prognosis, but with some important limitations regarding the data analysis, which included the small size of the cohort[647]. We observed the same limitation our samples set. The expression of CXCR4 is significantly higher in primary tumor and metastatic samples compare to normal mucosa, but when we assessed the correlation with prognosis, we did not observe significantly differences, likely due to the small set of patients, and also because our cohort exclusively included stage II colon cancer patients. When we studied the location of CXCR4 in cell, nearly all samples showed citoplasmatic staining, contradicting the results publish in the studies of Speetjens and Wang, where they demonstrated that a high expression of nuclear CXCR4 in tumor cells is a predictor for poor survival for CRC patients[648,649], as it is suggested to happen in other cancer types[650]. A potential explanation for these differences might be the use of a different antibody, after unsuccessful attempts to use the same antibody previously reported in our samples set, we observed nuclear staining in all samples, including normal mucosa, leading us to sort out that antibody and look for another one with higher specificity for our IHC experiments.

Taken together, our data suggest that CXCR4 expression may be a useful biomarker in CRC, but extended studies, unifying methodologies and conditions, are necessary to draw a solid conclusion.

Lately, another GPCR from cannabinoids family (CB_2 R) has been described as an interesting target in CRC due to its up-regulation in tumor cells[544]. These results were based on mRNA levels analysis, and concluding than the overexpression of the receptor is a poor prognostic factor for patients in advanced stages (lymph node positives or tumors with vascular invasion). In addition, these patients were submitted to adjuvant treatment. This led them the authors to suggest that CB_2 could be a marker for treatment resistance.

Focused on the prognostic value of CB_2 expression in CRC is not very extensive, therefore no major comparisons with our results could be accomplished. Nevertheless, our data confirm previous published results. In fact, we observed that CB_2 is overexpressed in tumor epithelial cells compared with their normal counterpart. Likewise, epithelial cells from metastasis shown higher CB_2 expression compare to normal epithelial cells. Unfortunately, we did not observe any prognostic value in our cohort. Compared to the aforementioned study, our results were based on IHC assays, and we only evaluated the expression of CB_2 in tumor cells (excluding the expression in cells from the tumor microenvironment), and at protein level in early stages patients (stage II). Therefore, we conclude that there are differences at the CB_2 levels expression between tumor cells and normal epithelial cells, but CB_2 expression is not associated with poor prognosis in stage II CRC patients. In fact, CB_2 should be considered as a possible specific therapeutic target against colon cancer cells. Furthermore, the fact that cannabinoid system is currently used in clinical practical as palliative treatment, since them capability to lessen chemotherapy sides-effects could contribute to use this kind of treatments in a specific set of patients.

A growing amount of evidence is emphasizing in the important and innovative notion of GPCRs heterodimerization. In fact, the heterodimerization of CXCR4 and CB_2,has been shown to have an impact in cancer cell invasion in breast cancer[651]. Another study in prostate cancer cell, along with breast cancer, supports the finding of CXCR4 and CB_2 heterodimers, and its implication in tumor progression[556].

In this thesis project, we observed that the high expression of both receptors at protein level in the same sample showed a tendency to worse prognosis compared to those patients that has low expression levels for both receptors. Our results did not exhibit significant differences between both groups, most likely due to the limited number of patients in our cohort.

Nonetheless, to our knowledge, the results presented in our study are the first ones to provide a strong evidence that the CXCR4-CB$_2$ heterodimer formation causes a more aggressive phenotype in CRC patients. By proximity ligation assay, we demonstrated that patients with distant metastasis within the next 5-years after detection of the primary tumor, showed a higher amount of heterodimers formation compared to those patients who did not relapse. Similarly, we reported significantly higher amount of heterodimers formation in primary samples compared to normal mucosa, suggesting a role of the CXCR4-CB$_2$ formation in the colon tumorigenesis.

In order to better understand the function of CXCR4-CB$_2$ heterodimers, we sought to use an *in vitro* model to elucidate the biological function of CXCR4 and CB$_2$ heterodimers. Among an array of different CRC cell lines, we chose SW480 cells because of their high expression levels of both receptors, and because it was the cell line that showed higher number of heterodimers. We found that endogenously-expressed CXCR4 and CB$_2$ in these cells were forming heterodimers. Based on previous studies that already explored the function of different GPCR receptors heterodimers, such as the cannabinoids receptors CB$_1$ and CB$_2$[458], or CB$_2$ and GPR55[557], we performed several assays to demonstrate the crosstalk between CXCR4 and CB$_2$ in CRC. Few studies have already attempted to address the functional role of CXCR4-CB$_2$ heterodimers in cancer, which suggested the role of heterodimers in the effects of CXCR4-induced migration in cancer cells[556,652]. Interestingly, another study demonstrated similar functional modulation in T lymphocytes[653]. Thus both receptors have been associated with proliferative and migration in cancer cells. However, the cross-talk between the two receptors remains still rather unknown. In our study, we observed that the inhibition of CB$_2$ showed a more potent effect in blocking the CXCR4 downstream signaling, than the activation of CB$_2$ receptor. Thus, our data suggest that CXCR4 and CB$_2$ display a cross-talk and bidirectional cross-antagonism at the functional level (i.e., inhibition of the p-ERK-1/2 pathway). Indeed, for a subset of CRC cells, in which CXCR4 and CB$_2$ receptors form heterodimers, the blockade of one receptor and the stimulation of the other reduces the activation of the corresponding downstream signaling pathway, and vice-versa. To our surprise, exposing cells to JTE907 (CB$_2$ antagonist) appeared to function as an antagonist for CXCR4, reducing the cell signaling levels and compromising the

migratory function. As mentioned above, previous reports have been suggested the same effect using the CB_2 agonist, but the authors did not provide any result of CB_2 inhibition[556,652]. Furthermore, this cross-antagonism mechanism showed an intriguing effect in cell migration. Our results demonstrated that CB_2 inhibition was capable of reducing CXCL12-induced cell migration.

Proposed model for CXCR4-CB_2 cross-talk:
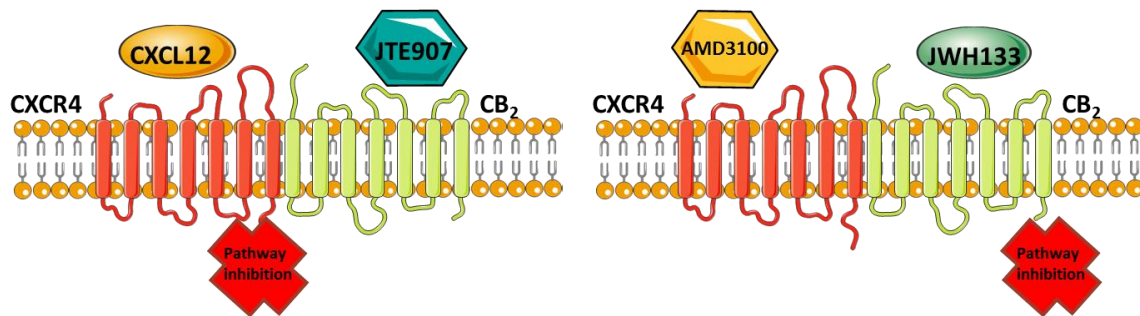
To further demonstration of CXCR4-CB_2 heterodimer functionally *in vivo*, we assessed the benefits of CXCR4 treatment (antagonist), CB_2 treatment (antagonist), and combinatorial therapy by inhibiting both receptors using an orthotopic mouse model. For this purpose, we generated a metastatic cell line, which was able to slowly growth in the cecum of the mice to provide sufficient time to allow cells migrate to distant organs. Based on previous study[618], we establish a derivate of the SW620 cell lines obtained from liver colonization after intrasplenic injection. This derivate SW620 cell line showed intermediate features between SW480 (cell lines chosen for *in vitro* experiments and able to migrate slowly to liver or lung in mouse model), and SW620 (lymph node metastasis cell line derived from SW480 same patient, which grew quickly in mouse cecum causing an intestinal obstruction producing mouse death before cells started to migrate). In a 40 day experiment, treating daily mice from day 4 on with CXCR4 antagonist, CB_2 antagonist, or combinatorial therapy by inhibiting both receptors, we observed effects at different levels. First. we detected a decrease in primary tumor growth in all treated groups compare to control animals. The group treated with the CXCR4 inhibitor, KRH-3955, showed a non-significant reduction in tumor size compare to the control. Within this group, we observed differences in the response to the treatment among different animals. Some animals responded well to the treatment, but others did non. Subsequently, we demonstrated the reduction of tumor sizes by KRH-3955 was partially due to a reduction on cell proliferation (i.e., decrease in mitoses). Similarly, the group treated with the CB_2

inhibitor, JTE907, also showed a non-significant reduction in the tumor size compared to control. These animals were treated orally (animals from KRH-3955 group were treated intraperitoneal), and also showed different responses within the group. In contrast to the animals from the previous group, these tumors now revealed a higher number of mitotic cells compare to control samples. Therefore, the increase in mitosis, accompanied by the reduction on tumor size, led us to hypothesize that JTE907 treatment induced mitotic catastrophe in tumor cells, as was described by Santoro and colleagues[654]. These authors demonstrated that rimonabant (selective CB_1 receptor antagonist) inhibits human colon cancer cell growth, induces cell death, alters cell cycle distribution (G2/M phase arrest) without inducing apoptosis, and reduces the formation of precancerous lesions in the mouse colon. These results suggest that CB_1 antagonist, rimonabant, is able to inhibit cell growth at different stages of the colon cancer pathogenesis by inducing mitotic catastrophe. Finally, animals treated with both inhibitors simultaneously, KRH-3955 and JTE907, showed a better response compare to the individually treated groups. Additionally, tumor sizes were also significantly reduced compared to the untreated animals. Furthermore, all animals from the combinatorial group showed similar response to the treatment, suggesting a higher consistency in the effect. Second, we detected a reduction in liver metastasis in mice treated with CXCR4 and CB_2 inhibitors compare to untreated animals. These results confirm previous findings in *in vivo* models of osteosarcoma and melanoma cancer using a small peptide CXCR4 antagonist to inhibit lung metastasis[655]. Surprisingly, animals treated with both inhibitors simultaneously showed a significant reduction on bioflumiscence signal. Moreover, these results were confirmed by Ki67 IHC, showing a small focus of tumor cells in liver samples. In summary, our results revealed a significant reduction of tumor size and liver metastases after simultaneous treatment with CXCR4 and CB_2 inhibitors in ortothopically-injected mice with highly metastatic CRC cells.

Taken together, our findings that CXCR4-CB_2 complexes have a particular signaling and function properties, and are critically involved in the response of cancer cells to KRH-3955 and JTE907 *in vitro* and *in vivo*, suggest the potential usage of both inhibitors for patients that present high amounts of heterodimers, thus a more aggressive phenotype. In addition, our results shed light on the development of compounds targeting these heterodimers. Whereas a single antagonist would inhibit CXCR4 function in a wide spectrum of cell types, including immune cells or hematopoietic stem cells, a combination of CXCR4 and CB_2 antagonists intended to promote inhibition via

heterodimerization could provide a higher specificity on tumor cells due to the increased expression levels of both receptors. Thus, targeted therapy against CXCR4-CB$_2$ heterodimers could be an innovative alternative approach to treat metastatic CRC patient granted that metastasis is not resectable and the associated poor overall survival rate.

CONCLUSIONS

The main conclusions derived from this thesis are:

First study: Idelalisib Interferes with the Crosstalk of Follicular Lymphoma and its Immune Microenvironment and Potentiates the Activity of ABT-199

1. Idelalisib modulates key pathways in the germinal center and downregulates the FDC-induced pathways in a selected group of patients.

2. Idelalisib shapes the FL immune microenvironment by decreasing the recruitment of TFH and Treg to the tumor site leading to less immunesuppresive phenotype

3. Idelalisib induces a moderate cytotoxic effect on FL cells that is maintained in FL- FDC and FL-M2 co-cultures.

4. FDC and M2 decrease FL dependence on BCL-2 and consequently, venetoclax cytotoxicity. Idelalisib sensitizes FL-FDC and FL-M2 co-cultures to venetoclax

Second study: GPCRs heterodimers as a new therapeutic target in colorectal cancer

5. CXCR4 and CB_2 expression is increased in primary colon tumor cells and in metastasis cells compared to normal epithelial cells from colon mucosa.

6. CXCR4 and CB_2 form heterodimers in colon tumoral cells and are associated with more aggressive phenotypes.

7. A bidirectional cross-antagonism crosstalk is established between these receptors.

8. CXCR4 and CB_2 heterodimers regulate *in vitro* CXCL12-induced migration.

9. *In vivo*, simultaneous CXCR4 and CB_2 inhibition shows superior anti-tumoral and anti-metastatic activities than the single agent inhibition.

BIBLIOGRAPHY

1   Mukherjee, S. *The emperor of all maladies: a biography of cancer*. (Simon and Schuster, 2010).

2   Maloney, D. G. *et al.* IDEC-C2B8 (Rituximab) anti-CD20 monoclonal antibody therapy in patients with relapsed low-grade non-Hodgkin's lymphoma. *Blood* **90**, 2188-2195 (1997).

3   Bishop, J. M. & Weinberg, R. A. *Scientific American molecular oncology*. (Scientific American, 1996).

4   Hanahan, D. & Weinberg, R. A. Hallmarks of cancer: the next generation. *cell* **144**, 646-674 (2011).

5   Hanahan, D. & Weinberg, R. A. The hallmarks of cancer. *cell* **100**, 57-70 (2000).

6   Esteller, M. Cancer epigenomics: DNA methylomes and histone-modification maps. *Nature Reviews Genetics* **8**, 286 (2007).

7   Berdasco, M. & Esteller, M. Aberrant epigenetic landscape in cancer: how cellular identity goes awry. *Developmental cell* **19**, 698-711 (2010).

8   Lane, D. P. Cancer. p53, guardian of the genome. *Nature* **358**, 15-16 (1992).

9   Dvorak, H. F. Tumors: wounds that do not heal. *New England Journal of Medicine* **315**, 1650-1659 (1986).

10   Grivennikov, S. I., Greten, F. R. & Karin, M. Immunity, inflammation, and cancer. *Cell* **140**, 883-899 (2010).

11   DeNardo, D. G., Andreu, P. & Coussens, L. M. Interactions between lymphocytes and myeloid cells regulate pro-versus anti-tumor immunity. *Cancer and Metastasis Reviews* **29**, 309-316 (2010).

12   Lemmon, M. A. & Schlessinger, J. Cell signaling by receptor tyrosine kinases. *Cell* **141**, 1117-1134 (2010).

13   Bhowmick, N. A., Neilson, E. G. & Moses, H. L. Stromal fibroblasts in cancer initiation and progression. *Nature* **432**, 332 (2004).

14   Salomon, D. S., Brandt, R., Ciardiello, F. & Normanno, N. Epidermal growth factor-related peptides and their receptors in human malignancies. *Critical reviews in oncology/hematology* **19**, 183-232 (1995).

15   Jiang, B. H. & Liu, L. Z. PI3K/PTEN signaling in angiogenesis and tumorigenesis. *Advances in cancer research* **102**, 19-65 (2009).

16   Yuan, T. & Cantley, L. PI3K pathway alterations in cancer: variations on a theme. *Oncogene* **27**, 5497 (2008).

17   Burkhart, D. L. & Sage, J. Cellular mechanisms of tumour suppression by the retinoblastoma gene. *Nature Reviews Cancer* **8**, 671 (2008).

18   Sherr, C. J. & McCormick, F. The RB and p53 pathways in cancer. *Cancer cell* **2**, 103-112 (2002).

19   Curto, M., Cole, B. K., Lallemand, D., Liu, C.-H. & McClatchey, A. I. Contact-dependent inhibition of EGFR signaling by Nf2/Merlin. *J Cell Biol* **177**, 893-903 (2007).

20   Bierie, B. & Moses, H. L. Tumour microenvironment: TGFβ: the molecular Jekyll and Hyde of cancer. *Nature Reviews Cancer* **6**, nrc1926 (2006).

21   Massagué, J. TGFβ in cancer. *Cell* **134**, 215-230 (2008).

22   Evan, G. & Littlewood, T. A matter of life and cell death. *Science* **281**, 1317-1322 (1998).

23   Lowe, S. W., Cepero, E. & Evan, G. Intrinsic tumour suppression. *Nature* **432**, 307 (2004).

24   Adams, J. M. & Cory, S. The Bcl-2 apoptotic switch in cancer development and therapy. *Oncogene* **26**, 1324 (2007).

25   Harris, C. C. Structure and function of the p53 tumor suppressor gene: clues for rational cancer therapeutic strategies. *JNCI: Journal of the National Cancer Institute* **88**, 1442-1455 (1996).

26   Junttila, M. R. & Evan, G. I. p53—a Jack of all trades but master of none. *Nature reviews cancer* **9**, 821 (2009).

27   Levine, B. & Kroemer, G. Autophagy in the pathogenesis of disease. *Cell* **132**, 27-42 (2008).

28   Blasco, M. A. Telomeres and human disease: ageing, cancer and beyond. *Nature Reviews Genetics* **6**, 611 (2005).

29   Kuilman, T., Michaloglou, C., Mooi, W. J. & Peeper, D. S. The essence of senescence. *Genes & development* **24**, 2463-2479 (2010).

30   Hanahan, D. & Folkman, J. Patterns and emerging mechanisms of the angiogenic switch during tumorigenesis. *cell* **86**, 353-364 (1996).

31   Carmeliet, P. VEGF as a key mediator of angiogenesis in cancer. *Oncology* **69**, 4-10 (2005).

32   Ferrara, N. Vascular endothelial growth factor. *Arteriosclerosis, thrombosis, and vascular biology* **29**, 789-791 (2009).

33   Baeriswyl, V. & Christofori, G. in *Seminars in cancer biology.* 329-337 (Elsevier).

34   Bergers, G. & Benjamin, L. E. Angiogenesis: tumorigenesis and the angiogenic switch. *Nature reviews cancer* **3**, 401 (2003).

35   Murdoch, C., Muthana, M., Coffelt, S. B. & Lewis, C. E. The role of myeloid cells in the promotion of tumour angiogenesis. *Nature Reviews Cancer* **8**, nrc2444 (2008).

36   Qian, B.-Z. & Pollard, J. W. Macrophage diversity enhances tumor progression and metastasis. *Cell* **141**, 39-51 (2010).

37   Ferrara, N. Pathways mediating VEGF-independent tumor angiogenesis. *Cytokine & growth factor reviews* **21**, 21-26 (2010).

38   Sporn, M. B. The war on cancer. *Lancet (London, England)* **347**, 1377-1381 (1996).

39   Cavallaro, U. & Christofori, G. Cell adhesion and signalling by cadherins and Ig-CAMs in cancer. *Nature Reviews Cancer* **4**, 118 (2004).

40   Berx, G. & Van Roy, F. Involvement of members of the cadherin superfamily in cancer. *Cold Spring Harbor perspectives in biology*, a003129 (2009).

41   Polyak, K. & Weinberg, R. A. Transitions between epithelial and mesenchymal states: acquisition of malignant and stem cell traits. *Nature Reviews Cancer* **9**, 265 (2009).

42   Thiery, J. P., Acloque, H., Huang, R. Y. & Nieto, M. A. Epithelial-mesenchymal transitions in development and disease. *cell* **139**, 871-890 (2009).

43   Egeblad, M., Nakasone, E. S. & Werb, Z. Tumors as organs: complex tissues that interface with the entire organism. *Developmental cell* **18**, 884-901 (2010).

44   Karnoub, A. E. *et al.* Mesenchymal stem cells within tumour stroma promote breast cancer metastasis. *Nature* **449**, 557 (2007).

45   Warburg, O. H. & Dickens, F. *The metabolism of tumours: investigations from the Kaiser Wilhelm Institute for Biology, Berlin-Dahlem.* (Constable & Company, 1930).

46   DeBerardinis, R. J., Lum, J. J., Hatzivassiliou, G. & Thompson, C. B. The biology of cancer: metabolic reprogramming fuels cell growth and proliferation. *Cell metabolism* **7**, 11-20 (2008).

47   Kim, R., Emi, M. & Tanabe, K. Cancer immunoediting from immune surveillance to immune escape. *Immunology* **121**, 1-14 (2007).

48   Pages, F. *et al.* Immune infiltration in human tumors: a prognostic factor that should not be ignored. *Oncogene* **29**, 1093 (2010).

49   Yang, L., Pang, Y. & Moses, H. L. TGF-β and immune cells: an important regulatory axis in the tumor microenvironment and progression. *Trends in immunology* **31**, 220-227 (2010).

50   Al-Hajj, M., Wicha, M. S., Benito-Hernandez, A., Morrison, S. J. & Clarke, M. F. Prospective identification of tumorigenic breast cancer cells. *Proceedings of the National Academy of Sciences* **100**, 3983-3988 (2003).

51   Marusyk, A. & Polyak, K. Tumor heterogeneity: causes and consequences. *Biochimica et Biophysica Acta (BBA)-Reviews on Cancer* **1805**, 105-117 (2010).

52   Ansell, S. M. & Vonderheide, R. H. in *American Society of Clinical Oncology educational book. American Society of Clinical Oncology. Meeting.*

53   Küppers, R. Mechanisms of B-cell lymphoma pathogenesis. *Nature Reviews Cancer* **5**, 251 (2005).

54   Hanahan, D. & Coussens, L. M. Accessories to the crime: functions of cells recruited to the tumor microenvironment. *Cancer cell* **21**, 309-322 (2012).

55   Mounier, M. *et al.* Changes in dynamics of excess mortality rates and net survival after diagnosis of follicular lymphoma or diffuse large B-cell lymphoma: comparison between European population-based data (EUROCARE-5). *The Lancet Haematology* **2**, e481-e491 (2015).

56   Siegel, R., Miller, K. & Jemal, A. Cancer Statistics, 2017 CA Cancer J Clin 2017; 67: 7-30. *External Resources Pubmed/Medline (NLM) Crossref (DOI)*.

57   Subramanian, J., Cavenagh, J., Desai, B. & Jacobs, I. Rituximab in the treatment of follicular lymphoma: the future of biosimilars in the evolving therapeutic landscape. *Cancer management and research* **9**, 131 (2017).

58   Kahl, B. S. Follicular lymphoma: are we ready for a risk-adapted approach? *ASH Education Program Book* **2017**, 358-364 (2017).

59   Kridel, R., Sehn, L. H. & Gascoyne, R. D. Pathogenesis of follicular lymphoma. *The Journal of clinical investigation* **122**, 3424-3431 (2012).

60   de Jong, D. & Fest, T. The microenvironment in follicular lymphoma. *Best Practice & Research Clinical Haematology* **24**, 135-146 (2011).

61   Horning, S. J. & Rosenberg, S. A. The natural history of initially untreated low-grade non-Hodgkin's lymphomas. *New England Journal of Medicine* **311**, 1471-1475 (1984).

62   Kahl, B. S. & Yang, D. Follicular lymphoma: evolving therapeutic strategies. *Blood*, blood-2015-2011-624288 (2016).

63   Tan, D. *et al.* Improvements in observed and relative survival in follicular grade 1-2 lymphoma over four decades: the Stanford University experience. *Blood*, blood-2013-2003-491514 (2013).

64   Magnano, L. *et al.* Life Expectancy of Follicular Lymphoma Patients in Complete Response at 30 Months is Similar to that of the Spanish General Population. (2018).

65   Rivas-Delgado, A. *et al.* Response duration and survival shorten after each relapse in patients with follicular lymphoma treated in the rituximab era. *British journal of haematology* (2018).

66   Montoto, S. & Fitzgibbon, J. Transformation of indolent B-cell lymphomas. *Journal of clinical oncology* **29**, 1827-1834 (2011).

67   Roulland, S. *et al.* Follicular lymphoma-like B cells in healthy individuals: a novel intermediate step in early lymphomagenesis. *Journal of Experimental Medicine* **203**, 2425-2431 (2006).

68   Tsujimoto, Y., Finger, L. R., Yunis, J., Nowell, P. C. & Croce, C. M. Cloning of the chromosome breakpoint of neoplastic B cells with the t (14; 18) chromosome translocation. *Science* **226**, 1097-1099 (1984).

69   Tsujimoto, Y., Cossman, J., Jaffe, E. & Croce, C. M. Involvement of the bcl-2 gene in human follicular lymphoma. *Science* **228**, 1440-1443 (1985).

70   Horsman, D. E. *et al.* Follicular lymphoma lacking the t (14; 18)(q32; q21): identification of two disease subtypes. *British journal of haematology* **120**, 424-433 (2003).

71   Leich, E. *et al.* Follicular lymphomas with and without translocation t (14; 18) differ in gene expression profiles and genetic alterations. *Blood* **114**, 826-834 (2009).

72   Leich, E. *et al.* Similar clinical features in follicular lymphomas with and without breaks in the BCL2 locus. *Leukemia* **30**, 854 (2016).

73   Tsujimoto, Y., Gorham, J., Cossman, J., Jaffe, E. & Croce, C. M. The t (14; 18) chromosome translocations involved in B-cell neoplasms result from mistakes in VDJ joining. *Science* **229**, 1390-1393 (1985).

74   Roulland, S. *et al.* in *Advances in immunology* Vol. 111   1-46 (Elsevier, 2011).

75   McDonnell, T. J. *et al.* bcl-2-immunoglobulin transgenic mice demonstrate extended B cell survival and follicular lymphoproliferation. *Cell* **57**, 79-88 (1989).

76   McDonnell, T. J. & Korsmeyer, S. J. Progression from lymphoid hyperplasia to high-grade malignant lymphoma in mice transgenic for the t (14; 18). *Nature* **349**, 254 (1991).

77   Sungalee, S. *et al.* Germinal center reentries of BCL2-overexpressing B cells drive follicular lymphoma progression. *The Journal of clinical investigation* **124**, 5337-5351 (2014).

78   Strasser, A., Cory, S. & Adams, J. M. Deciphering the rules of programmed cell death to improve therapy of cancer and other diseases. *The EMBO journal* **30**, 3667-3683 (2011).

79   Brunelle, J. K. & Letai, A. Control of mitochondrial apoptosis by the Bcl-2 family. *Journal of cell science* **122**, 437-441 (2009).

80   Llambi, F. *et al.* A unified model of mammalian BCL-2 protein family interactions at the mitochondria. *Molecular cell* **44**, 517-531 (2011).

81   Küppers, R. & Stevenson, F. K. Critical influences on the pathogenesis of follicular lymphoma. *Blood*, blood-2017-2011-764365 (2018).

82   Limpens, J. *et al.* Lymphoma-associated translocation t (14; 18) in blood B cells of normal individuals. *Blood* **85**, 2528-2536 (1995).

83   Dölken, G., Illerhaus, G., Hirt, C. & Mertelsmann, R. BCL-2/JH rearrangements in circulating B cells of healthy blood donors and patients with nonmalignant diseases. *Journal of Clinical Oncology* **14**, 1333-1344 (1996).

84   Schüler, F. *et al.* Prevalence and frequency of circulating t (14; 18)-MBR translocation carrying cells in healthy individuals. *International journal of cancer* **124**, 958-963 (2009).

85   Hirt, C. *et al.* Risk of follicular lymphoma associated with BCL2 translocations in peripheral blood. *Leukemia & lymphoma* **56**, 2625-2629 (2015).

86   Green, M. R. *et al.* Hierarchy in somatic mutations arising during genomic evolution and progression of follicular lymphoma. *Blood*, blood-2012-2009-457283 (2013).

87   Green, M. R. *et al.* Mutations in early follicular lymphoma progenitors are associated with suppressed antigen presentation. *Proceedings of the National Academy of Sciences*, 201501199 (2015).

88   Cha, S.-C. *et al.* Nonstereotyped lymphoma B cell receptors recognize vimentin as a shared autoantigen. *The Journal of Immunology*, 1300179 (2013).

89   Coelho, V. *et al.* Glycosylation of surface Ig creates a functional bridge between human follicular lymphoma and microenvironmental lectins. *Proceedings of the National Academy of Sciences* **107**, 18587-18592 (2010).

90   Linley, A. *et al.* Lectin binding to surface Ig variable regions provides a universal persistent activating signal for follicular lymphoma cells. *Blood*, blood-2015-2004-640805 (2015).

91   Morin, R. D. *et al.* Somatic mutations altering EZH2 (Tyr641) in follicular and diffuse large B-cell lymphomas of germinal-center origin. *Nature genetics* **42**, 181 (2010).

92   Morin, R. D. *et al.* Frequent mutation of histone-modifying genes in non-Hodgkin lymphoma. *Nature* **476**, 298 (2011).

93   Pasqualucci, L. *et al.* Inactivating mutations of acetyltransferase genes in B-cell lymphoma. *Nature* **471**, 189 (2011).

94   Okosun, J. *et al.* Integrated genomic analysis identifies recurrent mutations and evolution patterns driving the initiation and progression of follicular lymphoma. *Nature genetics* **46**, 176 (2014).

95   Bödör, C. *et al.* EZH2 mutations are frequent and represent an early event in follicular lymphoma. *Blood*, blood-2013-2004-496893 (2013).

96   Zhang, J. *et al.* The CREBBP acetyltransferase is a haploinsufficient tumor suppressor in B-cell lymphoma. *Cancer discovery* (2017).

97   Zhang, J. *et al.* Disruption of KMT2D perturbs germinal center B cell development and promotes lymphomagenesis. *Nature medicine* **21**, 1190 (2015).

98   Béguelin, W. *et al.* EZH2 is required for germinal center formation and somatic EZH2 mutations promote lymphoid transformation. *Cancer cell* **23**, 677-692 (2013).

99   Ortega-Molina, A. *et al.* The histone lysine methyltransferase KMT2D sustains a gene expression program that represses B cell lymphoma development. *Nature medicine* **21**, 1199 (2015).

100   Jiang, Y. *et al.* CREBBP inactivation promotes the development of HDAC3 dependent lymphomas. *Cancer discovery*, CD-16-0975 (2016).

101   Caganova, M. *et al.* Germinal center dysregulation by histone methyltransferase EZH2 promotes lymphomagenesis. *The Journal of clinical investigation* **123**, 5009-5022 (2013).

102   García-Ramírez, I. *et al.* Crebbp loss cooperates with Bcl2 over-expression to promote lymphoma in mice. *Blood*, blood-2016-2008-733469 (2017).

103   Béguelin, W. *et al.* EZH2 and BCL6 cooperate to assemble CBX8-BCOR complex to repress bivalent promoters, mediate germinal center formation and lymphomagenesis. *Cancer Cell* **30**, 197-213 (2016).

104   Ying, C. Y. *et al.* MEF2B mutations lead to deregulated expression of the oncogene BCL6 in diffuse large B cell lymphoma. *Nature immunology* **14**, 1084 (2013).

105   Pon, J. R. *et al.* MEF2B mutations in non-Hodgkin lymphoma dysregulate cell migration by decreasing MEF2B target gene activation. *Nature communications* **6**, 7953 (2015).

106   Trinh, D. L. *et al.* Analysis of FOXO1 mutations in diffuse large B-cell lymphoma. *Blood*, blood-2013-2001-479865 (2013).

107   Sander, S. *et al.* PI3 kinase and FOXO1 transcription factor activity differentially control B cells in the germinal center light and dark zones. *Immunity* **43**, 1075-1086 (2015).

108   Li, H. *et al.* Mutations in linker histone genes HIST1H1 B, C, D and E, OCT2 (POU2F2), IRF8 and ARID1A underlying the pathogenesis of follicular lymphoma. *Blood*, blood-2013-2005-500264 (2014).

109   Krysiak, K. *et al.* Recurrent somatic mutations affecting B-cell receptor signaling pathway genes in follicular lymphoma. *Blood*, blood-2016-2007-729954 (2016).

110   Huet, S., Sujobert, P. & Salles, G. From genetics to the clinic: a translational perspective on follicular lymphoma. *Nature Reviews Cancer* **18**, 224 (2018).

111   Dominguez, P. M. *et al.* DNA methylation dynamics of germinal center B cells are mediated by AID. *Cell reports* **12**, 2086-2098 (2015).

112   Kulis, M. *et al.* Whole-genome fingerprint of the DNA methylome during human B cell differentiation. *Nature genetics* **47**, 746 (2015).

113   O'Riain, C. *et al.* Array-based DNA methylation profiling in follicular lymphoma. *Leukemia* **23**, 1858 (2009).

114   De, S. *et al.* Aberration in DNA methylation in B-cell lymphomas has a complex origin and increases with disease severity. *PLoS genetics* **9**, e1003137 (2013).

115   Kretzmer, H. *et al.* DNA methylome analysis in Burkitt and follicular lymphomas identifies differentially methylated regions linked to somatic mutation and transcriptional control. *Nature genetics* **47**, 1316 (2015).

116   Young, R. M. & Staudt, L. M. Targeting pathological B cell receptor signalling in lymphoid malignancies. *Nature reviews Drug discovery* **12**, 229 (2013).

117   Lenz, G. *et al.* Oncogenic CARD11 mutations in human diffuse large B cell lymphoma. *Science* **319**, 1676-1679 (2008).

118   Lamason, R. L., McCully, R. R., Lew, S. M. & Pomerantz, J. L. Oncogenic CARD11 mutations induce hyperactive signaling by disrupting autoinhibition by the PKC-responsive inhibitory domain. *Biochemistry* **49**, 8240-8250 (2010).

119   Okosun, J. *et al.* Recurrent mTORC1-activating RRAGC mutations in follicular lymphoma. *Nature genetics* **48**, 183 (2016).

120   Sancak, Y. *et al.* Ragulator-Rag complex targets mTORC1 to the lysosomal surface and is necessary for its activation by amino acids. *Cell* **141**, 290-303 (2010).

121   Rebsamen, M. *et al.* SLC38A9 is a component of the lysosomal amino acid sensing machinery that controls mTORC1. *Nature* **519**, 477 (2015).

122   Bouska, A. *et al.* Combined copy number and mutation analysis identifies oncogenic pathways associated with transformation of follicular lymphoma. *Leukemia* **31**, 83 (2017).

123   Karube, K. *et al.* Recurrent mutations of NOTCH genes in follicular lymphoma identify a distinctive subset of tumours. *The Journal of pathology* **234**, 423-430 (2014).

124   Kreutz, B., Hajicek, N., Yau, D. M., Nakamura, S. & Kozasa, T. Distinct regions of Gα13 participate in its regulatory interactions with RGS homology domain-containing RhoGEFs. *Cellular signalling* **19**, 1681-1689 (2007).

125   Cai, G. & Freeman, G. J. The CD160, BTLA, LIGHT/HVEM pathway: a bidirectional switch regulating T-cell activation. *Immunological reviews* **229**, 244-258 (2009).

126   Murphy, K. M., Nelson, C. A. & Šedý, J. R. Balancing co-stimulation and inhibition with BTLA and HVEM. *Nature Reviews Immunology* **6**, 671 (2006).

127   Cheung, K.-J. J. *et al.* Acquired TNFRSF14 mutations in follicular lymphoma are associated with inferior prognosis. *Cancer research*, canres. 2460.2010 (2010).

128   Launay, E. *et al.* High rate of TNFRSF14 gene alterations related to 1p36 region in de novo follicular lymphoma and impact on prognosis. *Leukemia* **26**, 559 (2012).

129   Wagner-Johnston, N. D. *et al.* Outcomes of transformed follicular lymphoma in the modern era: a report from the National LymphoCare Study (NLCS). *Blood*, blood-2015-2001-621375 (2015).

130   Sarkozy, C. *et al.* Risk factors and outcomes for patients with follicular lymphoma who had histologic transformation after response to first-line immunochemotherapy in the PRIMA trial. *Journal of Clinical Oncology* **34**, 2575-2582 (2016).

131   Lossos, I. S. & Gascoyne, R. D. Transformation of follicular lymphoma. *Best practice & research Clinical haematology* **24**, 147-163 (2011).

132   Kridel, R. *et al.* Cell-of-origin of transformed follicular lymphoma. *Blood*, blood-2015-2006-649905 (2015).

133   Kridel, R., Sehn, L. H. & Gascoyne, R. D. Can histologic transformation of follicular lymphoma be predicted and prevented? *Blood*, blood-2017-2003-691345 (2017).

134   Carlotti, E. *et al.* Transformation of follicular lymphoma to diffuse large B-cell lymphoma may occur by divergent evolution from a common progenitor cell or by direct evolution from the follicular lymphoma clone. *Blood* **113**, 3553-3557 (2009).

135   Swerdlow, S. H. *et al.* The 2016 revision of the World Health Organization (WHO) classification of lymphoid neoplasms. *Blood*, blood-2016-2001-643569 (2016).

136   Kridel, R. *et al.* Histological transformation and progression in follicular lymphoma: a clonal evolution study. *PLoS medicine* **13**, e1002197 (2016).

137   Pasqualucci, L. *et al.* Genetics of follicular lymphoma transformation. *Cell reports* **6**, 130-140 (2014).

138   Sander, C. *et al.* p53 mutation is associated with progression in follicular lymphomas. *Blood* **82**, 1994-2004 (1993).

139   Yano, T., Jaffe, E., Longo, D. & Raffeld, M. MYC rearrangements in histologically progressed follicular lymphomas. *Blood* **80**, 758-767 (1992).

140   Lossos, I. S. *et al.* Transformation of follicular lymphoma to diffuse large-cell lymphoma: alternative patterns with increased or decreased expression of c-myc and its regulated genes. *Proceedings of the National Academy of Sciences* **99**, 8886-8891 (2002).

141   Bouska, A. *et al.* Genome-wide copy number analyses reveal genomic abnormalities involved in transformation of follicular lymphoma. *Blood*, blood-2013-2005-500595 (2013).

142   Lackraj, T., Goswami, R. & Kridel, R. Pathogenesis of follicular lymphoma. *Best Practice & Research Clinical Haematology* (2017).

143   Scherer, F. *et al.* Distinct biological subtypes and patterns of genome evolution in lymphoma revealed by circulating tumor DNA. *Science translational medicine* **8**, 364ra155-364ra155 (2016).

144   Glas, A. M. *et al.* Gene-expression and immunohistochemical study of specific T-cell subsets and accessory cell types in the transformation and prognosis of follicular lymphoma. *Journal of clinical oncology* **25**, 390-398 (2007).

145   Smeltzer, J. *et al.* Pattern of CD14+ follicular dendritic cells and PD1+ T cells independently predicts time to transformation in follicular lymphoma. *Clinical Cancer Research*, clincanres. 2367.2013 (2014).

146   Blaker, Y. N. *et al.* The tumour microenvironment influences survival and time to transformation in follicular lymphoma in the rituximab era. *British journal of haematology* **175**, 102-114 (2016).

147   Farinha, P. *et al.* The architectural pattern of FOXP3-positive T cells in follicular lymphoma is an independent predictor of survival and histologic transformation. *Blood* **115**, 289-295 (2010).

148   Farinha, P. *et al.* Vascularization predicts overall survival and risk of transformation in follicular lymphoma. *haematologica*, haematol. 2009.021766 (2010).

149   Wrench, D. *et al.* SNP rs6457327 in the HLA region on chromosome 6p is predictive of the transformation of follicular lymphoma. *Blood*, blood-2010-2010-315382 (2011).

150   Gentles, A. J. *et al.* A pluripotency signature predicts histologic transformation and influences survival in follicular lymphoma patients. *Blood* **114**, 3158-3166 (2009).

151   Brodtkorb, M. *et al.* Whole-genome integrative analysis reveals expression signatures predicting transformation in follicular lymphoma. *Blood*, blood-2013-2007-512392 (2013).

152   Yunis, J. J. *et al.* Multiple recurrent genomic defects in follicular lymphoma. *New England Journal of Medicine* **316**, 79-84 (1987).

153   Tilly, H. *et al.* Prognostic value of chromosomal abnormalities in follicular lymphoma. *Blood* **84**, 1043-1049 (1994).

154   Cheung, K.-J. J. *et al.* Genome-wide profiling of follicular lymphoma by array comparative genomic hybridization reveals prognostically significant DNA copy number imbalances. *Blood* **113**, 137-148 (2009).

155   Eide, M. B. *et al.* Genomic alterations reveal potential for higher grade transformation in follicular lymphoma and confirm parallel evolution of tumor cell clones. *Blood*, blood-2010-2003-272278 (2010).

156   O'Shea, D. *et al.* The presence of TP53 mutation at diagnosis of follicular lymphoma identifies a high-risk group of patients with shortened time to disease progression and poorer overall survival. *Blood* **112**, 3126-3129 (2008).

157   Akasaka, T., Lossos, I. S. & Levy, R. BCL6 gene translocation in follicular lymphoma: a harbinger of eventual transformation to diffuse aggressive lymphoma. *Blood* **102**, 1443-1448 (2003).

158   Correia, C. *et al.* BCL2 mutations are associated with increased risk of transformation and shortened survival in follicular lymphoma. *Blood*, blood-2014-2004-571786 (2014).

159   Dave, S. S. *et al.* Prediction of survival in follicular lymphoma based on molecular features of tumor-infiltrating immune cells. *New England Journal of Medicine* **351**, 2159-2169 (2004).

160   Tew, J. G., Wu, J., Fakher, M., Szakal, A. K. & Qin, D. Follicular dendritic cells: beyond the necessity of T-cell help. *Trends in immunology* **22**, 361-367 (2001).

161   Guilloton, F. *et al.* Mesenchymal stromal cells orchestrate follicular lymphoma cell niche through the CCL2-dependent recruitment and polarization of monocytes. *Blood*, blood-2011-2008-370908 (2012).

162   Pandey, S. *et al.* IL-4/CXCL12 loop is a key regulator of lymphoid stroma function in follicular lymphoma. *Blood*, blood-2016-2008-737239 (2017).

163   Amé-Thomas, P. & Tarte, K. in *Seminars in cancer biology.* 23-32 (Elsevier).

164   Mueller, S. N. & Germain, R. N. Stromal cell contributions to the homeostasis and functionality of the immune system. *Nature Reviews Immunology* **9**, 618 (2009).

165   Roozendaal, R. & Mebius, R. E. Stromal cell–immune cell interactions. *Annual review of immunology* **29**, 23-43 (2011).

166   Dierks, C. *et al.* Essential role of stromally induced hedgehog signaling in B-cell malignancies. *Nature medicine* **13**, 944 (2007).

167   Park, C.-S., Yoon, S.-O., Armitage, R. J. & Choi, Y. S. Follicular dendritic cells produce IL-15 that enhances germinal center B cell proliferation in membrane-bound form. *The Journal of Immunology* **173**, 6676-6683 (2004).

168   Tjin, E. P. *et al.* Follicular dendritic cells catalyze hepatocyte growth factor (HGF) activation in the germinal center microenvironment by secreting the serine protease HGF activator. *The Journal of Immunology* **175**, 2807-2813 (2005).

169   Lwin, T. *et al.* Lymphoma cell adhesion-induced expression of B cell-activating factor of the TNF family in bone marrow stromal cells protects non-Hodgkin's B lymphoma cells from apoptosis. *Leukemia* **23**, 170 (2009).

170   Amé-Thomas, P. *et al.* Human mesenchymal stem cells isolated from bone marrow and lymphoid organs support tumor B-cell growth: role of stromal cells in follicular lymphoma pathogenesis. *Blood* **109**, 693-702 (2007).

171   Chraa, D., Naim, A., Olive, D. & Badou, A. T lymphocyte subsets in cancer immunity: Friends or foes. *Journal of leukocyte biology* (2018).

172   Laurent, C. *et al.* Distribution, function and prognostic value of cytotoxic T lymphocytes in follicular lymphoma: a 3-D tissue imaging study. *Blood*, blood-2011-2004-345777 (2011).

173   Kim, H.-J. & Cantor, H. CD4 T-cell subsets and tumor immunity: the helpful and the not-so-helpful. *Cancer immunology research* **2**, 91-98 (2014).

174   Fridman, W. H., Pages, F., Sautes-Fridman, C. & Galon, J. The immune contexture in human tumours: impact on clinical outcome. *Nature Reviews Cancer* **12**, 298 (2012).

175   Lorvik, K. B. *et al.* Adoptive transfer of tumor-specific Th2 cells eradicates tumors by triggering an in situ inflammatory immune response. *Cancer research*, canres. 1219.2016 (2016).

176   Ellyard, J., Simson, L. & Parish, C. Th2-mediated anti-tumour immunity: friend or foe? *Tissue antigens* **70**, 1-11 (2007).

177   Tepper, R. I., Coffman, R. L. & Leder, P. An eosinophil-dependent mechanism for the antitumor effect of interleukin-4. *Science* **257**, 548-551 (1992).

178   Maniati, E., Soper, R. & Hagemann, T. Up for Mischief? IL-17/Th17 in the tumour microenvironment. *Oncogene* **29**, 5653 (2010).

179   Dhodapkar, K. M. *et al.* Dendritic cells mediate the induction of polyfunctional human IL17-producing cells (Th17-1 cells) enriched in the bone marrow of patients with myeloma. *Blood* **112**, 2878-2885 (2008).

180   Kryczek, I. *et al.* Phenotype, distribution, generation, and functional and clinical relevance of Th17 cells in the human tumor environments. *Blood* **114**, 1141-1149 (2009).

181   Schreck, S. *et al.* Prognostic impact of tumour-infiltrating Th2 and regulatory T cells in classical Hodgkin lymphoma. *Hematological oncology* **27**, 31-39 (2009).

182   Carreras, J. *et al.* High numbers of tumor-infiltrating FOXP3-positive regulatory T cells are associated with improved overall survival in follicular lymphoma. *Blood* **108**, 2957-2964 (2006).

183   Tzankov, A. *et al.* Correlation of high numbers of intratumoral FOXP3+ regulatory T cells with improved survival in germinal center-like diffuse large B-cell lymphoma, follicular lymphoma and classical Hodgkin's lymphoma. *haematologica* **93**, 193-200 (2008).

184   Fazilleau, N., Mark, L., McHeyzer-Williams, L. J. & McHeyzer-Williams, M. G. Follicular helper T cells: lineage and location. *Immunity* **30**, 324-335 (2009).

185   Amé-Thomas, P. *et al.* Characterization of intratumoral follicular helper T cells in follicular lymphoma: role in the survival of malignant B cells. *Leukemia* **26**, 1053 (2012).

186   Le, K.-S. *et al.* Follicular B lymphomas generate regulatory T cells via the ICOS/ICOSL pathway and are susceptible to treatment by anti-ICOS/ICOSL therapy. *Cancer research* (2016).

187   Taskinen, M., Karjalainen-Lindsberg, M.-L., Nyman, H., Eerola, L.-M. & Leppä, S. A high tumor-associated macrophage content predicts favorable outcome in follicular lymphoma patients treated with rituximab and cyclophosphamide-doxorubicin-vincristine-prednisone. *Clinical cancer research* **13**, 5784-5789 (2007).

188   Kridel, R. *et al.* The prognostic impact of CD163-positive macrophages in follicular lymphoma: a study from the BC Cancer Agency and the Lymphoma Study Association. *Clinical Cancer Research* (2015).

189   Mantovani, A., Sozzani, S., Locati, M., Allavena, P. & Sica, A. Macrophage polarization: tumor-associated macrophages as a paradigm for polarized M2 mononuclear phagocytes. *Trends in immunology* **23**, 549-555 (2002).

190   Sica, A. & Mantovani, A. Macrophage plasticity and polarization: in vivo veritas. *The Journal of clinical investigation* **122**, 787-795 (2012).

191   Schmieder, A., Michel, J., Schönhaar, K., Goerdt, S. & Schledzewski, K. in *Seminars in cancer biology.* 289-297 (Elsevier).

192   Hu, X., Park-Min, K.-H., Ho, H. H. & Ivashkiv, L. B. IFN-γ-primed macrophages exhibit increased CCR2-dependent migration and altered IFN-γ responses mediated by Stat1. *The Journal of Immunology* **175**, 3637-3647 (2005).

193   Hildebrand, J. M. *et al.* A BAFF-R mutation associated with non-Hodgkin lymphoma alters TRAF recruitment and reveals new insights into BAFF-R signaling. *Journal of Experimental Medicine* **207**, 2569-2579 (2010).

194   Domínguez-Soto, A. *et al.* Dendritic Cell-Specific ICAM-3–Grabbing Nonintegrin Expression on M2-Polarized and Tumor-Associated Macrophages Is Macrophage-CSF Dependent and Enhanced by Tumor-Derived IL-6 and IL-10. *The Journal of Immunology*, 1000475 (2011).

195   Epron, G. *et al.* Monocytes and T cells cooperate to favor normal and follicular lymphoma B-cell growth: role of IL-15 and CD40L signaling. *Leukemia* **26**, 139 (2012).

196   Carbonnelle-Puscian, A. *et al.* The novel immunosuppressive enzyme IL4I1 is expressed by neoplastic cells of several B-cell lymphomas and by tumor-associated macrophages. *Leukemia* **23**, 952 (2009).

197   Dreyling, M. *et al.* Newly diagnosed and relapsed follicular lymphoma: ESMO Clinical Practice Guidelines for diagnosis, treatment and follow-up. *Annals of Oncology* **27**, v83-v90 (2016).

198   Carbone, P. P., Kaplan, H. S., Musshoff, K., Smithers, D. W. & Tubiana, M. Report of the committee on Hodgkin's disease staging classification. *Cancer res* **31**, 1860-1861 (1971).

199   Ott, G. *et al.* Cytomorphologic, immunohistochemical, and cytogenetic profiles of follicular lymphoma: 2 types of follicular lymphoma grade 3. *Blood* **99**, 3806-3812 (2002).

200   Tilly, H. *et al.* Diffuse large B-cell lymphoma (DLBCL): ESMO Clinical Practice Guidelines for diagnosis, treatment and follow-up. *Annals of oncology* **26**, v116-v125 (2015).

201   Solal-Céligny, P. *et al.* Follicular lymphoma international prognostic index. *Blood* (2004).

202   Federico, M. *et al.* Follicular lymphoma international prognostic index 2: a new prognostic index for follicular lymphoma developed by the international follicular lymphoma prognostic factor project. *Journal of Clinical Oncology* **27**, 4555-4562 (2009).

203   Buske, C. *et al.* The Follicular Lymphoma International Prognostic Index (FLIPI) separates high-risk from intermediate-or low-risk patients with advanced-stage follicular lymphoma treated front-line with rituximab and the combination of cyclophosphamide, doxorubicin, vincristine, and prednisone (R-CHOP) with respect to treatment outcome. *Blood* **108**, 1504-1508 (2006).

204   Casulo, C., Nastoupil, L., Fowler, N., Friedberg, J. & Flowers, C. Unmet needs in the first-line treatment of follicular lymphoma. *Annals of Oncology* **28**, 2094-2106 (2017).

205   Pastore, A. *et al.* Integration of gene mutations in risk prognostication for patients receiving first-line immunochemotherapy for follicular lymphoma: a retrospective analysis of a prospective clinical trial and validation in a population-based registry. *The lancet oncology* **16**, 1111-1122 (2015).

206   López-Guillermo, A. A novel clinicogenetic prognostic score for follicular lymphoma. *The Lancet Oncology* **16**, 1011-1012 (2015).

207   Andorsky, D. J. *et al.*   (American Society of Clinical Oncology, 2017).

208   Sander, B. *et al.* The reliability of immunohistochemical analysis of the tumor microenvironment in follicular lymphoma: a validation study from the Lunenburg Lymphoma Biomarker Consortium. *haematologica*, haematol. 2013.095257 (2014).

209   Huet, S. *et al.* A gene-expression profiling score for prediction of outcome in patients with follicular lymphoma: a retrospective training and validation analysis in three international cohorts. *The Lancet Oncology* **19**, 549-561 (2018).

210   Leonard, J. P., Nastoupil, L. J. & Flowers, C. R. Where to start? Upfront therapy for follicular lymphoma in 2018. *ASH Education Program Book* **2018**, 185-188 (2018).

211   Mac Manus, M. P. & Hoppe, R. T. Is radiotherapy curative for stage I and II low-grade follicular lymphoma? Results of a long-term follow-up study of patients treated at Stanford University. *Journal of Clinical Oncology* **14**, 1282-1290 (1996).

212   Hoskin, P. J. *et al.* 4 Gy versus 24 Gy radiotherapy for patients with indolent lymphoma (FORT): a randomised phase 3 non-inferiority trial. *The Lancet Oncology* **15**, 457-463 (2014).

213   Solal-Céligny, P. *et al.* Watchful waiting in low–tumor burden follicular lymphoma in the rituximab era: results of an F2-study database. *Journal of Clinical Oncology* **30**, 3848-3853 (2012).

214   Friedberg, J. W. *et al.* Effectiveness of first-line management strategies for stage I follicular lymphoma: analysis of the National LymphoCare Study. *Journal of Clinical Oncology* **30**, 3368 (2012).

215   Ardeshna, K. M. *et al.* Rituximab versus a watch-and-wait approach in patients with advanced-stage, asymptomatic, non-bulky follicular lymphoma: an open-label randomised phase 3 trial. *The lancet oncology* **15**, 424-435 (2014).

216   Nastoupil, L. J. *et al.* Comparison of the effectiveness of frontline chemoimmunotherapy regimens for follicular lymphoma used in the United States. *Leukemia & lymphoma* **56**, 1295-1302 (2015).

217   Marcus, R. *et al.* Phase III study of R-CVP compared with cyclophosphamide, vincristine, and prednisone alone in patients with previously untreated advanced follicular lymphoma. *Journal of Clinical Oncology* **26**, 4579-4586 (2008).

218   Rummel, M. J. *et al.* Bendamustine plus rituximab versus CHOP plus rituximab as first-line treatment for patients with indolent and mantle-cell lymphomas: an open-label, multicentre, randomised, phase 3 non-inferiority trial. *The Lancet* **381**, 1203-1210 (2013).

219   Bachy, E. *et al.* Long-term follow-up of the FL2000 study comparing CHVP-interferon to CHVP-interferon plus rituximab in follicular lymphoma. *haematologica*, haematol. 2012.082412 (2013).

220   Becnel, M. R. & Nastoupil, L. J. Follicular Lymphoma: Past, Present, and Future. *Current Treatment Options in Oncology* **19**, 32 (2018).

221   Federico, M. *et al.* R-CVP versus R-CHOP versus R-FM for the initial treatment of patients with advanced-stage follicular lymphoma: results of the FOLL05 trial conducted by the Fondazione Italiana Linfomi. *Journal of Clinical Oncology* **31**, 1506-1513 (2013).

222   Vitolo, U. *et al.* Rituximab maintenance compared with observation after brief first-line R-FND chemoimmunotherapy with rituximab consolidation in patients age older than 60 years with advanced follicular lymphoma: a phase III randomized study by the Fondazione Italiana Linfomi. *Journal of Clinical Oncology* **31**, 3351-3359 (2013).

223   Martinelli, G. *et al.* Long-term follow-up of patients with follicular lymphoma receiving single-agent rituximab at two different schedules in trial SAKK 35/98. *Journal of clinical oncology* **28**, 4480-4484 (2010).

224   Scholz, C. W. *et al.* 90Yttrium-ibritumomab-tiuxetan as first-line treatment for follicular lymphoma: 30 months of follow-up data from an international multicenter phase II clinical trial. *Journal of Clinical Oncology* **31**, 308-313 (2012).

225   Marcus, R. *et al.* Obinutuzumab for the first-line treatment of follicular lymphoma. *New England Journal of Medicine* **377**, 1331-1344 (2017).

226   Salles, G. A. *et al.*   (Am Soc Hematology, 2017).

227   Hill, B. T. *et al.*   (Am Soc Hematology, 2017).

228   Canales, M. A. *et al.*   (Am Soc Hematology, 2013).

229   Casulo, C. *et al.* Early relapse of follicular lymphoma after rituximab plus cyclophosphamide, doxorubicin, vincristine, and prednisone defines patients at high risk for death: an analysis from the National LymphoCare Study. *Journal of Clinical Oncology* **33**, 2516 (2015).

230   Montoto, S. *et al.* Indications for hematopoietic stem cell transplantation in patients with follicular lymphoma: a consensus project of the EBMT-Lymphoma Working Party. *Haematologica* **98**, 1014-1021 (2013).

231   Gopal, A. K. *et al.*   (Am Soc Hematology, 2014).

232   Cheson, B. D. *et al.* Overall survival benefit in patients with rituximab-refractory indolent non-Hodgkin lymphoma who received obinutuzumab plus bendamustine induction and

obinutuzumab maintenance in the GADOLIN study. *Journal of Clinical Oncology*, JCO. 2017.2076. 3656 (2018).

233   Gallagher, C. *et al.* Follicular lymphoma: prognostic factors for response and survival. *Journal of Clinical Oncology* **4**, 1470-1480 (1986).

234   Courtney, K. D., Corcoran, R. B. & Engelman, J. A. The PI3K pathway as drug target in human cancer. *Journal of clinical oncology* **28**, 1075 (2010).

235   Soler, A. *et al.* Inhibition of the p110α isoform of PI 3-kinase stimulates nonfunctional tumor angiogenesis. *Journal of Experimental Medicine* **210**, 1937-1945 (2013).

236   Hirsch, E., Ciraolo, E., Franco, I., Ghigo, A. & Martini, M. PI3K in cancer–stroma interactions: bad in seed and ugly in soil. *Oncogene* **33**, 3083 (2014).

237   Fruman, D. A. & Rommel, C. PI3K and cancer: lessons, challenges and opportunities. *Nature reviews Drug discovery* **13**, 140 (2014).

238   Vivanco, I. & Sawyers, C. L. The phosphatidylinositol 3-kinase–AKT pathway in human cancer. *Nature Reviews Cancer* **2**, 489 (2002).

239   Lannutti, B. J. *et al.* CAL-101, a p110δ selective phosphatidylinositol-3-kinase inhibitor for the treatment of B-cell malignancies, inhibits PI3K signaling and cellular viability. *Blood* **117**, 591-594 (2011).

240   Greenwell, I. B., Ip, A. & Cohen, J. B. PI3K Inhibitors: Understanding Toxicity Mechanisms and Management: Page 2 of 3. *Oncology* **31** (2017).

241   Herman, S. E. *et al.* The phosphatidylinositol 3-kinase-δ inhibitor CAL-101 demonstrates promising pre-clinical activity in chronic lymphocytic leukemia by antagonizing intrinsic and extrinsic cellular survival signals. *Blood*, blood-2010-2002-271171 (2010).

242   Flinn, I. W. *et al.* Idelalisib, a selective inhibitor of phosphatidylinositol 3-kinase-δ, as therapy for previously treated indolent non-Hodgkin lymphoma. *Blood*, blood-2013-2011-538546 (2014).

243   Cheah, C. Y. & Fowler, N. H. Idelalisib in the management of lymphoma. *Blood*, blood-2016-2002-702761 (2016).

244   Gopal, A. K. *et al.* PI3Kδ inhibition by idelalisib in patients with relapsed indolent lymphoma. *New England Journal of Medicine* **370**, 1008-1018 (2014).

245   Gopal, A. K. *et al.*   (Am Soc Hematology, 2015).

246   Gopal, A. K. *et al.* Idelalisib is effective in patients with high-risk follicular lymphoma and early relapse after initial chemoimmunotherapy. *Blood* **129**, 3037-3039 (2017).

247   Dal Col, J. *et al.* Distinct functional significance of Akt and mTOR constitutive activation in mantle cell lymphoma. *Blood* **111**, 5142-5151 (2008).

248   Kahl, B. S. *et al.* Results of a phase I study of idelalisib, a PI3Kδ inhibitor, in patients with relapsed or refractory mantle cell lymphoma (MCL). *Blood*, blood-2013-2011-537555 (2014).

249   Lampson, B. L. & Brown, J. R. PI3Kδ-selective and PI3Kα/δ-combinatorial inhibitors in clinical development for B-cell non-Hodgkin lymphoma. *Expert opinion on investigational drugs* **26**, 1267-1279 (2017).

250   Lampson, B. L. *et al.* Idelalisib given front-line for treatment of chronic lymphocytic leukemia causes frequent immune-mediated hepatotoxicity. *Blood*, blood-2016-2003-707133 (2016).

251   Furman, R. R. *et al.* Idelalisib and rituximab in relapsed chronic lymphocytic leukemia. *New England Journal of Medicine* **370**, 997-1007 (2014).

252   Cheah, C. Y. *et al.* Lenalidomide, idelalisib, and rituximab are unacceptably toxic in patients with relapsed/refractory indolent lymphoma. *Blood* **125**, 3357-3359 (2015).

253   Graupera, M. *et al.* Angiogenesis selectively requires the p110α isoform of PI3K to control endothelial cell migration. *Nature* **453**, 662 (2008).

254   Dreyling, M. *et al.* Phosphatidylinositol 3-kinase inhibition by copanlisib in relapsed or refractory indolent lymphoma. *Journal of Clinical Oncology* **35**, 3898-3905 (2017).

255   Younes, A. *et al.* Pan-phosphatidylinositol 3-kinase inhibition with buparlisib in patients with relapsed and refractory non-Hodgkin lymphoma. *haematologica*, haematol. 2017.169656 (2017).

256   Dreyling, M. *et al.* Phase II study of copanlisib, a PI3K inhibitor, in relapsed or refractory, indolent or aggressive lymphoma. *Annals of Oncology* **28**, 2169-2178 (2017).

257   Sayers, T. J. Targeting the extrinsic apoptosis signaling pathway for cancer therapy. *Cancer Immunology, Immunotherapy* **60**, 1173-1180 (2011).

258   Shamas-Din, A., Brahmbhatt, H., Leber, B. & Andrews, D. W. BH3-only proteins: Orchestrators of apoptosis. *Biochimica et Biophysica Acta (BBA)-Molecular Cell Research* **1813**, 508-520 (2011).

259   Echeverry, N. *et al.* Intracellular localization of the BCL-2 family member BOK and functional implications. *Cell death and differentiation* **20**, 785 (2013).

260   Yamaguchi, H., Bhalla, K. & Wang, H.-G. Bax plays a pivotal role in thapsigargin-induced apoptosis of human colon cancer HCT116 cells by controlling Smac/Diablo and Omi/HtrA2 release from mitochondria. *Cancer research* **63**, 1483-1489 (2003).

261   Susin, S. A. *et al.* Bcl-2 inhibits the mitochondrial release of an apoptogenic protease. *Journal of Experimental Medicine* **184**, 1331-1341 (1996).

262   Green, D. R. & Reed, J. C. Mitochondria and apoptosis. *science*, 1309-1312 (1998).

263   Kim, M. S., Kim, S. S., Yoo, N. J. & Lee, S. H. Rare somatic mutation of pro-apoptotic BAX and BAK genes in common human cancers. *Tumori Journal* **98**, 149-151 (2012).

264   Youle, R. J. & Strasser, A. The BCL-2 protein family: opposing activities that mediate cell death. *Nature reviews Molecular cell biology* **9**, 47 (2008).

265   Willis, S. N. & Adams, J. M. Life in the balance: how BH3-only proteins induce apoptosis. *Current opinion in cell biology* **17**, 617-625 (2005).

266   Khan, N. & Kahl, B. Targeting BCL-2 in hematologic malignancies. *Targeted oncology*, 1-11 (2018).

267   Klasa, R. J., Gillum, A. M., Klem, R. E. & Frankel, S. R. Oblimersen Bcl-2 antisense: facilitating apoptosis in anticancer treatment. *Antisense and Nucleic Acid Drug Development* **12**, 193-213 (2002).

268   Oltersdorf, T. *et al.* An inhibitor of Bcl-2 family proteins induces regression of solid tumours. *Nature* **435**, 677 (2005).

269   Rudin, C. M. *et al.* Phase II study of single-agent navitoclax (ABT-263) and biomarker correlates in patients with relapsed small cell lung cancer. *Clinical Cancer Research* (2012).

270   Kaefer, A. *et al.* Mechanism-based pharmacokinetic/pharmacodynamic meta-analysis of navitoclax (ABT-263) induced thrombocytopenia. *Cancer chemotherapy and pharmacology* **74**, 593-602 (2014).

271   Souers, A. J. *et al.* ABT-199, a potent and selective BCL-2 inhibitor, achieves antitumor activity while sparing platelets. *Nature medicine* **19**, 202 (2013).

272   Roberts, A. W. *et al.* Targeting BCL2 with venetoclax in relapsed chronic lymphocytic leukemia. *New England Journal of Medicine* **374**, 311-322 (2016).

273   Stilgenbauer, S. *et al.* Venetoclax in relapsed or refractory chronic lymphocytic leukaemia with 17p deletion: a multicentre, open-label, phase 2 study. *The Lancet Oncology* **17**, 768-778 (2016).

274   Seymour, J. F. *et al.* Venetoclax plus rituximab in relapsed or refractory chronic lymphocytic leukaemia: a phase 1b study. *The Lancet Oncology* **18**, 230-240 (2017).

275   Davids, M. S. *et al.* Phase I First-in-Human Study of Venetoclax in Patients With Relapsed or Refractory Non-Hodgkin Lymphoma. *Journal of clinical oncology: official journal of the American Society of Clinical Oncology* **35**, 826-833 (2017).

276   Zinzani, P. L. *et al.*   (Am Soc Hematology, 2016).

277   de Vos, S. *et al.*   (Am Soc Hematology, 2015).

278   Fowler, N. H. *et al.* Role of the tumor microenvironment in mature B-cell lymphoid malignancies. *Haematologica* **101**, 531-540 (2016).

279   Witzig, T. E. *et al.* Lenalidomide oral monotherapy produces durable responses in relapsed or refractory indolent non-Hodgkin's Lymphoma. *Journal of Clinical Oncology* **27**, 5404-5409 (2009).

280   Bartlett, N. L. *et al.* Single-agent ibrutinib in relapsed or refractory follicular lymphoma: a phase 2 consortium trial. *Blood*, blood-2017-2009-804641 (2017).

281   Kirschbaum, M. *et al.* Phase II study of vorinostat for treatment of relapsed or refractory indolent non-Hodgkin's lymphoma and mantle cell lymphoma. *Journal of clinical oncology* **29**, 1198 (2011).

282   Ogura, M. *et al.* A multicentre phase II study of vorinostat in patients with relapsed or refractory indolent B-cell non-Hodgkin lymphoma and mantle cell lymphoma. *British journal of haematology* **165**, 768-776 (2014).

283   Evens, A. M. *et al.* A phase I/II multicenter, open-label study of the oral histone deacetylase inhibitor abexinostat in relapsed/refractory lymphoma. *Clinical cancer research*, clincanres. 0624.2015 (2015).

284   Ribrag, V. *et al.* Safety and efficacy of abexinostat, a pan-histone deacetylase inhibitor, in non-Hodgkin lymphoma and chronic lymphocytic leukemia: Results of a phase 2 study. *haematologica*, haematol. 2016.154377 (2017).

285   Gulati, N., Béguelin, W. & Giulino-Roth, L. Enhancer of zeste homolog 2 (EZH2) inhibitors. *Leukemia & lymphoma*, 1-12 (2018).

286   Morschhauser, F. *et al.* Interim report from a phase 2 multicenter study of tazemetostat, an EZH2 inhibitor, in patients with relapsed or refractory B-cell non-Hodgkin lymphomas. *Hematological Oncology* **35**, 24-25 (2017).

287   Lesokhin, A. M. *et al.* Nivolumab in patients with relapsed or refractory hematologic malignancy: preliminary results of a phase Ib study. *Journal of Clinical Oncology* **34**, 2698 (2016).

288   Schuster, S. J. *et al.*   (Am Soc Hematology, 2015).

289   Schuster, S. J. *et al.* Chimeric antigen receptor T cells in refractory B-cell lymphomas. *New England Journal of Medicine* **377**, 2545-2554 (2017).

290   Turtle, C. J. *et al.*   (Am Soc Hematology, 2015).

291   Michot, J. *et al.* PHASE IB STUDY OF CC-122 IN COMBINATION WITH OBINUTUZUMAB (GA101): RELAPSED OR REFRACTORY (R/R) PATIENTS WITH B-CELL NON-HODGKIN LYMPHOMAS (NHL). *Hematological Oncology* **35**, 53-53 (2017).

292   Michot, J.-M. *et al.*   (Am Soc Hematology, 2017).

293   Fowler, N. H. *et al.*   (American Society of Clinical Oncology, 2018).

294   Morschhauser, F. *et al.* Rituximab plus lenalidomide in advanced untreated follicular lymphoma. *New England Journal of Medicine* **379**, 934-947 (2018).

295   Stewart, B. W. & Wild, C. World Cancer Report 2014. Lyon, France: International Agency for Research on Cancer. *World Health Organization*, 630 (2014).

296   Cronin, K. A. *et al.* Annual Report to the Nation on the Status of Cancer, part I: National cancer statistics. *Cancer* (2018).

297   Holleczek, B. *et al.* On-going improvement and persistent differences in the survival for patients with colon and rectum cancer across Europe 1999–2007–results from the EUROCARE-5 study. *European Journal of Cancer* **51**, 2158-2168 (2015).

298   Burt, R. W., Bronner, M. P. & Jasperson, K. W. Polyposis syndromes. *Yamada's Atlas of Gastroenterology*, 246-265 (2016).

299   Hampel, H. *et al.* Screening for the Lynch syndrome (hereditary nonpolyposis colorectal cancer). *New England Journal of Medicine* **352**, 1851-1860 (2005).

300   Jasperson, K. W., Tuohy, T. M., Neklason, D. W. & Burt, R. W. Hereditary and familial colon cancer. *Gastroenterology* **138**, 2044-2058 (2010).

301   Carballal, S. *et al.* Colorectal cancer risk factors in patients with serrated polyposis syndrome: a large multicentre study. *Gut* **65**, 1829-1837 (2016).

302   IJspeert, J. *et al.* Detection rate of serrated polyps and serrated polyposis syndrome in colorectal cancer screening cohorts: a European overview. *Gut* **66**, 1225-1232 (2017).

303   Maida, M. *et al.* Screening of colorectal cancer: present and future. *Expert review of anticancer therapy* **17**, 1131-1146 (2017).

304   Haggar, F. A. & Boushey, R. P. Colorectal cancer epidemiology: incidence, mortality, survival, and risk factors. *Clinics in colon and rectal surgery* **22**, 191 (2009).

305   Vogelstein, B. *et al.* Genetic alterations during colorectal-tumor development. *New England Journal of Medicine* **319**, 525-532 (1988).

306   Grady, W. M. & Markowitz, S. D. The molecular pathogenesis of colorectal cancer and its potential application to colorectal cancer screening. *Digestive diseases and sciences* **60**, 762-772 (2015).

307   Nucci, M. R., Robinson, C. R., Longo, P., Campbell, P. & Hamilton, S. R. Phenotypic and genotypic characteristics of aberrant crypt foci in human colorectal mucosa. *Human pathology* **28**, 1396-1407 (1997).

308   Bird, R. P. Observation and quantification of aberrant crypts in the murine colon treated with a colon carcinogen: preliminary findings. *Cancer letters* **37**, 147-151 (1987).

309   Pretlow, T. P. *et al.* Aberrant crypts: putative preneoplastic foci in human colonic mucosa. *Cancer research* **51**, 1564-1567 (1991).

310   Roncucci, L., Stamp, D., Medline, A., Cullen, J. B. & Bruce, W. R. Identification and quantification of aberrant crypt foci and microadenomas in the human colon. *Human pathology* **22**, 287-294 (1991).

311   Takayama, T. *et al.* Analysis of K-ras, APC, and β-catenin in aberrant crypt foci in sporadic adenoma, cancer, and familial adenomatous polyposis. *Gastroenterology* **121**, 599-611 (2001).

312   Heinen, C. D., Shivapurkar, N., Tang, Z., Groden, J. & Alabaster, O. Microsatellite instability in aberrant crypt foci from human colons. *Cancer research* **56**, 5339-5341 (1996).

313   Chan, A. O.-O. *et al.* CpG island methylation in aberrant crypt foci of the colorectum. *The American journal of pathology* **160**, 1823-1830 (2002).

314   Li, H. *et al.* SLC5A8, a sodium transporter, is a tumor suppressor gene silenced by methylation in human colon aberrant crypt foci and cancers. *Proceedings of the National Academy of Sciences* **100**, 8412-8417 (2003).

315   Cho, N. L. *et al.* Aberrant crypt foci in the adenoma prevention with celecoxib trial. *Cancer Prevention Research*, 1940-6207. CAPR-1907-0011 (2008).

316   Mutch, M. G. *et al.* A multicenter study of prevalence and risk factors for aberrant crypt foci. *Clinical Gastroenterology and Hepatology* **7**, 568-574 (2009).

317   Quintanilla, I. *et al.* LINE-1 hypomethylation is neither present in rectal aberrant crypt foci nor associated with field defect in sporadic colorectal neoplasia. *Clinical epigenetics* **6**, 24 (2014).

318   Snover, D. C. Update on the serrated pathway to colorectal carcinoma. *Human pathology* **42**, 1-10 (2011).

319   Yan, D. *et al.* Elevated expression of axin2 and hnkd mRNA provides evidence that Wnt/β-catenin signaling is activated in human colon tumors. *Proceedings of the National Academy of Sciences* **98**, 14973-14978 (2001).

320   Bienz, M. The subcellular destinations of APC proteins. *Nature reviews Molecular cell biology* **3**, 328 (2002).

321   Kaplan, K. B. *et al.* A role for the Adenomatous Polyposis Coli protein in chromosome segregation. *Nature cell biology* **3**, 429 (2001).

322   Green, R. A. & Kaplan, K. B. Chromosome instability in colorectal tumor cells is associated with defects in microtubule plus-end attachments caused by a dominant mutation in APC. *The Journal of cell biology* **163**, 949-961 (2003).

323   Tighe, A., Johnson, V. L. & Taylor, S. S. Truncating APC mutations have dominant effects on proliferation, spindle checkpoint control, survival and chromosome stability. *Journal of cell science* **117**, 6339-6353 (2004).

324   Bettington, M. *et al.* The serrated pathway to colorectal carcinoma: current concepts and challenges. *Histopathology* **62**, 367-386 (2013).

325   Goldstein, N. S. Serrated pathway and APC (conventional)-type colorectal polyps: molecular-morphologic correlations, genetic pathways, and implications for classification. *American journal of clinical pathology* **125**, 146-153 (2006).

326   Kambara, T. *et al.* BRAF mutation is associated with DNA methylation in serrated polyps and cancers of the colorectum. *Gut* **53**, 1137-1144 (2004).

327   Nagasaka, T. *et al.* Colorectal cancer with mutation in BRAF, KRAS, and wild-type with respect to both oncogenes showing different patterns of DNA methylation. *Journal of Clinical Oncology* **22**, 4584-4594 (2004).

328   Chan, T. L., Zhao, W., Leung, S. Y. & Yuen, S. T. BRAF and KRAS mutations in colorectal hyperplastic polyps and serrated adenomas. *Cancer research* **63**, 4878-4881 (2003).

329   Yang, S., Farraye, F. A., Mack, C., Posnik, O. & O'brien, M. J. BRAF and KRAS Mutations in hyperplastic polyps and serrated adenomas of the colorectum: relationship to histology and CpG island methylation status. *The American journal of surgical pathology* **28**, 1452-1459 (2004).

330   Fearon, E. R. & Vogelstein, B. A genetic model for colorectal tumorigenesis. *Cell* **61**, 759-767 (1990).

331   Walther, A. *et al.* Genetic prognostic and predictive markers in colorectal cancer. *Nature Reviews Cancer* **9**, 489 (2009).

332   Grady, W. M. & Carethers, J. M. Genomic and epigenetic instability in colorectal cancer pathogenesis. *Gastroenterology* **135**, 1079-1099 (2008).

333   Lengauer, C., Kinzler, K. W. & Vogelstein, B. Genetic instabilities in human cancers. *Nature* **396**, 643 (1998).

334   Hermsen, M. *et al.* Colorectal adenoma to carcinoma progression follows multiple pathways of chromosomal instability. *Gastroenterology* **123**, 1109-1119 (2002).

335   Grady, W. M. Genomic instability and colon cancer. *Cancer and Metastasis Reviews* **23**, 11-27 (2004).

336   Shin, H.-J. *et al.* Dual roles of human BubR1, a mitotic checkpoint kinase, in the monitoring of chromosomal instability. *Cancer cell* **4**, 483-497 (2003).

337   Anderhub, S. J., Krämer, A. & Maier, B. Centrosome amplification in tumorigenesis. *Cancer letters* **322**, 8-17 (2012).

338   Roger, L. *et al.* Extensive telomere erosion in the initiation of colorectal adenomas and its association with chromosomal instability. *Journal of the National Cancer Institute* **105**, 1202-1211 (2013).

339   Gilad, O. *et al.* Combining ATR suppression with oncogenic Ras synergistically increases genomic instability, causing synthetic lethality or tumorigenesis in a dosage-dependent manner. *Cancer research* (2010).

340   Vilar, E. & Gruber, S. B. Microsatellite instability in colorectal cancer—the stable evidence. *Nature reviews Clinical oncology* **7**, 153 (2010).

341   Boland, C. R. *et al.*   (AACR, 1998).

342   O'brien, M. J. *et al.* Comparison of microsatellite instability, CpG island methylation phenotype, BRAF and KRAS status in serrated polyps and traditional adenomas indicates separate pathways to distinct colorectal carcinoma end points. *The American journal of surgical pathology* **30**, 1491-1501 (2006).

343   Inoue, A. *et al.* B-RAF mutation and accumulated gene methylation in aberrant crypt foci (ACF), sessile serrated adenoma/polyp (SSA/P) and cancer in SSA/P. *British journal of cancer* **112**, 403 (2015).

344   Palles, C. *et al.* Germline mutations affecting the proofreading domains of POLE and POLD1 predispose to colorectal adenomas and carcinomas. *Nature genetics* **45**, 136 (2013).

345   Handel, A. E., Ebers, G. C. & Ramagopalan, S. V. Epigenetics: molecular mechanisms and implications for disease. *Trends in molecular medicine* **16**, 7-16 (2010).

346   Kim, Y. S. & Deng, G. Epigenetic changes (aberrant DNA methylation) in colorectal neoplasia. *Gut and liver* **1**, 1 (2007).

347   Toyota, M. *et al.* CpG island methylator phenotype in colorectal cancer. *Proceedings of the National Academy of Sciences* **96**, 8681-8686 (1999).

348   Weisenberger, D. J. *et al.* CpG island methylator phenotype underlies sporadic microsatellite instability and is tightly associated with BRAF mutation in colorectal cancer. *Nature genetics* **38**, 787 (2006).

349   Tahara, T. *et al.* Colorectal carcinomas with CpG island methylator phenotype 1 frequently contain mutations in chromatin regulators. *Gastroenterology* **146**, 530-538. e535 (2014).

350   Bachman, K. E. *et al.* Histone modifications and silencing prior to DNA methylation of a tumor suppressor gene. *Cancer cell* **3**, 89-95 (2003).

351   Hinshelwood, R. A. *et al.* Aberrant de novo methylation of the p16 INK4A CpG island is initiated post gene silencing in association with chromatin remodelling and mimics nucleosome positioning. *Human molecular genetics* **18**, 3098-3109 (2009).

352   Groden, J. *et al.* Identification and characterization of the familial adenomatous polyposis coli gene. *Cell* **66**, 589-600 (1991).

353   Aberle, H., Bauer, A., Stappert, J., Kispert, A. & Kemler, R. β-catenin is a target for the ubiquitin–proteasome pathway. *The EMBO journal* **16**, 3797-3804 (1997).

354   Huang, D. & Du, X. Crosstalk between tumor cells and microenvironment via Wnt pathway in colorectal cancer dissemination. *World journal of gastroenterology: WJG* **14**, 1823 (2008).

355   Booth, R. A. Minimally invasive biomarkers for detection and staging of colorectal cancer. *Cancer letters* **249**, 87-96 (2007).

356   Andreyev, H. J. N., Norman, A. R., Clarke, P. A., Cunningham, D. & Oates, J. R. Kirsten ras mutations in patients with colorectal cancer: the multicenter "RASCAL" study. *JNCI: Journal of the National Cancer Institute* **90**, 675-684 (1998).

357   Vogelstein, B. & Kinzler, K. W. Cancer genes and the pathways they control. *Nature medicine* **10**, 789 (2004).

358   Downward, J. Targeting RAS signalling pathways in cancer therapy. *Nature Reviews Cancer* **3**, 11 (2003).

359   Karapetis, C. S. *et al.* K-ras mutations and benefit from cetuximab in advanced colorectal cancer. *New England Journal of Medicine* **359**, 1757-1765 (2008).

360   Misale, S. *et al.* Emergence of KRAS mutations and acquired resistance to anti-EGFR therapy in colorectal cancer. *Nature* **486**, 532 (2012).

361   Spring, K. J. *et al.* High prevalence of sessile serrated adenomas with BRAF mutations: a prospective study of patients undergoing colonoscopy. *Gastroenterology* **131**, 1400-1407 (2006).

362   Rosenberg, D. W. *et al.* Mutations in BRAF and KRAS differentially distinguish serrated versus non-serrated hyperplastic aberrant crypt foci in humans. *Cancer research* **67**, 3551-3554 (2007).

363   Nosho, K. *et al.* Comprehensive biostatistical analysis of CpG island methylator phenotype in colorectal cancer using a large population-based sample. *PloS one* **3**, e3698 (2008).

364   Levine, A. J. p53, the cellular gatekeeper for growth and division. *cell* **88**, 323-331 (1997).

365   Menendez, D., Inga, A. & Resnick, M. A. The expanding universe of p53 targets. *Nature reviews Cancer* **9**, 724 (2009).

366   Béroud, C. & Soussi, T. The UMD-p53 database: new mutations and analysis tools. *Human mutation* **21**, 176-181 (2003).

367   Leslie, A., Carey, F., Pratt, N. & Steele, R. The colorectal adenoma–carcinoma sequence. *British Journal of Surgery* **89**, 845-860 (2002).

368   Samuels, Y. *et al.* High frequency of mutations of the PIK3CA gene in human cancers. *Science* **304**, 554-554 (2004).

369   Jehan, Z. *et al.* Frequent PIK3CA gene amplification and its clinical significance in colorectal cancer. *The Journal of Pathology: A Journal of the Pathological Society of Great Britain and Ireland* **219**, 337-346 (2009).

370   Barault, L. *et al.* Mutations in the RAS-MAPK, PI (3) K (phosphatidylinositol-3-OH kinase) signaling network correlate with poor survival in a population-based series of colon cancers. *International journal of cancer* **122**, 2255-2259 (2008).

371   Nosho, K. *et al.* PIK3CA mutation in colorectal cancer: relationship with genetic and epigenetic alterations. *Neoplasia* **10**, 534-541 (2008).

372   Deschoolmeester, V., Baay, M., Specenier, P., Lardon, F. & Vermorken, J. B. A review of the most promising biomarkers in colorectal cancer: one step closer to targeted therapy. *The oncologist* **15**, 699-731 (2010).

373   Popat, S. & Houlston, R. S. A systematic review and meta-analysis of the relationship between chromosome 18q genotype, DCC status and colorectal cancer prognosis. *European journal of cancer* **41**, 2060-2070 (2005).

374   Fearon, E. R. Molecular genetics of colorectal cancer. *Annual Review of Pathology: Mechanisms of Disease* **6**, 479-507 (2011).

375   Zoratto, F. *et al.* Focus on genetic and epigenetic events of colorectal cancer pathogenesis: implications for molecular diagnosis. *Tumor Biology* **35**, 6195-6206 (2014).

376   Jen, J. *et al.* Allelic loss of chromosome 18q and prognosis in colorectal cancer. *New England Journal of Medicine* **331**, 213-221 (1994).

377   Pino, M. S. & Chung, D. C. The chromosomal instability pathway in colon cancer. *Gastroenterology* **138**, 2059-2072 (2010).

378 Hui, L. & Chen, Y. Tumor microenvironment: Sanctuary of the devil. *Cancer letters* **368**, 7-13 (2015).

379 Calon, A. *et al.* Stromal gene expression defines poor-prognosis subtypes in colorectal cancer. *Nature genetics* **47**, 320 (2015).

380 Eaden, J., Abrams, K. & Mayberry, J. The risk of colorectal cancer in ulcerative colitis: a meta-analysis. *Gut* **48**, 526-535 (2001).

381 Xu, X., Fu, X.-Y., Plate, J. & Chong, A. S. IFN-γ induces cell growth inhibition by Fas-mediated apoptosis: requirement of STAT1 protein for up-regulation of Fas and FasL expression. *Cancer research* **58**, 2832-2837 (1998).

382 Street, S. E., Trapani, J. A., MacGregor, D. & Smyth, M. J. Suppression of lymphoma and epithelial malignancies effected by interferon γ. *Journal of Experimental Medicine* **196**, 129-134 (2002).

383 Wu, P. *et al.* γδT17 cells promote the accumulation and expansion of myeloid-derived suppressor cells in human colorectal cancer. *Immunity* **40**, 785-800 (2014).

384 Kryczek, I. *et al.* IL-22+ CD4+ T cells promote colorectal cancer stemness via STAT3 transcription factor activation and induction of the methyltransferase DOT1L. *Immunity* **40**, 772-784 (2014).

385 Grivennikov, S. I. *et al.* Adenoma-linked barrier defects and microbial products drive IL-23/IL-17-mediated tumour growth. *Nature* **491**, 254 (2012).

386 Shiao, S. L., Ganesan, A. P., Rugo, H. S. & Coussens, L. M. Immune microenvironments in solid tumors: new targets for therapy. *Genes & development* **25**, 2559-2572 (2011).

387 Galon, J. *et al.* Cancer classification using the Immunoscore: a worldwide task force. *Journal of translational medicine* **10**, 205 (2012).

388 Pagès, F. *et al.* International validation of the consensus Immunoscore for the classification of colon cancer: a prognostic and accuracy study. *The Lancet* **391**, 2128-2139 (2018).

389 Galon, J. *et al.* Type, density, and location of immune cells within human colorectal tumors predict clinical outcome. *Science* **313**, 1960-1964 (2006).

390 Nakagawa, K. *et al.* Low infiltration of peritumoral regulatory T cells predicts worse outcome following resection of colorectal liver metastases. *Annals of surgical oncology* **22**, 180-186 (2015).

391 Yu, P. & Fu, Y.-X. Tumor-infiltrating T lymphocytes: friends or foes? *Laboratory investigation* **86**, 231 (2006).

392 Hori, S., Nomura, T. & Sakaguchi, S. Control of regulatory T cell development by the transcription factor Foxp3. *Science* **299**, 1057-1061 (2003).

393 Yaghoubi, N., Soltani, A., Ghazvini, K., Hassanian, S. M. & Hashemy, S. I. PD-1/PD-L1 blockade as a novel treatment for colorectal cancer. *Biomedicine & Pharmacotherapy* **110**, 312-318 (2019).

394 Cook, J. & Hagemann, T. Tumour-associated macrophages and cancer. *Current opinion in pharmacology* **13**, 595-601 (2013).

395 Ostuni, R., Kratochvill, F., Murray, P. J. & Natoli, G. Macrophages and cancer: from mechanisms to therapeutic implications. *Trends in immunology* **36**, 229-239 (2015).

396 Noy, R. & Pollard, J. W. Tumor-associated macrophages: from mechanisms to therapy. *Immunity* **41**, 49-61 (2014).

397 Cardoso, A. *et al.* Macrophages stimulate gastric and colorectal cancer invasion through EGFR Y 1086, c-Src, Erk1/2 and Akt phosphorylation and smallGTPase activity. *Oncogene* **33**, 2123 (2014).

398 Pansa, M. F. *et al.* Contribution of resident and recruited macrophages to the photodynamic intervention of colorectal tumor microenvironment. *Tumor Biology* **37**, 541-552 (2016).

399   Mantovani, A., Marchesi, F., Malesci, A., Laghi, L. & Allavena, P. Tumour-associated macrophages as treatment targets in oncology. *Nature reviews Clinical oncology* **14**, 399 (2017).

400   Barbera-Guillem, E., Nyhus, J. K., Wolford, C. C., Friece, C. R. & Sampsel, J. W. Vascular endothelial growth factor secretion by tumor-infiltrating macrophages essentially supports tumor angiogenesis, and IgG immune complexes potentiate the process. *Cancer research* **62**, 7042-7049 (2002).

401   Gilkes, D. M., Semenza, G. L. & Wirtz, D. Hypoxia and the extracellular matrix: drivers of tumour metastasis. *Nature Reviews Cancer* **14**, 430 (2014).

402   Zhong, X., Chen, B. & Yang, Z. The Role of Tumor-Associated Macrophages in Colorectal Carcinoma Progression. *Cellular Physiology and Biochemistry* **45**, 356-365 (2018).

403   Coffelt, S. B. *et al.* Elusive identities and overlapping phenotypes of proangiogenic myeloid cells in tumors. *The American journal of pathology* **176**, 1564-1576 (2010).

404   Tarin, D. Fine structure of murine mammary tumours: the relationship between epithelium and connective tissue in neoplasms induced by various agents. *British journal of cancer* **23**, 417 (1969).

405   Kalluri, R. & Zeisberg, M. Fibroblasts in cancer. *Nature Reviews Cancer* **6**, 392 (2006).

406   Öhlund, D., Elyada, E. & Tuveson, D. Fibroblast heterogeneity in the cancer wound. *Journal of Experimental Medicine* **211**, 1503-1523 (2014).

407   Parsonage, G. *et al.* A stromal address code defined by fibroblasts. *Trends in immunology* **26**, 150-156 (2005).

408   Paauwe, M. *et al.* Endoglin expression on cancer-associated fibroblasts regulates invasion and stimulates colorectal cancer metastasis. *Clinical Cancer Research*, clincanres. 0329.2018 (2018).

409   Kalluri, R. The biology and function of fibroblasts in cancer. *Nature Reviews Cancer* **16**, 582 (2016).

410   Patel, R., Filer, A., Barone, F. & Buckley, C. D. Stroma: fertile soil for inflammation. *Best Practice & Research Clinical Rheumatology* **28**, 565-576 (2014).

411   Orimo, A. *et al.* Stromal fibroblasts present in invasive human breast carcinomas promote tumor growth and angiogenesis through elevated SDF-1/CXCL12 secretion. *Cell* **121**, 335-348 (2005).

412   De Veirman, K. *et al.* Cancer associated fibroblasts and tumor growth: focus on multiple myeloma. *Cancers* **6**, 1363-1381 (2014).

413   Calon, A. *et al.* Dependency of colorectal cancer on a TGF-β-driven program in stromal cells for metastasis initiation. *Cancer cell* **22**, 571-584 (2012).

414   Ao, M. *et al.* Cross-talk between paracrine-acting cytokine and chemokine pathways promotes malignancy in benign human prostatic epithelium. *Cancer research* **67**, 4244-4253 (2007).

415   Carmeliet, P. & Jain, R. K. Angiogenesis in cancer and other diseases. *nature* **407**, 249 (2000).

416   Bouck, N., Stellmach, V. & Hsu, S. C. in *Advances in cancer research* Vol. 69   135-174 (Elsevier, 1996).

417   Ahmed, Z. & Bicknell, R. in *Angiogenesis Protocols*   3-24 (Springer, 2009).

418   Dejana, E., Orsenigo, F., Molendini, C., Baluk, P. & McDonald, D. M. Organization and signaling of endothelial cell-to-cell junctions in various regions of the blood and lymphatic vascular trees. *Cell and tissue research* **335**, 17-25 (2009).

419   Tammela, T. & Alitalo, K. Lymphangiogenesis: molecular mechanisms and future promise. *Cell* **140**, 460-476 (2010).

420   Wan, L., Pantel, K. & Kang, Y. Tumor metastasis: moving new biological insights into the clinic. *Nature medicine* **19**, 1450 (2013).

421   Senthebane, D. A. *et al.* The role of tumor microenvironment in chemoresistance: To survive, keep your enemies closer. *International journal of molecular sciences* **18**, 1586 (2017).

422   Pyke, C. *et al.* Laminin-5 is a marker of invading cancer cells in some human carcinomas and is coexpressed with the receptor for urokinase plasminogen activator in budding cancer cells in colon adenocarcinomas. *Cancer research* **55**, 4132-4139 (1995).

423   Lu, P., Weaver, V. M. & Werb, Z. The extracellular matrix: a dynamic niche in cancer progression. *J Cell Biol* **196**, 395-406 (2012).

424   Pietras, K. & Östman, A. Hallmarks of cancer: interactions with the tumor stroma. *Experimental cell research* **316**, 1324-1331 (2010).

425   Gaengel, K., Genové, G., Armulik, A. & Betsholtz, C. Endothelial-mural cell signaling in vascular development and angiogenesis. *Arteriosclerosis, thrombosis, and vascular biology* **29**, 630-638 (2009).

426   Gout, S. & Huot, J. Role of cancer microenvironment in metastasis: focus on colon cancer. *Cancer Microenvironment* **1**, 69-83 (2008).

427   Fidler, I. J. The pathogenesis of cancer metastasis: the'seed and soil'hypothesis revisited. *Nature Reviews Cancer* **3**, 453 (2003).

428   Gerhardt, H. & Semb, H. Pericytes: gatekeepers in tumour cell metastasis? *Journal of molecular medicine* **86**, 135-144 (2008).

429   Klein, C. A. Parallel progression of primary tumours and metastases. *Nature Reviews Cancer* **9**, 302 (2009).

430   Coghlin, C. & Murray, G. I. Current and emerging concepts in tumour metastasis. *The Journal of pathology* **222**, 1-15 (2010).

431   Cao, P. D., Cheung, W. K. & Nguyen, D. X. Cell lineage specification in tumor progression and metastasis. *Discovery medicine* **12**, 329-340 (2011).

432   Nguyen, D. X. *et al.* WNT/TCF signaling through LEF1 and HOXB9 mediates lung adenocarcinoma metastasis. *Cell* **138**, 51-62 (2009).

433   Oskarsson, T. *et al.* Breast cancer cells produce tenascin C as a metastatic niche component to colonize the lungs. *Nature medicine* **17**, 867 (2011).

434   Suvà, M. L., Riggi, N. & Bernstein, B. E. Epigenetic reprogramming in cancer. *Science* **339**, 1567-1570 (2013).

435   Spaderna, S. *et al.* A transient, EMT-linked loss of basement membranes indicates metastasis and poor survival in colorectal cancer. *Gastroenterology* **131**, 830-840 (2006).

436   Kalluri, R. & Weinberg, R. A. The basics of epithelial-mesenchymal transition. *The Journal of clinical investigation* **119**, 1420-1428 (2009).

437   Sánchez-Tilló, E. *et al.* EMT-activating transcription factors in cancer: beyond EMT and tumor invasiveness. *Cellular and molecular life sciences* **69**, 3429-3456 (2012).

438   Gupta, G. P. & Massagué, J. Cancer metastasis: building a framework. *Cell* **127**, 679-695 (2006).

439   Fichna, J. *Introduction to Gastrointestinal Diseases*. Vol. 2 (Springer, 2017).

440   Quail, D. F. & Joyce, J. A. Microenvironmental regulation of tumor progression and metastasis. *Nature medicine* **19**, 1423 (2013).

441   Wyckoff, J. *et al.* A paracrine loop between tumor cells and macrophages is required for tumor cell migration in mammary tumors. *Cancer research* **64**, 7022-7029 (2004).

442   Chambers, A. F., Groom, A. C. & MacDonald, I. C. Metastasis: dissemination and growth of cancer cells in metastatic sites. *Nature Reviews Cancer* **2**, 563 (2002).

443 Bos, P. D. *et al.* Genes that mediate breast cancer metastasis to the brain. *Nature* **459**, 1005 (2009).

444 Karkkainen, M. J., Mäkinen, T. & Alitalo, K. Lymphatic endothelium: a new frontier of metastasis research. *Nature cell biology* **4**, E2 (2002).

445 Meijer, J., Zeelenberg, I. S., Sipos, B. & Roos, E. The CXCR5 chemokine receptor is expressed by carcinoma cells and promotes growth of colon carcinoma in the liver. *Cancer research* **66**, 9576-9582 (2006).

446 Müller, A. *et al.* Involvement of chemokine receptors in breast cancer metastasis. *nature* **410**, 50 (2001).

447 Schimanski, C. C. *et al.* Effect of chemokine receptors CXCR4 and CCR7 on the metastatic behavior of human colorectal cancer. *Clinical Cancer Research* **11**, 1743-1750 (2005).

448 Sakai, N. *et al.* CXCR4/CXCL12 expression profile is associated with tumor microenvironment and clinical outcome of liver metastases of colorectal cancer. *Clinical & experimental metastasis* **29**, 101-110 (2012).

449 Brand, S. *et al.* CXCR4 and CXCL12 are inversely expressed in colorectal cancer cells and modulate cancer cell migration, invasion and MMP-9 activation. *Experimental cell research* **310**, 117-130 (2005).

450 Zlotnik, A., Burkhardt, A. M. & Homey, B. Homeostatic chemokine receptors and organ-specific metastasis. *Nature Reviews Immunology* **11**, 597 (2011).

451 O'hayre, M. *et al.* The emerging mutational landscape of G proteins and G-protein-coupled receptors in cancer. *Nature Reviews Cancer* **13**, 412 (2013).

452 Bar-Shavit, R. *et al.* G protein-coupled receptors in cancer. *International journal of molecular sciences* **17**, 1320 (2016).

453 Rosenbaum, D. M., Rasmussen, S. G. & Kobilka, B. K. The structure and function of G-protein-coupled receptors. *Nature* **459**, 356 (2009).

454 Gahbauer, S. & Böckmann, R. A. Membrane-mediated oligomerization of G protein coupled receptors and its implications for GPCR function. *Frontiers in physiology* **7**, 494 (2016).

455 Gutkind, J. S. The pathways connecting G protein-coupled receptors to the nucleus through divergent mitogen-activated protein kinase cascades. *Journal of Biological Chemistry* **273**, 1839-1842 (1998).

456 Teicher, B. A. & Fricker, S. P. CXCL12 (SDF-1)/CXCR4 pathway in cancer. *Clinical cancer research*, 1078-0432. CCR-1009-2329 (2010).

457 Milligan, G. The prevalence, maintenance and relevance of GPCR oligomerization. *Molecular pharmacology*, mol. 113.084780 (2013).

458 Callén, L. *et al.* Cannabinoid receptors CB1 and CB2 form functional heteromers in brain. *Journal of Biological Chemistry* **287**, 20851-20865 (2012).

459 Ferré, S. *et al.* G protein–coupled receptor oligomerization revisited: functional and pharmacological perspectives. *Pharmacological reviews* **66**, 413-434 (2014).

460 Hasbi, A., O'Dowd, B. F. & George, S. R. Dopamine D1-D2 receptor heteromer signaling pathway in the brain: emerging physiological relevance. *Molecular brain* **4**, 26 (2011).

461 So, C. H. *et al.* D1 and D2 dopamine receptors form heterooligomers and co-internalize following selective activation of either receptor. *Molecular pharmacology* (2005).

462 Hillion, J. *et al.* Coaggregation, cointernalization, and codesensitization of adenosine A2A receptors and dopamine D2Receptors. *Journal of Biological Chemistry* **277**, 18091-18097 (2002).

463 Schonenbach, N. S., Hussain, S. & O'Malley, M. A. Structure and function of G protein-coupled receptor oligomers: implications for drug discovery. *Wiley Interdisciplinary Reviews: Nanomedicine and Nanobiotechnology* **7**, 408-427 (2015).

464 Rozenfeld, R. *et al.* Receptor heteromerization expands the repertoire of cannabinoid signaling in rodent neurons. *PLoS One* **7**, e29239 (2012).

465 Rozenfeld, R. & Devi, L. A. Receptor heterodimerization leads to a switch in signaling: β-arrestin2-mediated ERK activation by μ-δ opioid receptor heterodimers. *The FASEB Journal* **21**, 2455-2465 (2007).

466 Santos, R. *et al.* A comprehensive map of molecular drug targets. *Nature reviews Drug discovery* **16**, 19 (2017).

467 Sriram, K. & Insel, P. A. GPCRs as targets for approved drugs: How many targets and how many drugs? *Molecular pharmacology*, mol. 117.111062 (2018).

468 Allen, J. A. & Roth, B. L. Strategies to discover unexpected targets for drugs active at G protein–coupled receptors. *Annual review of pharmacology and toxicology* **51**, 117-144 (2011).

469 Wacker, D., Stevens, R. C. & Roth, B. L. How ligands illuminate GPCR molecular pharmacology. *Cell* **170**, 414-427 (2017).

470 Lazennec, G. & Richmond, A. Chemokines and chemokine receptors: new insights into cancer-related inflammation. *Trends in molecular medicine* **16**, 133-144 (2010).

471 Raman, D., Baugher, P. J., Thu, Y. M. & Richmond, A. Role of chemokines in tumor growth. *Cancer letters* **256**, 137-165 (2007).

472 Balkwill, F. Cancer and the chemokine network. *Nature Reviews Cancer* **4**, 540 (2004).

473 Rot, A. & Von Andrian, U. H. Chemokines in innate and adaptive host defense: basic chemokinese grammar for immune cells. *Annu. Rev. Immunol.* **22**, 891-928 (2004).

474 Zlotnik, A. & Yoshie, O. Chemokines: a new classification system and their role in immunity. *Immunity* **12**, 121-127 (2000).

475 Balkwill, F., Charles, K. A. & Mantovani, A. Smoldering and polarized inflammation in the initiation and promotion of malignant disease. *Cancer cell* **7**, 211-217 (2005).

476 Mantovani, A. Cancer: inflaming metastasis. *Nature* **457**, 36 (2009).

477 Zlotnik, A. Chemokines and cancer. *International journal of cancer* **119**, 2026-2029 (2006).

478 Günther, K. *et al.* Prediction of lymph node metastasis in colorectal carcinoma by expressionof chemokine receptor CCR7. *International journal of cancer* **116**, 726-733 (2005).

479 Kim, J. *et al.* Chemokine receptor CXCR4 expression in colorectal cancer patients increases the risk for recurrence and for poor survival. *Journal of Clinical Oncology* **23**, 2744-2753 (2005).

480 Fredriksson, R., Lagerström, M. C., Lundin, L.-G. & Schiöth, H. B. The G-protein-coupled receptors in the human genome form five main families. Phylogenetic analysis, paralogon groups, and fingerprints. *Molecular pharmacology* **63**, 1256-1272 (2003).

481 Balkwill, F. in *Seminars in cancer biology.* 171-179 (Elsevier).

482 Tilton, B. *et al.* Signal transduction by CXC chemokine receptor 4: stromal cell–derived factor 1 stimulates prolonged protein kinase B and extracellular signal–regulated kinase 2 activation in T lymphocytes. *Journal of experimental medicine* **192**, 313-324 (2000).

483 Ganju, R. K. *et al.* The α-chemokine, stromal cell-derived factor-1α, binds to the transmembrane G-protein-coupled CXCR-4 receptor and activates multiple signal transduction pathways. *Journal of Biological Chemistry* **273**, 23169-23175 (1998).

484 Busillo, J. M. & Benovic, J. L. Regulation of CXCR4 signaling. *Biochimica et Biophysica Acta (BBA)-Biomembranes* **1768**, 952-963 (2007).

485 Anders, H.-J., Romagnani, P. & Mantovani, A. Pathomechanisms: homeostatic chemokines in health, tissue regeneration, and progressive diseases. *Trends in molecular medicine* **20**, 154-165 (2014).

486   Nagasawa, T. *et al.* Defects of B-cell lymphopoiesis and bone-marrow myelopoiesis in mice lacking the CXC chemokine PBSF/SDF-1. *Nature* **382**, 635 (1996).

487   Takabatake, Y. *et al.* The CXCL12 (SDF-1)/CXCR4 axis is essential for the development of renal vasculature. *Journal of the American Society of Nephrology* **20**, 1714-1723 (2009).

488   Donà, E. *et al.* Directional tissue migration through a self-generated chemokine gradient. *Nature* **503**, 285 (2013).

489   Rankin, S. M. Chemokines and adult bone marrow stem cells. *Immunology letters* **145**, 47-54 (2012).

490   Heissig, B. *et al.* Recruitment of stem and progenitor cells from the bone marrow niche requires MMP-9 mediated release of kit-ligand. *Cell* **109**, 625-637 (2002).

491   Ansel, K. M. *et al.* A chemokine-driven positive feedback loop organizes lymphoid follicles. *Nature* **406**, 309 (2000).

492   Link, A. *et al.* Fibroblastic reticular cells in lymph nodes regulate the homeostasis of naive T cells. *Nature immunology* **8**, 1255 (2007).

493   Kokovay, E. *et al.* Adult SVZ lineage cells home to and leave the vascular niche via differential responses to SDF1/CXCR4 signaling. *Cell stem cell* **7**, 163-173 (2010).

494   Yang, Q.-E., Kim, D., Kaucher, A., Oatley, M. J. & Oatley, J. M. CXCL12–CXCR4 signaling is required for the maintenance of mouse spermatogonial stem cells. *J Cell Sci* **126**, 1009-1020 (2013).

495   Hu, T.-h. *et al.* SDF-1/CXCR4 promotes epithelial–mesenchymal transition and progression of colorectal cancer by activation of the Wnt/β-catenin signaling pathway. *Cancer letters* **354**, 417-426 (2014).

496   Fulton, A. M. The chemokine receptors CXCR4 and CXCR3 in cancer. *Current oncology reports* **11**, 125-131 (2009).

497   Xu, C. *et al.* CXCR4 overexpression is correlated with poor prognosis in colorectal cancer. *Life sciences* (2018).

498   Staller, P. *et al.* Chemokine receptor CXCR4 downregulated by von Hippel–Lindau tumour suppressor pVHL. *Nature* **425**, 307 (2003).

499   Romain, B. *et al.* Hypoxia differentially regulated CXCR4 and CXCR7 signaling in colon cancer. *Molecular cancer* **13**, 58 (2014).

500   Bachelder, R. E., Wendt, M. A. & Mercurio, A. M. Vascular endothelial growth factor promotes breast carcinoma invasion in an autocrine manner by regulating the chemokine receptor CXCR4. *Cancer research* **62**, 7203-7206 (2002).

501   Helbig, G. *et al.* NF-κ B promotes breast cancer cell migration and metastasis by inducing the expression of the chemokine receptor CXCR4. *Journal of biological chemistry* **278**, 21631-21638 (2003).

502   Libura, J. *et al.* CXCR4–SDF-1 signaling is active in rhabdomyosarcoma cells and regulates locomotion, chemotaxis, and adhesion: Presented at the Annual Meeting of the American Society of Hematology, Orlando, FL, December 7-11, 2001. *Blood* **100**, 2597-2606 (2002).

503   Zeelenberg, I. S., Ruuls-Van Stalle, L. & Roos, E. The chemokine receptor CXCR4 is required for outgrowth of colon carcinoma micrometastases. *Cancer research* **63**, 3833-3839 (2003).

504   Zhang, X. H.-F. *et al.* Latent bone metastasis in breast cancer tied to Src-dependent survival signals. *Cancer cell* **16**, 67-78 (2009).

505   Reya, T., Morrison, S. J., Clarke, M. F. & Weissman, I. L. Stem cells, cancer, and cancer stem cells. *nature* **414**, 105 (2001).

506   Liles, W. C. *et al.* Mobilization of hematopoietic progenitor cells in healthy volunteers by AMD3100, a CXCR4 antagonist. *Blood* **102**, 2728-2730 (2003).

507   Matsuda, L. A., Lolait, S. J., Brownstein, M. J., Young, A. C. & Bonner, T. I. Structure of a cannabinoid receptor and functional expression of the cloned cDNA. *Nature* **346**, 561 (1990).

508   Munro, S., Thomas, K. L. & Abu-Shaar, M. Molecular characterization of a peripheral receptor for cannabinoids. *Nature* **365**, 61 (1993).

509   Izzo, A. A. & Sharkey, K. A. Cannabinoids and the gut: new developments and emerging concepts. *Pharmacology & therapeutics* **126**, 21-38 (2010).

510   Borgelt, L. M., Franson, K. L., Nussbaum, A. M. & Wang, G. S. The P harmacologic and C linical E ffects of M edical C annabis. *Pharmacotherapy: The Journal of Human Pharmacology and Drug Therapy* **33**, 195-209 (2013).

511   Camilleri, M. Cannabinoids and gastrointestinal motility: Pharmacology, clinical effects, and potential therapeutics in humans. *Neurogastroenterology & Motility*, e13370 (2018).

512   Guzman, M. Cannabinoids: potential anticancer agents. *Nature Reviews Cancer* **3**, 745 (2003).

513   Mechoulam, R. *et al.* Identification of an endogenous 2-monoglyceride, present in canine gut, that binds to cannabinoid receptors. *Biochemical pharmacology* **50**, 83-90 (1995).

514   Sugiura, T. *et al.* 2-Arachidonoylglycerol: a possible endogenous cannabinoid receptor ligand in brain. *Biochemical and biophysical research communications* **215**, 89-97 (1995).

515   Di Marzo, V. The endocannabinoid system: its general strategy of action, tools for its pharmacological manipulation and potential therapeutic exploitation. *Pharmacological research* **60**, 77-84 (2009).

516   Devane, W. A. *et al.* Isolation and structure of a brain constituent that binds to the cannabinoid receptor. *Science* **258**, 1946-1949 (1992).

517   Ligresti, A. *et al.* Possible endocannabinoid control of colorectal cancer growth. *Gastroenterology* **125**, 677-687 (2003).

518   Deutsch, D. G. & Chin, S. A. Enzymatic synthesis and degradation of anandamide, a cannabinoid receptor agonist. *Biochemical pharmacology* **46**, 791-796 (1993).

519   Ahn, K., McKinney, M. K. & Cravatt, B. F. Enzymatic pathways that regulate endocannabinoid signaling in the nervous system. *Chemical reviews* **108**, 1687-1707 (2008).

520   Blankman, J. L., Simon, G. M. & Cravatt, B. F. A comprehensive profile of brain enzymes that hydrolyze the endocannabinoid 2-arachidonoylglycerol. *Chemistry & biology* **14**, 1347-1356 (2007).

521   Duncan, M. *et al.* Distribution and function of monoacylglycerol lipase in the gastrointestinal tract. *American Journal of Physiology-Gastrointestinal and Liver Physiology* **295**, G1255-G1265 (2008).

522   Sun, H. *et al.* Potential tumor-suppressive role of monoglyceride lipase in human colorectal cancer. *Oncogene* **32**, 234 (2013).

523   Abalo, R. & Martín-Fontelles, M. I. in *Handbook of Cannabis and Related Pathologies*   439-449 (Elsevier, 2017).

524   Duncan, M., Davison, J. & Sharkey, K. Endocannabinoids and their receptors in the enteric nervous system. *Alimentary pharmacology & therapeutics* **22**, 667-683 (2005).

525   Wright, K. *et al.* Differential expression of cannabinoid receptors in the human colon: cannabinoids promote epithelial wound healing. *Gastroenterology* **129**, 437-453 (2005).

526   Ihenetu, K., Molleman, A., Parsons, M. E. & Whelan, C. J. Inhibition of interleukin-8 release in the human colonic epithelial cell line HT-29 by cannabinoids. *European journal of pharmacology* **458**, 207-215 (2003).

527   Klein, T. W. *et al.* The cannabinoid system and immune modulation. *Journal of leukocyte biology* **74**, 486-496 (2003).

528   Samson, M.-T. *et al.* Differential roles of CB1 and CB2 cannabinoid receptors in mast cells. *The Journal of Immunology* **170**, 4953-4962 (2003).

529   Klein, T. W. & Cabral, G. A. Cannabinoid-induced immune suppression and modulation of antigen-presenting cells. *Journal of Neuroimmune Pharmacology* **1**, 50 (2006).

530   Chang, Y. H., Lee, S. T. & Lin, W. W. Effects of cannabinoids on LPS-stimulated inflammatory mediator release from macrophages: involvement of eicosanoids. *Journal of cellular biochemistry* **81**, 715-723 (2001).

531   Facchinetti, F., Del Giudice, E., Furegato, S., Passarotto, M. & Leon, A. Cannabinoids ablate release of TNFα in rat microglial cells stimulated with lypopolysaccharide. *Glia* **41**, 161-168 (2003).

532   Small-Howard, A. L., Shimoda, L. M. & TURNER, H. Anti-inflammatory potential of CB1-mediated cAMP elevation in mast cells. *Biochemical Journal* **388**, 465-473 (2005).

533   Munson, A., Harris, L., Friedman, M., Dewey, W. & Carchman, R. Antineoplastic activity of cannabinoids. *Journal of the National Cancer Institute* **55**, 597-602 (1975).

534   De Petrocellis, L. *et al.* The endogenous cannabinoid anandamide inhibits human breast cancer cell proliferation. *Proceedings of the National Academy of Sciences* **95**, 8375-8380 (1998).

535   Galve-Roperh, I. *et al.* Anti-tumoral action of cannabinoids: involvement of sustained ceramide accumulation and extracellular signal-regulated kinase activation. *Nature medicine* **6**, 313 (2000).

536   Nithipatikom, K. *et al.* 2-Arachidonoylglycerol: a novel inhibitor of androgen-independent prostate cancer cell invasion. *Cancer research* **64**, 8826-8830 (2004).

537   Ma, M. *et al.* Monoacylglycerol lipase inhibitor JZL184 regulates apoptosis and migration of colorectal cancer cells. *Molecular medicine reports* **13**, 2850-2856 (2016).

538   Winkler, K. *et al.* Fatty acid amide hydrolase inhibitors confer anti-invasive and antimetastatic effects on lung cancer cells. *Oncotarget* **7**, 15047 (2016).

539   Picardi, P., Ciaglia, E., Proto, M. C. & Pisanti, S. Anandamide inhibits breast tumor-induced angiogenesis. *Translational Medicine@ UniSa* **10**, 8 (2014).

540   Ramer, R., Fischer, S., Haustein, M., Manda, K. & Hinz, B. Cannabinoids inhibit angiogenic capacities of endothelial cells via release of tissue inhibitor of matrix metalloproteinases-1 from lung cancer cells. *Biochemical pharmacology* **91**, 202-216 (2014).

541   Blázquez, C. *et al.* Cannabinoid receptors as novel targets for the treatment of melanoma. *The FASEB journal* **20**, 2633-2635 (2006).

542   Caffarel, M. M., Sarrió, D., Palacios, J., Guzmán, M. & Sánchez, C. Δ9-tetrahydrocannabinol inhibits cell cycle progression in human breast cancer cells through Cdc2 regulation. *Cancer research* **66**, 6615-6621 (2006).

543   Wang, D. *et al.* Loss of cannabinoid receptor 1 accelerates intestinal tumor growth. *Cancer research* **68**, 6468-6476 (2008).

544   Martínez-Martínez, E. *et al.* Cannabinoids receptor type 2, CB2, expression correlates with human colon cancer progression and predicts patient survival. *Oncoscience* **2**, 131 (2015).

545   Felder, C. C. *et al.* Comparison of the pharmacology and signal transduction of the human cannabinoid CB1 and CB2 receptors. *Molecular pharmacology* **48**, 443-450 (1995).

546   Slipetz, D. M. *et al.* Activation of the human peripheral cannabinoid receptor results in inhibition of adenylyl cyclase. *Molecular pharmacology* **48**, 352-361 (1995).

547   Bouaboula, M. *et al.* Signaling pathway associated with stimulation of CB2 peripheral cannabinoid receptor: involvement of both mitogen-activated protein kinase and induction of Krox-24 expression. *European journal of biochemistry* **237**, 704-711 (1996).

548 Lopez-Ilasaca, M. Signaling from G-protein-coupled receptors to mitogen-activated protein (MAP)-kinase cascades. *Biochemical pharmacology* **56**, 269-277 (1998).

549 Grimsey, N. L., Goodfellow, C. E., Dragunow, M. & Glass, M. Cannabinoid receptor 2 undergoes Rab5-mediated internalization and recycles via a Rab11-dependent pathway. *Biochimica et Biophysica Acta (BBA)-Molecular Cell Research* **1813**, 1554-1560 (2011).

550 Atwood, B. K., Wager-Miller, J., Haskins, C., Straiker, A. & Mackie, K. Functional selectivity in CB2 cannabinoid receptor signaling and regulation: implications for the therapeutic potential of CB2 ligands. *Molecular pharmacology*, mol. 111.074013 (2011).

551 Galiègue, S. *et al.* Expression of central and peripheral cannabinoid receptors in human immune tissues and leukocyte subpopulations. *European journal of biochemistry* **232**, 54-61 (1995).

552 Deng, L. *et al.* Chronic cannabinoid receptor 2 activation reverses paclitaxel neuropathy without tolerance or cannabinoid receptor 1–dependent withdrawal. *Biological psychiatry* **77**, 475-487 (2015).

553 Leleu-Chavain, N. *et al.* Recent advances in the development of selective CB2 agonists as promising anti-inflammatory agents. *Current medicinal chemistry* **19**, 3457-3474 (2012).

554 Han, S., Thatte, J., Buzard, D. J. & Jones, R. M. Therapeutic utility of cannabinoid receptor type 2 (CB2) selective agonists. *Journal of medicinal chemistry* **56**, 8224-8256 (2013).

555 Pérez-Gómez, E. *et al.* Role of cannabinoid receptor CB2 in HER2 pro-oncogenic signaling in breast cancer. *JNCI: Journal of the National Cancer Institute* **107** (2015).

556 Coke, C. J. *et al.* Simultaneous activation of induced heterodimerization between CXCR4 chemokine receptor and cannabinoid receptor 2 (CB2) reveal a mechanism for regulation of tumor progression. *Journal of Biological Chemistry*, jbc. M115. 712661 (2016).

557 Moreno, E. *et al.* Targeting CB2-GPR55 receptor heteromers modulates cancer cell signaling. *Journal of Biological Chemistry* **289**, 21960-21972 (2014).

558 Sánchez, C. *et al.* Inhibition of glioma growth in vivo by selective activation of the CB2 cannabinoid receptor. *Cancer research* **61**, 5784-5789 (2001).

559 Guzman, M. *et al.* A pilot clinical study of Δ 9-tetrahydrocannabinol in patients with recurrent glioblastoma multiforme. *British journal of cancer* **95**, 197 (2006).

560 Julien, B. *et al.* Antifibrogenic role of the cannabinoid receptor CB2 in the liver. *Gastroenterology* **128**, 742-755 (2005).

561 Hamilton, W., Round, A., Sharp, D. & Peters, T. Clinical features of colorectal cancer before diagnosis: a population-based case–control study. *British journal of cancer* **93**, 399 (2005).

562 Moreno, C. C. *et al.* Colorectal cancer initial diagnosis: screening colonoscopy, diagnostic colonoscopy, or emergent surgery, and tumor stage and size at initial presentation. *Clinical colorectal cancer* **15**, 67-73 (2016).

563 Majumdar, S. R., Fletcher, R. H. & Evans, A. T. How does colorectal cancer present? Symptoms, duration, and clues to location. *The American journal of gastroenterology* **94**, 3039-3045 (1999).

564 Sobin, L. H. & Fleming, I. D. TNM classification of malignant tumors, (1997). *Cancer: Interdisciplinary International Journal of the American Cancer Society* **80**, 1803-1804 (1997).

565 Eriksen, A. C. *et al.* Does heterogeneity matter in the estimation of tumour budding and tumour stroma ratio in colon cancer? *Diagnostic pathology* **13**, 20 (2018).

566 Dienstmann, R., Salazar, R. & Tabernero, J. Personalizing colon cancer adjuvant therapy: selecting optimal treatments for individual patients. *Journal of Clinical Oncology* **33**, 1787-1796 (2015).

567   Dienstmann, R. *et al.* Prediction of overall survival in stage II and III colon cancer beyond TNM system: a retrospective, pooled biomarker study. *Annals of Oncology* **28**, 1023-1031 (2017).

568   Sargent, D. J. *et al.*   (American Society of Clinical Oncology, 2014).

569   Popovici, V. *et al.* Context-dependent interpretation of the prognostic value of BRAF and KRAS mutations in colorectal cancer. *BMC cancer* **13**, 439 (2013).

570   Galon, J. *et al.* Towards the introduction of the 'Immunoscore'in the classification of malignant tumours. *The Journal of pathology* **232**, 199-209 (2014).

571   Mesker, W. E. *et al.* The carcinoma–stromal ratio of colon carcinoma is an independent factor for survival compared to lymph node status and tumor stage. *Analytical Cellular Pathology* **29**, 387-398 (2007).

572   van Pelt, G. W. *et al.* The tumour–stroma ratio in colon cancer: the biological role and its prognostic impact. *Histopathology* (2018).

573   Horcic, M. *et al.* Tumor budding score based on 10 high-power fields is a promising basis for a standardized prognostic scoring system in stage II colorectal cancer. *Human pathology* **44**, 697-705 (2013).

574   Bupathi, M. & Wu, C. Biomarkers for immune therapy in colorectal cancer: mismatch-repair deficiency and others. *Journal of gastrointestinal oncology* **7**, 713 (2016).

575   Guinney, J. *et al.* The consensus molecular subtypes of colorectal cancer. *Nature medicine* **21**, 1350 (2015).

576   Vogel, J. D., Eskicioglu, C., Weiser, M. R., Feingold, D. L. & Steele, S. R. The American Society of Colon and Rectal Surgeons clinical practice guidelines for the treatment of colon cancer. *Diseases of the Colon & Rectum* **60**, 999-1017 (2017).

577   Sauer, R. *et al.* Preoperative versus postoperative chemoradiotherapy for rectal cancer. *New England Journal of Medicine* **351**, 1731-1740 (2004).

578   Cukier, M. *et al.* Neoadjuvant chemoradiotherapy and multivisceral resection for primary locally advanced adherent colon cancer: a single institution experience. *European Journal of Surgical Oncology (EJSO)* **38**, 677-682 (2012).

579   Taylor, W. E. *et al.* The Mayo Clinic experience with multimodality treatment of locally advanced or recurrent colon cancer. *Annals of surgical oncology* **9**, 177-185 (2002).

580   Group, F. C. Feasibility of preoperative chemotherapy for locally advanced, operable colon cancer: the pilot phase of a randomised controlled trial. *The Lancet Oncology* **13**, 1152 (2012).

581   Buyse, M., Zeleniuch-Jacquotte, A. & Chalmers, T. C. Adjuvant therapy of colorectal cancer: why we still don't know. *Jama* **259**, 3571-3578 (1988).

582   Wolmark, N. *et al.* Postoperative Adjuvant Chemotherapy or BCG for Colon Cancer: Results From NSABP Protocol C-011. *JNCI: Journal of the National Cancer Institute* **80**, 30-36 (1988).

583   Wolmark, N. *et al.* The benefit of leucovorin-modulated fluorouracil as postoperative adjuvant therapy for primary colon cancer: results from National Surgical Adjuvant Breast and Bowel Project protocol C-03. *Journal of Clinical Oncology* **11**, 1879-1887 (1993).

584   André, T. *et al.* Oxaliplatin, fluorouracil, and leucovorin as adjuvant treatment for colon cancer. *New England Journal of Medicine* **350**, 2343-2351 (2004).

585   M McQuade, R., Stojanovska, V., C Bornstein, J. & Nurgali, K. Colorectal cancer chemotherapy: the evolution of treatment and new approaches. *Current medicinal chemistry* **24**, 1537-1557 (2017).

586   Kannarkatt, J., Joseph, J., Kurniali, P. C., Al-Janadi, A. & Hrinczenko, B. Adjuvant chemotherapy for stage II colon cancer: a clinical dilemma. *Journal of oncology practice* **13**, 233-241 (2017).

587   Varghese, A. Chemotherapy for stage II colon cancer. *Clinics in colon and rectal surgery* **28**, 256 (2015).

588   Rodriguez-Bigas, M. A., Grothey, A. & Goldberg, R. M. Overview of the management of primary colon cancer. *Waltham MA: UpTodate* (2017).

589   Tournigand, C. *et al.* Adjuvant therapy with fluorouracil and oxaliplatin in stage II and elderly patients (between ages 70 and 75 years) with colon cancer: subgroup analyses of the Multicenter International Study of Oxaliplatin, Fluorouracil, and Leucovorin in the Adjuvant Treatment of Colon Cancer trial. *Journal of clinical oncology* **30**, 3353-3360 (2012).

590   Lund, C. *et al.* Efficacy and toxicity of adjuvant chemotherapy in elderly patients with colorectal cancer: the ACCORE study. *ESMO open* **1**, e000087 (2016).

591   André, T. *et al.* Improved overall survival with oxaliplatin, fluorouracil, and leucovorin as adjuvant treatment in stage II or III colon cancer in the MOSAIC trial. *Journal of Clinical Oncology* **27**, 3109-3116 (2009).

592   Saltz, L. B. *et al.* Bevacizumab in combination with oxaliplatin-based chemotherapy as first-line therapy in metastatic colorectal cancer: a randomized phase III study. *Journal of clinical oncology* **26**, 2013-2019 (2008).

593   Stintzing, S. *et al.* FOLFIRI plus cetuximab versus FOLFIRI plus bevacizumab for metastatic colorectal cancer (FIRE-3): a post-hoc analysis of tumour dynamics in the final RAS wild-type subgroup of this randomised open-label phase 3 trial. *The Lancet Oncology* **17**, 1426-1434 (2016).

594   Oki, E. *et al.* Recent advances in treatment for colorectal liver metastasis. *Annals of gastroenterological surgery* **2**, 167-175 (2018).

595   Giantonio, B. J. *et al.* Bevacizumab in combination with oxaliplatin, fluorouracil, and leucovorin (FOLFOX4) for previously treated metastatic colorectal cancer: results from the Eastern Cooperative Oncology Group Study E3200. *Journal of Clinical Oncology* **25**, 1539-1544 (2007).

596   Van Cutsem, E. *et al.* Cetuximab plus irinotecan, fluorouracil, and leucovorin as first-line treatment for metastatic colorectal cancer: updated analysis of overall survival according to tumor KRAS and BRAF mutation status. *J Clin Oncol* **29**, 2011-2019 (2011).

597   Peeters, M. *et al.* Final results from a randomized phase 3 study of FOLFIRI±panitumumab for second-line treatment of metastatic colorectal cancer. *Annals of Oncology* **25**, 107-116 (2014).

598   Van Cutsem, E. *et al.* Addition of aflibercept to fluorouracil, leucovorin, and irinotecan improves survival in a phase III randomized trial in patients with metastatic colorectal cancer previously treated with an oxaliplatin-based regimen. *J Clin Oncol* **30**, 3499-3506 (2012).

599   Grothey, A. *et al.* Regorafenib monotherapy for previously treated metastatic colorectal cancer (CORRECT): an international, multicentre, randomised, placebo-controlled, phase 3 trial. *The Lancet* **381**, 303-312 (2013).

600   Kagami, Y. *et al.* Establishment of a follicular lymphoma cell line (FLK-1) dependent on follicular dendritic cell-like cell line HK. *Leukemia* **15**, 148 (2001).

601   Shaffer, A. L. *et al.* A library of gene expression signatures to illuminate normal and pathological lymphoid biology. *Immunological reviews* **210**, 67-85 (2006).

602   Nadeu, F. *et al.* Clinical impact of clonal and subclonal TP53, SF3B1, BIRC3, NOTCH1 and ATM mutations in chronic lymphocytic leukemia. *Blood*, blood-2015-2007-659144 (2016).

603   Li, H. & Durbin, R. Fast and accurate short read alignment with Burrows–Wheeler transform. *bioinformatics* **25**, 1754-1760 (2009).

604   McKenna, A. *et al.* The Genome Analysis Toolkit: a MapReduce framework for analyzing next-generation DNA sequencing data. *Genome research* (2010).

605   Van der Auwera, G. A. *et al.* From FastQ data to high-confidence variant calls: the genome analysis toolkit best practices pipeline. *Current protocols in bioinformatics* **43**, 11.10. 11-11.10. 33 (2013).

606   Li, H. *et al.* The sequence alignment/map format and SAMtools. *Bioinformatics* **25**, 2078-2079 (2009).

607   Koboldt, D. C. *et al.* VarScan 2: somatic mutation and copy number alteration discovery in cancer by exome sequencing. *Genome research* (2012).

608   Lai, Z. *et al.* VarDict: a novel and versatile variant caller for next-generation sequencing in cancer research. *Nucleic acids research* **44**, e108-e108 (2016).

609   Gerstung, M., Papaemmanuil, E. & Campbell, P. J. Subclonal variant calling with multiple samples and prior knowledge. *Bioinformatics* **30**, 1198-1204 (2014).

610   Cingolani, P. *et al.* A program for annotating and predicting the effects of single nucleotide polymorphisms, SnpEff: SNPs in the genome of Drosophila melanogaster strain w1118; iso-2; iso-3. *Fly* **6**, 80-92 (2012).

611   Ruden, D. M. *et al.* Using Drosophila melanogaster as a model for genotoxic chemical mutational studies with a new program, SnpSift. *Frontiers in genetics* **3**, 35 (2012).

612   Kleinman HK, C. M. Preparation of endothelial cells. *CurrProtocCell* **831** (2001).

613   Jenson, J. M., Ryan, J. A., Grant, R. A., Letai, A. & Keating, A. E. Epistatic mutations in PUMA BH3 drive an alternate binding mode to potently and selectively inhibit anti-apoptotic Bfl-1. *Elife* **6**, e25541 (2017).

614   Söderberg, O. *et al.* Characterizing proteins and their interactions in cells and tissues using the in situ proximity ligation assay. *Methods* **45**, 227-232 (2008).

615   Rasband, W. S. Imagej, us national institutes of health, bethesda, maryland, usa. *http://imagej. nih. gov/ij/* (2011).

616   Li, C. & Tam, P. K.-S. An iterative algorithm for minimum cross entropy thresholding. *Pattern recognition letters* **19**, 771-776 (1998).

617   Giavazzi, R., Campbell, D. E., Jessup, J., Cleary, K. & Fidler, I. J. Metastatic behavior of tumor cells isolated from primary and metastatic human colorectal carcinomas implanted into different sites in nude mice. *Cancer Research* **46**, 1928-1933 (1986).

618   Urosevic, J. *et al.* Colon cancer cells colonize the lung from established liver metastases through p38 MAPK signalling and PTHLH. *Nature cell biology* **16**, 685 (2014).

619   Céspedes, M. V. *et al.* Orthotopic microinjection of human colon cancer cells in nude mice induces tumor foci in all clinically relevant metastatic sites. *The American journal of pathology* **170**, 1077-1085 (2007).

620   Matas-Céspedes, A. *et al.* Disruption of follicular dendritic cells-follicular lymphoma crosstalk by the pan-PI3K inhibitor BKM120 (buparlisib). *Clinical Cancer Research*, clincanres. 0154.2014 (2014).

621   Gobert, M. *et al.* Regulatory T cells recruited through CCL22/CCR4 are selectively activated in lymphoid infiltrates surrounding primary breast tumors and lead to an adverse clinical outcome. *Cancer research* (2009).

622   Curiel, T. J. *et al.* Specific recruitment of regulatory T cells in ovarian carcinoma fosters immune privilege and predicts reduced survival. *Nature medicine* **10**, 942 (2004).

623   Rawal, S. *et al.* Cross talk between follicular Th cells and tumor cells in human follicular lymphoma promotes immune evasion in the tumor microenvironment. *The Journal of Immunology*, 1201363 (2013).

624   Yoshie, O. & Matsushima, K. CCR4 and its ligands: from bench to bedside. *International immunology* **27**, 11-20 (2014).

625   Ryan, J., Montero, J., Rocco, J. & Letai, A. iBH3: simple, fixable BH3 profiling to determine apoptotic priming in primary tissue by flow cytometry. *Biological chemistry* **397**, 671-678 (2016).

626   Potter, D. S. & Letai, A. in *Cold Spring Harbor symposia on quantitative biology.* 030841 (Cold Spring Harbor Laboratory Press).

627   Yang, Q., Modi, P., Newcomb, T., Qu, C. & Gandhi, V. Idelalisib: first-in-class PI3K delta inhibitor for the treatment of chronic lymphocytic leukemia, small lymphocytic leukemia, and follicular lymphoma. *Clinical cancer research*, clincanres. 2034.2014 (2015).

628   de Weerdt, I., Koopmans, S. M., Kater, A. P. & van Gelder, M. Incidence and management of toxicity associated with ibrutinib and idelalisib: a practical approach. *Haematologica* **102**, 1629-1639 (2017).

629   Cuneo, A. *et al.* Management of adverse events associated with idelalisib treatment in chronic lymphocytic leukemia and follicular lymphoma: A multidisciplinary position paper. *Hematological oncology* (2018).

630   Migault, C. *et al.* Pulmonary adverse events related to idelalisib therapy: A single centre experience. *Journal of Chemotherapy*, 1-5 (2018).

631   Yusuf, I. *et al.* Germinal center T follicular helper cell IL-4 production is dependent on signaling lymphocytic activation molecule receptor (CD150). *The Journal of Immunology*, ji_0903505 (2010).

632   Rolf, J. *et al.* Phosphoinositide 3-kinase activity in T cells regulates the magnitude of the germinal center reaction. *The Journal of Immunology*, 1001730 (2010).

633   Zhou DM, X. Y., Zhang LY, . The role of follicular T helper cells in patients with malignant lymphoid disease. *Hematology* **22**, 412-418 (2017).

634   Couper, K. N., Blount, D. G. & Riley, E. M. IL-10: the master regulator of immunity to infection. *The Journal of Immunology* **180**, 5771-5777 (2008).

635   Linterman, M. A. *et al.* Foxp3+ follicular regulatory T cells control the germinal center response. *Nature medicine* **17**, 975 (2011).

636   Wing, J. B., Tekgüç, M. & Sakaguchi, S. Control of germinal center responses by T-follicular regulatory cells. *Frontiers in immunology* **9** (2018).

637   Drillenburg, P. & Pals, S. T. Cell adhesion receptors in lymphoma dissemination. *Blood* **95**, 1900-1910 (2000).

638   Terol, M.-J. *et al.* Expression of beta-integrin adhesion molecules in non-Hodgkin's lymphoma: correlation with clinical and evolutive features. *Journal of clinical oncology* **17**, 1869-1875 (1999).

639   de Rooij, M. F. *et al.* Ibrutinib and idelalisib synergistically target BCR-controlled adhesion in MCL and CLL: a rationale for combination therapy. *Blood* **125**, 2306-2309 (2015).

640   Leverson, J. D. & Cojocari, D. Hematologic Tumor Cell Resistance to the BCL-2 Inhibitor Venetoclax: A Product of Its Microenvironment? *Frontiers in oncology* **8**, 458 (2018).

641   Jayappa, K. D. *et al.* Microenvironmental agonists generate de novo phenotypic resistance to combined ibrutinib plus venetoclax in CLL and MCL. *Blood advances* **1**, 933-946 (2017).

642   Oppermann, S. *et al.* High-content screening identifies kinase inhibitors that overcome venetoclax resistance in activated CLL cells. *Blood* **128**, 934-947 (2016).

643   Thijssen, R. *et al.* Resistance to ABT-199 induced by microenvironmental signals in chronic lymphocytic leukemia can be counteracted by CD20 antibodies or kinase inhibitors. *Haematologica* **100**, e302-e306 (2015).

644   Chiron, D. *et al.* Biological rational for sequential targeting of Bruton tyrosine kinase and Bcl-2 to overcome CD40-induced ABT-199 resistance in mantle cell lymphoma. *Oncotarget* **6**, 8750 (2015).

645   Kim, J., Takeuchi, H., Foshag, L., Bilchik, A. & Hoon, D. Colorectal cancer expression of chemokine receptor CXCR4 promotes liver metastasis. *Journal of Clinical Oncology* **22**, 3582-3582 (2004).

646   Yoshitake, N. *et al.* Expression of SDF-1α and nuclear CXCR4 predicts lymph node metastasis in colorectal cancer. *British Journal of Cancer* **98**, 1682 (2008).

647   Li, L.-N. *et al.* Prognosis and clinicopathology of CXCR4 in colorectal cancer patients: a meta-analysis. *Asian Pac J Cancer Prev* **16**, 4077-4080 (2015).

648   Speetjens, F. M. *et al.* Nuclear localization of CXCR4 determines prognosis for colorectal cancer patients. *Cancer Microenvironment* **2**, 1 (2009).

649   Wang, S.-C. *et al.* Nuclear expression of CXCR4 is associated with advanced colorectal cancer. *International journal of colorectal disease* **25**, 1185-1191 (2010).

650   Wang, L. *et al.* CXCR4 nuclear localization follows binding of its ligand SDF-1 and occurs in metastatic but not primary renal cell carcinoma. *Oncology reports* **22**, 1333-1339 (2009).

651   Nasser, M. W. *et al.* Crosstalk between chemokine receptor CXCR4 and cannabinoid receptor CB2 in modulating breast cancer growth and invasion. *PloS one* **6**, e23901 (2011).

652   Scarlett, K. A. *et al.* Agonist-induced CXCR4 and CB2 Heterodimerization Inhibits Gα13/RhoA-mediated Migration. *Molecular Cancer Research* (2018).

653   Ghosh, S., Preet, A., Groopman, J. E. & Ganju, R. K. Cannabinoid receptor CB2 modulates the CXCL12/CXCR4-mediated chemotaxis of T lymphocytes. *Molecular immunology* **43**, 2169-2179 (2006).

654   Santoro, A. *et al.* Rimonabant inhibits human colon cancer cell growth and reduces the formation of precancerous lesions in the mouse colon. *International journal of cancer* **125**, 996-1003 (2009).

655   Kim, S. Y. *et al.* Inhibition of the CXCR4/CXCL12 chemokine pathway reduces the development of murine pulmonary metastases. *Clinical & experimental metastasis* **25**, 201-211 (2008).

ANNEXES

## Supplemental Table 1 Recurrent somatic mutations in FL

Study label	CREBBP	TNFRSF14	KMT2D	EP300	MEF2B	EZH2	TNFAIP3	TP53	RRAGC
FL2	p.Phe1484del	p.Cys42Tyr	p.Gln4609* p.Pro868fs						
FL3	p.Asp1037fs	p.Arg62Gly	p.Trp339*						
FL4	p.Gln1209fs	p.Cys54Ser	p.Cys1474Tyr		p.Thr70Arg				
FL6	p.Pro1948Leu p.Ser1436Arg p.Cys1219*								
FL7	p.Tyr1503Asn p.Gln338fs		p.Gln2819* p.Pro2557Leu						
FL8	p.Tyr1450Cys	p.His134fs	p.Pro2382Ser			p.Tyr646Asn			
FL9	p.Arg1446Leu	p.Trp201*	p.Glu1588* p.Pro1460fs						p.Trp115Arg
FL10	p.Asn1978Ser p.Arg1498*		p.Ile1208fs	p.Trp1436Arg			p.His195fs	p.Ser240Arg	
FL11	p.Tyr1503Ser		p.Val5155fs p.His3588fs p.Glu902fs		p.Pro340Leu			p.Arg248Trp	
FL12		p.Pro55Ser							
FL13			p.Tyr2199fs p.Cys276fs,			p.Tyr646Phe			
FL14	p.Arg1446Cys,		p.Tyr1495fs p.Ile982fs p.Tyr343Cys						
FL15	p.Gln442*			p.Glu1246*					
FL16	p.Tyr1450Ser		p.Gln3737* p.Arg3452*				p.Thr647Pro		p.Pro87Leu
FL17			p.Ser2488fs		p.Thr70Lys				
FL18	p.Ser1680del								
FL19		p.Gln158*	p.Thr3384fs				p.Gln370*		
FL20	p.Gln1491Lys		p.Ser4456fs, p.Gln4412*						
FL21			p.Gln4347fs p.Val2551fs						
FL22	p.Leu1454Arg	p.Cys127Tyr	p.Gly2493Glu						
FL23			p.Pro2931fs p.Arg1388Leu						
FL24	p.His1487Tyr	p.Ser112Pro	p.Arg5154Gln p.Cys5117* p.Arg348Cys	p.Pro925Thr		p.Tyr646Phe			
FL25	p.Ser1680del	p.Cys93*	c.7333C>T c.5124_5125del AC						
FL26		p.Lys17fs	p.Val4642fs p.Leu3245*	p.Gln1720His					
FL27	p.Arg1446His	p.Gly8fs	p.Arg4198* p.Gln3265fs						
FL29	p.Ser1680del p.Tyr1503Asp	p.Cys138Tyr	p.Arg3321* p.Gln425*			p.Ala692Val			
FL31	p.Tyr1503His p.Ala981Thr		p.His5114Tyr		p.Arg24Gln	p.Ala682Gly	p.Thr647Pro		
FL32							p.Gln350fs p.His351Tyr		

Supplemental Figure 1
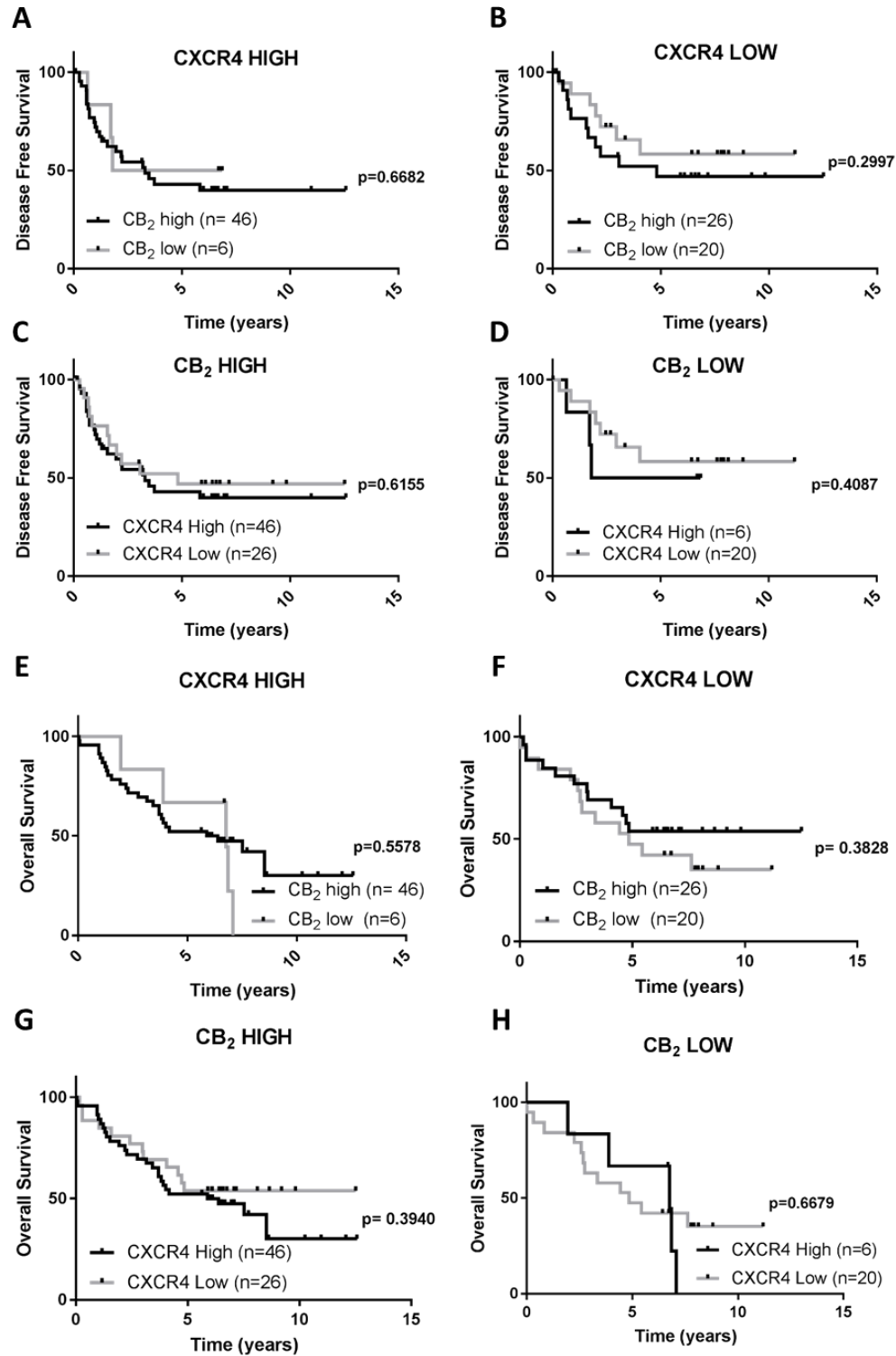
Figure S1. Prognostic value of CXCR4 and CB₂. **(A-D)** Data plotted in Kaplan-Meier curves for disease free survival combining both receptors expression levels. **(E-H)** Data plotted in Kaplan-Meier curves for overall survival combining both receptors expression levels.

Supplemental Figure 2
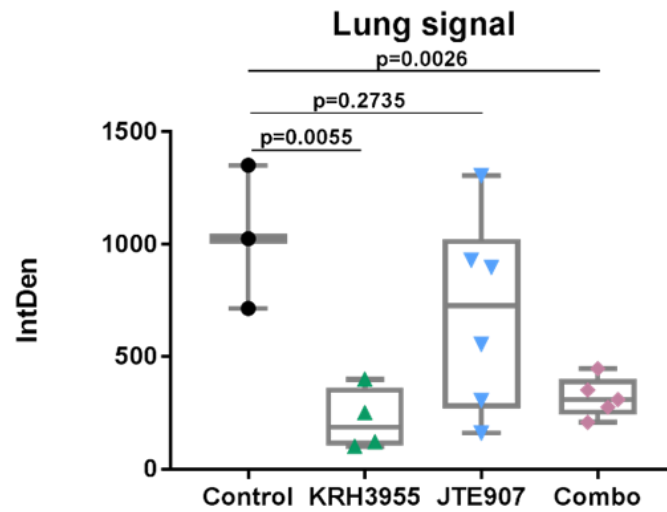
Figure S2. Targeting the crosstalk between CXCR4 and CB₂ showed anti-lung metastatic effect. *Ex-vivo* evaluation of mice lungs. At the experiment endpoint, a significant decrease in lungs metastases in animals treated with the CXCR4 antagonist, KRH3955 (P=0.0055) was observed. Additionally, even a more pronounced decrease was detected in animals treated with a combination of CXCR4 antagonist, KRH3955 and CB2 antagonist, JTE907, (P=0.0026).